UNIVERSITAT DE BARCELONA

Spontaneous and perturbation-based electroencephalographic markers of brain health

Ruben Perellón Alfonso

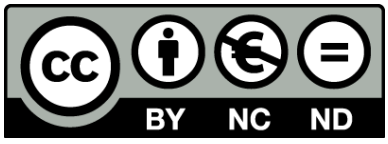

Spontaneous and perturbation-based electroencephalographic markers of brain health

Doctoral Thesis

Ruben Perellón Alfondo

Universitat de Barcelona

2024

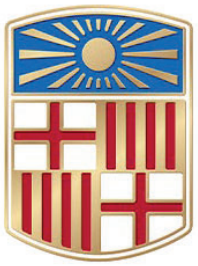

UNIVERSITAT DE BARCELONA

Spontaneous and perturbation-based electroencephalographic markers of brain health

Doctoral thesis dissertation presented by Ruben Perellón Alfonso to apply for the degree of doctor at the University of Barcelona

Directed by Dr. David Bartrés Faz and Dr. Kilian Abellaneda Pérez

Doctoral Program in Medicine and Translational Research.
School of Medicine and Health Sciences. University of Barcelona.

January 2024

Life is beautiful!

Indre Pileckyte

Als meus pares i al meu germà

A la Indre i la Sara

ACKNOWLEDGEMENTS

First, I want to thank my supervisors, David Bartrés Faz and Kilian Abellaneda Pérez, whose invaluable and unwavering guidance throughout this journey has been instrumental in getting this thesis to a satisfactory conclusion. I also thank you for all you have taught me about neuroscience, non-invasive brain stimulation, and scientific methodology, and all the opportunities you have given me to become a better scientist. But more importantly, I thank you for your personal support and friendship, which has brought me confidence and joy in equal measure. I also want to thank all other lab members, Lídia Vaqué Alcázar, Lídia Mulet Pons, María Cabello Toscano, Cristina Solé Padullés and Pablo Martín Trias. Thank you all for sharing this journey with me. I will treasure every day in the lab and every night out with all of you. Getting to know you all has made me a better person and a much stronger scientist.

I want to thank my wife, Indre Pileckyte, who has been my scientific and life partner ever since we met 12 years ago in Vienna. You are my anchor to happiness and optimism and the ideal of scientist I strive to become one day myself. Without your support and patience this thesis would never have been completed. You pick me up when I am down and send me soaring when I rise.

Finally, to my daughter Sara, *my little*, now I truly have it all.

FUNDING

I was fully funded to conduct the doctoral work that has given rise to this thesis from an INPhINIT fellowship form “la Caixa” Foundation (ID 100010434. Fellowship code: LCF/BQ/DI19/ 11730050). Additionally, the work conducted in this thesis was partially supported by grants from the Agencia de Gestio d'Ajuts Universitaris i de Recerca (AGAUR) “PANDEMIES 2020” (Grant Number: 2020PANDE00043), the “La Marato de TV3” MARATO 2020 COVID-19 (Grant Number: 202129-31), the “la Caixa” Foundation (Grant Number: LCF/PR/PR16/11110004) and the Spanish Ministry of Science and Innovation (Grant Number: RTI2018-095181-B-C2).

TABLE OF CONTENTS

ABBREVIATIONS AND ACRONYMS 16

LIST OF ARTICLES IN THE THESIS 19

RESUM DE LA TESI 21

CHAPTER 1. General Introduction 26

1.1. Brain Health challenges and biomarkers 26

1.2. Non-invasive capture and modulation of electric synaptic transmission 28

1.2.1. Physiological basis of EEG 28

1.2.2. Transcranial electric and magnetic stimulation 30

1.2.3. Concurrent TMS-EEG 33

1.3. Biomarkers of mental health resilience during the COVID-19 pandemic 35

1.3.1. The mental health impact of the COVID-19 pandemic 35

1.3.2. Mental health resilience 36

1.3.3. A toy model of brain resilience 39

1.4. Biomarkers of cognitive disfunction in schizophrenia 40

1.4.1. The heterogeneity problem in psychiatry and schizophrenia 40

1.4.2. Neuroimaging and EEG correlates of schizophrenia 41

1.4.3. Working memory deficits in schizophrenia 45

1.4.4. Data-driven diagnostic and patient classification in schizophrenia 46

1.5. Biomarkers of cortical excitability and protein pathology in AD 48

1.5.1. The pathophysiology of Alzheimer's disease 48

1.5.2. Biomarkers for early detection of Alzheimer's disease 49

1.5.3. The role of cortical excitability in Alzheimer's disease 50

CHAPTER 2. Hypotheses and Objectives 55

2.1. General Hypothesis 55

2.2. Specific Hypotheses 55

2.2.1. Study 1 55

2.2.2. Study 2 55

2.2.3. Study 3 55

2.3. General Objective 56

2.4. Specific Objectives 56

2.4.1. Study 1 56

2.4.2. Study 2 56

2.4.3. Study 3 56
CHAPTER 3. Materials, Methods, and Results 58
3.1. STUDY 1 59
3.2. STUDY 2 78
3.3. STUDY 3 102
CHAPTER 4. General Discussion 124
CONCLUSIONS 136
BIBLIOGRAPHY 138

ABBREVIATIONS AND ACRONYMS

AD	Alzheimer's disease
AMPA	α-amino-3-hydroxy-5-methyl-4-isoxazolepropionic acid
Aβ	Amyloid-β
CA1	Cornu ammonis 1
CDA	Contralateral delay activity
COVID-19	Coronavirus disease 2019
CSF	Cerebrospinal fluid
cTBS	Continuous theta burst stimulation
EEG	Electroencephalography / Electroencephalogram
ERP	Event-related potential
fMRI	Functional magnetic resonance imaging
FPN	Frontoparietal control network
GABA	Gamma-aminobutyric acid
iTBS	Intermittent theta burst stimulation
L-IPL	Left inferior parietal lobule
L-PFC	Left prefrontal cortex
LTD	Long-term depression
LTP	Long-term potentiation
M1	Primary motor cortex
MRI	Magnetic resonance imaging
NfL	Neurofilament light
NMDA	N-methyl-D-aspartate
PET	Positron emission tomography
p-tau	Phosphorylated tau
p-tau181	tau phosphorylated at amino acid 181
rTMS	Repetitive transcranial magnetic stimulation
SN	Salience network

SV2A	Synaptic vesicle protein 2A
TBS	Theta burst stimulation
tDCS	Transcranial direct current stimulation
TES	Transcranial electric stimulation
TMS	Transcranial magnetic stimulation
TMS-EEG	TMS with concurrent EEG
VGSC	Voltage-gated sodium channel
WM	Working memory

LIST OF ARTICLES IN THE THESIS

This thesis dissertation is presented to apply for the degree of doctor at the University of Barcelona and is the result of several studies conducted at the Medical Psychology Unit, Department of Medicine, University of Barcelona.

The thesis is presented in a compendium of publications format, consisting of two peer-reviewed published articles and one manuscript under review:

1. **Perellón-Alfonso. R.**, Redondo-Camós, M., Abellaneda-Pérez, K., Cattaneo, G., Delgado-Gallén, S., España-Irla, G., Sánchez, JS., Tormos, JM., Pascual-Leone, A., Bartrés-Faz, D. 2022. Prefrontal reactivity to TMS perturbation as a toy model of mental health outcomes during the COVID-19 pandemic. Heliyon, 8(8), e10208. Impact Factor 4.0; Quartile 1 (Scimago Journal Rank).

2. **Perellón-Alfonso, R.**, Oblak, A., Kuclar, M., Škrlj, B., Skodlar, B., Pregelj, P., Pileckyte, I., Abellaneda-Pérez, K., Bartrés-Faz, D., Repovš, G. and Bon, J. 2023. Dense Attentional Network identifies EEG abnormalities during working memory performance of patients with schizophrenia. Frontiers in Psychiatry, 14, 1205119. Impact Factor 4.7; Quartile 1 (Scimago Journal Rank).

3. **Perellón-Alfonso, R.**, Abellaneda-Pérez, K., Pileckyte, I., Cabello-Toscano, M., Mulet-Pons, L., Vaqué-Alcázar, L., Cattaneo G., Redondo-Camós, M., España-Irla, G., Delgado-Gallen, S., Sánchez, JS., Zetterberg, H., Tormos JM., Franzmeier N., Pascual-Leone A., Bartrés-Faz D. Spontaneous and perturbation-based EEG markers of cortical excitability are associated with blood p-tau181 concentration in healthy middle aged adults. Under Review.

RESUM DE LA TESI

Títol: Marcadors electroencefalogràfics espontanis i basats en pertorbacions en l'estudi de la salut cerebral

introducció: La salut cerebral és l'estat òptim del funcionament cerebral que permet a l'individu assolir el seu màxim potencial al llarg de la vida, independentment de la presència o absència de malalties. Per poder promoure i preservar la salut cerebral enfront de la malaltia, és fonamental descobrir els seus determinants cerebrals. Alguns dels principals reptes per a la salut cerebral són els trastorns mentals i les malalties neurodegeneratives, els més prevalents dels quals són els trastorns de l'estat d'ànim, l'esquizofrènia i la malaltia d'Alzheimer. Des del punt de vista fisiopatològic, aquestes malalties comparteixen disfuncions en la transmissió sinàptica, arrelades en processos inhibitoris i excitatoris, que podrien ser detectables mitjançant l'electroencefalografia i potencialment modificables mitjançant tècniques d'estimulació cerebral no invasives. Per tant, en aquesta tesi hem investigat biomarcadors candidats de la salut cerebral que podrien ser neurofisiològicament rellevants en el context de malalties comunes que la desafien, i, el que és més important, que són potencialment modificables.

Hipòtesis: Les hipòtesis generals són: 1) els biomarcadors candidats de la salut cerebral són detectables mitjançant mètodes no invasius i potencialment escalables, i 2) revelen mecanismes rellevants per a malalties que presenten disfuncions en la transmissió sinàptica , arrelades en processos excitatoris i inhibitoris. Les hipòtesis específiques per a cadascun dels tres estudis d'aquesta tesi són: 1) Es pot construir un "model de joguina" de la resiliència cerebral utilitzant una pertorbació cerebral controlada per simular l'estressor i avaluar la reactivitat cerebral com a indicador de la resposta de l'organisme. Aquest model integrat permetrà identificar una signatura distintiva de la resiliència cerebral davant de l'impacte anticipat dels estressors psicosocials associats a la pandèmia de la COVID-19. 2) Les anomalies inhibitòries dels pacients amb esquizofrènia durant una tasca de memòria de treball visual són detectables i es poden aprofundir mitjançant un model interpretable d'aprenentatge automàtic, per tal de diferenciar pacients de controls utilitzant només dades d'electroencefalografia (EEG). 3) l'excitabilitat cortical més elevada es correlaciona amb

concentracions més altes de tau fosforilada secretada en plasma, mentre que no s'observà cap associació amb la concentració de 'neurofilament light' de secreció passiva.

Objectius: L'objectiu principal d'aquesta tesi és investigar biomarcadors candidats de la salut cerebral que siguin potencialment translacionals i modificables en el context d'alguns dels seus reptes més prevalents. Els objectius específics de cadascun dels tres estudis són: 1) construir un "model de joguina" de la resiliència cerebral i emprar-lo en el context dels estressors psicosocials associats a la pandèmia de la COVID-19. 2) implementar un algoritme interpretable d'aprenentatge automàtic que pugui diferenciar pacients de controls basant-se únicament en dades d'EEG, alhora que reveli els mecanismes neurofisiològiques específics que donat lloc a la classificació. 3) establir la relació entre l'excitabilitat cortical i les proteïnes implicades en la fisiopatologia de la malaltia d'Alzheimer utilitzant mètodes no invasius.

Mètodes: S'ha utilitzat electroencefalografia (EEG) en repòs i durant tasca, així com també amb estimulació magnètica transcranial concurrent (EMT-EEG), per tal d'obtenir mètriques d'excitabilitat cortical espontànies i basades en pertorbacions. El potencial d'aquestes mètriques com a biomarcadors candidats de la salut cerebral es va investigar en tres escenaris diferents corresponents a tres estudis. L'estudi 1 va incloure una submostra de 74 participants del projecte Barcelona Brain Health Initiative (BBHI), que van completar EMT-EEG, una bateria de proves neuropsicològiques i avaluació de la salut mental abans de l'inici de la pandèmia i en tres moments addicionals durant aquesta. L'estudi 2 va incloure 15 pacients amb esquizofrènia i 15 controls sans, que van realitzar una tasca de memòria de treball visual amb EEG. Es van utilitzar mètodes d'anàlisi estadística univariable per avaluar les dades conductuals i d'EEG, mentre que es va utilitzar un algoritme interpretable d'aprenentatge automàtic únicament amb dades d'EEG. A l'estudi 3, es van emprar la concentració de tau fosforilada a l'aminoàcid 181 (p-tau181) i cadena lleugera(NfL) en plasma, així com les dades d'EEG en repòs en 648 participants de la cohort del BBHI. Addicionalment, en una submostra de 47 participants també disposàvem de EMT-EEG.

Resultats: A l'estudi 1, els individus que varen experimentar un efecte negatiu en la seva salut mental durant la pandèmia, van mostrar una resposta significativament més alta de la resposta d'EEG evocada per EMT a l'escorça prefrontal esquerre, quan la comparem amb la resposta d'individus que van romandre estables. Aquesta signatura, juntament amb els nivells d'educació, va ser significativament predictiva de l'estat de salut mental durant la pandèmia. A l'estudi 2, els pacients van mostrar una supressió significativament més baixa de la banda de freqüència alfa que els controls en moments crítics de la tasca de memòria de treball. L'algoritme d'aprenentatge automàtic interpretable va discriminar amb èxit els pacients dels controls. Les regions de la sèrie temporal d'EEG que van resultar més discriminants coincidien amb els regions temporals on les diferències en alfa eren més pronunciades. A l'estudi 3, tant les mesures d'excitabilitat cortical espontànies com les basades en pertorbacions estaven significativament associades amb la concentració de p-tau181, però no amb NfL.

Discussió: En aquesta tesi, composta per tres estudis, hem revelat nous biomarcadors candidats de la salut cerebral en el context de la resiliència mental, l'esquizofrènia i la malaltia d'Alzheimer en els seus estadis inicials. A més, això s'ha aconseguit utilitzant mètodes no invasius i potencialment escalables. Els biomarcadors candidats identificats revelen alteracions potencials de la transmissió sinàptica, arrelades en processos inhibitoris i excitatoris que, per tant, són potencialment modificables mitjançant mètodes no invasius d'estimulació transcranial elèctrica i magnètica.

Conclusions: Les conclusions de la tesi són les següents: 1) La resiliència en salut mental es pot modelar entenent-la com a la resposta del cervell a una pertorbació controlada que, a més a més, és predictiva de la potencial vulnerabilitat a estressors psicosocials futurs, tals com aquells associats a la pandèmia de la COVID-19. 2) Els algoritmes d'aprenentatge automàtic interpretable i el EEG durant tasques poden identificar dèficits inhibitoris en l'esquizofrènia, fins i tot quan el rendiment cognitiu es troba preservat. 3) Els marcadors d'excitabilitat cortical estan associats a les concentracions de p-tau en individus sans de mitjana edat, de manera coherent amb el paper presumpte de l'excitabilitat neuronal en la secreció de p-tau. 4) Per tant, el EEG

espontani i també el basat en pertorbacions ha revelat biomarcadors candidats no invasius de la salut cerebral que estan arrelats en la transmissió sinàptica inhibitòria i excitatòria.

CHAPTER 1. General Introduction

1.1. Brain Health challenges and biomarkers

The World Health Organization recently defined Brain Health as “the state of brain functioning across cognitive, sensory, social-emotional, behavioral and motor domains, allowing a person to realize their full potential over the life course, irrespective of the presence or absence of disorders” (Word Health Organization, 2022). Importantly, this definition underscores that brain health does not mean absence of disease, but rather that there is a potentially quantifiable set of factors that determine optimal cognitive, mental and social functioning, regardless of disease (Hachinski et al., 2021). This optimal state results from the continuous and dynamic interaction of individual and environmental factors across the lifespan; including genetic endowment, personality and life experiences, as well as a safe, healthy and positively engaging environment (Hachinski, 2023). This lifespan perspective, in turn, puts the accent on the cerebral determinants of neuronal development, adaptation, repair and compensation, as the brain grows and faces disease- and aging-related changes. This thesis is motivated by the timely and pressing need for scalable and potentially modifiable brain health biomarkers that are relevant for the early detection and neurophysiological understanding of the most globally prevalent disorders threatening it. Neuropsychiatric and neurodegenerative disorders stand as some of the most significant and prevalent threats to brain health. In our increasingly aging population, we have seen a sharp increase in the number of people affected by neurodegenerative diseases, such as Alzheimer’s and Parkinson’s disease, affecting over 7 million people in Europe alone. This figure is expected to double every 20 years as the population ages (Long et al., 2023). Alzheimer’s disease (AD) is the most prevalent neurodegenerative disorder and the leading cause of dementia and currently has no cure. Similarly, even before the coronavirus disease 2019 (COVID-19) pandemic, mental health problems affected around 20% of the population in the European Union (European Commission, 2023), and 970 million people worldwide (Word Health Organization, 2022). In the first year of the pandemic, estimates point to a 25% increase in the general prevalence of depression and anxiety symptoms (Bueno-Notivol

et al., 2021). Although effective treatments exist, around one in three patients with most prevalent disorders —major depressive disorder and schizophrenia— are treatment resistant (McIntyre et al., 2023; Mørup et al., 2020). Neurodegenerative and mental health disorders are, therefore, pandemics in their own right. Consequently, researchers and public health agencies around the world have been focusing their efforts not only in improving our understanding of these prevalent disorders to develop more effective treatments, but also on early detection and prevention strategies, to either halt or slow down disease onset and progression. In this context, it is crucial to develop early disease biomarkers that are capable of accurately predicting the risk of developing disease, while providing insights that are pathophysiologically relevant. Furthermore, the candidate biomarkers for preclinical early detection should rely on non-invasive, inexpensive, and readily available methods, if they are to be scalable to an early detection screening scenario (Abi-Dargham et al., 2023; Chimthanawala et al., 2023). In this context, electroencephalography (EEG) is a tool that can capture the electrical activity of the brain while fulfilling these scalability criteria. Indeed, the underlaying neurophysiopathology of mood disorders, schizophrenia and AD are closely linked to dysfunctions in electric synaptic transmission (Duman and Aghajanian, 2012; Howes et al., 2023; Pichet Binette et al., 2022), which further makes EEG a well suited method for biomarker discovery for these disorders. Furthermore, electric brain activity can be induced in a controlled and precise manner via transcranial electric and magnetic stimulation techniques, which can selectively recruit different neuronal elements and circuits, while also fulfilling the scalability criteria, for they are non-invasive, inexpensive, and already commonly available in research and clinical settings. Current technical advances make it possible to combine non-invasive brain stimulation and EEG, allowing the interference of the ongoing electrical activity of the brain and the capture of its direct response in real-time. Thus, by combining these methods, we can probe the implication and significance of specific neuronal circuits in the neurophysiology of disease. Importantly, electric synaptic transmission is plastic and directly regulated by excitatory and inhibitory processes, which can also be promoted via long-term depression- and potentiation-like mechanisms by these non-invasive stimulation techniques. This highlights the translational utility of these methods to reveal candidate biomarkers, that are also modifiable by these very same methods,

offering potentially disease-modifying interventions within the same methodological framework. Consequently, in this thesis we focus on the discovery of EEG candidate biomarkers for early detection of mental health disorders and AD. These biomarkers should also provide mechanistic insights on the neurophysiology of disease and be informative of new potential treatment targets using non-invasive brain stimulation, with the overarching goal of promoting and maintaining optimal brain health when facing disease.

1.2. Non-invasive capture and modulation of electric synaptic transmission

1.2.1. Physiological basis of EEG

As this thesis is focused on the discovery of EEG candidate biomarkers relying on synaptic transmission mechanisms, the findings and implications of the studies that form this thesis should be interpreted within the scope of what EEG can actually measure. EEG devices consist of a set of electrodes connected to a differential signal amplifier and digitization unit. Electrodes placed on the scalp record the electrical activity of the brain as a differential voltage signal reflecting the summation of postsynaptic potentials from tenths of thousands of synchronized pyramidal neurons (Figure 1. A; Buzsaki, 2006). Corresponding evidence from local field potential — electrodes inserted into the brain— research shows that scalp EEG reflects what local field potentials record, but spatiotemporally smoothed, due to the distortions and attenuations produced by the tissues the electric field must pass through before reaching the electrodes on the scalp; pia matter, cerebrospinal fluid, arachnoid space, bone and skin (Figure 1. B; Buzsáki et al., 2012). Therefore, only the summation of many synchronous individual extracellular field changes will be detectable at the scalp (Cohen, 2017). Local field potential recordings pick up the intra- and extracellular electric fields resulting from the superposition of all neuronal transmembrane currents generated by the movement of ions in and out of the membrane. Thus, the main contributor to these extracellular fields are synaptic currents generated by excitatory NMDA and AMPA neurotransmission at the synapse of the cell's soma and dendrites, which effectively cause depolarization of these cells. While GABA mediated inhibitory neurotransmission would be thought to add little to the extracellular field,

paradoxically, its action often causes depolarization of spiking pyramidal neurons until they hyperpolarize (Glickfeld et al., 2009), effectively yielding a significant contribution to the extracellular field. Therefore, EEG registers the spatiotemporally smoothed extracellular fields generated by the synchronous activation of many pyramidal cortical neurons, which is, in turn, regulated by afferent excitatory and inhibitory synaptic transmission.

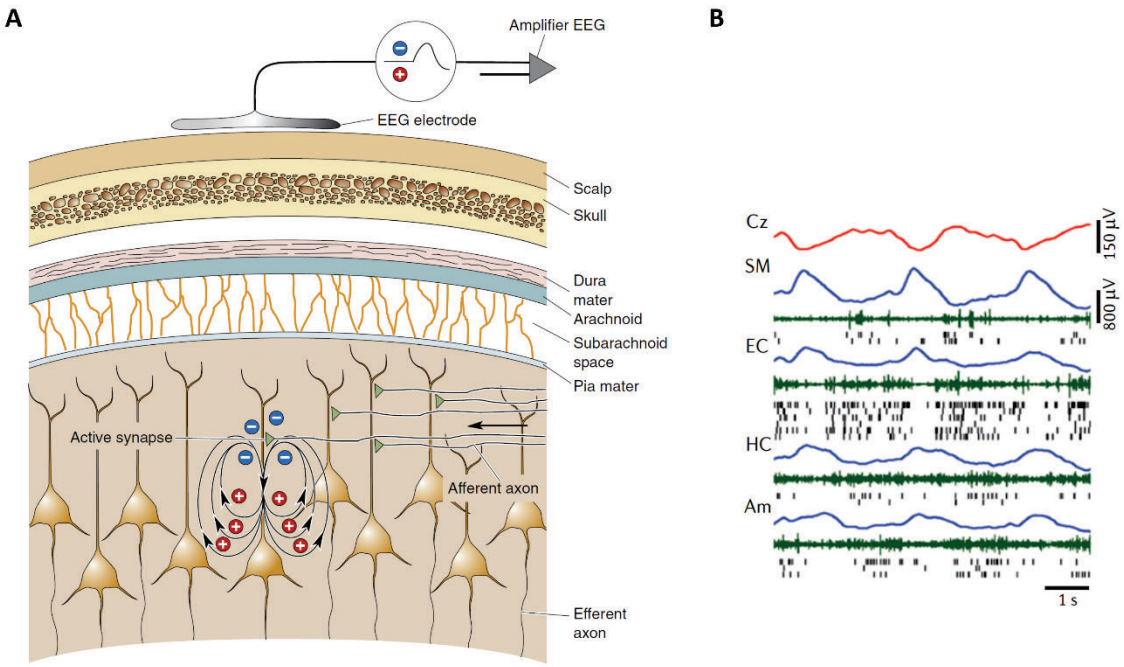

Figure 1. Basic physiological principles of EEG and correspondence with local field potentials. A) shows the extracellular field generated by an active synapse between a pyramidal cortical neuron and an afferent axon; as the electric activity must then pass though the different tissues separating the cortex from the electrode placed on top of the scalp, which then picks up the signal and send it to a diferential amplifier. B) shows a 6 second recording of slow EEG waves during sleep (in red), with the electrode placed on the scalp at the vertex (Cz), and the simultaneous local field potential recordings (in blue) from the supplementary motor area (SM), entorhinal cortex (EC), hypocampus (HC) and amygdala. The black dots show neuron activity spikes, while the green lines show multi-unit activity. A) was extracted from Bear et. al., (2020) and B) was extracted from (Buzsáki et al., 2012)

1.2.2. Transcranial electric and magnetic stimulation

Electric brain activity can be perturbed, modulated, or modified using non-invasive transcranial electric and magnetic stimulation (from now on TES and TMS, respectively), thus offering an additional avenue over EEG to further investigate synaptic transmission and potentially modify it. Therefore, given the translational focus of this thesis, which is aimed at candidate biomarker discovery that can also be informative of potential disease modifying interventions, here we offer a general overview of the non-invasive stimulation methods that will be referenced throughout the thesis.

The most ubiquitous TES technique in research and clinical practice is tDCS. In this technique, a low-amplitude direct electric current between 1 and 2mA in amplitude, is passed between two or more electrodes placed on the scalp, so that some of the current will pass not only through the path of least resistance (i.e., skin), but also through the brain. The effect of this current on the cortex is the increase or decrease (i.e., excitation or inhibition) of the neuronal resting membrane potential, thus modulating the firing likelihood of neurons. The direction of this membrane polarization effect is selectively modulated by the polarity of the stimulating electrodes, whereby a cathodal montage tends towards depolarization or excitation, while an anodal montage tends to promote hyperpolarization or inhibition (Figure 2. A; Lefaucheur and Wendling, 2019; Yamada and Sumiyoshi, 2021). Stimulation is usually delivered over a period of 20 to 30 minutes and its effects on cortical excitability can outlast stimulation for up to 120 minutes (Jamil et al., 2017). These plastic changes have been linked to long-term depression and potentiation (LTP and LTD, respectively) synaptic processes (Kronberg et al., 2017). By repeatedly delivering tDCS sessions over the course of multiple days, it is believed that the plastic changes become progressively more durable (Monte-Silva et al., 2013, 2010), lasting for days, or even months (Brunoni et al., 2012). This potentially cumulative effect is thought to be the basis of successful therapeutic applications of tDCS (Lefaucheur and Wendling, 2019). This method has the added advantage of being inexpensive, mobile and easy to use, making it a viable candidate for home-based therapeutic interventions (Silva-Filho et al., 2022).

TMS relies on the basic principles of electromagnetic induction (Faraday, 1832), to deliver electromagnetic pulses through a coil that, unlike tDCS, can induce an effective electric current on the axons and bodies of neurons causing them to depolarize (Barker et al., 1985). The intensity of a single TMS pulse, relative to the threshold from which effective pyramidal neuronal depolarization is induced, can be modulated to selectively target different neuronal populations; a subthreshold pulse will mostly affect afferent interneuron circuits, while near threshold stimulation will also recruit excitatory afferents, finally, suprathreshold stimulation will additionally directly depolarize pyramidal cortical neurons (Schmidt and Brandt, 2021). Thus, by pairing pulses (i.e., paired pulse TMS) at different intensities relative to the threshold and with different time intervals between them (ranging from 1ms up to 100ms), it is possible to probe the effect of a conditioning pulse on a suprathreshold stimulus test pulse, revealing the contribution of different interneuron circuits to the test stimulus (Cash and Ziemann, 2021). If pulses are repeated in succession for at least 30 minutes, it is possible to induce plastic changes akin to LTP and LTD of synaptic transmission that outlast stimulation for at least 30min (Pascual-Leone et al., 1994; Wagner et al., 2007). Repeated TMS (rTMS) at a frequency below 5Hz (typically 1 Hz) promotes inhibition of cortical activity, while frequencies above (typically 10, 15 or 20 Hz) promote excitability. For safety reasons, high-frequency protocols are typically delivered in trains with pauses in between (Rossini et al., 2015). A new generation of patterned rTMS protocols deliver bursts of gamma frequency pulse triplets (50 Hz) repeated at theta frequency (5 Hz), these protocols have thus been termed theta burst stimulation (TBS), and produce analogous effects to conventional rTMS protocols, but with a significantly shorter total stimulation durations of around 3 minutes (Huang et al., 2005a). The choice of gamma stimulation within theta cycles is grounded on observations of patterned neuronal firing in CA1 pyramidal hippocampal neurons in rats during spatial exploration, as well as in cell cultures, whereby LTP mediated plasticity was found to result from gamma bursts of spike activity at a theta frequency (Capocchi et al., 1992; Larson and Munkácsy, 2015). When TBS is delivered continuously, it promotes inhibition of cortical activity and when delivered in trains with a pause of 8 seconds in between, it promotes excitability (Figure 2. B). As with tDCS, when rTMS stimulation is repeated for several

sessions throughout multiple days, the plastic changes appear to become more durable, extending for days or even months after stimulation (Lefaucheur et al., 2014).

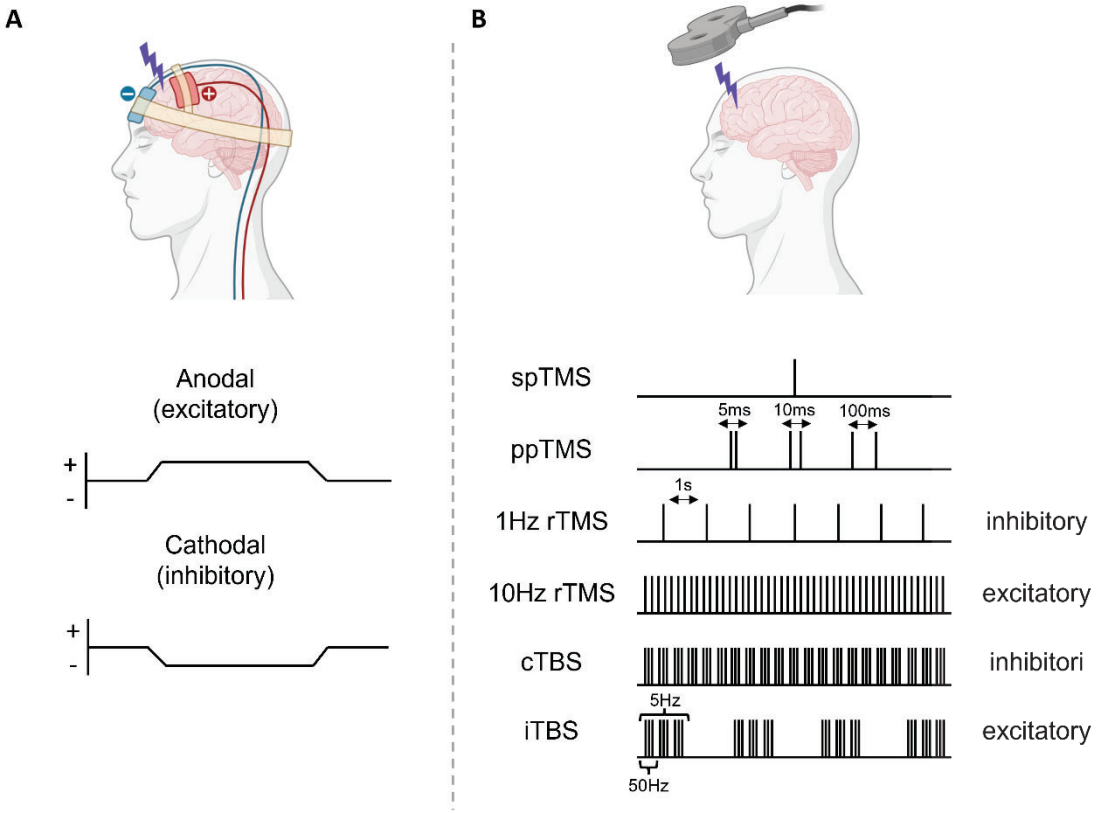

Figure 2. Illustration of A) tDCS and B) TMS protocols. Original figure created with BioRender.com.

Importantly, it has been shown that the effects of these non-invasive stimulation techniques propagate from the site of stimulation to other anatomically and functionally connected brain regions (Jog et al., 2023; Kabakov et al., 2012; Kearney-Ramos et al., 2018; Kunze et al., 2016; Ozdemir et al., 2020; Vink et al., 2018; Voineskos et al., 2010). This characteristic makes these methods suitable to study and potentially modulate brain connectivity patterns. Given the outlined capacity of TES and TMS techniques to induce plastic changes that outlast stimulation and propagate beyond the stimulation site, these methods have been extensively used to treat a great variety of neurologic and psychiatric conditions coursing with connectivity and inhibition/excitation imbalances, such as stroke, chronic pain, cognitive impairment, schizophrenia or major depressive disorder (Bhattacharya et al., 2022).

1.2.3. Concurrent TMS-EEG

The effects of TES and TMS on cortical excitability have been extensively studied on the primary motor cortex, as the output of the corticospinal tract can be reliably measured peripherally. For instance, single pulse TMS of the motor cortex induces the depolarization of cortical motor neurons, triggering action potentials that travel down through the corticospinal tract to the peripheral nerves until they reach the muscle fibers, consequently triggering a muscle contraction (Hallett, 2000). In this case, the brain response is thus indirectly measured at the targeted muscles (Figure 3; e.g., using electromyography).

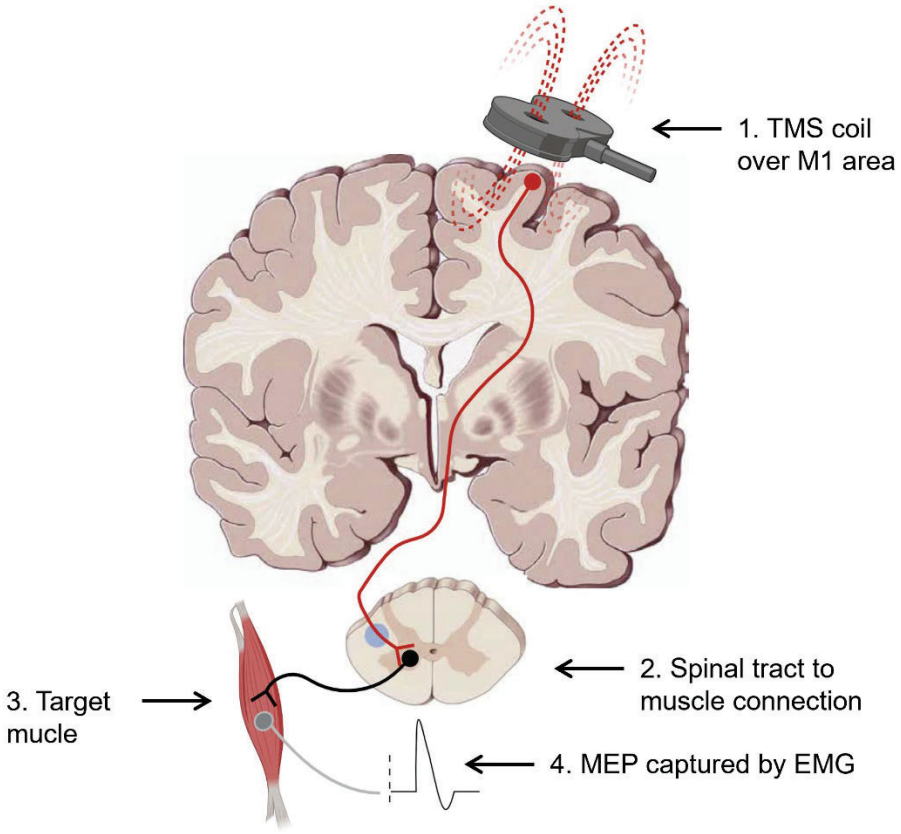

Figure 3. Simplified schematic of TMS stimulation of the primary motor cortex (M1) as it travels down the corticospinal tract and to the muscle, causing a motor contraction which can be captured as a motor evoked potential (MEP) using electromyography (EMG). Modified from Bear et al., (2020) with BioRender.com

The direct neuronal effects of stimulation can be captured with concurrent EEG during TMS (TMS-EEG). Single pulse TMS has been shown to induce stable and

reproducible cortical responses (Ozdemir et al., 2021a, 2021b), termed TMS-evoked potentials, that reflect the dynamic shifts in the inhibition/excitation balance in cortical circuits, with its different peaks and troughs reflecting the contributions of different neurotransmission systems (Belardinelli et al., 2021; Darmani et al., 2016; Ghazaleh Darmani et al., 2019; Du et al., 2018; Ferrarelli et al., 2010; I Premoli et al., 2014; Isabella Premoli et al., 2017, 2014; Salavati et al., 2018; Sarasso et al., 2015; Ziemann et al., 2015), throughout the time-course of the brain response to the TMS pulse, which lasts up to 300ms after the pulse (Figure 4).

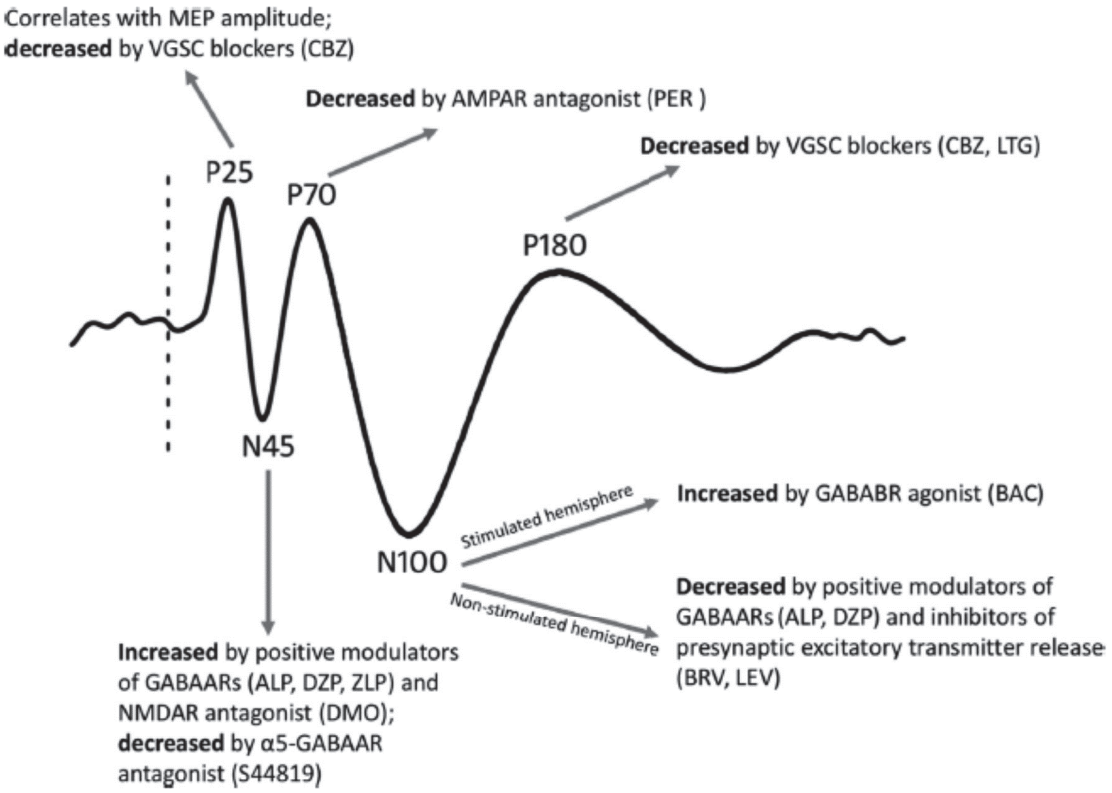

Figure 4. Schematic of the pharmaco-physiological mechanisms of TMS evoked EEG potentials after single-pulse TMS of the primary motor cortex. The dashed vertical line represents the time of the TMS pulse (0ms). The peaks and troughs are labeled ‘P’ and ‘N’, respectively, followed by the approximate time in milliseconds at which they typically occur. ALP, alprazolam; BAC, baclofen; BRV, brivaracetam; CBZ, carbamazepine; DMO, dextromethorphan; DZP, diazepam; LTG, lamotrigine; LEV, levetiracetam; PER, perampanel; ZLP, zolpidem. Extracted from Darmani et al., (2019).

1.3. Biomarkers of mental health resilience during the COVID-19 pandemic

1.3.1. The mental health impact of the COVID-19 pandemic

Mental health has long been one of the main public health challenges, but its relevance and impact were brought into a bright focus after the severe acute respiratory syndrome coronavirus 2 outbreak gave rise to the COVID-19. As cases surged worldwide and healthcare systems faced immense pressure and collapse, on March 11th of 2020 the WHO declared COVID-19 a pandemic. To try and contain the spread of the virus, most governments enforced drastic measures, such as lockdowns, travel bans, social distancing measures and quarantines, with unprecedented societal and economic consequences. As a result of the fear of the pandemic and the psychosocial stress produced by the enforced measures, the prevalence of depression and anxiety increased globally by 25% in 2020. As illustrated in Figure 5, Santomauro et al., (2021) reported an additional 53.2 million new cases of major depressive disorder and 76.2 million cases of anxiety that were directly caused by the psychosocial stressors produced by the pandemic, with and uneven impact across age groups and gender; younger people and females being hit the hardest.

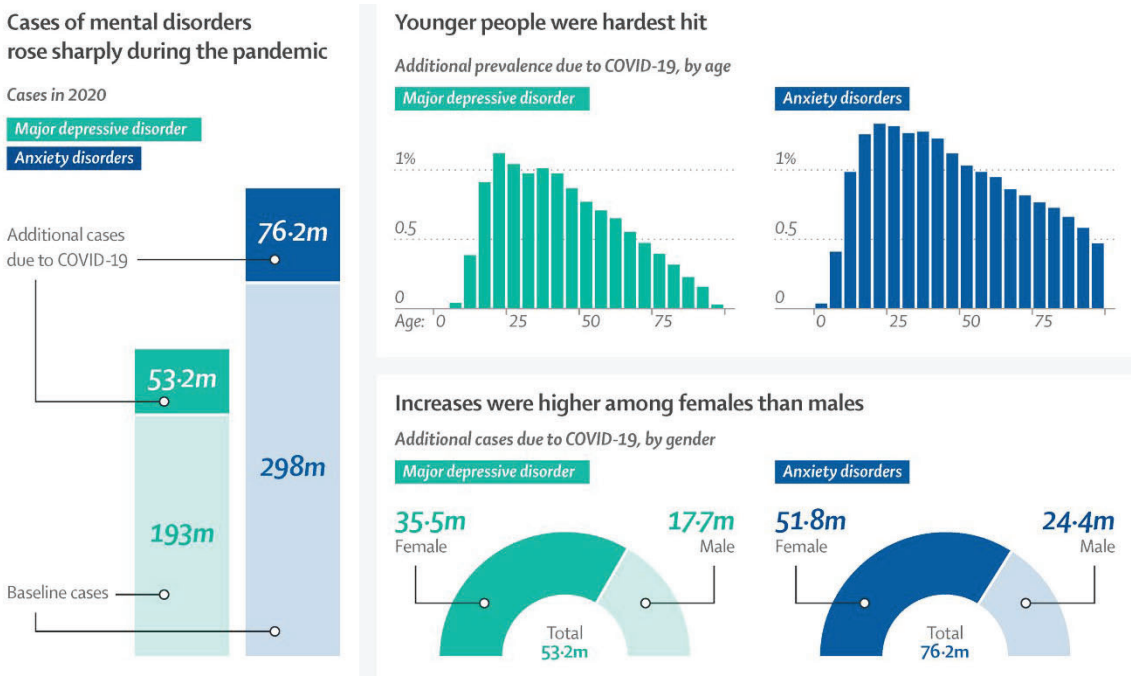

Figure 5. Increased prevalence of major depressive and anxiety disorders in 2020 as a direct result of the COVID-19 pandemic. Adapted from Santomauro et al., (2021).

While the pandemic had a global overall negative impact on mental health, when confronted with similar stressors or insults, individuals exhibit varying degrees of vulnerability; some may experience more pronounced negative effects, while others, owing to their inherent “resilience”, demonstrate minimal or no impact and may even thrive in the face of adversity (Pascual-Leone and Bartres-Faz, 2021).

1.3.2. Mental health resilience

Pascual-Leone and Bartres-Faz (2021) recognized that the concept of resilience is highly heterogeneous, with its definition changing across different disciplines and fields of study. In this thesis, we adhere to the general definition proposed by the authors that resilience is essentially a homeostatic mechanism, whereby an organism is able to cope with a given stressor by either resisting it or adapting to successfully compensate its impact. In this definition the stressor can be acute or chronic, psychological or physical, and internal or external in origin. Importantly, in this definition, resilience is a capacity that can be present both in health and in the presence of disease. Within this framework, in the particular case of mental health, resilience comprises the mechanisms that help an individual avoid developing illnesses, mental health issues, or distress when faced with stressful or traumatic situations (Moore et al., 2020; Russo et al., 2012). In this context, resilience is contraposed to psychological vulnerability, which refers to a diminished capacity to manage stressors and is considered a predisposing factor for psychopathological conditions (Wright et al., 2013). However, resilience and vulnerability are not simply opposites but rather represent two extremes of a spectrum. This spectrum is believed to be the dynamic result of complex interactions between individual and contextual factors (Cathomas et al., 2019; Rutter, 2012; Tost et al., 2015). Such factors include genetic makeup, demographic characteristics, socio-economic background, early developmental experiences, access to healthcare, living conditions, adherence to certain lifestyle behaviors (like cognitive, physical activities, nutritional choices, and sleep patterns), participation in emotion-regulation strategies such as meditation, the quality of social connections and early support, and educational attainment (Campbell-Sills et al., 2009; Frankish and Horton, 2017; Gelfo et al., 2018; Livingston et al., 2017; Di Marco et al., 2014).

Resilience in the context of mental health has also been shown to rely on a specific neurophysiological substrate (Cathomas et al., 2019; Russo et al., 2012). Research involving animal subjects and human neuroimaging has identified several brain regions and functional networks that are likely significant in determining resilience and vulnerability to mental health disorders. These discoveries are heavily grounded in the concept of 'functional brain networks', which is the result of decades of research made possible by functional magnetic resonance imaging (fMRI), a neuroimaging technique that detects changes in the blood-oxygen level dependent signal, with the assumption that increased blood flow indicates increased neural activity in a given brain region (Biswal et al., 1995). This approach to understanding brain function represented a major paradigm shift from the classical model that considered brain function as arranged in discrete modules corresponding to isolated brain regions (Brodmann, 1909; Fodor, 1983). Instead, fMRI revealed that brain activity is rather distributed across interconnected groups of brain regions that form networks working in synchrony to support brain function (Biswal et al., 1995; Raichle et al., 2001), furthermore, these networks are themselves connected with one another and balance each other in a dynamic manner (Rubinov and Sporns, 2010). Therefore, the resulting picture of brain functional organization looks more like a complex and dynamic interplay of juxtaposing systems whereby the whole brain is interconnected and recruitment of neural resources for a particular function takes the form of balance shifts between such networks (Hansen et al., 2015; Menon and Uddin, 2010). While still an evolving field it is generally recognized that there are at least seven fundamental functional networks in the adult human brain supporting basic processes subtending cognitive function (Figure 6; Thomas Yeo et al., 2011).

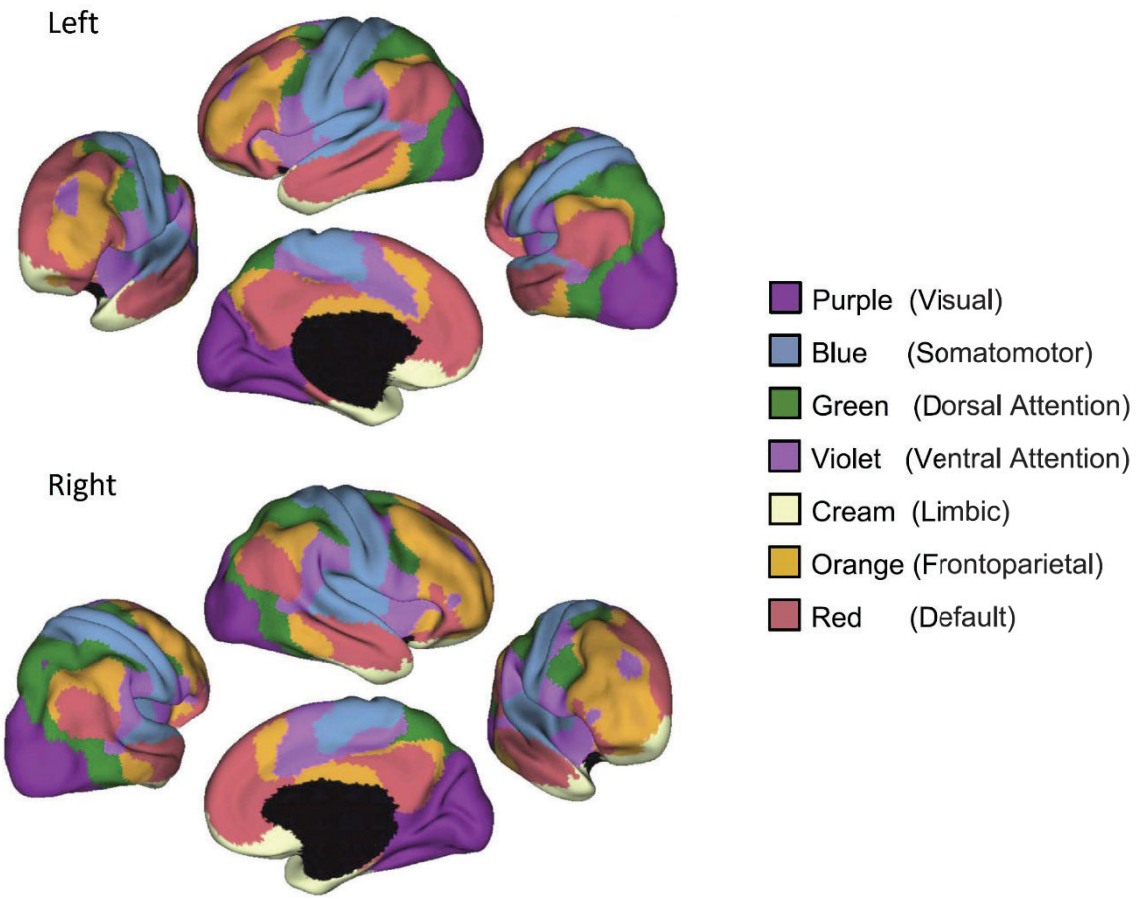

Figure 6. Seven-functional network parcellation of the human cerebral cortex based on 1000 subjects. Extracted form Yeo at al., (2011)

In the field of psychological resilience, functional and structural neuroimaging research consistently highlights, both cortical and subcortical structures implicated in stress response and emotional regulation, including the amygdala, insular, anterior cingulate and prefrontal cortices (Kong et al., 2015; Waugh et al., 2008). Furthermore, large-scale functional systems associated with these regions have also been found to relate to psychological resilience, particularly the relative activity between three functional networks implicated in higher-level cognitive functioning and emotional processing, the default mode network (DMN), the salience network (SN, also known as ventral attention network) and the frontoparietal control network (FPN; Cathomas et al., 2019; van Oort et al., 2017; Watanabe and Takeda, 2022).

A singular cortical structure, that is part of the FPN, the left prefrontal cortex, is recognized as a key player (Maier and Watkins, 2010; Varela et al., 2012), with its size,

activity, and connectivity with limbic areas being positively associated with resilience to trauma and adverse childhood events (Bolsinger et al., 2018). Furthermore, longitudinal fMRI studies have observed that children who effectively manage the amygdala's emotional reactions through the FPN are more resilient to depression after maltreatment (Rodman et al., 2019). The role of prefrontal function extends to the pathophysiology and management of psychiatric disorders, especially major depressive disorder (Hare & Duman, 2020 or Pizzagalli & Roberts, 2022) and schizophrenia (Dienel et al., 2022; Smucny et al., 2022). Lastly, the prefrontal cortex is not just central to psychological resilience and psychiatric disorders but is also suggested as a key area for cognitive resilience during normal aging and in relation to brain deterioration and pathology in AD (Ewers et al., 2021; Franzmeier et al., 2018, 2017; Neitzel et al., 2019). While the neural substrate of resilience is likely distributed throughout several brain networks and regions, given its transversal implication across the resilience spectrum, it is plausible that the prefrontal cortex is a central node that serves as their anchor. This anchor is also likely a key mediator of the positive influences of developmental, environmental, and socioeconomic factors (Pascual-Leone and Bartres-Faz, 2021).

1.3.3. A toy model of brain resilience

The recognition that resilience serves as a fundamental defense for mental health when facing stressors (Feder et al., 2019), underscores the importance of comprehending its determinants and neurophysiological underpinnings. This understanding is crucial for fostering resilience as a proactive measure to prevent the onset of mental health disorders. In this context, global psychologically stressful events such as the pandemic and associated lockdowns provide an unprecedented opportunity to elucidate the neuropsychological factors and inherent neurophysiological mechanisms that contribute to either resilience or vulnerability.

We have seen that the neural substrate of resilience is a complex phenomenon resulting from the interaction of many internal and external factors. However, it is possible to study complex systems by building on a simplified model first. This idea is well stablished in theoretical physics, where ‘toy models’ refer to simplified models of more complex phenomena that can however be used to provide a quantitative

explanation and make reliable predictions (Georgescu, 2012; Marzuoli, 2008). To achieve this, we can draw inspiration from the animal studies on the neurophysiological substrate of resilience that employ stimuli that can be precisely quantified and controlled, for example using tail-shock stress paradigms (Seligman et al., 1975), in which a mild electric shock is given to the tail of rats or mice. This paradigm was used, among others, to establish the mechanism of 'learned helplessness', whereby, after being exposed to uncontrollable stress, an animal will be unable to escape from subsequent aversive situations, even when it has control over them (Landgraf et al., 2015). Similarly, TMS can be used to induce precisely controlled and transient perturbations of brain activity *in vivo* in awake humans on a specific brain location, and the reaction of the brain can then be captured in real-time with concurrent EEG. This makes the basis for a toy-model: we can induce a controlled perturbation of a region found to be part of the neurophysiological substrate of resilience — the prefrontal cortex— and measure the brain response profile of a given individual to this perturbation, as if it were a stressor or insult the brain must cope with. Then we can evaluate how the TMS-EEG response profile correlates with resilience or vulnerability to an event such as the COVID-19 pandemic or in the presence of diseases such as schizophrenia or AD.

1.4. Biomarkers of cognitive disfunction in schizophrenia

1.4.1. The heterogeneity problem in psychiatry and schizophrenia

It is a common issue in psychiatry that a particular disorder may be caused by a different set of causal mechanisms, moreover, clinical manifestation is also variable across individuals with apparently similar pathophysiological conditions; meaning, there is no clear necessary conditions to be meet for a disease to develop with a particular set of symptoms. Thus, psychiatric diagnosis, treatment and management are 'heterogeneous' in nature and, therefore, challenging (Feczko et al., 2019). A Disease that has been recognized as particularly heterogeneous in psychiatry is schizophrenia (Wolfers et al., 2018).

Schizophrenia is a serious and disabling mental health condition with a worldwide occurrence of approximately 0.28% (Charlson et al., 2018), that leads to

considerable social and economic impacts. Moreover, around 30% of patients are treatment resistant at some point during the disease (Mørup et al., 2020). Its symptoms are categorized into two main categories: positive symptoms such as hallucinations, delusions, and disorganized thought processes, and negative symptoms including reduced emotional expression, withdrawal from social interactions, and cognitive deficits affecting memory and decision-making abilities (Batinic, 2019; Mosolov and Yaltonskaya, 2022). It is a neurodevelopmental disorder believed to originate from a combination of genetic predispositions and early environmental influences (Van Os et al., 2010; Robinson and Bergen, 2021; Seidman and Mirsky, 2017), which disrupt the brain's development and result in compromised functional brain network connectivity (Howes and Shatalina, 2022; Liu et al., 2021) and abnormal brain activity (Anticevic et al., 2015a, 2015b). The underlying mechanisms may involve changes in dopamine, GABA and glutamate neurotransmission, leading to an imbalance between excitatory and inhibitory signals within brain circuits that ultimately affects the synchronization of brain oscillatory activity (Hirano and Uhlhaas, 2021). Despite over one-hundred years after the term was first used and a growing body of research on all aspects of the disease, our understanding and treatment of schizophrenia has not advanced enough to provide effective interventions for this largely developmental disorder. This lack can be attributed, at least in part, to the inherent difficulties in diagnosing the disease in the first place, owing to the heterogeneity of its pathophysiology (Alnæs et al., 2019; Wolfers et al., 2018) and clinical manifestation (Bosia et al., 2019; Dollfus and Brazo, 1997). This led to diving the disease into an ever-growing number of subtypes, and the inevitable conclusion that schizophrenia is a spectrum disorder (for a historical overview see Jablensky, 2010) covering a variety of genetic and neurophysiological abnormalities, and clinical symptoms.

1.4.2. Neuroimaging and EEG correlates of schizophrenia

Decades of neuroimaging research on the neurophysiological underpinnings of schizophrenia lead to the identification of several brain abnormalities associated with schizophrenia, these include macroscopic structural brain changes, and most consistently, alterations in synaptic microstructure and metabolism. The most

consistent findings in structural magnetic resonance imaging of schizophrenia —when compared to healthy controls— are decreased grey matter volume and density (Kuo & Pogue-Geile, 2019) and cortical gyrification (Sasabayashi et al., 2021), which indexes the ratio of the length of the folded cortical contour to the length of the outer brain surface (Zilles et al., 1988). At the level of synapse, abnormalities have been reported regarding density and metabolism. Common findings include decreased synaptic density, which can be measured by-proxy from synaptic vesicle protein 2A (SV2A) using positron emission tomography (PET), and has been shown to be decreased in patients with chronic schizophrenia compared to matched controls (Onwordi et al., 2020; Radhakrishnan et al., 2021), as well as microstructural abnormalities measured by neurite orientation and density imaging, which has been reported to be decreased in schizophrenia patients when compared to healthy controls (Kraguljac et al., 2023; Nazeri et al., 2017). Metabolic abnormalities include reduced levels of N-acetylaspartase (Onwordi et al., 2020; Radhakrishnan et al., 2021), measured using magnetic resonance spectroscopy, as well as reduced glucose reuptake during resting state (Townsend et al., 2023), measured using fluorodeoxyglucose-PET. Nevertheless, these findings are not always consistent across studies, possibly owing to the variability in the disease subtypes sampled and methods used. Moreover, the candidate biomarkers with higher sensitivity to detect the most specific synaptic abnormalities in schizophrenia are expensive and require exposure to radioactivity (Figure 7; Howes et al., 2023).

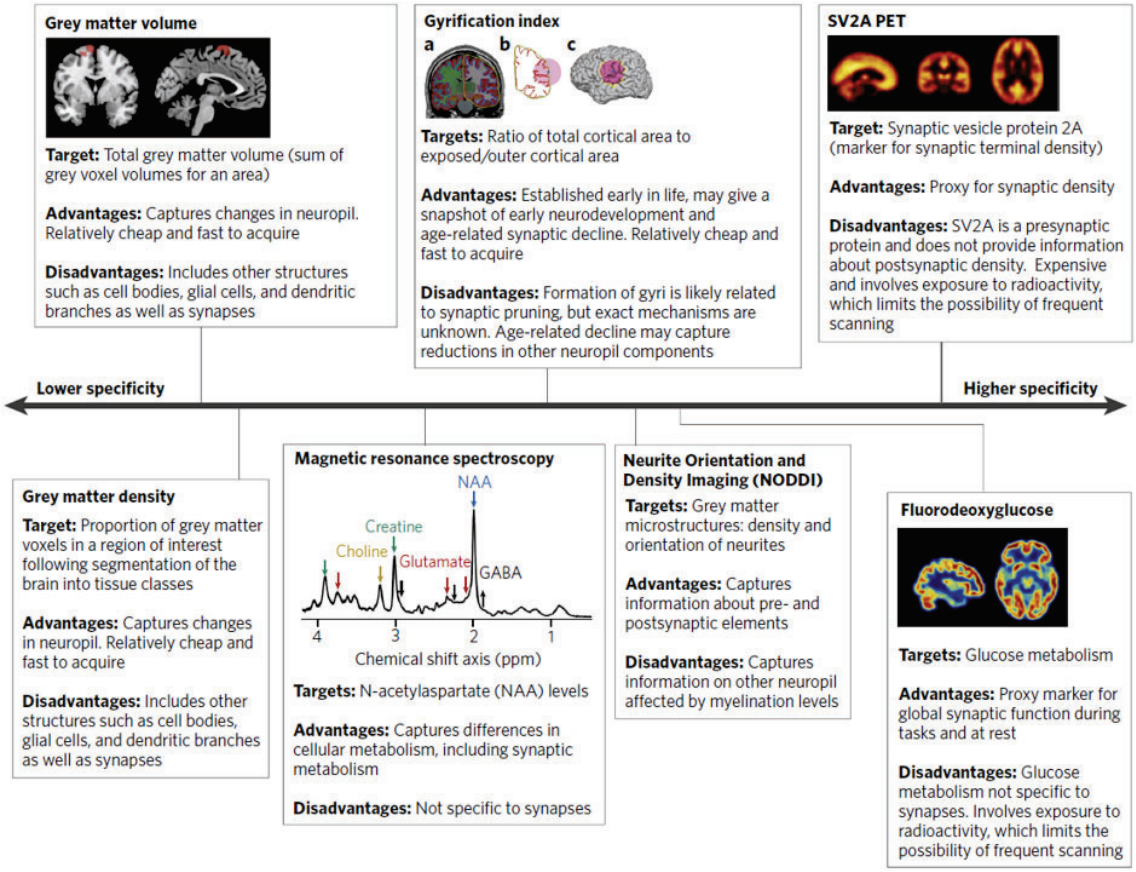

Figure 7. Schematic of neuroimaging abnormalities reported in schizophrenia, with an emphasis on the advantages and disadvantages of each method regarding its specificity to detect synaptic disfunction. Extracted from Howes et al., (2023).

The reviewed structural and synaptic abnormalities constitute the pathophysiological substrate for the functional brain abnormalities reported in an ample body of research using resting and task-based fMRI in schizophrenia research. Research during resting state fMRI most consistently report abnormalities in the SN (Menon and Uddin, 2010; Palaniyappan and Liddle, 2012) and DMN networks (Hu et al., 2017), and thalamocortical dysconnectivity (Chen et al., 2020; Ramsay et al., 2023; Wei et al., 2022), when compared to healthy controls. Another common finding is overall decreased connectivity or brain synchrony, which has been attributed to GABAergic interneuron disfunction in schizophrenia (Pujol et al., 2023). While for task-based fMRI, a recent metanalysis by Picó-Pérez et al., (2022), most consistently identified decreased activation of the dorsomedial prefrontal cortex, the

supplementary motor area, and the right inferior frontal gyrus, when compared to healthy controls.

These methods have provided crucial insights on the neurobiology of schizophrenia and constitute valuable candidate biomarkers. However, findings are often inconsistent across studies (Dabiri et al., 2022; Howes et al., 2023; Picó-Pérez et al., 2022), and the methods used are expensive and may involve exposure to radioactivity. Therefore, these candidate biomarkers are inevitably restricted to research settings. EEG on the other hand, is a cheaper, more practical, thus, potentially clinically scalable method. An ample body of research on differential diagnostic of schizophrenia and prediction of transition to psychosis, has identified several resting state and task-based EEG correlates. The most consistent findings across EEG studies targeting the frequency domain include abnormalities in alpha (Trajkovic et al., 2021) and gamma (Reilly et al., 2018) oscillations. Alpha rhythms (between 8 to 12Hz), constitute a dominant frequency in the human brain mediating long-range and thalamocortical connectivity (Scheeringa et al., 2012), as well as inhibition and gating processes related to attention, resource allocation and inhibition of task-irrelevant brain regions (Jensen and Mazaheri, 2010; Klimesch, 2012). A recent metanalysis of resting state alpha power differences between patients with high and low risk for transition to psychosis found that those at high risk had significantly lower alpha power and peak alpha (i.e., alpha slowing) —the frequency at which alpha band peaks in the power spectrum— at the right frontoparietal control network. Similarly, resting state studies comparing patient and healthy controls found consistently decreased alpha power and peak alpha at frontal, parietal and temporal cortices (Begré et al., 2003; Murphy and Öngür, 2019; Pascual-Marqui et al., 1999; Ramyead et al., 2016). Gamma band oscillations (between 30 and 100HZ) have been shown to be generated by the synchronized activation of cortical pyramidal neuronal assemblies (Fries et al., 2007; Womelsdorf et al., 2007) which is mediated by parvalbumin-positive GABAergic interneurons (Bartos et al., 2007), and are therefore fundamental in cortico-cortical communication supporting general cognitive functioning (Fries, 2009; Roux et al., 2012). Resting state studies comparing schizophrenia patients with healthy controls consistently find increases in gamma power, most prominently over the frontal cortex

(Ramyead et al., 2016, 2015; Tikka et al., 2014). During tasks, the most consistent findings also include abnormalities in the alpha and gamma bands. Specifically, event related studies find decreased desynchronization of alpha, particularly during events related to inhibition of distractors, possibly indicating an attentional inhibitory deficit (Boudewyn and Carter, 2018; Kayser et al., 2014). In the gamma band, studies most consistently report decreased evoked and induced power throughout a variety of cognitive tasks in patients after a first psychotic episode or at high risk of developing psychosis (Reilly et al., 2018), also pointing at inhibitory deficits. Another group of EEG abnormalities in schizophrenia comes from event-related potential (ERP) studies, which most consistently report impairments in the sensory gating-related P50 (Atagun et al., 2020) and N100 (Rosburg, 2018) ERP components, as well as amplitude reductions in memory- and attention-related mismatch negativity (Erickson et al., 2016) and P300 (Qiu et al., 2014) ERPs.

1.4.3. Working memory deficits in schizophrenia

Among the heterogenous landscape of symptoms in schizophrenia, perhaps the most consistent core cognitive impairment affects working memory (WM), which has been found to be strongly predictive of functional outcome and prognosis (Chan et al., 2000; Fu et al., 2017; Gold et al., 2019; Jenkins et al., 2018) an might be an early indicator for transition into psychosis (Tao et al., 2023). WM is typically described as a system with a limited capacity for temporarily holding and manipulating information needed for complex, goal-oriented behaviors such as understanding, learning, and reasoning (Baddeley, 2010; D'Esposito and Postle, 2015) and it depends on and interacts with other cognitive processes, including attention and executive function (D'Esposito and Postle, 2015; Luck and Vogel, 2013). It has been shown that schizophrenia patients exhibit widespread deficits across various WM subprocesses and modalities (Luck and Vogel, 2013), including issues with proactive cognitive control, which involves maintaining goal-related information in WM to influence behavior (Barch and Ceaser, 2012), and unusually concentrated and intense attentional focus of processing resources (Luck et al., 2019). Even among high-functioning patients with generally intact WM capabilities, inconsistencies like increased variability in

reaction times have been reported (Rentrop et al., 2010a), suggesting subtle information processing impairments.

1.4.4. Data-driven diagnostic and patient classification in schizophrenia

While the body of research outlined in the previous sections has brought us closer to understanding the neurophysiology of schizophrenia and its cognitive impacts —owing to the proverbial heterogeneity problem— they had limited translation in the improvement of differential diagnostic and the development of novel treatment strategies. With the growing advances in artificial intelligence, the field of psychiatry has recently turned to machine learning to progress in these areas. This move is partly motivated by the limitations posed by conventional univariate statistical methods, which are suitable for group-level distinction of patients from controls or patient subgroups, but fall short in differential diagnostic at the individual level (Scangos et al., 2023).

Machine learning is a subset of artificial intelligence where algorithms learn from and make decisions based on data. Unlike traditional programming, where rules are explicitly coded, machine learning algorithms build a model from sample data or experience to predict or decide without explicit programming. Classic machine learning models include linear regression, where a linear equation is fit to observed data to predict a continuous output (Galton, 1886); decision trees, which split the data into smaller subsets based on feature values, creating a tree-like structure of decisions that lead to predictions or classifications (Quinlan, 1986); and K-nearest neighbors, which classify a data point based on how its 'k' nearest neighbors in the feature space are classified (Kaplan and Meier, 1958). Modern and more complex machine learning algorithms are becoming popular tools in precision psychiatry research to enhance diagnostic differentiation at the individual level. Particularly, support vector machines, which can classify high-dimensional data (i.e., when the number of features is greater than the number of observations) by finding the best boundary (or hyperplane) that separates data points in a given dataset into classes or subsets (Cortes and Vapnik, 1995); deep neural networks (DNNs), that mimic the human brain’s interconnected neuronal computations to learn hierarchical representations of the input data

(Rumelhart et al., 1986); and convolutional neural networks (CNNs), which are DNNs specialized in finding spatial hierarchies and patterns in input data that has the shape of a matrix or grid (e.g., images; Krizhevsky et al., 2012), which makes them particularly well suited for neuroimaging.

Recent studies have demonstrated the use of machine learning using neuroimaging data in patients with schizophrenia to distinguish patients from controls and patient subtypes with notable accuracy, using variations of the algorithms described above (for a recent review see Cortes-Briones et al., 2022). A limited number of this studies have used EEG data alone, either during resting state (Phang et al., 2020; Ruiz De Miras et al., 2023; Shim et al., 2016; Shoeibi et al., 2021; Sun et al., 2021) or during working memory (Johannesen et al., 2016) or oddball tasks (Shim et al., 2016), showcasing unprecedented potential for clinically applicable diagnostic enhancements. However, while efficient in classification, these algorithms pose one major drawback, they are 'black-boxes', due to the opaque manner in which they process input data to produce specific outcomes (Sheu, 2020). This means that the potentially neurophysiology revealing features in the data that led to a successful classification remain hidden. As a result, there's a growing demand for more transparent and interpretable deep learning models (Barros et al., 2021).

One promising solution is the revolutionary concept of the self-attention mechanism, as outlined in the influential paper by Bahdanau, Cho, and Bengio (2015). Originally developed for machine language processing and generation, this mechanism allows inputs to interact with each other (i.e., each word in a sentence can look at other words) and weigh their influence on the model's output. This was a major shift from previous models that processed inputs sequentially. The mechanism mimics how human visual perception works. For example, when looking at a scene containing a salient feature, such as a lion in the jungle, traditional CNN models would first extract texture and structural features and then generalize them to a semantic level, while a human might spot the lion at first glance. Another crucial feature of models incorporating the attention mechanism is their interpretability; the network's attention layers provide a probability distribution over the input space, offering insights into the

network's internal operations by directly mapping the relative importance of each feature in reaching a decision or performing a classification to the input space (de Santana Correia and Colombini, 2022; Škrlj et al., 2020).

Therefore, by leveraging modern machine learning algorithms that incorporate the attention mechanism and are intrinsically interpretable, we can target one of the most consistent symptoms of schizophrenia —working memory impairment— using a well stablished and sensitive experimental paradigm, the visuospatial change detection task. By relying on inexpensive and potentially scalable methods like EEG, we can produce a diagnostic enhancement that is clinically usable for discriminating between patients at an individual level. Finally, these methods might provide insights into the neurophysiological mechanisms behind the impairment.

1.5. Biomarkers of cortical excitability and protein pathology in AD

1.5.1. The pathophysiology of Alzheimer's disease

Alzheimer's disease (AD) is a slowly progressing neurodegenerative disease with no effective treatment that affects an estimated 10% of people older than 65 years of age, with an estimated 50 million people worldwide currently living with the disease. The majority of AD cases have a late onset at 65 years or older and prevalence increases with age and depending on biological sex; at age 85 and older at least 30% of people have AD and, regardless of age of onset, woman are more prone to develop AD than men (Figure 8), according to the latest estimates (Gustavsson et al., 2023; Rajan et al., 2021). With the increase in life expectancy over the last century the number of people suffering from AD has increased exponentially (Valenza and Scuderi, 2022), and it is projected to triple by 2050 as population grows and ages (Nichols et al., 2022).

AD has been described as a continuum (Jack et al., 2018), since its time course spans several decades, and pathological molecular brain changes begin as early as 20 years before the apparition of first symptoms (Montine et al., 2012). AD is believed to be caused by the confluence of aging, environmental influences, cardiovascular, genetic and lifestyle risk factors (Breijyeh and Karaman, 2020). In the early stages, the gradual accumulation of misfolded amyloid-beta (Aβ) protein forms plaques in the

extracellular space, triggering the secretion and increased deposition of soluble phosphorylated tau (p-tau) protein, which then forms insoluble and toxic neurofibrillary tangles intracellularly, ensuing neurodegeneration and the onset of cognitive symptoms as pathology spreads throughout the brain (Jack and Holtzman, 2013). The mechanisms of spread are poorly understood, but recent research has shown that tau pathology has an initial epicenter at the temporal cortex that will then spread through anatomically and functionally connected regions until reaching a plateau in the late stage of AD (Pichet Binette et al., 2022; Steward et al., 2023), at which point dementia will often be evident. See Figure 8 for a timeline of the AD hallmark events described.

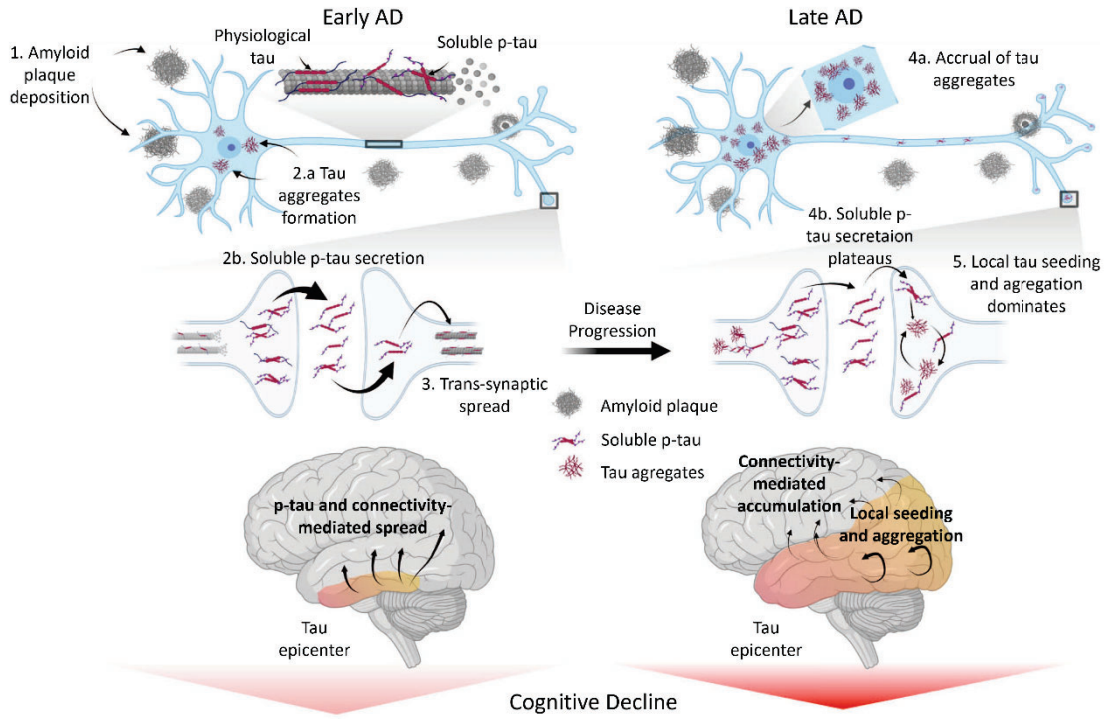

Figure 8. Schematic model of tau pathology accumulation and spread throughout the course of Alzheimer's disease. Adapted from Binette et al., (2022).

1.5.2. Biomarkers for early detection of Alzheimer's disease

Currently, the most stablished biomarkers for AD detection and disease progression monitoring include the proteins implicated in the pathogenesis of the disease. Early disease biomarkers include Aβ and tau concentrations measured in cerebrospinal fluid (CSF) via lumbar puncture, as well as Aβ using PET. These markers

can detect AD in the preclinical stage, years before the onset of symptoms (Hansson, 2021). As first symptoms appear, often in the form of mild cognitive impairment (MCI), Aβ and tau pathology will have already spread throughout the brain and caused significant neurodegeneration, therefore, increased tau concentrations become detectable in PET imaging (Ossenkoppele et al., 2016) and significant concentrations of neurofilament light (NfL; Gaetani et al., 2019) —which is released as a byproduct of neuroaxonal injury (Gaetani et al., 2019)— are detectable in CSF, while widespread synaptic dysfunction can be detected at this stage as increased neurogranin concentrations in CSF, which is a postsynaptic protein involved in long-term potentiation and synaptic plasticity (Portelius et al., 2015). Due to neurodegeneration, brain volume reductions can also be detected using magnetic resonance imaging (Frisoni et al., 2010). As the disease progress into its late-stage with severe cognitive impact and dementia, brain wide synaptic dysfunction will be detectable by PET imaging of the SV2A, which assesses synaptic density (Carson et al., 2022), and fluorodeoxyglucose PET, which asses glucose metabolism (Chételat et al., 2020). Finally, astrocyte activation and degeneration can be assessed by the YKL-40 neuroinflammation biomarker in CSF (Craig-Schapiro et al., 2010).

The reviewed biomarkers are correlated with the different pathophysiological stages of AD and can detect AD years before symptoms onset. However, owing to their costly and invasive nature, they are not ideal candidates for early pre-clinical population screening, which would allow detecting individuals at risk of developing the disease early on. However, a new generation of blood-based biomarkers for measuring Aβ, p-tau and NfL concentrations have been recently developed and found to correlate with the more stablished CSF and PET biomarkers (Blennow et al., 2010; Mattsson-Carlgren et al., 2023; Simrén et al., 2021; Teunissen et al., 2022). Given their relatively lower cost and non-invasive nature, these are better candidates for early population screening.

1.5.3. The role of cortical excitability in Alzheimer's disease

While the hallmark pathophysiological events that occur throughout the course of AD have been consistently described, and we have a broad range of biomarkers that

correlate with them, we lack an understanding about the links in this chain of events. A crucial missing link is the mechanism by which Aβ pathology leads to the increased deposition of hyperphosphorylated tau. Research in mouse models of AD and cell cultures consistently shows that even before Aβ plaque formation, the introduction of extracellular soluble Aβ, triggers hyperexcitability in hippocampal CA1 pyramidal neurons (Busche et al., 2012, 2008). While administration of γ-secretase inhibitors, which reduces soluble Aβ levels, restores neuronal activity to control levels (Busche et al., 2012; Ghatak et al., 2019). Further *in vivo* research in mice has shown that neuronal activation promotes and enhances tau secretion in the post-synaptic neuron (Pooler et al., 2013; Schultz et al., 2018; Wu et al., 2016; Yamada et al., 2014). Thus, trans-synaptic activation promoted by soluble Aβ is a candidate mechanism for the secretion and propagation of tau pathology. While the specific mechanisms are poorly understood (Targa Dias Anastacio et al., 2022), it has been proposed that the presence of soluble Aβ can form ionic pores in the neuronal membrane (Arispe et al., 1993; Ho et al., 2001), thereby increasing Ca^{2+} influx, and reduce the expression of voltage-gated potassium channels, while increasing NMDA receptor activation via increased D-serine (Wu et al., 2004) and glutamate release and reduced glutamate uptake (Arias et al., 1995; Li et al., 2009; Parpura-Gill et al., 1997). Next it has been proposed that tau could further promote hyperexcitability, by altering glutamate levels as well as the expression and function of voltage-gated potassium channels and NMDA receptors, which would further potentiate the effects of Aβ pathology in a vicious cycle (Zott et al., 2019). This model is consistent with the known fact that in early AD, general hyperexcitability is another early hallmark of the disease (Samudra et al., 2023), leading to epileptiform discharges (Kural et al., 2020) and seizures (Pandis and Scarmeas, 2012), and coincides with the rapid spread of tau pathology, until it plateaus and hyperexcitability resolves in advanced AD (Pichet Binette et al., 2022).

Given that the evidence reviewed points at neuronal excitability as the putative mechanism by which increases in soluble Aβ may trigger p-tau secretion and trans-synaptic spread, early changes in cortical excitability in AD constitute a promising candidate biomarker for early AD detection (Samudra et al., 2023; Targa Dias Anastacio

et al., 2022). In this context, it is now possible to measure cortical excitability non-invasively in humans *in vivo* using EEG.

Recent research has shown that we can capture the overall cortical balance of excitation and inhibition using simple resting state EEG. After decomposing the EEG activity into the frequency domain, the power decreases as a function of frequency, whereby lower frequencies will contain most of the power in the spectra. This function follows a power distribution that can be described as $1/f^x$, where f is frequency, and the exponent x denotes the steepness or slope of the power spectrum. This aperiodic non-oscillatory feature was originally regarded as background noise that should be removed to capture the 'true' oscillatory activity in the power spectrum (Gyurkovics et al., 2021). However, recent research in mice and macaque, as well as computational modeling, show that, far from being irrelevant noise, the slope of the power spectrum likely reflects the overall balance of excitation and inhibition (Clements et al., 2021; Donoghue et al., 2020; Gao et al., 2017), whereby steeper slopes reflect a shift in the balance towards inhibition and vice versa.

Cortical excitability can also be measured more directly using TMS-EEG. As introduced in section 1.1.3, the peaks and troughs of the TMS evoked potentials reflect the contributions of distinct excitatory and inhibitory neurotransmitter systems. Of particular interest to derive a cortical excitability biomarker that potentially interacts with Aβ and p-tau pathology, is the latter components of the evoked potential (160-240ms after the TMS pulse), which have been shown to reflect voltage gated sodium channel (VGSC)-excitability. This was demonstrated in pharmacological studies employing VGSC blockers commonly used to treat epilepsy (Meisel et al., 2015), such as carbamazepine and lamotrigine, which consistently suppresses these late evoked components (Ghazaleh Darmani et al., 2019; Isabella Premoli et al., 2017).

Therefore, cortical excitability can be effectively modified via readily available pharmacological interventions that act by reducing excitability through the selective blocking of ion channels, thereby inhibiting excitatory synaptic transmission (Bialer and White, 2010). However, these drugs affect whole brain neurotransmitter systems and have a certain degree of toxicity. Hence, they produce unwanted side effects, such as

coordination disturbances, cognitive dysfunctions or adverse psychiatric effects, and cutaneous, hematological and hepatic or pancreatic reactions (Perucca and Gilliam, 2012). Alternatively, non-invasive transcranial stimulation techniques such as low-frequency rTMS, cTBS and cathodal tDCS can effectively induce long lasting decreases of cortical excitability, via long-term depression-like mechanisms (Houdayer et al., 2008; Huang et al., 2005b; Kronberg et al., 2017; Pascual-Leone et al., 1994; Valero-Cabré et al., 2007), and importantly, without comparable side effects. Furthermore, unlike antiepileptic drugs, these stimulation techniques can selectively target brain regions of interest (Lynch et al., 2022; Momi et al., 2021), for instance, they could be used to target tau epicenters such as the temporal cortex, to inhibit spread to other connected regions.

Therefore, there is now non-invasive and potentially scalable methods —blood-based Aβ, p-tau and NfL concentrations, and resting state EEG and TMS-EEG— to study biomarkers of cortical excitability in preclinical AD while investigating their interaction with Aβ and p-tau *in vivo* in humans. The findings derived from this research can then be used to inform non-invasive interventions to target cortical excitability. Current new generation interventions for AD aim at clearing of Aβ and tau, therefore, given the potential mediating role of excitability, reducing excitability could complement and potentially augment the effects of Aβ and p-tau clearing drugs.

CHAPTER 2. Hypotheses and Objectives

2.1. General Hypothesis

1) Candidate biomarkers of brain health are detectable using non-invasive and potentially scalable methods.
2) The proposed candidate biomarkers provide mechanistic insights relevant to diseases presenting disfunctions in synaptic transmission related to excitatory and inhibitory processes.

2.2. Specific Hypotheses

2.2.1. Study 1

1) A 'toy model' of brain resilience can be built with a controlled TMS brain perturbation modeling the stressor and the EEG reactivity to it modeling the response of the organism.
2) The proposed 'toy model' identifies a signature of brain resilience to the future impact of psychosocial stressors associated with the COVID-19 pandemic.

2.2.2. Study 2

1) Behavioral and neurophysiological abnormalities of schizophrenia patients can be detected in the EEG during a standard visual working memory task using univariate statistical methods.
2) An interpretable machine learning model incorporating the attention mechanism, can discriminate patients from matched healthy controls, relying on EEG data alone and provide insights relevant to the underlying neurophysiological abnormalities detected by univariate statistical methods.

2.2.3. Study 3

1) Spontaneous and perturbation-based EEG markers of cortical excitability are correlated with plasma concentration of secreted phosphorylated tau in healthy middle-aged adults.

2) Higher cortical excitability is associated with higher p-tau concentrations but not with passively released neurofilament light concentration in plasma.

2.3. General Objective

1) The objective of the experimental work reported in this thesis is to investigate translational and modifiable candidate biomarkers of brain health in the context of some of its most prevalent challenges: mental health vulnerability, schizophrenia, and Alzheimer's disease.

2.4. Specific Objectives

2.4.1. Study 1

1) Build a 'toy model' of brain resilience and vulnerability and showcase it in the context of the negative mental health impact of the psychosocial stressors associated with the COVID-19 pandemic.

2.4.2. Study 2

1) Implement an interpretable machine learning model based on the attention mechanism, that can distinguish patients from controls, based on EEG data alone, and reveal the neurophysiological signatures differentiating them.

2.4.3. Study 3

1) Establish the relationship between cortical excitability and secreted p-tau in a healthy middle-aged population using non-invasive methods.

CHAPTER 3. Materials, Methods, and Results

3.1. STUDY 1

Perellón-Alfonso. R., Redondo-Camós, M., Abellaneda-Pérez, K., Cattaneo, G., Delgado-Gallén, S., España-Irla, G., Sánchez, JS., Tormos, JM., Pascual-Leone, A., Bartrés-Faz, D. 2022. Prefrontal reactivity to TMS perturbation as a toy model of mental health outcomes during the COVID-19 pandemic. Heliyon, 8(8), e10208.

Heliyon 8 (2022) e10208

Contents lists available at ScienceDirect

Heliyon

journal homepage: www.cell.com/heliyon

Research article

Prefrontal reactivity to TMS perturbation as a toy model of mental health outcomes during the COVID-19 pandemic

Ruben Perellón-Alfonso [a,b], María Redondo-Camós [c,d,e], Kilian Abellaneda-Pérez [a,b,c], Gabriele Cattaneo [c,d,e], Selma Delgado-Gallén [c,d,e], Goretti España-Irla [c,d,e], Javier Solana Sánchez [c,d,e], José M. Tormos [c,d,e], Alvaro Pascual-Leone [c,f,g,**,1], David Bartrés-Faz [a,b,c,*,1]

[a] Faculty of Medicine and Health Sciences, and Institute of Neurosciences, University of Barcelona, Barcelona, Spain
[b] Institute of Biomedical Research August Pi i Sunyer (IDIBAPS), Barcelona, Spain
[c] Institut Guttmann, Institut Universitari de Neurorehabilitació adscrit a la UAB, Badalona, Barcelona, Spain
[d] Universitat Autònoma de Barcelona, Bellaterra (Cerdanyola del Vallès), Spain
[e] Fundació Institut d'Investigació en Ciències de la Salut Germans Trias i Pujol, Badalona, Barcelona, Spain
[f] Hinda and Arthur Marcus Institute for Aging Research and Deanna and Sidney Wolk Center for Memory Health, Hebrew Senior Life, Boston, MA, USA
[g] Department of Neurology, Harvard Medical School; Boston, MA, USA

ARTICLE INFO

Keywords:
TMS-EEG
Mental health
Resilience
COVID-19

ABSTRACT

Psychosocial hardships associated with the COVID-19 pandemic led many individuals to suffer adverse mental health consequences, however, others show no negative effects. We hypothesized that the electroencephalographic (EEG) response to transcranial magnetic stimulation (TMS) could serve as a toy-model of an individual's capacity to resist psychological stress, in this case linked to the COVID-19 pandemic. We analyzed data from 74 participants who underwent mental health monitoring and concurrent electroencephalography with transcranial magnetic stimulation of the left dorsolateral prefrontal cortex (L-DLPFC) and left inferior parietal lobule (L-IPL). Within the following 19 months, mental health was reassessed at three timepoints during lock-down confinement and different phases of de-escalation in Spain. Compared with participants who remained stable, those who experienced increased mental distress showed, months earlier, significantly larger late EEG responses locally after L-DLPFC stimulation (but not globally nor after L-IPL stimulation). This response, together with years of formal education, was significantly predictive of mental health status during the pandemic. These findings reveal that the effect of TMS perturbation offers a predictive toy model of psychosocial stress response, as exemplified by the COVID-19 pandemic.

1. Introduction

The stressors associated with the coronavirus disease (COVID-19) pandemic, as well as the restrictions imposed to contain the spread of the virus, are expected to increase the global burden on mental health (Pfefferbaum and North, 2020; Torales et al., 2020). The World Health Organization has acknowledged this fact (Giacalone et al., 2020) and highlighted the importance of integrating mental health into the preparedness and response plans to public health emergencies (WHO, 2021). Some studies estimate a 25% increase in the general prevalence of depression and anxiety symptoms (Bueno-Notivol et al., 2021). However, whereas some individuals' mental wellbeing will be negatively impacted, others - on account of their 'resilience' - will not be affected, or even thrive in the face of adversity (Pascual-Leone and Bartres-Faz, 2021).

The concept of resilience is highly heterogeneous with various meanings across different fields of study (Pascual-Leone and Bartres-Faz, 2021). Here we use resilience to refer to the processes that enable an individual to resist the development of illness, mental health problems or distress when confronted with stressful events or trauma (Moore et al., 2020; Russo et al., 2012). Conversely, psychological vulnerability is

* Corresponding author.
** Corresponding author.
E-mail addresses: apleone@hsl.harvard.edu (A. Pascual-Leone), dbartres@ub.edu (D. Bartrés-Faz).
[1] Drs. Alvaro Pascual-Leone and David Bartrés-Faz contributed equally to this manuscript.

https://doi.org/10.1016/j.heliyon.2022.e10208
Received 22 March 2022; Received in revised form 24 May 2022; Accepted 3 August 2022

reduced ability to cope with stressors, which would constitute a risk factor for developing psychopathology (Wright et al., 2013). Rather than a dichotomy, resilience and vulnerability can be understood as opposite ends of a continuum, which likely reflects the dynamic product of a complex interplay of individual and environmental factors (Cathomas et al., 2019; Rutter, 2012; Tost et al., 2015), including genetic and demographic characteristics, socio-economic status, developmental circumstances, access to health care, living conditions, adherence to certain lifestyle factors (e.g. cognitive, physical, nutritional and sleep habits), engagement in emotion-regulation practices such as meditation, social relations and support (particularly early in life), and years of education (Campbell-Sills et al., 2009; Di Marco et al., 2014; Frankish and Horton, 2017; Gelfo et al., 2018; Livingston et al., 2017).

Evidence from animal models and human neuroimaging studies have identified several brain regions and networks that likely play a role in the continuum of resilience and vulnerability. Converging evidence points at the crucial roles of anterior cingulate and insular cortices and their connections within the salience network (Menon, 2015; Menon and Uddin, 2010), as well as limbic structures, such as the amygdala and the ventral striatum (Holz et al., 2020). Additionally, the prefrontal cortex has been identified as an important structure (Maier and Watkins, 2010). Specifically, prefrontal cortical volume, activation and connectivity with limbic structures, positively correlate with resilience to traumatic events (Bolsinger et al., 2018); and longitudinal studies using functional magnetic resonance imaging (fMRI) found that children who were better able to regulate amygdala's emotional response through recruitment of the frontoparietal network exhibited greater resilience to developing depressive symptoms following maltreatment (Rodman et al., 2019). Prefrontal function is also involved in the pathophysiology and treatment of psychiatric conditions, most prominently, major depressive disorder (Hare and Duman, 2020) and schizophrenia (Selemon and Zecevic, 2015). Finally, the prefrontal cortex appears to not only play a central role in psychological resilience and psychiatric pathophysiology, but has been also proposed as a hub region for cognitive resilience in normal aging (Franzmeier et al., 2017b) as well as to brain atrophy and pathology associated with Alzheimer's disease (Franzmeier et al., 2018; Neitzel et al., 2019). Therefore, in the present study we focused on the prefrontal cortex to investigate the neural substrate of resilience to mental health impact of the COVID-19 pandemic and, argued that single pulse transcranial magnetic stimulation (TMS) in combination with electroencephalography (EEG) could be used in human experimental designs akin to the intervention-based animal studies of the neural substrate of resilience.

Animal studies that employ stimuli that can be precisely quantified and controlled, for example using tail-shock stress paradigms (Seligman et al., 1975) in which a mild electric shock is given to the tail of rats or mice, illustrate the power of such interventional experimental approaches to gain mechanistic insights into the substrate of resilience. Similar approaches in human research combining non-invasive brain stimulation with neuroimaging are possible. For example, Shafi and colleagues (Shafi et al., 2015) have shown that brain responses to TMS allow identifying abnormal cortical activity patterns before the manifestation of clinical symptoms in some forms of epilepsy. More recently, Abellaneda-Pérez and colleagues (Abellaneda-Pérez et al., 2019) have shown that the default mode network's response profile to intermittent theta burst stimulation of the inferior parietal lobule can be used to predict cognitive decline or maintenance after a three-year follow-up in an aging population, well over and above of what baseline neuroimaging data alone could predict. Furthermore, recent methodological advances (Ozdemir et al., 2020, 2021b), have revealed that single pulse TMS can be used concurrently with EEG to produce highly specific and reliable cortical response profiles.

We propose that TMS-EEG can be a 'toy model' of the impact of a perturbation onto an individual brain and provide a quantitative observation of the effect of the controlled external perturbation on brain dynamics that can be used to test specific predictions about a complex system. In theoretical physics 'toy-models' refer to simple models which nevertheless provide a quantitative explanation and reliable prediction of a given phenomenon (Georgescu, 2012; Marzuoli, 2008). Specifically, as illustrated in Figure 1, here we use the EEG response to TMS as a 'toy model' predictive of the eventual (months later) impact of the COVID pandemic and confinement on mental health. We hypothesized that individual differences in the electrophysiological cortical response to single pulse TMS brain perturbation of the left dorsolateral prefrontal cortex, compared to another control cortical target (i.e., inferior parietal lobule), and recorded using EEG, would be predictive of psychological distress outcomes during the COVID-19 pandemic and confinement. Our findings contribute to the understanding of biological brain mechanisms of resilience processes and identify a potential target and novel strategy to promote individual resilience.

2. Results

2.1. The dynamics of the EEG response to TMS perturbation differentiate individuals eventually found to have a 'negative' impact on mental health status, from those who remained 'stable', during the COVID-19 pandemic

Assessments of mental health using the four-item patient health questionnaire (PHQ-4), an ultra-brief depression and anxiety screening self-report questionnaire, were obtained prior to the COVID-19 pandemic and up to three additional times during the pandemic. If during all timepoints across the confinement, the PHQ-4 score was lower or equal than before the pandemic outbreak, subjects were classified as 'stable' (n = 32). Conversely, if a given subject had a higher score at any timepoint during the pandemic, they were classified as having a 'negative' impact (n = 32). Because not all participants completed stimulation at both target locations, the subgroups used in this analysis were actually smaller for each stimulation target (for L-DLPFC, 23 stable and 25 negative; for L-IPL, 22 stable and 23 negative). To make sure that the mental health impact of the pandemic was related to the levels of stress perceived during the outbreak, we tested for correlation between the average score of the three pandemic PHQ-4 timepoints, and the scores of the 14-item perceived stress scale (Cohen et al., 1983), which was also completed by participants during the pandemic, and found a strong positive correlation ($R_s = .69$; $p < .001$), indicating that subjects experiencing more stress during the pandemic also had a larger mental health impact. Overall, participants had a low to moderate level of perceived stress during the pandemic ($Mdn = 14$; range from 2 to 32). Additionally, to rule out that the groups significantly differed demographically, in resting motor threshold or pre-COVID PHQ-4 score, a multivariate ANOVA was used to compare both groups regarding four independent variables (age, years of education, pre-COVID PHQ4 score and resting motor threshold; see supplementary table S1 for descriptive statistics), which showed that the groups did not differ in any of these variables ($F(4, 63) = 3.869$, $p = 0.130$; Wilk's lambda = 0.888, partial $\eta 2 = 7.111$).

Point-by-point non-parametric permutation testing (1000 permutations) with cluster correction for multiple comparisons (Cohen, 2014) on the TMS-EEG evoked time-series, revealed a single broad cluster (i.e., 202–269 ms post-stimulus) surviving correction for multiple comparisons, only during stimulation of the left dorsolateral prefrontal cortex (L-DLPFC) (Figure 2, A). Inspection of the topographical distributions in source space for the surviving cluster, confirms that individuals whose mental health was negatively impacted had a qualitatively stronger frontal activation than those who remained stable (Figure 2, B). There were no significant clusters revealed after analysis of the responses to the left inferior parietal lobule (L-IPL) control target (Figure 2, C and D), nor for the distributed responses to stimulation on either target (Figure S2).

Finally, given that only a subsample (i.e., 50% of participants) completed stimulation of both targets, we additionally run permutation testing of the local TMS-EEG evoked time-series after DLPFC stimulation, but including only the participants that had undergone stimulation of both targets. The results on this subsample of participants are comparable

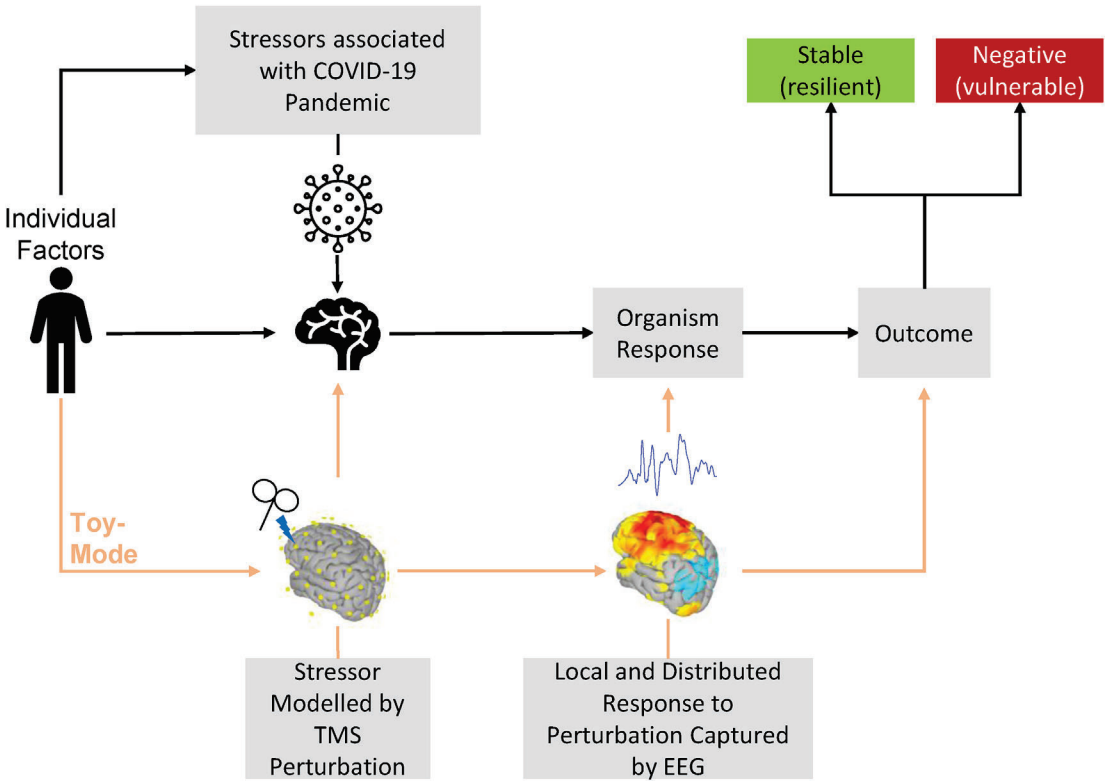

Figure 1. Schematic Illustration of the toy-model approach in our study design. MRI-guided single pulse TMS perturbation is used to experimentally model as the stressor, captured by evoked EEG reactivity, and measured at local and distributed (i.e., global) levels. We examined whether this 'toy-model' can predict the eventual impact of the COVID-19 on mental health assessed months later. We further hypothesized the stressor would be moderated by demographic and individual factors such as years of formal education. Modified from Pascual-Leone and Bartrés-Faz (Pascual-Leone and Bartres-Faz, 2021).

to the full sample (Figure S3), since the broad cluster surviving multiple comparisons correction remains in the same location, albeit slightly shorter in duration (i.e., from 200 to 253 ms after the TMS pulse).

2.2. Local EEG response to TMS perturbation of the left dorsolateral prefrontal cortex predicts mental health during the pandemic's lockdown confinement

Without dividing the sample into two groups, a multiple linear regression model was fit to determine the potential of TMS evoked EEG perturbation of the L-DLPFC to predict mental health outcomes after the COVID-19 pandemic outbreak and the strict lock-down confinement imposed to curb community transmission of the virus. The model's response variable was the mean of the total scores for the three PHQ-4 questionnaires, which were completed by participants during the lock-down confinement. Candidate predictors were the local and global (i.e., distributed) brain EEG reactivity to the TMS pulse — recorded before the pandemic outbreak —, as well as their interaction with the stimulation target definition method (i.e., functional or anatomical). Additionally, we included age, gender, and years of formal education as predictors, because these are demographic and individual factors partially predictive of resilience to stress (Campbell-Sills et al., 2009). Finally, we included as a predictor the number of months before the pandemic since each subject underwent TMS-EEG. This was included to control for the possibility that the amount of time passed from stimulation to pandemic would have an impact in the prediction.

The full linear regression model for the L-DLPFC stimulation target significantly predicted mental health during the pandemic (F (8,47) = 3.1, p = .007, R^2_{adj} = .234), and revealed as significant predictors the local brain reactivity to TMS (t = 3.27, p < .002) and years of formal education (t = -2.86, p = .006). See supplementary Table S2 (model "Full DLPFC") for detailed results. Both predictors were independent from each other, as reveled by the lack of correlation between them (R^2 = .187, p = .167). Subsequently, we tested a reduced model (F (2,53) = 10.5, p < .001, R^2_{adj} = .257) retaining only as predictors local brain reactivity (t = 3.66, p < .001) and education (t = -3.40, p = .001). See supplementary table S2 (model "Reduced DLPFC") for detailed results. Likelihood ratio test comparing the two models showed that the full model did not provide a better fit than the reduced one (χ^2 (6) = 4.98, p = .546). The lower Akaik and Bayesian information criteria (AIC and BIC, respectively) values for the reduced model further suggest a better and more parsimonious fit (AIC_{full} = 79.83, $AIC_{reduced}$ = 72.82; BIC_{full} = 98.06, $BIC_{reduced}$ = 78.89). Figure 3 illustrates the linear relationship between the significant predictors and the response variable in the reduced model. Analysis of variance of the reduced model revealed that local L-DLPFC reactivity explained 12.79% of total variance in mental health during the pandemic, while education explained 15.64%.

To confirm that our findings were specifically associated with pre-frontal reactivity, we fitted a model replacing the predictors for local and global EEG reactivity with those measured when stimulating the L-IPL. The regression model for this control stimulation target did not significantly predict mental health during the pandemic (F (8,46) = 0.4, p = .915, R^2_{adj} = -.097). See supplementary table S2 (model "Full IPL") for detailed results.

To demonstrate the specificity of the stimulation itself, a model was fitted where we added the local baseline pre-TMS activity as an additional predictor to the reduced L-DLPFC model. The resulting model, while still significant (F (3,47) = 7.09, p < .001, R^2_{adj} = .25), revealed that baseline pre-TMS EEG activity did not significantly contribute to predict mental health during the pandemic (t = .67, p = .507). See supplementary table S2 (model "Reduced + Baseline") for detailed results.

Finally, to ensure that the results are consistent, even when only considering the subsample of participants who completed stimulation of both targets, a model was fitted with only this subsample and the local

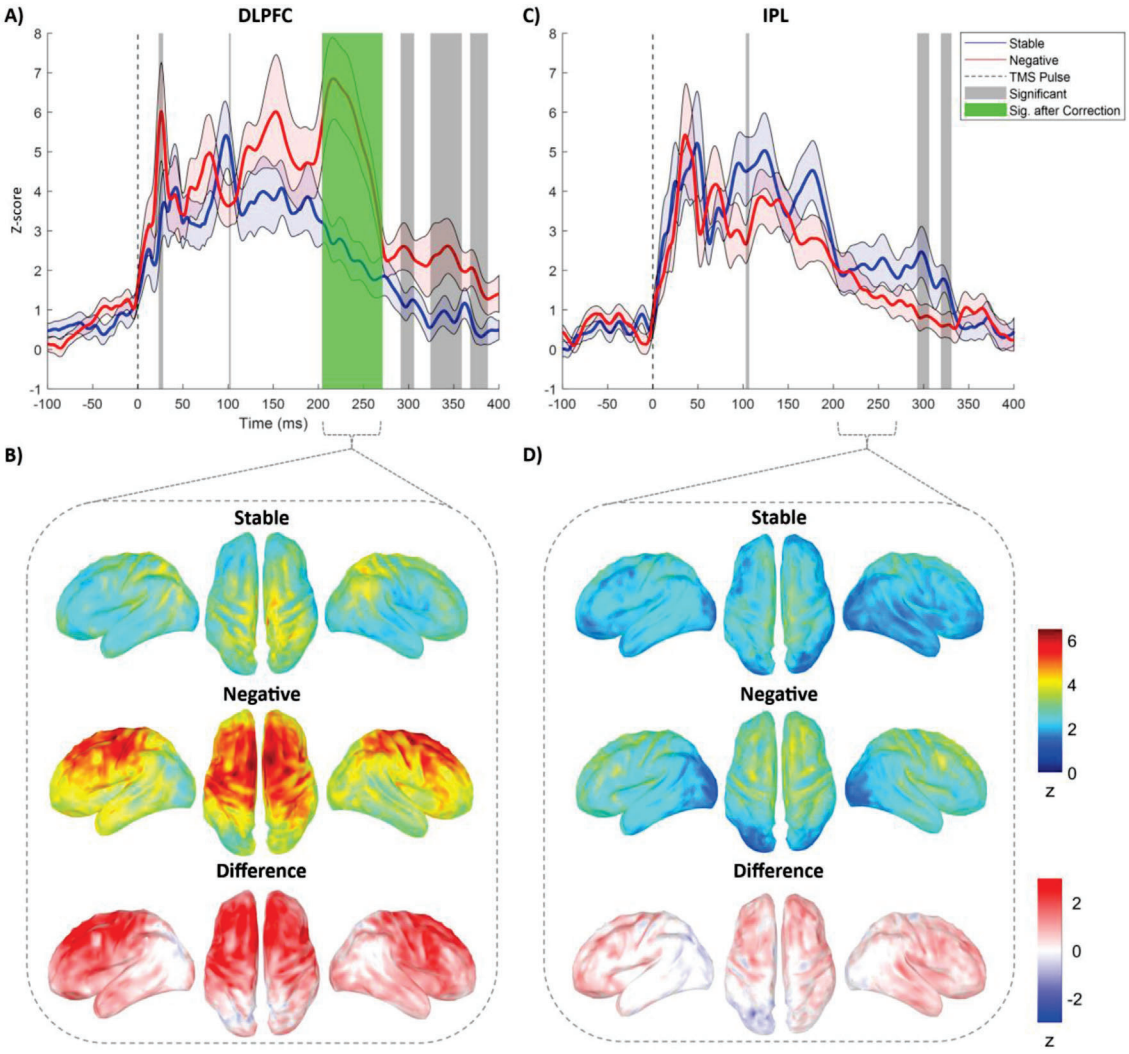

Figure 2. Results of permutation testing of the difference between stable and negatively impacted individuals on the TMS evoked EEG time-series. A) shows the significant differences at the local EEG time-series during L-DLPFC stimulation in grey vertical bands, while the vertical green band highlights the cluster surviving correction for multiple comparisons. B) shows the topographical distribution in source space of the response to L-DLPFC stimulation during the green shaded time-window in A, for both groups and their difference. C) depicts the results of permutation testing for the control stimulation of the L-IPL. D) shows the topographical distribution for the same time window as B, for both groups and their difference. Red and blue contours along the plot lines in A and C depict the standard error of the mean. DLPFC, dorsolateral prefrontal cortex; IPL, inferior parietal lobule.

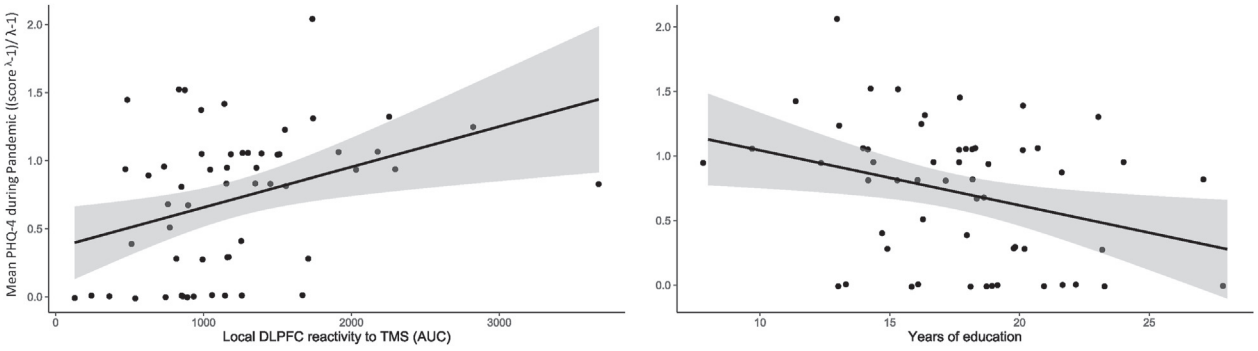

Figure 3. Scatter plots illustrating the linear relationship between the predictors and the response variable in the reduced model. Black line in each plot depicts the least squares regression line; shaded grey contours depict 95% confidence intervals. The response variable depicted here in the y-axis is Box-Cox transformed ($\lambda = -0.078$). PHQ-4, four item patient health questionnaire; DLPFC, dorsolateral prefrontal cortex; AUC, area under the curve.

response to IPL stimulation added as a predictor to the reduced model. The resulting model was still significant (F (3,33) = 3.25; p = .034) and revealed that, while local DLPFC reactivity (t = 2.44, p = .021) and education (t = -2.46, p = .019) were significant, local IPL reactivity was not (t = -1.03, p = .311). See supplementary table S2 (model "Reduced Subsample + IPL) for detailed results.

3. Discussion

We tested the EEG brain reactivity to TMS perturbation as a toy model of mental health outcomes in the face of the COVID-19 pandemic and lockdown confinement. The results show that the local response to TMS perturbation of the left DLPFC — measured months *before* the pandemic outbreak — offers a predictive marker of the future mental health impact of the pandemic and confinement. These results serve as a proof of concept that understanding the TMS pulse as an external transitory insult allows quantification of the brain responses and identifies critical and specific substrates of susceptibility to more complex stressors. At the core of this 'toy-model' is the assumption that single TMS stimuli can be understood as transitory perturbations or insults in themselves. This is supported by evidence showing that the stimuli interfere with ongoing brain activity by suddenly injecting an amount of current into the neural circuitry that disrupts ongoing brain activity, resulting in phase resetting and TMS-evoked perturbation of the ongoing EEG (Rocchi et al., 2018). Indeed, failure to suppress this perturbation can lead — in the presence of pathological conditions such as stroke or epilepsy — to a cascading synchronization of neuronal activity that in turn might lead to a seizure (Kimiskidis, 2019; Kimiskidis et al., 2017). Thus, we can interpret the present results as showing that in the presence of such a brain state disruption, a more resilient brain is better able to tolerate the perturbation. A link between the ability of the brain to withstand a targeted attack and resilience, has also been proposed by Santarnecchi and colleagues employing in-silico models (Santarnecchi et al., 2015), but the present study is the first to offer direct experimental support on a topic of substantial timely relevance.

Our findings are specific to TMS prefrontal perturbation, because neither the response to L-IPL stimulation, nor the pre-TMS baseline EEG activity held significant predictive value. Moreover, we show that the findings are restricted locally to the stimulated area, because the distributed measure of response could not differentiate stable from negatively impacted individuals and did not yield significant predictive value. Nevertheless, years of formal education was also found to be predictive of mental health during the pandemic, which is unsurprising given the well-known epidemiological-level notion that individuals with higher socioeconomic status (encompassing, among others, educational attainment and income) have lower odds of being depressed (Lorant et al., 2003), and that education might be a protective factor both against cognitive as well as emotional vulnerability, by boosting a higher efficiency on top-down emotional regulatory processes (Huang et al., 2019). In this context, and while education and TMS-EEG reactivity were independent from one another in this analysis, it is still plausible that both reflect prefrontal function, and is therefore, their joint inclusion that best predicted mental health status during the pandemic.

Dividing the sample into participants who remained stable and those who had a negative change in mental health during the pandemic, allowed us to directly compare the dynamics of the EEG response to the TMS perturbation, revealing that the most discriminative time segment after TMS perturbation of the local L-DLPFC is the late TMS evoked response between 202 ms and 269 ms post-TMS. Interestingly, this occurs in the vicinity of the commonly found P180 EEG evoked component in response to single TMS pulses of the primary motor cortex (Lioumis et al., 2009). This component has been found to significantly decrease after application of voltage-gated sodium channel blockers, such as lamotrigine and carbamazepine (Darmani and Ziemann, 2019; Premoli et al., 2017), indicating that this component reflects cortical excitability. Therefore, we propose that higher amplitudes found in vulnerable individuals may be reflective of cortical hyperexcitability. Furthermore, the amplitude of late TMS-EEG responses (=>180 ms) is related to GABA-B mediated inhibition, as it is significantly reduced after long interval intracortical inhibition (de Goede et al., 2020). Therefore, the increased amplitude in late EEG responses found in individuals that had a negative impact, when compared to the ones who remained stable, might reflect a relatively lower intracortical inhibitory capacity and point to differential levels of activation of parvo-albumin positive cells and integrity of peri-neural nets – main substrates of intracortical excitability-inhibition balance (Favuzzi et al., 2017; Xue et al., 2014). This would predict that conditions that alter and disrupt parvo-albumin positive cells and integrity of peri-neural nets, such as status post traumatic brain injury, early stages of Alzheimer's disease, or schizophrenia, would be associated with a loss of resilience and increased vulnerability to stressors. Epidemiologic data appear to support such notions (Buckley et al., 2009; Ehrenberg et al., 2018; Hammond et al., 2019).

Our results are novel and relevant in advancing our understanding of the neural mechanisms of resilience. However, this study has some limitations. We had to conduct the regression analysis on each stimulation target separately due to missing data, which may have hindered statistical power. The regression analysis results would benefit from further validation on a separate independent sample to be able to make reliable predictions of mental health outcomes based on the response to TMS perturbation. Moreover, due to the limited number of participants relative to the number of mental health monitoring timepoints during the pandemic, we were unable to account for all the mental health trajectories that have been described in the literature, such as people who have a negative impact but eventually recover (e.g., Gambin et al., 2021). Instead, in the permutation analysis, we focused on dichotomizing the two main trajectories (i.e., resilient vs vulnerable). Future studies should investigate the neurophysiological signature in response to stimulation of subjects who recover in the medium or long term, and that here were all classified as vulnerable. Finally, the changes in mental health observed during the pandemic were small overall, with most participants not surpassing clinical screening thresholds for depression and anxiety, therefore, a sample with a broader range of mental health impact could provide a clearer picture of the neurophysiological determinants of such impact. However, despite the narrow range of mental health changes, we are still able to show that TMS-EEG can detect a neurophysiological signature underlying the future differential impact of the pandemic on mental health.

The presented results are not only relevant as a proof of concept for using intervention-based designs in neuroimaging investigations of the neural basis of resilience, but also add to the existing evidence of a primary role of the left prefrontal cortex in resilience processes (Bolsinger et al., 2018; Dedovic et al., 2009; Franzmeier et al., 2017a, 2017b, 2017b, 2018, 2017b; Holz et al., 2020; Neitzel et al., 2019; Rodman et al., 2019; Stern et al., 2018). This, in turn, singles out the prefrontal cortex as a promising target for interventions aiming to promote positive outcomes after disrupting events such as the pandemic and associated social restrictions, including the potentially transformative possibility of using non-invasive stimulation to promote brain resilience by modulating prefrontal brain activity. Several of our results and other lines of evidence support such potentially transformative therapeutic intervention: (1) the known protective role of higher prefrontal function to the deleterious mental health effects of stress and trauma (Bolsinger et al., 2018; Rodman et al., 2019); (2) the link we have demonstrated between the L-DLPFC response to a brain perturbation and the mental health outcomes when facing the stressors associated with the pandemic; (3) our finding of exaggerated response to TMS perturbation of the L-DLPFC in individuals that would be negatively impacted by pandemic related stress; and (4) the established ability of non-invasive stimulation techniques to induce long lasting brain plastic changes (Huang et al., 2017). Finally, the identified electrophysiological dynamics in the local DLPFC response to TMS perturbation is a potential neurophysiological marker that might be useful in a preventive precision medicine framework, when

assessing the potential risk of deleterious mental health impacts for a given individual, when exposed to future stressful events such as a new pandemic.

4. Methods

4.1. Study design

In the present study we analyzed existing data from participants of the longitudinal study 'Barcelona Brain Health Initiative', BBHI for short (Cattaneo et al., 2018). In mid-March 2020, during the COVID-19 epidemic, the BBHI launched a longitudinal substudy to investigate the mental and brain health impact of societal and personal restrictions imposed by the pandemic (Bartrés-Faz et al., 2021; Pascual-Leone et al., 2021). For the present report, we selected those BBHI participants who had undergone concurrent TMS-EEG between July 2018 and February 2020, before the COVID-19 pandemic outbreak, as well as mental health monitoring before and during the lockdown using the Patient Health Questionnaire for Depression and Anxiety (PHQ-4), a standardized ultra-brief tool for detecting both anxiety and depressive disorders (Kroenke et al., 2009). The scale was administered at four different timepoints; one between November 2018 and January 2020, hence before a mandatory lockdown that was issued by the Spanish Government on March 14th 2020, and another three timepoints during the pandemic, spanning a total of 3 months during the strictest home-confinement and initial phases of de-escalation (Figure 4).

The sample included 74 healthy adults (45 male) ranging from 42 to 66 years ($M = 55.07$; $SD = 7.1$), with a range of years of formal education from 8 to 28 years ($M = 18.01$; $SD = 3.85$). Consistent with the BBHI general inclusion criteria, none of these individuals reported a medical diagnosis of any major neuropsychiatric disorder (including mood and anxiety disorders) at study entrance and had normal cognitive function as assessed by comprehensive neuropsychological testing (Cattaneo et al., 2018). All participants gave written informed consent, and the local ethics committee (Comité d'Ètica i Investigació Clínica de la Unió Catalana d'Hospitals) approved the protocols here described and conformed to the Declaration of Helsinki for research involving human subjects.

The objective of this analysis was to evaluate the potential of using the brain response to TMS perturbation – quantified by EEG – as a toy model of the mental health impact of a complex stressor, namely, the COVID-19 pandemic and confinement, the impact of which was quantified with the PHQ-4 questionnaires. Given the known involvement of the prefrontal cortex in various forms of resilience, we hypothesized that the EEG response to left dorsolateral prefrontal stimulation would be predictive of mental health during the pandemic. Stimulation on the left inferior parietal lobule was included in the analysis as a control stimulation condition.

4.2. Neuronavigated TMS-EEG

Transcranial magnetic stimulation was delivered over the left dorsolateral prefrontal cortex (L-DLPFC) and the left inferior parietal lobule (L-IPL). Stimulation was guided by a BrainSight neuronavigation system (RogueResearch, Inc., Canada). Targets were determined for each individual based on either anatomy or the cortical parcellation by Yeo and colleagues (Thomas Yeo et al., 2011). See supplementary materials for MRI acquisition parameters and target determination procedures. Stimulation intensity was 120% of resting motor threshold, determined as the minimum intensity required to elicit motor evoked potentials in the first dorsal interosseous muscle of the relaxed right hand, of at least 50μV peak-to-peak, in at least five out of ten trials (Rossini et al., 2015). For each target, 120 single biphasic pulses were delivered through an MCF-B65 butterfly coil, using a MagPro X100 stimulator (Magventure, Inc., Denmark), with a random inter-pulse interval between four and six seconds. The order of targets was randomized for each participant. In order to attenuate auditory evoked responses induced by the TMS coil click, participants listened to white-noise through earplug-earbuds at their maximum comfortable volume. Stimulation was performed concurrently with EEG using a TMS compatible ActiChamp 64-channel amplifier system, coupled with an ActiCap Slim with active electrodes (BrainProducts, GmbH., Germany). While the use of active electrodes is relatively novel in the context of TMS-EEG, recent research has successfully used them to evaluate TMS evoked brain reactivity (to cite some, Gamboa Arana et al., 2020; Ozdemir et al., 2021b, 2021a, 2020; Redondo-Camós et al., 2022; Rocchi et al., 2021). Moreover, it has been recently shown that the TMS evoked potential waveforms are reliable and comparable to those obtained with passive electrodes (Mancuso et al., 2021), provided that interelectrode impedance is kept low. Therefore, we monitored electrode impedance to make sure it was kept under 5kΩ for all electrodes and throughout the experiment. EEG data was recorded DC to 500Hz and digitized at a 1KHz sampling rate. While 76% of participants completed stimulation of the L-DLPFC and 74% completed stimulation of the L-IPL, only 50% of participants completed stimulation on both targets. For this reason, statistical analysis was conducted separately for each stimulation target.

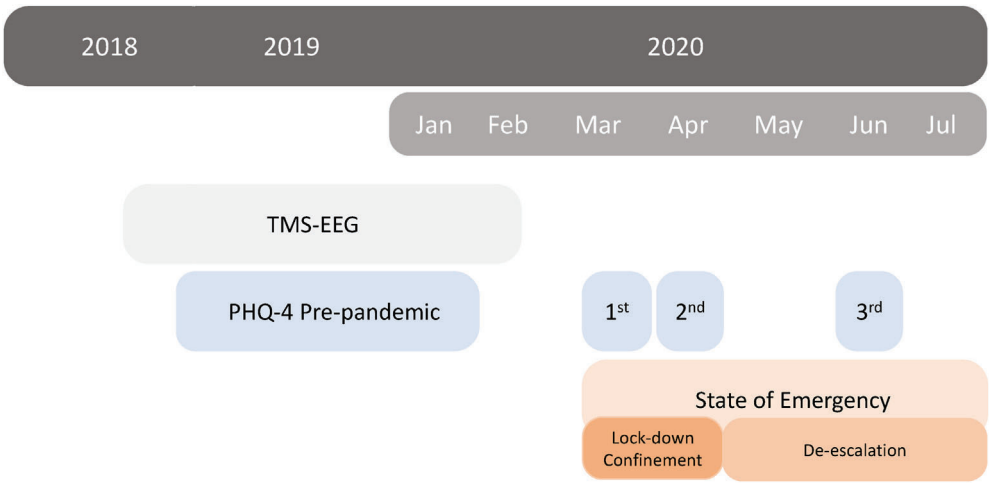

Figure 4. Timeline of relevant events for the study cohort. According to the Spanish Government state of alarm dictation orders and subsequent de-escalation (https://www.boe.es/eli/es/rd/2020/03/14/463/con). 1st, 2nd and 3rd indicate the three PHQ-4 based mental health monitoring timepoints during the pandemic. PHQ-4, four item patient health questionnaire; COVID-19, coronavirus diesease 2019; TMS-EEG, transcraneal magnetic stimulation with concurrent electroencephalography.

4.3. Mental health assessment

Mental health was measured using the PHQ-4, an ultra-brief four item depression and anxiety screening self-report questionnaire, that consists of a 2-item depression scale (PHQ-2) and a 2-item anxiety scale (GAD-2). Each subitem scores in the range of 0–6, with combined range from 0 to 12. On each subscale a score of 3 or greater is considered positive for screening purposes. The test was administered a total of four times in an online format, once before the pandemic and at three timepoints during the confinement and de-escalation. All participants in this analysis completed the pre-pandemic questionnaire and most completed the three additional ones during the pandemic (69%), however, few participants completed only two (23%) or one (8%) of them. For the purposes of quantifying mental health status during the pandemic in the regression models, we used the mean of total scores from the completed questionnaires during the pandemic.

4.4. EEG data preprocessing and analysis

All EEG data was preprocessed using functions from the EEGLAB toolbox (Delorme and Makeig, 2004) and the TESA plugin (Mutanen et al., 2020; Rogasch et al., 2017). Source reconstruction and analysis was performed using Brainstorm (Tadel et al., 2019) and custom made Matlab (The MathWorks, Inc., USA) scripts.

First, the data was segmented around the TMS pulse (−1000 to 1000 ms from the pulse) and baseline corrected (−900 ms to -100 ms from the pulse). Then the direct electrical pulse artifact (between -2 ms and 14 ms from pulse) was zero-padded. Bad channels were then identified via visual inspection and removed (range from 0 to 3; $M = 0.49$, $SD = 0.76$). Bad epochs were first tagged based on threshold voltage (>100 μV), probability and kurtosis using the inbuilt TESA plugin functions, visual inspection ensured that the epochs were correctly tagged and that no bad epochs were missed, then they were removed from further analysis (range from 0 to 53; $M = 20.59$; $SD = 9.66$). A first round of fast independent component analysis (ICA) was used to reject any remains of the immediate electrical pulse artifact (range from 0 to 3; $M = 0.67$; $SD = 0.65$). The zero-padded pulse artifact was then linearly interpolated, and the data was re-referenced to the average of all channels. Finally, a second round of ICA was used to reject any other remaining artifacts (e.g., muscle, eye-movements, heartbeat and others), as well as the somatosensory and auditory potentials evoked by transcutaneous scalp nerve excitation and coil firing sounds, respectively (range from 21 to 23: $M = 28.37$; $SD = 2.77$). These are commonplace preprocessing procedures for TMS-EEG data and have been described in greater detail elsewhere (Rogasch et al., 2017).

The cleaned preprocessed data was then used for source reconstruction in Brainstorm. For each subject a forward model was estimated via the openMEEG algorithm (Kybic et al., 2005) using the default settings (i.e., 3 layers with 1922 vertices each; skull and scalp conductivities of 1 and brain conductivity of 0.0125; adaptative integration), and based on each subject's T1 and T2 weighted MRI images and digitized real electrode locations, when available (the 29 subjects for which anatomical target determination was used, had no digitized electrode locations, therefore, the standard 10-10 electrode locations were used instead). The inverse solution was estimated using the minimum norm imaging method (Salmelin and Baillet, 2009). Sources were then computed as current density maps for constrained orientations only (i.e., normal to cortex). These are commonplace source reconstruction procedures for TMS-EEG data and have been described in greater detail elsewhere (Ozdemir et al., 2020, 2021a, 2021b).

4.5. Local and distributed EEG measures of the response to TMS perturbation

To quantify EEG derived brain reactivity measures to the TMS pulse we computed the following global (i.e., distributed) and local reactivity measures:

Global response: the global mean field amplitude (GMFA; Lehmann and Skrandies, 1980) of the TMS evoked potentials (TEPs) in sensor space, was taken as the estimated time-series of the global brain response to the TMS pulse. This measure was computed according to the following formula:

$$GMFA(t) = \sqrt{\left\{\frac{\sum_i^k (\mathrm{Vi}\ (t) - \mathrm{V}_{mean(t)})2}{K}\right\}}$$

Where $V_i(t)$ is the voltage at electrode i at a certain point in time, $V_{mean(t)}$ is the mean of instantaneous TEP across electrodes, and K is the number of electrodes.

Local response: To extract local measures, we first defined a region of interest (ROI) of 100 vertices around each subject's stimulation target coordinate, which corresponds to a cortex surface area of approximately 10 cm^2. Then the TEP response at the targeted location in source space was taken as the local reactivity time-series. To allow group level statistics, the TEP time-series in source space of each vertex within the target ROI were rectified, averaged together, and then normalized via z-score transformation:

$$z=(TEP-\mu)/\sigma$$

Where μ is the average of the pre-stimulus baseline (-500 ms to -3 ms) and σ is the standard deviation of the baseline.

For both global and local TMS response measures, the trapezoidal integration from 15 ms to 400 ms post-TMS stimulus was used in the regression analyses as an estimate of the overall response to TMS perturbation.

4.6. Statistical analysis

Statistical analysis was performed in RStudio (RStudio Team, 2020) and Matlab 2020b.

To compare the global and local TMS evoked time-series for each target we conducted four permutation-based tests. In each test, we computed the difference of means for each data point within the time-series time-window of interest (from 15 ms to 400 ms after the TMS pulse). In each of the 1000 permutations, the labels for each group (resilient or vulnerable) were scrambled. The resulting p-values were adjusted for multiple comparisons using cluster correction (Cohen, 2014), whereby the size and magnitude of a given cluster of significant timepoints is considered to survive correction if the size and magnitude of the cluster is above 95% of all cluster sizes and magnitudes discovered during permutation testing. To test the consistency of the significant results on the subsample of participants that completed stimulation on both targets, an additional permutation-based test was run on this subsample. To test the correlation between perceived stress and mental health during the pandemic a Spearman rank correlation was used.

To investigate the predictive value of TMS reactivity at a local and global levels we used two multiple linear regression models, one for each stimulation target (i.e., L-DLPFC and L-IPL). The full model included as predictors the local and global TMS brain reactivity measures, age, gender, and years of education. Additionally, and to control for the possibility that the target definition method influenced the candidate reactivity measures, we included the interaction between the targeting method (2 levels: anatomical or functional) and both local and global reactivity measures, for each model. In each regression model the response variable was each subject's mean of the completed pandemic PHQ-4 scores. In the presence of significant predictors, a reduced model including only those was defined and compared against the full model. To determine the better fitting model, we used the likelihood ratio test and further confirmed the result based on the AIC and BIC values. To assert the TMS induced specificity of the findings, we fitted an additional model where the possible contribution of the pre-TMS stimulus baseline to the prediction of mental health was tested. Finally, to confirm the

consistency of the results on the subsample of participants that completed stimulation on both targets, a model was fitted adding the local IPL reactivity as a predictor and including only the subsample participants.

Lilliefors test on each model's residuals revealed that they were not normally distributed, therefore, we transformed the response variable in each model using Box-Cox transformation, resulting in normally distributed residuals, therefore, the results reported in this work correspond to the regression models with the transformed response variable. Assumptions of multicollinearity, autocorrelation and heteroscedasticity were met in each model.

Declarations

Author contribution statement

Ruben Perellón-Alfonso: Conceived and designed the experiments; Analyzed and interpreted the data; Contributed analysis tools; Wrote the paper.

María Redondo-Camós: Conceived and designed the experiments; Performed the experiments; Analyzed and interpreted the data.

Kilian Abellaneda-Pérez: Conceived and designed the experiments; Interpreted the data; Wrote the paper.

Gabriele Cattaneo, Javier Solana Sánchez: Conceived and designed the experiments; Interpreted the data.

Selma Delgado-Gallén, Goretti España-Irla: Performed the experiments.

José M. Tormos: Conceived and designed the experiments; Contributed materials and data.

Alvaro Pascual-Leone, David Bartrés-Faz: Conceived and designed the experiments; Interpreted the data; Contributed materials and data; Wrote the paper.

Funding statement

This work was supported by a grant from the Agencia de Gestio d'Ajuts Universitaris i de Recerca (AGAUR) "PANDEMIES 2020" [2020PANDE00043] and a grant from "La Marato de TV3" MARATO 2020 COVID-19 [202129-31].

Dr. Bartres-Faz was supported by an ICREA Academia 2019 award.

David Bartrés-Faz and Kilian Abellaneda-Pérez were supported by Ministerio de Ciencia, Innovación y Universidades de España [RTI2018-095181-B-C21].

Ruben Perellón-Alfonso was supported by a fellowship from "la Caixa" Foundation [ID 100010434. Fellowship code: LCF/BQ/DI19/11730050].

Alvaro Pascual-Leone was supported by the National Institutes of Health, United States [R24AG06142 and P01AG031720].

The research leading to these results has received funding from "la Caixa" Foundation [LCF/PR/PR16/11110004].

Data availability statement

The authors encourage interested investigators to reach out and we will honor all reasonable and scientifically motivated requests for data access and make the raw data available when required.

Declaration of interest's statement

The authors declare the following conflict of interests: Dr. A. Pascual-Leone is listed as an inventor on several issued and pending patents on the real-time integration of noninvasive brain stimulation with electroencephalography and magnetic resonance imaging. He is co-founder of Linus Health and TI Solutions AG; serves on the scientific advisory boards for Starlab Neuroscience, Magstim Inc., Radiant Hearts, and MedRhythms, and is an Associate Editor for Annals of Neurology. None of the other authors reports any conflict of interest.

Additional information

Supplementary content related to this article has been published online at https://doi.org/10.1016/j.heliyon.2022.e10208.

Acknowledgements

Authors thank the Barcelona Brain Health Initiative project participants, whose invaluable contribution made this research possible. We are thankful for the contribution of Indre Pileckyte to the statistical analysis in this work, as well as for her review of the manuscript.

References

Abellaneda-Pérez, K., Vaqué-Alcázar, L., Vidal-Piñeiro, D., Jannati, A., Solana, E., Bargalló, N., Santarnecchi, E., Pascual-Leone, A., Bartrés-Faz, D., 2019. Age-related differences in default-mode network connectivity in response to intermittent theta-burst stimulation and its relationships with maintained cognition and brain integrity in healthy aging. Neuroimage 188, 794–806.

Bartrés-Faz, D., Macià, D., Cattaneo, G., Borràs, R., Tarrero, C., Solana, J., Tormos, J.M., Pascual-Leone, A., 2021. The paradoxical effect of COVID-19 outbreak on loneliness. BJ Psych Open 7, 1–4.

Bolsinger, J., Seifritz, E., Kleim, B., Manoliu, A., 2018. Neuroimaging correlates of resilience to traumatic events—a comprehensive review. Front. Psychiatr. 9.

Buckley, P.F., Miller, B.J., Lehrer, D.S., Castle, D.J., 2009. Psychiatric comorbidities and schizophrenia. Schizophr. Bull. 35, 383–402.

Bueno-Notivol, J., Gracia-García, P., Olaya, B., Lasheras, I., López-Antón, R., Santabárbara, J., 2021. Prevalence of depression during the COVID-19 outbreak: a meta-analysis of community-based studies. Int. J. Clin. Health Psychol. 21.

Campbell-Sills, L., Forde, D.R., Stein, M.B., 2009. Demographic and childhood environmental predictors of resilience in a community sample. J. Psychiatr. Res. 43, 1007–1012.

Cathomas, F., Murrough, J.W., Nestler, E.J., Han, M.H., Russo, S.J., 2019. Neurobiology of resilience: interface between mind and body. Biol. Psychiatr. 86, 410–420.

Cattaneo, G., Bartrés-Faz, D., Morris, T.P., Sánchez, J.S., Macià, D., Tarrero, C., Tormos, J.M., Pascual-Leone, A., 2018. The Barcelona brain health initiative: a cohort study to define and promote determinants of brain health. Front. Aging Neurosci. 10.

Cohen, M.X., 2014. Analyzing Neural Time Series Data: Theory and Practice. MIT press.

Cohen, S., Kamarck, T., Mermelstein, R., 1983. A global measure of perceived stress. J. Health Soc. Behav. 24, 385–396.

Darmani, G., Ziemann, U., 2019. Pharmacophysiology of TMS-evoked EEG potentials: a mini-review. Brain Stimul. 12, 829–831.

de Goede, A.A., Cumplido-Mayoral, I., van Putten, M.J.A.M., 2020. Spatiotemporal dynamics of single and paired pulse TMS-EEG responses. Brain Topogr. 33, 425–437.

Dedovic, K., D'Aguiar, C., Pruessner, J.C., 2009. What stress does to your brain: a review of neuroimaging studies. Can. J. Psychiatr. 54, 6–15.

Delorme, A., Makeig, S., 2004. Eeglab_Jnm03.Pdf. Tech. Soc 134, 9–21.

Di Marco, L.Y., Marzo, A., Muñoz-Ruiz, M., Ikram, M.A., Kivipelto, M., Ruefenacht, D., Venneri, A., Soininen, H., Wanke, I., Ventikos, Y.A., Frangi, A.F., 2014. Modifiable lifestyle factors in dementia: a systematic review of longitudinal observational cohort studies. J. Alzheim. Dis. 42, 119–135.

Ehrenberg, A.J., Suemoto, C.K., França Resende, E. de P., Petersen, C., Leite, R.E.P., Rodriguez, R.D., Ferretti-Rebustini, R.E. de L., You, M., Oh, J., Nitrini, R., Pasqualucci, C.A., Jacob-Filho, W., Kramer, J.H., Gatchel, J.R., Grinberg, L.T., 2018. Neuropathologic correlates of psychiatric symptoms in Alzheimer's disease. J. Alzheimers. Dis. 66, 115–126.

Favuzzi, E., Marques-Smith, A., Deogracias, R., Winterflood, C.M., Sánchez-Aguilera, A., Mantoan, L., Maeso, P., Fernandes, C., Ewers, H., Rico, B., 2017. Activity-Dependent gating of parvalbumin interneuron function by the perineuronal net protein brevican. Neuron 95, 639–655.e10.

Frankish, H., Horton, R., 2017. Prevention and management of dementia: a priority for public health. Lancet 390, 2614–2615.

Franzmeier, N., Göttler, J., Grimmer, T., Drzezga, A., Áraque-Caballero, M.A., Simon-Vermot, L., Taylor, A.N.W., Bürger, K., Catak, C., Janowitz, D., Müller, C., Duering, M., Sorg, C., Ewers, M., 2017a. Resting-state connectivity of the left frontal cortex to the default mode and dorsal attention network supports reserve in mild cognitive impairment. Front. Aging Neurosci. 9, 1–11.

Franzmeier, N., Hartmann, J., Taylor, A.N.W., Araque-Caballero, M., Simon-Vermot, L., Kambeitz-Ilankovic, L., Bürger, K., Catak, C., Janowitz, D., Müller, C., Ertl-Wagner, B., Stahl, R., Dichgans, M., Duering, M., Ewers, M., 2018. The left frontal cortex supports reserve in aging by enhancing functional network efficiency Rik Ossenkoppele. Alzheimer's Res. Ther. 10, 1–12.

Franzmeier, N., Hartmann, J.C., Taylor, A.N.W., Caballero, M.Á.A., Simon-Vermot, L., Buerger, K., Kambeitz-Ilankovic, L.M., Ertl-Wagner, B., Mueller, C., Catak, C., Janowitz, D., Stahl, R., Dichgans, M., Duering, M., Ewers, M., 2017b. Left frontal hub connectivity during memory performance supports reserve in aging and mild cognitive impairment. J. Alzheim. Dis. 59, 1381–1392.

Gambin, M., Oleksy, T., Sękowski, M., Wnuk, A., Woźniak-Prus, M., Kmita, G. 1/4yna, Holas, P., Pisula, E., Łojek, E., Hansen, K., Gorgol, J., Kubicka, K., Huflejt-ŁUkasik, M., Cudo, A., Łyś, A.E., Szczepaniak, A., Bonanno, G.A., 2021. Pandemic

trajectories of depressive and anxiety symptoms and their predictors: five-wave study during the COVID-19 pandemic in Poland. Psychol. Med. 19, 1–3.
Gamboa Arana, O.L., Palmer, H., Dannhauer, M., Hile, C., Liu, S., Hamdan, R., Brito, A., Cabeza, R., Davis, S.W., Peterchev, A.V., Sommer, M.A., Appelbaum, L.G., 2020. Intensity- and timing-dependent modulation of motion perception with transcranial magnetic stimulation of visual cortex. Neuropsychologia 147, 107581.
Gelfo, F., Mandolesi, L., Serra, L., Sorrentino, G., Caltagirone, C., 2018. The neuroprotective effects of experience on cognitive functions: evidence from animal studies on the neurobiological bases of brain reserve. Neuroscience 370, 218–235.
Georgescu, I., 2012. Quantum simulation: Toy model. Nat. Phys. 8, 444.
Giacalone, A., Rocco, G., Ruberti, E., 2020. Physical health and psychosocial considerations during the coronavirus disease 2019 outbreak. Psychosomatics 61, 851–852.
Hammond, F.M., Corrigan, J.D., Ketchum, J.M., Malec, J.F., Dams-O'Connor, K., Hart, T., Novack, T.A., Bogner, J., Dahdah, M.N., Whiteneck, G.G., 2019. Prevalence of medical and psychiatric comorbidities following traumatic brain injury. J. Head Trauma Rehabil. 34, E1–E10.
Hare, B.D., Duman, R.S., 2020. Prefrontal cortex circuits in depression and anxiety: contribution of discrete neuronal populations and target regions. Mol. Psychiatr. 25, 2742–2758.
Holz, N.E., Tost, H., Meyer-Lindenberg, A., 2020. Resilience and the brain: a key role for regulatory circuits linked to social stress and support. Mol. Psychiatr. 25, 379–396.
Huang, C.M., Fan, Y.T., Lee, S.H., Liu, H.L., Chen, Y.L., Lin, C., Lee, T.M.C., 2019. Cognitive reserve-mediated neural modulation of emotional control and regulation in people with late-life depression. Soc. Cognit. Affect Neurosci. 14, 849–860.
Huang, Y.Z., Lu, M.K., Antal, A., Classen, J., Nitsche, M., Ziemann, U., Ridding, M., Hamada, M., Ugawa, Y., Jaberzadeh, S., Suppa, A., Paulus, W., Rothwell, J., 2017. Plasticity induced by non-invasive transcranial brain stimulation: a position paper. Clin. Neurophysiol. 128, 2318–2329.
Kimiskidis, V., 2019. The dynamics of TMS-induced seizures and epileptiform discharges. Brain Stimul. 12, 484.
Kimiskidis, V.K., Tsimpiris, A., Ryvlin, P., Kalviainen, R., Koutroumanidis, M., Valentin, A., Laskaris, N., Kugiumtzis, D., 2017. TMS combined with EEG in genetic generalized epilepsy: a phase II diagnostic accuracy study. Clin. Neurophysiol. 128, 367–381.
Kroenke, K., Spitzer, R.L., Williams, J.B.W., Löwe, B., 2009. An ultra-brief screening scale for anxiety and depression: the PHQ–4. Psychosomatics 50, 613–621.
Kybic, J., Clerc, M., Abboud, T., Faugeras, O., Keriven, R., Papadopoulo, T., 2005. A common formalism for the integral formulations of the forward EEG problem. IEEE Trans. Med. Imag. 24, 12–28.
Lehmann, D., Skrandies, W., 1980. Reference-free identification of components of checkerboard-evoked multichannel potential fields. Electroencephalogr. Clin. Neurophysiol. 48, 609–621.
Lioumis, P., Kičić, D., Savolainen, P., Mäkelä, J.P., Kähkönen, S., 2009. Reproducibility of TMS - evoked EEG responses. Hum. Brain Mapp. 30, 1387–1396.
Livingston, G., Sommerlad, A., Orgeta, V., Costafreda, S.G., Huntley, J., Ames, D., Ballard, C.G., Banerjee, S., Burns, A., Cohen-Mansfield, J., Cooper, C., Fox, N., Gitlin, L.N., Howard, R., Kales, H.C., Larson, E., Ritchie, K., Rockwood, K., Sampson, E.L., Samus, Q.M., Schneider, L.S., Selbæk, G., Teri, L., Mukadam, N., 2017. The lancet international commission on dementia prevention and care. Lancet 390, 2673–2734.
Lorant, V., Deliège, D., Eaton, W., Robert, A., Philippot, P., Ansseau, M., 2003. Socioeconomic inequalities in depression: a meta-analysis. Am. J. Epidemiol. 157, 98–112.
Maier, S.F., Watkins, L.R., 2010. Role of the medial prefrontal cortex in coping and resilience. Brain Res. 1355, 52–60.
Mancuso, M., Sveva, V., Cruciani, A., Brown, K., Ibáñez, J., Rawji, V., Casula, E., Premoli, I., D'Ambrosio, S., Rothwell, J., Rocchi, L., 2021. Transcranial evoked potentials can be reliably recorded with active electrodes. Brain Sci. 11, 1–16.
Marzuoli, A., 2008. Toy models in physics and the reasonable effectiveness of mathematics. In: Deduction, Computation, Experiment. Springer, pp. 49–64.
Menon, V., 2015. Salience Network, Brain Mapping: an Encyclopedic Reference. Elsevier Inc.
Menon, V., Uddin, L.Q., 2010. Saliency, switching, attention and control: a network model of insula function. Brain Struct. Funct. 214, 655–667.
Moore, T.M., White, L.K., Barzilay, R., Calkins, M.E., Jones, J.D., Young, J.F., Gur, R.C., Gur, R.E., 2020. Development of a scale battery for rapid assessment of risk and resilience. Psychiatr. Res. 288, 112996.
Mutanen, T.P., Biabani, M., Sarvas, J., Ilmoniemi, R.J., Rogasch, N.C., 2020. Source-based artifact-rejection techniques available in TESA, an open-source TMS–EEG toolbox. Brain Stimul. 13, 1349–1351.
Neitzel, J., Franzmeier, N., Rubinski, A., Ewers, M., 2019. Left frontal connectivity attenuates the adverse effect of entorhinal tau pathology on memory. Neurology 93, E347–E357.
Ozdemir, R.A., Boucher, P., Fried, P.J., Momi, D., Jannati, A., Pascual-Leone, A., Santarnecchi, E., Shafi, M.M., 2021a. Reproducibility of cortical response modulation induced by intermittent and continuous theta-burst stimulation of the human motor cortex. Brain Stimul. 14, 949–964.
Ozdemir, R.A., Tadayon, E., Boucher, P., Momi, D., Karakhanyan, K.A., Fox, M.D., Halko, M.A., Pascual-Leone, A., Shafi, M.M., Santarnecchi, E., 2020. Individualized perturbation of the human connectome reveals reproducible biomarkers of network dynamics relevant to cognition. Proc. Natl. Acad. Sci. U. S. A. 117, 8115–8125.
Ozdemir, R.A., Tadayon, E., Boucher, P., Sun, H., Momi, D., Ganglberger, W., Westover, M.B., Pascual-Leone, A., Santarnecchi, E., Shafi, M.M., 2021b. Cortical responses to noninvasive perturbations enable individual brain fingerprinting. Brain Stimul. 14.
Pascual-Leone, A., Bartres-Faz, D., 2021. Human brain resilience: a call to action. Ann. Neurol. 1–14.
Pascual-Leone, A., Cattaneo, G., Macià, D., Solana, J., Tormos, J.M., Bartrés-Faz, D., 2021. Beware of optimism bias in the context of the COVID-19 pandemic. Ann. Neurol. 11, 2019–2021.
Pfefferbaum, B., North, C.S., 2020. Mental health and the covid-19 pandemic. N. Engl. J. Med. 383, 510–512.
Premoli, I., Biondi, A., Carlesso, S., Rivolta, D., Richardson, M.P., 2017. Lamotrigine and levetiracetam exert a similar modulation of TMS-evoked EEG potentials. Epilepsia 58, 42–50.
Redondo-Camós, M., Cattaneo, G., Perellón-Alfonso, R., Alviarez-Schulze, V., Morris, T.P., Solana-Sanchez, J., España-Irla, G., Delgado-Gallén, S., Pachón-García, C., Albu, S., Zetterberg, H., Tormos, J.M., Pascual-Leone, A., Bartres-Faz, D., 2022. Local prefrontal cortex TMS-induced reactivity is related to working memory and reasoning in middle-aged adults. Front. Psychol. 13, 1–10.
Rocchi, L., Di Santo, A., Brown, K., Ibáñez, J., Casula, E., Rawji, V., Di Lazzaro, V., Koch, G., Rothwell, J., 2021. Disentangling EEG responses to TMS due to cortical and peripheral activations. Brain Stimul. 14, 4–18.
Rocchi, L., Ibáñez, J., Benussi, A., Hannah, R., Rawji, V., Casula, E., Rothwell, J., 2018. Variability and predictors of response to continuous theta burst stimulation: a TMS-EEG study. Front. Neurosci. 12, 1–11.
Rodman, A.M., Jenness, J.L., Weissman, D.G., Pine, D.S., McLaughlin, K.A., 2019. Neurobiological markers of resilience to depression following childhood maltreatment: the role of neural circuits supporting the cognitive control of emotion. Biol. Psychiatr. 86, 464–473.
Rogasch, N.C., Sullivan, C., Thomson, R.H., Rose, N.S., Bailey, N.W., Fitzgerald, P.B., Farzan, F., Hernandez-pavon, J.C., 2017. NeuroImage Analysing concurrent transcranial magnetic stimulation and electroencephalographic data : a review and introduction to the open-source TESA software. Neuroimage 147, 934–951.
Rossini, P.M., Burke, D., Chen, R., Cohen, L.G., Daskalakis, Z., Di Iorio, R., Di Lazzaro, V., Ferreri, F., Fitzgerald, P.B., George, M.S., Hallett, M., Lefaucheur, J.P., Langguth, B., Matsumoto, H., Miniussi, C., Nitsche, M.A., Pascual-leone, A., Paulus, W., Rossi, S., Rothwell, J.C., Siebner, H.R., Ugawa, Y., Walsh, V., Ziemann, U., Committee, I.F.C.N., Rossini, P.M., Burke, D., Chen, R., Cohen, L.G., Daskalakis, Z., Iorio, R., Di Lazzaro, V., Di Ferreri, F., Fitzgerald, P.B., George, M.S., Hallett, M., Lefaucheur, J.P., Langguth, B., Matsumoto, H., Miniussi, C., Nitsche, M.A., Pascual-leone, A., Paulus, W., Rossi, S., Rothwell, J.C., Siebner, H.R., 2015. Clinical Neurophysiology Non-invasive electrical and magnetic stimulation of the brain , spinal cord , roots and peripheral nerves : basic principles and procedures for routine clinical and research application . An updated report from an. Clin. Neurophysiol. 126, 1071–1107.
RStudio Team, 2020. RStudio. Integrated Development Environment for R.
Russo, S.J., Murrough, J.W., Han, M., Charney, D.S., Nestler, E.J., 2012. Review Neurobiology of resilience. Nat. Neurosci. 15, 1475–1484.
Rutter, M., 2012. Resilience as a dynamic concept. Dev. Psychopathol. 24, 335–344.
Salmelin, R., Baillet, S., 2009. Electromagnetic brain imaging. Hum. Brain Mapp. 30, 1753–1757.
Santarnecchi, E., Rossi, S., Rossi, A., 2015. The smarter, the stronger: intelligence level correlates with brain resilience to systematic insults. Cortex 64, 293–309.
Selemon, L.D., Zecevic, N., 2015. Schizophrenia: a tale of two critical periods for prefrontal cortical development. Transl. Psychiatry 5.
Seligman, M.E., Rosellini, R.A., Kozak, M.J., 1975. Learned helplessness in the rat: time course, immunization, and reversibility. J. Comp. Physiol. Psychol. 88, 542–547.
Shafi, M.M., Vernet, M., Klooster, D., Chu, C.J., Boric, K., Barnard, M.E., Romatoski, K., Westover, M.B., Christodoulou, J.A., Gabrieli, J.D.E., Whitfield-Gabrieli, S., Pascual-Leone, A., Chang, B.S., 2015. Physiological consequences of abnormal connectivity in a developmental epilepsy. Ann. Neurol. 77, 487–503.
Stern, Y., Arenaza-Urquijo, E.M., Bartrés-Faz, D., Belleville, S., Cantilon, M., Chetelat, G., Ewers, M., Franzmeier, N., Kempermann, G., Kremen, W.S., Okonkwo, O., Scarmeas, N., Soldan, A., Udeh-Momoh, C., Valenzuela, M., Vemuri, P., Vuoksimaa, E., Arenaza Urquiljo, E.M., Bartrés-Faz, D., Belleville, S., Cantillon, M., Chetelat, G., Clouston, S.A.P., Estanga, A., Ewers, M., Franzmeier, N., Gold, B., Habeck, C., Jones, R., Kempermann, G., Kochhann, R., Kremen, W., Lim, Y.Y., Martínez-Lage, P., Morbelli, S., Okonkwo, O., Ossenkoppele, R., Pettigrew, C., Rosen, A.C., Scarmeas, N., Soldan, A., Song, X., Udeh-Momoh, C., Stern, Y., Valenzuela, M., Van Loenhoud, A.C., Vemuri, P., Vuoksimaa, E., 2018. Whitepaper: defining and investigating cognitive reserve, brain reserve, and brain maintenance. Alzheimer's Dementia 1–7.
Tadel, F., Bock, E., Niso, G., Mosher, J.C., Cousineau, M., Pantazis, D., Leahy, R.M., Baillet, S., 2019. MEG/EEG group analysis with brainstorm. Front. Neurosci. 13, 1–21.
Thomas Yeo, B.T., Krienen, F.M., Sepulcre, J., Sabuncu, M.R., Lashkari, D., Hollinshead, M., Roffman, J.L., Smoller, J.W., Zöllei, L., Polimeni, J.R., Fisch, B., Liu, H., Buckner, R.L., 2011. The organization of the human cerebral cortex estimated by intrinsic functional connectivity. J. Neurophysiol. 106, 1125–1165.
Torales, J., O'Higgins, M., Castaldelli-Maia, J.M., Ventriglio, A., 2020. The outbreak of COVID-19 coronavirus and its impact on global mental health. Int. J. Soc. Psychiatr. 66, 317–320.
Tost, H., Champagne, F.A., Meyer-Lindenberg, A., 2015. Environmental influence in the brain, human welfare and mental health. Nat. Neurosci. 18, 4121–4131.
WHO. WHO Executive Board stresses need for improved response to mental health impact of public health emergencies [WWW Document]. URL. https://www.who.int/news/item/11-02-2021-who-executive-board-stresses-need-for-improved-response-to-mental-health-impact-of-public-health-emergencies. (Accessed 23 February 2021).
Wright, M.O., Masten, A.S., Narayan, A.J., 2013. Resilience processes in development: four waves of research on positive adaptation in the context of adversity. In: Goldstein, S., Brooks, R.B. (Eds.), Handbook of Resilience in Children. Springer US, Boston, MA, pp. 15–37.
Xue, M., Atallah, B.V., Scanziani, M., 2014. Equalizing excitation-inhibition ratios across visual cortical neurons. Nature 511, 596–600.

Supplementary Materials for

TMS-evoked prefrontal reactivity as a toy model of mental health outcomes during the COVID-19 pandemic

Ruben Perellón-Alfonso, María Redondo-Camós, Kilian Abellaneda-Pérez, Gabriele Cattaneo, Selma Delgado-Gallén, Goretti España-Irla, Javier Solana Sánchez, José M. Tormos, Alvaro Pascual-Leone, David Bartrés-Faz

Correspondence to: DBF, dbartres@ub.edu; APL, apleone@hsl.harvard.edu

Included here:

Structural MRI acquisition parameters

TMS target determination procedures

Figs. S1, S2 and S3

Supplementary References

Tables S1 and S2

PHQ-4 Questionnaire

PSS Questionnaire

Structural MRI acquisition parameters

T1 and T2-weighted anatomical MRI scans were obtained for all participants and used for neuronavigation and EEG source reconstruction. Participants undertook a high resolution (0.8x0.8x0.8mm^3) 3D MP-RAGE T1 weighted structural magnetic resonance image obtained from a 3T Siemens Magnetom Prisma machine. A total of 208 contiguous axial slices were obtained in ascending fashion (sequence parameters of repetition time = 2400ms, echo time = 2.22ms, TI = 1000ms, flip angle = 8º, slice thickness=0.8 mm and field of view =256mm). Additionally, a high resolution (0.8x0.8x0.8mm^3) 3D SPC T2 weighted structural magnetic resonance image was obtained from the same machine (sequence parameters of repetition time = 3200ms, echo time = 563ms, flip angle = 120º, slice thickness=0.8 mm and field of view =256mm). Image quality control measures were implemented manually by a trained MRI technician to ensure that these did not contain MRI artifacts or excessive motion. The T1 was used for neuronavigation, while the T2 was used, together with the T1, to produce high quality segmentations and meshes for EEG source reconstruction.

TMS target determination procedures

For the 29 first subjects of the sample, which were recorded in 2018, individualized targets were determined anatomically. Left-DLPFC stimulation was targeted at the superior half of the middle frontal gyrus, approximately 3 cm anterior to the precentral sulcus. Left-IPL was targeted at the superior edge of the angular gyrus, roughly 1cm inferior to the intraparietal sulcus. For the remaining 45 subjects, which were recorded between 2019 and 2020, targets were determined based on the group-level resting-state seven functional networks parcellation by Yeo and colleagues (Thomas Yeo et al., 2011), according to the method described first by Ozdemir and

colleagues (Ozdemir et al., 2020). Briefly, confidence maps for each resting state network across a sample of 1000 healthy subjects were used. In these maps, each vertex has a confidence value of belonging to a particular network (ranging from -1 to 1), with larger values indicating higher confidence. Using these maps at the group level it is possible to select the most consistent and reliable regions, within the angular gyrus and the middle frontal gyrus. Each individual's T1 was then linearly transformed to the MNI space. Finally, the invers transform was used to return the coordinates of interest to each subject's native space, by using the FSL's (Jenkinson et al., 2012) FNIRT tool. These individual coordinates were then used to guide stimulation using a BrainSight neuronavigation system (RogueResearch, Inc., Canada).

The mean MNI coordinates of the anatomical targeting method were x=-44, y=-67, z=44 for IPL and x=-33, y=37, z=48 for L-DLPFC. While mean coordinates of the functional targeting method were x=-53, y=-51, z=18 for IPL and x=-43, y=34, z=42 for L-DLPFC. Figure S1 shows these mean target coordinates on the MNI template.

In order to account for a possible effect of the targeting method on the predictors of interest, target determination method was included in the main analysis as an interaction term for each TMS-EEG reactivity measure.

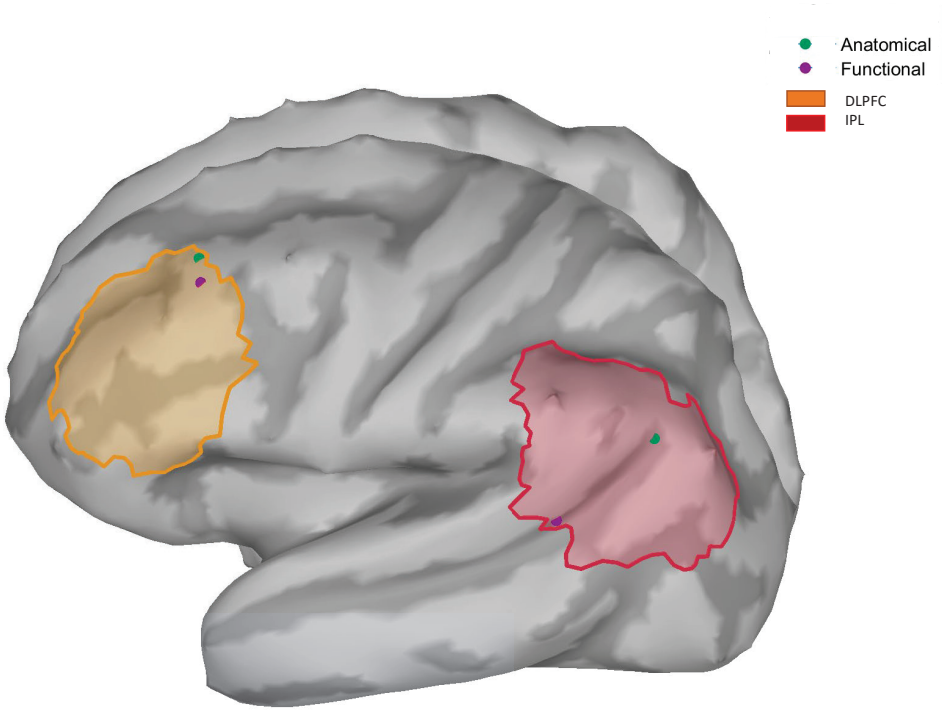

Fig. S1. Mean L-IPL and L-DLPFC coordinates for each targeting method overlayed on the MNI template. Yellow and red ROIs correspond to a projection of the PFC and IPL, respectively, from the 17- network Schaefer parcellation of the Yeo atlas (Schaefer et al., 2018).

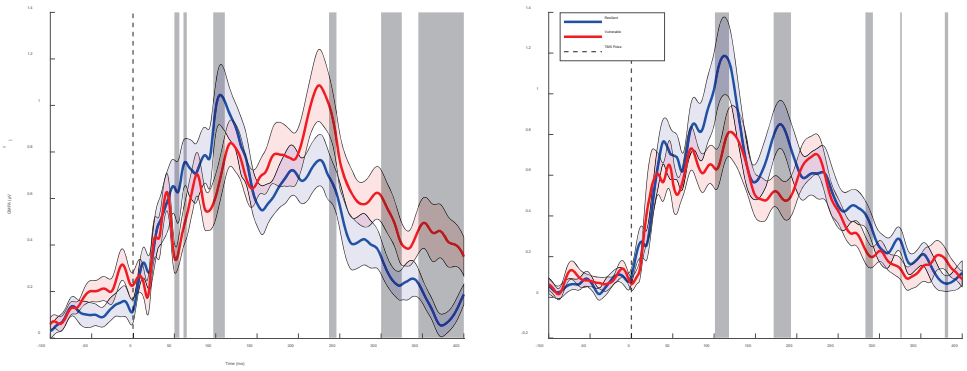

Fig. S2. Uncorrected significant results after permutation testing, of stable against individuals with a negative mental health impact, for global reactivity to DLPFC and IPL stimulation. Grey regions highlight significant differences between curves prior to cluster correction for multiple comparisons. Shaded blue and red contours along the curves depict the standard error of the mean. GMFA: global mean field amplitude. DLPFC, dorsolateral prefrontal cortex; IPL, inferior parietal lobule.

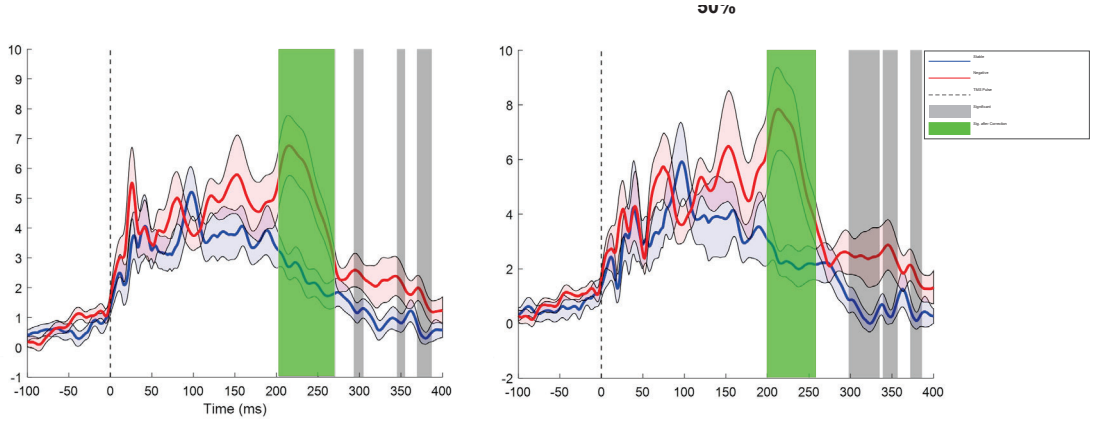

Fig. S3. Results of permutation testing for local reactivity after DLPFC stimulation with all participants and only with participants that completed stimulation at both targets (which corresponds to 50% of the sample). Grey regions highlight significant differences between curves prior to cluster correction for multiple comparisons. Green regions highlight significant differences after correction for multiple comparisons.

Shaded blue and red contours along the curves depict the standard error of the mean. Note that the curves are similar in both graphs and the green regions have similar locations and lengths. Any discrepancies between the grey areas of the original graph depicted in Figure 2.A and the left panel of this figure are inherent to permutation testing inconsistencies between test runs for uncorrected results.

Supplementary References

Jenkinson, M., Beckmann, C.F., Behrens, T.E.J., Woolrich, M.W., Smith, S.M., 2012. NeuroImage 62, 782–790. https://doi.org/10.1016/j.neuroimage.2011.09.015

Ozdemir, R.A., Tadayon, E., Boucher, P., Momi, D., Karakhanyan, K.A., Fox, M.D., Halko, M.A., Pascual-Leone, A., Shafi, M.M., Santarnecchi, E., 2020. Individualized perturbation of the human connectome reveals reproducible biomarkers of network dynamics relevant to cognition. Proc. Natl. Acad. Sci. U. S. A. 117, 8115–8125. https://doi.org/10.1073/pnas.1911240117

Schaefer, A., Kong, R., Gordon, E.M., Laumann, T.O., Zuo, X.-N., Holmes, A.J., Eickhoff, S.B., Yeo, B.T.T., 2018. Local-Global Parcellation of the Human Cerebral Cortex from Intrinsic Functional Connectivity MRI. Cereb. Cortex 28, 3095–3114. https://doi.org/10.1093/cercor/bhx179

Thomas Yeo, B.T., Krienen, F.M., Sepulcre, J., Sabuncu, M.R., Lashkari, D., Hollinshead, M., Roffman, J.L., Smoller, J.W., Zöllei, L., Polimeni, J.R., Fisch, B., Liu, H., Buckner, R.L., 2011. The organization of the human cerebral cortex estimated by intrinsic functional connectivity. J. Neurophysiol. 106, 1125–1165. https://doi.org/10.1152/jn.00338.2011

Table S1. Descriptive statistics of variables used in multivariate MANOVA. Means and standard deviations are reported. PHQ4, four-item patient health questionnaire; COVID, coronavirus disease; RMT, resting motor threshold; MSO, maximum stimulator output.

Mental Health Outcome	*Age*	*Gender*	*Years of Education*	*PHQ4 Score Pre-COVID*	*RMT (%MSO)*
Stable (*n*=32)	55.16 ±7.23	18 male	18.47 ±3.46	2.16 ±2.49	61.47 ±9.17
Negative (*n*=32)	55.34 ±7.21	22 male	17.72 ±3.98	1 ±1.29	63.28 ±10.70

Table S2. Detailed results of the five regression models employed. The three values for each predictor report regression estimates, standard errors in parenthesis and the t-statistic.

	Dependent variable:				
	Mental Health During Lock-down				
	(Full DLPFC)	(Reduced DLPFC)	(Full IPL)	(Reduced+Baseline EEG)	(Reduced Subsample+IPL)
DLPFC Local	0.001**	0.0004***		0.0004***	0.0004*
	(0.0002)	(0.0001)		(0.0001)	(0.0002)
	t = 3.270	t = 3.662		t = 3.631	t = 2.437
DLPFC Global	-0.000				
	(0.000)				
	t = -1.619				
IPL Local			-0.0001		-0.0003
			(0.0003)		(0.0003)
			t = -0.217		t = -1.029
IPL Global			-0.000		
			(0.000)		
			t = -0.219		
Age	-0.013		-0.011		
	(0.009)		(0.013)		
	t = -1.420		t = -0.823		
Gender	0.163		-0.067		
	(0.147)		(0.201)		
	t = 1.107		t = -0.334		
Education	-0.049**	-0.053**	-0.028	-0.053**	-0.071*
	(0.017)	(0.016)	(0.025)	(0.016)	(0.029)
	t = -2.863	t = -3.404	t = -1.109	t = -3.361	t = -2.458
TMS Date	0.013		-0.026		
	(0.020)		(0.024)		
	t = 0.674		t = -1.105		
DLPFC Local : Targeting Method	-0.0003				
	(0.0002)				
	t = -1.349				
DLPFC Global : Targeting Method	0.000				
	(0.000)				
	t = 0.976				
IPL Local : Targeting Method			0.0001		
			(0.0004)		
			t = 0.307		
IPL Global : Targeting Method			0.000		
			(0.000)		
			t = 0.281		
DLPFC Local pre-TMS Baseline				0.003	
				(0.004)	
				t = 0.668	
Constant	1.798**	1.219***	2.254*	0.221	1.924**
	(0.614)	(0.285)	(1.003)	(1.522)	(0.561)
	t = 2.926	t = 4.279	t = 2.247	t = 0.145	t = 3.427
Observations	56	56	55	56	37
R^2	0.345	0.284	0.065	0.291	0.228
Adjusted R^2	0.234	0.257	-0.097	0.250	0.158
Residual Std. Error	0.459 (df = 47)	0.452 (df = 53)	0.643 (df = 46)	0.454 (df = 52)	0.673 (df = 33)
F Statistic	3.099** (df = 8; 47)	10.533*** (df = 2; 53)	0.400 (df = 8; 46)	7.098*** (df = 3; 52)	3.248* (df = 3; 33)
Note:					*p<.05; **p<.01; ***p<.001

4 item Patient Health Questionnaire (PHQ-4)

Over the last 2 weeks, how often have you been bothered by the following problems?	Not at all	Several days	More than half the days	Nearly every day
1. Feeling nervous, anxious or on edge	0	1	2	3
2. Not being able to stop or control worrying	0	1	2	3
3. Little interest or pleasure in doing things	0	1	2	3
4. Feeling down, depressed, or hopeless	0	1	2	3

Scoring

PHQ-4 total score ranges from 0 to 12, with categories of psychological distress being:

- None 0-2
- Mild 3-5
- Moderate 6-8
- Severe 9-12

Anxiety subscale = sum of items 1 and 2 (score range, 0 to 6)

Depression subscale = sum of items 3 and 4 (score range, 0 to 6)

On each subscale, a score of 3 or greater is considered positive for screening purposes

Kroenke, K., Spitzer, R.L., Williams, J.B.W., Löwe, B., 2009. An Ultra-Brief Screening Scale for Anxiety and Depression: The PHQ–4. Psychosomatics 50, 613–621. https://doi.org/10.1016/s0033-3182(09)70864-3

Perceived Stress Scale (PSS)

1. In the last month, how often have you been upset because of something that happened unexpectedly?
2. In the last month, how often have you felt that you were unable to control important things in your life?
3. In the last month, how often have you felt nervous and “stressed”?
4. In the last month, how often have you dealt successfully with irritating life hassles?
5. In the last month, how often have you felt that you were effectively coping with important changes that were occurring in your life?
6. In the last month, how often have you felt confident about your ability to handle your personal problems?
7. In the last month, how often have you felt that things were going your way?
8. In the last month, how often have you found that you could not cope with all the things that you had to do?
9. In the last month, how often have you been able to control irritations in your life?
10. In the last month, how often have you felt that you were on top of things?
11. In the last month, how often have you been angered because of things that happened that were outside of your control?
12. In the last month, how often have you found yourself thinking about things that you have to accomplish?
13. In the last month, how often have you been able to control the way you spend your time?
14. In the last month, how often have you felt difficulties were piling up so high that you could not overcome them?

Scoring

- [0=never; 1=almost never; 2=sometimes; 3=fairly often; 4=very often]
- Items 4, 5, 6, 7, 9, 10, and 13 are scored in reverse direction.

3.2. STUDY 2

Perellón-Alfonso, R., Oblak, A., Kuclar, M., Škrlj, B., Skodlar, B., Pregelj, P., Pileckyte, I., Abellaneda-Pérez, K., Bartrés-Faz, D., Repovš, G. and Bon, J. 2023. Dense Attentional Network identifies EEG abnormalities during working memory performance of patients with schizophrenia. Frontiers in Psychiatry, 14, 1205119.

frontiers | Frontiers in Psychiatry

TYPE Original Research
PUBLISHED 25 September 2023
DOI 10.3389/fpsyt.2023.1205119

OPEN ACCESS

EDITED BY
Elisabetta C. del Re,
Harvard Medical School, United States

REVIEWED BY
Mohammad S. E. Sendi,
Harvard Medical School, United States
Rebekah Trotti,
Beth Israel Deaconess Medical Center
and Harvard Medical School, United States

*CORRESPONDENCE
Ruben Perellón-Alfonso
✉ ruben.perellon@ub.edu
Jurij Bon
✉ jurij.bon@mf.uni-lj.si

RECEIVED 13 April 2023
ACCEPTED 04 September 2023
PUBLISHED 25 September 2023

CITATION
Perellón-Alfonso R, Oblak A, Kuclar M, Škrlj B, Pileckyte I, Škodlar B, Pregelj P, Abellaneda-Pérez K, Bartrés-Faz D, Repovš G and Bon J (2023) Dense attention network identifies EEG abnormalities during working memory performance of patients with schizophrenia.
Front. Psychiatry 14:1205119.
doi: 10.3389/fpsyt.2023.1205119

Dense attention network identifies EEG abnormalities during working memory performance of patients with schizophrenia

Ruben Perellón-Alfonso[1,2]*, Aleš Oblak[3], Matija Kuclar[4], Blaž Škrlj[5], Indre Pileckyte[6], Borut Škodlar[3,4], Peter Pregelj[3,4], Kilian Abellaneda-Pérez[1,2,7], David Bartrés-Faz[1,2], Grega Repovš[8] and Jurij Bon[3,4]*

[1]Faculty of Medicine and Health Sciences, and Institute of Neurosciences, University of Barcelona, Barcelona, Spain, [2]Institute of Biomedical Research August Pi i Sunyer (IDIBAPS), Barcelona, Spain, [3]University Psychiatric Clinic Ljubljana, Ljubljana, Slovenia, [4]Department of Psychiatry, Faculty of Medicine, University of Ljubljana, Ljubljana, Slovenia, [5]Jožef Stefan Institute, Ljubljana, Slovenia, [6]Center for Brain and Cognition, Pompeu Fabra University, Barcelona, Spain, [7]Institut Guttmann, Institut Universitari de Neurorehabilitació Adscrit a la UAB, Barcelona, Spain, [8]Department of Psychology, Faculty of Arts, University of Ljubljana, Ljubljana, Slovenia

Introduction: Patients with schizophrenia typically exhibit deficits in working memory (WM) associated with abnormalities in brain activity. Alterations in the encoding, maintenance and retrieval phases of sequential WM tasks are well established. However, due to the heterogeneity of symptoms and complexity of its neurophysiological underpinnings, differential diagnosis remains a challenge. We conducted an electroencephalographic (EEG) study during a visual WM task in fifteen schizophrenia patients and fifteen healthy controls. We hypothesized that EEG abnormalities during the task could be identified, and patients successfully classified by an interpretable machine learning algorithm.

Methods: We tested a custom dense attention network (DAN) machine learning model to discriminate patients from control subjects and compared its performance with simpler and more commonly used machine learning models. Additionally, we analyzed behavioral performance, event-related EEG potentials, and time-frequency representations of the evoked responses to further characterize abnormalities in patients during WM.

Results: The DAN model was significantly accurate in discriminating patients from healthy controls, *ACC* = 0.69, SD = 0.05. There were no significant differences between groups, conditions, or their interaction in behavioral performance or event-related potentials. However, patients showed significantly lower alpha suppression in the task preparation, memory encoding, maintenance, and retrieval phases $F(1,28) = 5.93$, $p = 0.022$, $\eta^2 = 0.149$. Further analysis revealed that the two highest peaks in the attention value vector of the DAN model overlapped in time with the preparation and memory retrieval phases, as well as with two of the four significant time-frequency ROIs.

Discussion: These results highlight the potential utility of interpretable machine learning algorithms as an aid in diagnosis of schizophrenia and other psychiatric disorders presenting oscillatory abnormalities.

KEYWORDS

schizophrenia, working memory (WM), contralateral delay activity (CDA), electroencephalography (EEG), dense attention network (DAN)

1. Introduction

Schizophrenia is a severe neuropsychiatric disorder with a global prevalence of 0.28% and a significant socioeconomic burden (1). The symptoms of schizophrenia can be divided into positive (i.e., hallucinations, delusions and disorganized thinking) and negative [i.e., decreased emotional expression, social withdrawal, and cognitive impairments of memory and executive functions; (2, 3)]. Schizophrenia is thought to be a neurodevelopmental disorder caused by interaction of genetic and early environmental risk factors (4–6), resulting in impaired large-scale connectivity (7, 8) and aberrant brain activity (9, 10). Pathophysiological changes include altered dopamine and glutamate neurotransmission, which is thought to be related to a disruption in the balance of excitation and inhibition in cortical microcircuits, contributing to altered synchronization of neuronal oscillations (11).

Impairment of working memory (WM) is a core cognitive deficit in schizophrenia that significantly correlates with functional capacity and outcome (12), and has been proposed as a warning sign of conversion to psychosis (13). WM is often defined as a system with limited capacity for the temporary storage and manipulation of representations of information necessary to guide behavior in complex goal-directed tasks such as comprehension, learning, and reasoning (14), and it overlaps with other cognitive domains such as attention and executive function (15). In schizophrenia, deficits can be observed in all WM subprocesses and stimulus types (16), and are associated with impairments in proactive cognitive control [i.e., the ability to actively represent goal information in working memory to guide behavior (16)] or attention hyperfocus [i.e., an abnormally narrow and intense focusing of processing resources; (17)]. Deficits have also been detected, in high-functioning patients with preserved WM performance, in the form of increased reaction time variability (18), which has been interpreted as impaired information processing. The visual modality of WM is particularly relevant in schizophrenia, as it strongly correlates with measures of higher cognitive functions and, according to some estimates, may account for up to 40% of the cognitive deficit in patients with schizophrenia (19).

Working memory tasks can be constructed to engage different WM subprocesses either simultaneously [e.g., N-back tasks; (20, 21)] or sequentially [e.g., verbal span tasks, visuospatial change detection tasks; (22, 23)]. Sequential tasks are particularly useful to probe behavioral performance and brain activity during separate time periods of the WM task corresponding to task preparation, encoding, maintenance, and retrieval of information, all of which have been shown to be affected in schizophrenia (24–26).

Electroencephalographic (EEG) studies of event-related potentials (ERPs) elicited during working memory tasks, have shown abnormalities in electrical activity during early evoked responses and late, cognition-related components of schizophrenia patients (27). In visual WM, a lateralized change detection task (23) elicits a corresponding ERP component, the contralateral delay activity (CDA), which has been shown to be closely related to WM capacity and is modulated by load (28). CDA studies in schizophrenia have shown that visual WM capacity is lower, relative to healthy controls, and that patients also show specific impairments in attention control during the task (29). In addition to ERP abnormalities, studies also found changes on synchronized neuronal oscillations in several frequency bands. Specifically, gamma (>30 Hz), which is involved in sensory processing (30) and maintenance of WM information (31), shows lack of synchronization in schizophrenia patients during WM tasks [e.g., (32)]. Theta (4–7 Hz), which supports long range connectivity and coordination of WM items (33), has been reported to be abnormally high during resting state (34) and decoupled from gamma during WM performance (35). Finally, alpha (8–12 Hz) desynchronization (also known as alpha suppression), which reflects the active inhibition of task-irrelevant information (36, 37), has been shown to be impaired in schizophrenia patients and individuals at risk of psychosis during working memory and oddball tasks (24, 38–41).

While these studies have significantly advanced our understanding of the neurophysiological basis of schizophrenia, they typically rely on univariate statistical methods that, while suitable for group-level comparisons, are insufficient for the purposes of individual diagnosis within the framework of precision psychiatry (42, 43). Moreover, these studies highlight the fact that schizophrenia exhibits heterogenic symptoms and intricate neurophysiological foundations that cannot be attributed to a single brain area or neural process and that might be shared across psychiatric disorders (44). This complexity makes precise differential diagnosis and neurophysiological characterization of individual patients challenging. To confront these challenges, the field of psychiatry has increasingly turned to machine learning, a class of artificial intelligence approaches where algorithms are designed to make successful predictions without explicit programming (45). A growing number of studies have used EEG data to successfully classify patients and controls with high accuracy (46–52). These results have the potential to yield clinically translatable improvements in diagnosis. However, the best performance is often achieved by deep convolutional neural network models, which are said to be "black boxes," since there is no straightforward solution to disentangle how the

algorithm transforms the input data to model a particular output (53). This characteristic limits their utility for investigating the neurophysiological substrate of schizophrenia and identifying suitable biomarkers for early detection, consequently, more transparent and interpretable deep learning models are needed to fill this gap (54).

A promising alternative is the dense attention network (DAN), a type of deep learning model based on the attention model (55), a simple mechanism that scatters input signals and highlights only the parts of the feature space that are relevant to the task at hand. Crucially, the attention layers can output a probability distribution over the input space, thus providing an insight into the inner workings of the neural network, in the form of a one-to one mapping of the relative contribution of each feature in the input space (56, 57).

Here, we took a data-driven machine learning approach to determine the distribution of EEG signatures specific to schizophrenia patients over the time course of a visuospatial change detection task. Based on previous encouraging reports (46–52), we hypothesized that machine learning could be used to successfully classify patients from controls based on EEG alone. We chose an interpretable subtype of machine learning based on the attention model (55), with the hypothesis that specific temporal signatures would be most discriminative of patients and controls. We hypothesized that differences between schizophrenia patients and control subjects would also be evident using univariate statistical methods, particularly on oscillatory activity related to attention control (i.e., in the alpha frequency band), which has been consistently reported to be impaired in patients with schizophrenia, and would be most prominent during the task preparation, encoding, maintenance or memory retrieval phases of the task time-course (24, 39, 41). Finally, we expected this significantly different task segments to overlap with the features found to be most discriminative by the DAN model. This correspondence is of crucial importance if machine learning is to become not just a diagnostic aid, but also a tool capable of proving the neurophysiological substrate of schizophrenia (54).

2. Materials and methods

2.1. Study participants

Fifteen patients with a mean age of 28.1 years, *SD* = 3.9, and an average of 13.4 years of education, *SD* = 1.1, were recruited from the Department for Psychotherapy of Psychotic Disorders at the University Psychiatric Clinic Ljubljana (see **Supplementary Table 1** for descriptive statistics on demographics). All participants included in the study were male, due to a lack of a representative number of female participants available at the time of recruitment. All patients had a diagnosis of schizophrenia (12 subjects) or schizoaffective disorder (3 subjects). The diagnoses were confirmed according to the DSM-IV criteria by experienced clinicians (BŠ and JB) involved in the study. At the time of the experiment, all patients were taking second generation antipsychotic medication and were in stable symptomatic remission, with an average PANSS score (58) of 77.1 (*SD* = 15.3), and were cleared for inclusion in psychodynamic group psychotherapy. The patients' mean duration of illness was 6.1 years (*SD* = 3.3), and the mean number of hospitalizations was 2.9 (*SD* = 2.1). For further clinical details, see **Supplementary Table 1**.

Additionally, we recruited a control group of 15 male participants of comparable age, *M* = 26.8 years, *SD* = 5.5, and years of education, *M* = 14.4, *SD* = 1.2. The study was approved by the Medical Ethics Committee of the Republic of Slovenia and all participants signed an informed consent form according to the Declaration of Helsinki.

2.2. Visual working memory task and EEG recording

A lateralized change detection task with distractors (23, 59) was implemented using PsychoPy (60). First, participants were shown an arrow cue for 200 ms, the direction of which indicated to which half of the visual field they should direct their attention. This was followed first by a fixation cross shown for 400 ms and then by a memory array shown for 300 ms. The memory array consisted of 2 or 4 rectangles (in each half of the visual field). The rectangles were colored either blue, or blue and red (in the distractor condition), and were shown in one of 4 possible orientations (0°, 45°, 90°, or 135°). Participants were asked to remember the orientations of the blue rectangles shown on the cued side of the visual field. The presentation of the memory array was followed by a delay of 1400 ms before the presentation of a test array, that remained for 4 s and was then followed by 2 s without any stimulus. The test array was either identical to the memory array or with only one of the randomly selected (blue) rectangles on the cued side changing its orientation in half of the trials. The participants' task was to indicate whether any of the target items had changed by pressing the corresponding button on a response box (**Figure 1**).

There were three task conditions, differing in the number of target items and the presence of a distractor:

1. A condition with two blue rectangles shown on each side (low memory load; condition 2),
2. A condition with four blue rectangles shown on each side (high memory load: condition 4), and
3. A condition with two blue and two red rectangles shown on each side (distractor condition; condition 2+2).

In the 2+2 condition, participants had to successfully inhibit the two red distractor rectangles presented together with the two blue memory rectangles. The trials belonging to the different conditions were interleaved within a block. Participants were familiarized with the task during the practice trials, and the experimenter ensured that they all performed with at least 70% accuracy.

Participants performed 200 trials for each of the three conditions in an electrically shielded and soundproofed room while seated in a comfortable chair in front of a cathode ray monitor. Throughout the task, the EEG signal was recorded using four BrainAmp amplifiers connected to a 128-channel actiCAP system with active electrodes in a standard montage (Brain Products GmbH, Munich, Germany). The EEG was recorded with a 2000 Hz low-pass filter and digitized at a sampling rate of 500 Hz.

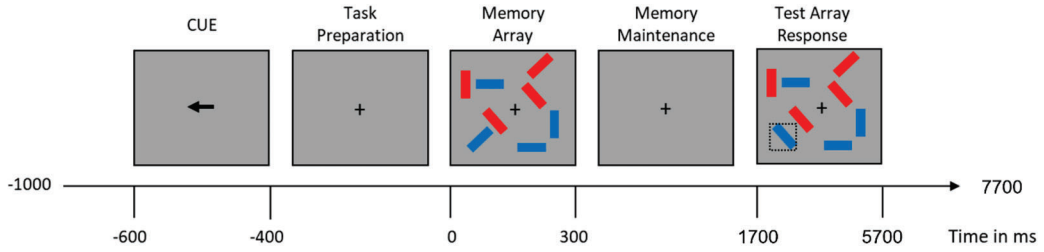

FIGURE 1
Visual working memory trial time-course. Doted square containing the blue item on the lower left part of the test array illustrates an item that changed from the memory array.

2.3. Working memory task performance metrics

To compare behavioral task performance between groups we computed memory capacity index K (61) and intra-individual reaction time variability (see **Supplementary Table 2** for detailed descriptive statistics of task performance).

2.3.1. Working memory capacity

WM capacity index K was calculated for each subject and condition using the Pashler variant of the formula appropriate for a whole-display variant of a change detection task (61):

$$K = N\left(\frac{HR - FAR}{1 - FAR}\right)$$

Where *HR* is the hit rate, *FAR* is the false alarm rate, and *N* is the number of to-be-remembered items.

2.3.2. Intra-individual reaction time variability

Rentrop and colleagues (18) reported schizophrenia patients with relatively well-preserved WM performance still showed higher intraindividual variability in reaction times. Therefore, we compared the coefficient of variation of reaction times between the two groups, which was defined as the ratio of the standard deviation to the mean of the reaction times.

2.4. EEG preprocessing

Electroencephalographic data were preprocessed using EEGLAB functions (62) and custom-made MATLAB (The MathWorks Inc., Massachusetts, USA) scripts. Data were first filtered with a high-pass filter with a 0.5 Hz frequency cutoff, then the line frequency noise was removed from the signal using the CleanLine algorithm (63). Visual inspection was aided by statistical thresholding based on variance and Kurtosis to identify bad channels, M = 15.3, SD = 4.6. Next data were referenced to the average of the mastoid channels (i.e., TP9 and TP10) and segmented into epochs around the onset of the memory array (−1,000 ms to 4,500 ms). At this point, epoched data were visually inspected, and epochs that contained obvious artifacts (e.g., high-frequency or muscular artifacts) were removed. Because lateral eye movements would impact the magnitude of the CDA, electrooculogram channels were visually inspected for the time period from the presentation of arrow cue to the presentation of memory array, and all epochs with eye blinks or horizontal eye movements in this period were also discarded, bringing the total average of epochs removed to 47.6.3, SD = 29.5. Next, the AMICA algorithm (64) was used to identify and then remove any remaining artifactual independent components M = 6.4, SD = 2.4. Last, the channels previously removed from the data were spline interpolated based on the signal from the neighboring electrodes.

2.5. Machine learning methods and empirical evaluation

The aim of this analysis was to investigate the potential of machine learning methods to discriminate patients from controls. Given the heterogeneous nature of schizophrenia, our aim was to produce a model capable of discriminating between patients and controls without relying on any specific clinical data, leveraging only EEG data that has been preprocessed using relatively simple and well-established procedures. The dense attention network model was deliberately chosen because it retains a sufficient level of interpretability to explain which events were most important in distinguishing patients from controls over the time course of the experiment (57) The dimensionality reduction of the data, the construction of the DAN architecture, and its evaluation, were performed using in house methods (a detailed description can be found in **Supplementary material**; scripts and data used to design, train, and evaluate the different machine learning models[1]). Briefly, the dimensionality of the preprocessed data was reduced from 4d to 1d by incremental stepwise averaging of three of the four original dimensions (i.e., 3 conditions left and 3 right, 128 channels, 2,750 time-points and 153 trials on average):

$$S_\gamma = \frac{1}{RNZ}\sum_{\mu=1}^{R}\left(\sum_{\nu=1}^{N}\left(\sum_{\sigma=1}^{Z} M_{\mu\nu\gamma\sigma}\right)\right)$$

Where μ, ν, γ, and σ stand for condition, channel, time, and trial, respectively. In this way, a 1d array was created for each subject while preserving the temporal characteristics of the data. This simplified dimensionality of the data allowed us to train a dense

1 https://gitlab.com/MaticKu/shizo

attention network model (DAN). The final input dataset used in the model was numeric and consisted of 30 instances (i.e., number of subjects), each described by 2,750 features (i.e., corresponding to the preserved time dimension after the incremental stepwise averaging of the original 4d EEG data set).

Empirical evaluation of model performance consisted of leave-one-out cross-validation repeated ten times for each model. For the DAN model there were 160 possible configurations evaluated. We used the Adam optimization algorithm (65) and we considered the following parameters: dropout rate (0.01, 0.05, 0.2, and 0.5) hidden layer size (16, 32, 64, and 128), number of epochs (2, 4, 8, 16, and 32) and learning rate (0.001 and 0.0001).

The performance of the model was compared with the performance of other simpler architectures (i.e., linear regression, radio frequency machine learning, support vector machine, radial basis function and k-nearest neighbor), and common deep learning models (convolutional neural network and feed forward neural network).

We report the average and standard deviation of the resulting accuracy, precision and recall from these iterations. We also report the F_1 scores, computed as follows:

$$F_1 = 2\frac{precision \cdot recall}{precision + recall}$$

All models were implemented using the PyTorch deep learning library (66) and evaluated on a Tesla graphics card accelerator (Nvidia Corp. Santa Clara, USA).

Throughout training of the DAN model, a bijection is maintained with the input space (i.e., the attention layer corresponds to the input space in a one-to-one relationship). Therefore, we were able to use the attention layer's output directly as a probability distribution over the input space. This attention value vector quantifies the contribution of each feature (EEG time-point in the WM task time-course) in the distinction between patients and controls.

2.6. Event related potential analysis

In order to capture the electrophysiological correlate of WM capacity, we computed the contralateral delayed activity (CDA) as the difference between the contralateral and ipsilateral (relative to the cued side for the memory array) ERP waveforms using an established procedure (23, 28). For each subject, the mean amplitude of the resulting CDA difference curves was measured for the average of all parieto-occipital electrodes and the time segment from 500 ms to 900 ms after the presentation of the memory array (**Figure 2**). The resulting mean CDA amplitude data were used for further statistical analysis.

2.7. Time-frequency analysis

To compare the oscillatory dynamics between patients and controls, throughout the trial time course, we performed a time-frequency analysis of total power (i.e., comprising induced and evoked power) for the epoched data. Data was decomposed into the time-frequency domain by convolving a set of complex Morlet wavelets from 1 Hz to 60 Hz, in steps of 1 Hz, with a logarithmically spaced wavelet width of 4–10 cycles. The resulting time-frequency maps were normalized as the decibel (db) change from baseline (i.e., −850 to −650 ms from the memory array presentation). Time-frequency regions of interest (ROIs) were then determined based on the main WM task phases and frequency bands. Specifically, the time segments of interest (i.e., ROIs x-axis) were, *preparation* for the task (−400 to 0 ms), *encoding* (0–300 ms), *maintenance* (300–1,700 ms) and *retrieval* of the memory array (1,700–3,060 ms). The end of the time window for the memory retrieval phase was chosen based on the average reaction time plus one standard deviation in the slower group (i.e., patients; **Supplementary Table 2**). We included four frequency bands of interest (i.e., ROIs y-axis), theta (4–7 Hz), alpha (8–12 Hz), beta (13–29 Hz) and gamma (30–60 Hz) to explore possible group differences across the frequency spectrum. For further statistical analysis, the average of all time-frequency data points within each ROI for each subject and condition was used.

2.8. Statistical analysis

For behavioral analysis a mixed design ANOVA was used for memory capacity K and another for reaction-time variability. For ERP analysis one mixed design ANOVA was used. For time-frequency total power four mixed design ANOVAs were used, one for each frequency band. All statistical tests were implemented in R (67). Greenhouse-Geisser correction was used in case of sphericity violations. All *post-hoc* comparisons were performed with paired or Welch's *t*-tests with Bonferroni corrections.

3. Results

3.1. Memory capacity K

To test for differences in memory capacity between groups and conditions we used a mixed design ANOVA with a within-subject factor *condition* (condition 2, condition 2+2 and condition 4) and a between-subject factor *group* (patient vs. control). The test revealed no significant main effect of *group*, $F(1,28) = 2.21$, $p = 0.149$, $\eta^2 = 0.043$, but there was a significant effect of *condition*, $F(2,56) = 33.74$, $p < 0.001$, $\eta^2 = 0.344$. *Post-hoc* analysis with a pairwise *t*-test revealed that in condition 4, $M = 2.57$, $SD = 0.86$, memory capacity K was significantly higher than in conditions 2, $M = 1.81$, $SD = 0.14$, $p < 0.001$, $d = 1.236$ and 2+2, $M = 1.76$, $SD = 0.32$ $p < 0.001$, $d = 1.245$. There was no interaction between *group* and *condition*, $F(2,56) = 1.13$, $p = 0.329$, $\eta^2 = 0.017$.

3.2. Reaction time's coefficient of variation

A mixed design ANOVA with a within-subject factor of *condition* (condition 2, condition 2+2 and condition 4) and a between-subject factor of *group* (patient vs. control) was used to test for differences in the coefficient of variation. The test revealed no significant main effect *condition*, $F(2,56) = 1.08$, $p = 0.345$, $\eta^2 = 0.007$, *group*, $F(1,28) = 2.49$, $p = 0.125$, $\eta^2 = 0.068$, or their interaction $F(2,56) = 1.14$, $p = 0.326$, $\eta^2 = 0.007$.

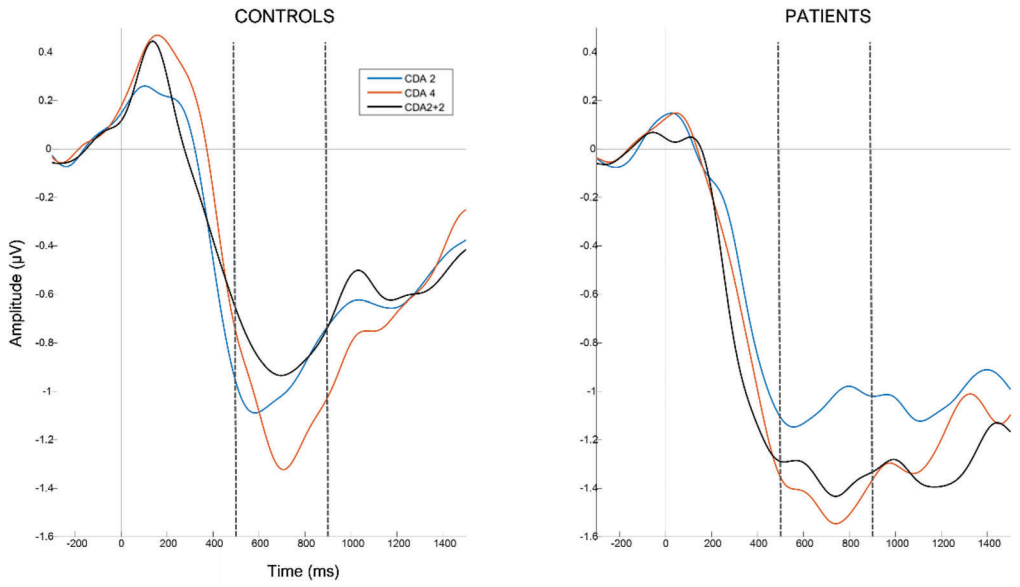

FIGURE 2
Grand average contralateral delayed activity waveforms per each group (i.e., patients **left panel** and controls **right panel**) and condition (2 items in blue, 4 items in red and 2+2 items in black), averaged over parieto-occipital electrodes. Vertical gray lines at time 0 correspond to the presentation of the memory array. Horizontal gray lines correspond to 0 amplitude. Horizontal doted black lines mark the time segment (500–900 ms after memory array onset) from which we extracted the average CDA amplitude for each subject.

3.3. Contralateral delay activity's mean amplitude

To examine the differences in mean CDA amplitude between the two groups and the three experimental conditions, we used a mixed design ANOVA with a within-subject factor *condition* (condition 2, condition 2+2, and condition 4) and a between-subject factor *of group* (patient vs. control). This analysis revealed no significant main effect of *group* $F(1,28) = 0.22$, $p = 0.642$, $\eta^2 = 0.004$, *condition,* $F(2,56) = 3.12$, $p = 0.065$, $\eta^2 = 0.048$, or their interaction $F(2,56) = 0.41$, $p = 0.617$, $\eta^2 = 0.007$.

3.4. Time-frequency power representation

To investigate possible differences between patients and controls in overall power at four frequency bands, we used a mixed design ANOVA for each frequency band with a within-subject factor *condition* (condition 2, condition 2+2, and condition 4), a within-subject factor WM task *phase* (preparation, encoding, maintenance, retrieval), and a between-subject factor *group* (patient vs. control). This analysis revealed a significant *group* effect, $F(1,28) = 5.93$, $p = 0.022$, $\eta^2 = 0.149$, and interaction between *group*, *condition* and task *phase*, $F(6,168) = 2.20$, $p = 0.046$, $\eta^2 = 0.002$, only for the alpha frequency band (for complete results in the theta, beta, and gamma bands see **Supplementary Section 5** and **Supplementary Figure 3**). *Post-hoc* analysis with Welch's *t*-test revealed that patients had overall higher alpha power (i.e., less alpha suppression), $M = -1.04$, $SD = 0.89$, than controls, $M = -2.33$, $SD = 1.84$, $t(20.24) = 2.43$, $p = 0.024$, $d = 0.889$.

To unravel the triple interaction, we ran an additional mixed design ANOVA for each of the four WM task phases, with a within-subject factor *condition* (condition 2, condition 2+2, and condition 4) and a between-subject factor *group* (patients vs. controls). We found that groups differed in each of the 4 WM task phases (**Figure 3**). During task preparation, $F(1,28) = 6.16$, $p = 0.019$, $\eta^2 = 0.167$, patients, $M = -1.09$, $SD = 0.81$, had higher alpha power than controls, $M = -2.36$, $SD = 1.81$, $t(19.41) = 2.48$, $p = 0.022$, $d = 0.906$. During memory encoding, $F(1,28) = 5.73$, $p = 0.024$, $\eta^2 = 0.159$, patients, $M = -0.83$, $SD = 1.00$, had higher alpha power than controls, $M = -2.17$, $SD = 1.93$, $t(21.04) = 2.39$, $p = 0.026$, $d = 0.874$. During memory maintenance, we found a significant interaction between group and condition, $F(2,56) = 3.28$, $p = 0.045$, $\eta^2 = 0.013$. A follow-up analysis revealed that the interaction was driven by the decrease in alpha power from condition 2+2, $M = -1.03$, $SD = 0.96$, to condition 4, $M = -1.13$, $SD = 0.99$, in patients, and increase in alpha power from condition 2+2, $M = -2.63$, $SD = 2.14$, to condition 4, $M = -1.96$, $SD = 1.75$, in controls. Finally, during memory retrieval, $F(1,28) = 4.73$, $p = 0.038$, $\eta^2 = 0.133$, patients, $M = -1.13$, $SD = 1.13$, had higher alpha power than controls, $M = -2.50$, $SD = 2.16$, $t(21.12) = 2.17$, $p = 0.041$, $d = 0.794$.

To summarize, there was a significant difference between patients and controls in the alpha frequency band, but not in other frequency bands. This difference was observed in all four task phases. In support to these univariate results, the difference between patients and controls can also be visually evaluated in time-frequency difference maps, where it can be seen that the differences in alpha band peak after the presentation of the main task stimuli, namely, directional cue, memory array and test array (**Figure 4**).

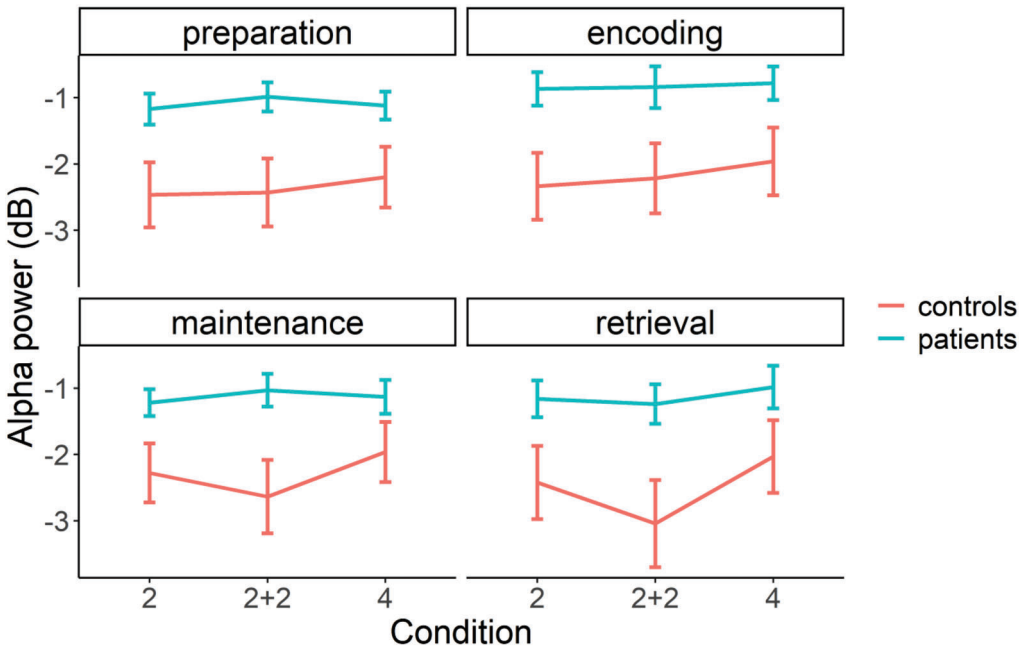

FIGURE 3
Average alpha power baseline normalized in patient (blue line) and control (red line) groups in three different conditions (2, 2+2, and 4) and four WM task phases (preparation, encoding, maintenance, and retrieval). The error bars represent standard error of the mean.

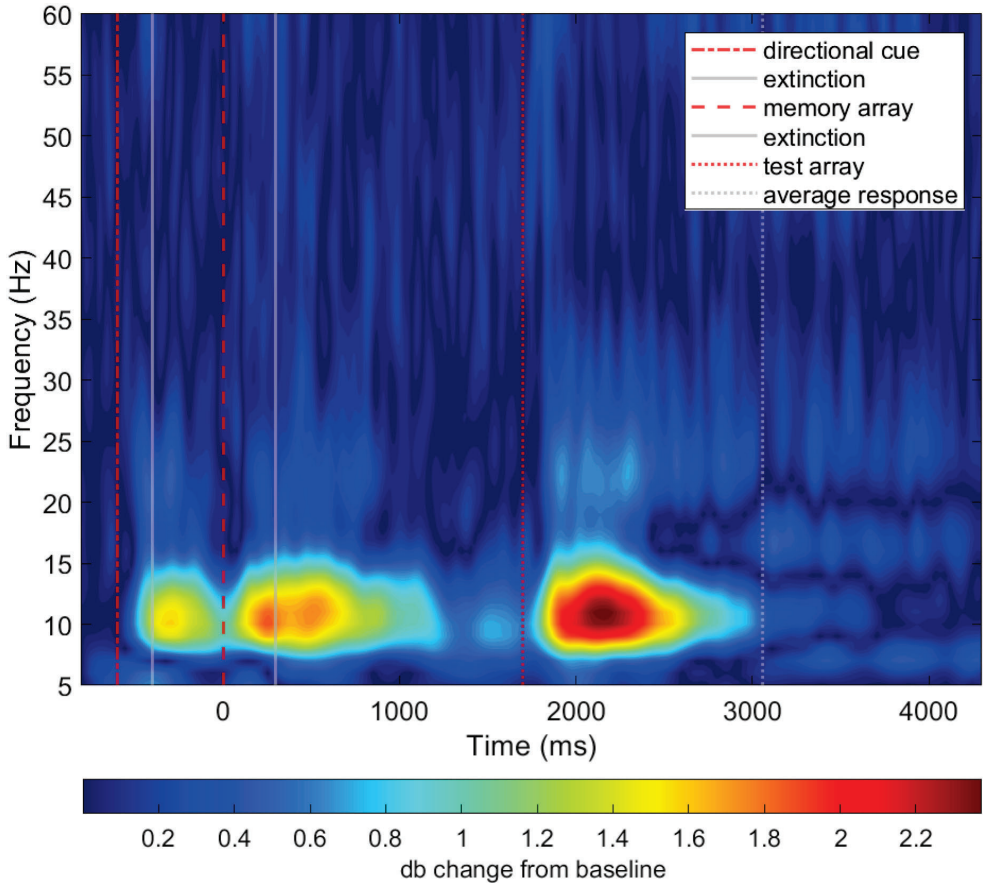

FIGURE 4
Unthresholded average time-frequency representation of total power difference of patients and controls (i.e., patients−controls).

TABLE 1 Summary of the empirical evaluation average results for the different machine learning architectures used.

Model	Accuracy	F1	Recall	Precision
DAN	0.69 ± (0.05)	0.71 ± (0.07)	0.77 ± (0.11)	0.67 ± (0.03)
FFNN	0.71 ± (0.03)	0.72 ± (0.03)	0.73 ± (0.05)	0.70 ± (0.02)
CNN	0.69 ± (0.05)	0.72 ± (0.05)	0.81 ± (0.05)	0.66 ± (0.04)
LR	0.65 ± (0.0)	0.67 ± (0.0)	0.69 ± (0.0)	0.64 ± (0.0)
SVM linear	0.62 ± (0.0)	0.62 ± (0.0)	0.62 ± (0.0)	0.62 ± (0.0)
SVM poly	0.62 ± (0.0)	0.58 ± (0.0)	0.54 ± (0.0)	0.64 ± (0.0)
KNN	0.69 ± (0.0)	0.71 ± (0.0)	0.77 ± (0.0)	0.67 ± (0.0)
RF	0.56 ± (0.08)	0.58 ± (0.09)	0.62 ± (0.11)	0.55 ± (0.07)
SVM rbf	0.58 ± (0.0)	0.62 ± (0.0)	0.69 ± (0.0)	0.56 ± (0.0)

Standard deviations in parenthesis. CNN, convolutional neural network; DAN, dense attention network; FFNN, feed forward neural network; KNN, K-nearest neighbor; LR, linear regression; RF, radio frequency machine learning; SVM, support vector machine; rbf, radial basis function.

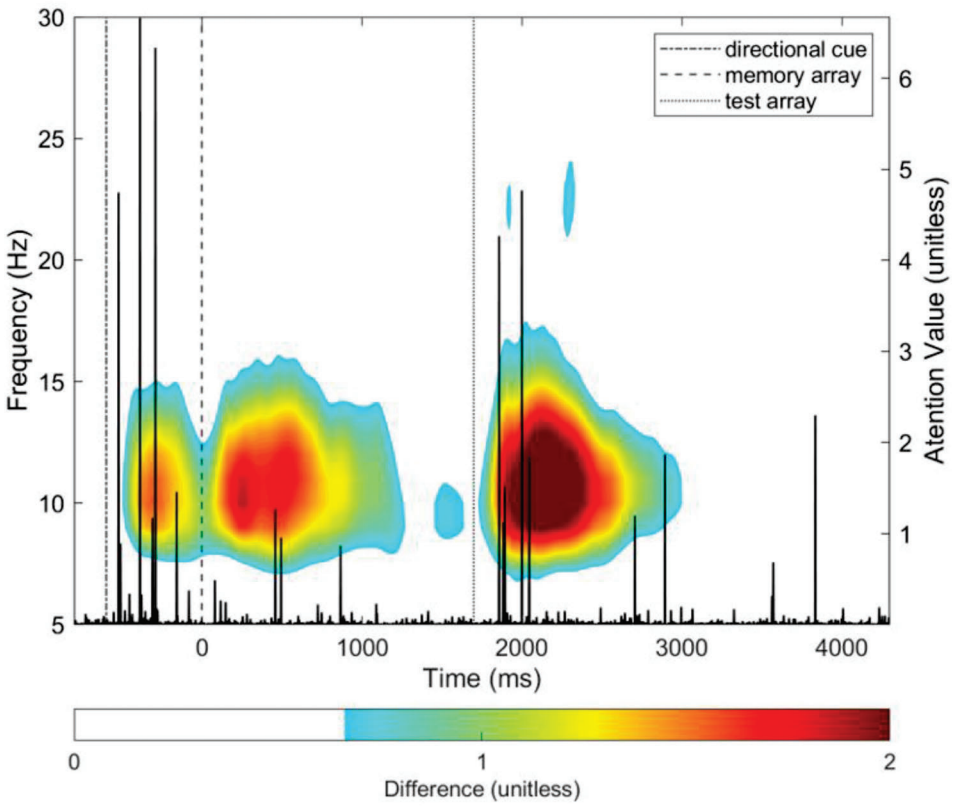

FIGURE 5
DAN attention value vector (in black; y-axis scale on the right side of plot) overlayed on the group difference time-frequency total power time-frequency map for the average of all parieto-occipital electrodes. The difference was computed by subtracting the grand average map of total power of controls from patients (i.e., patients−controls). The colormap is thresholded, for visualization purposes only, to show no color for values lower than 30% of the maximum difference value of 2. See **Figure 4** for unthresholded map.

3.5. Machine learning performance and interpretation

The results from the empirical evaluation show that the DAN model consistently demonstrated accuracy in discriminating patients from controls significantly above chance, *ACC* = 0.69, *SD* = 0.05, F_1 = 0.71, SD = 0.07, *Recall* = 0.77, SD = 0.11, *PRC* = 0.67, SD = 0.03 (**Table 1**). This model outperformed simpler architectures, such as the support vector machine, while performing similarly to other common deep neural network models, such as the convolutional neural network. Full results for all models tested under different subsets of the feature space (i.e., task conditions) can be found in **Supplementary Figure 1** and **Supplementary Table 3**.

Projecting the DAN attention value over the WM task timeline and onto the time-frequency map of group differences shows that the time points most relevant to the model's discrimination between groups (i.e., attention value) overlap with time-frequency ROIs that were found to be significantly different between groups (**Figure 5**),

and correspond to the task preparation and memory retrieval phases of the WM task.

4. Discussion

In this study, we investigated the WM performance and associated EEG signatures of schizophrenia patients and compared them to healthy controls. The results show that in our sample neither WM performance, measured by memory index K and reaction time variability, nor CDA amplitude showed a significant difference between patients and controls. However, statistical analysis in the time-frequency domain revealed, a significant group effect in all time segments of interest (task preparation, memory encoding, maintenance and retrieval) in the alpha-band range (8–12 Hz). We demonstrated that a simple dimensionality reduction procedure consisting of incremental stepwise averaging, that preserves the temporal characteristics of the EEG signal, can be used as input to train a DAN machine learning model capable of successfully discriminating patients from control subjects based on the EEG signal after standard preprocessing alone, with accuracy significantly above chance ($ACC = 0.69$). We then compared the model's performance with simpler machine learning architectures, as well as more common deep neural network models, showing similar performance. Finally, direct mapping of the attention value vector with the WM task trial time course, revealed that the most discriminative time points for the classification overlapped with the task preparation and memory retrieval phases, as well as with the identified time-frequency regions of interest that show significant group differences in alpha suppression, with patients showing less suppression than controls at these ROIs.

4.1. Normal WM performance and contralateral delay activity in schizophrenia patients

In our study, behavioral and CDA results did not differ significantly between patients and controls. This is in contrast with previous studies that generally find working memory performance deficits in schizophrenia (68, 69). Recent studies have found associations between poor performance and deficits in consolidation or early maintenance of stimuli (24), deficits in attention and executive control (70) or less efficient allocation of memory resources (71). Previous studies also report CDA amplitude differences between patients and controls, with amplitude being larger than that of control subjects at low memory load but smaller at high memory load (29), even when their maximum visual WM capacity is equal to that of control subjects. This pattern of impairment may support the theory of inefficient attention hyperfocus on a small number of items, especially when they are salient (17).

Normal behavioral and CDA results in our sample suggest that patients performed well on this particular visual WM task. These results are consistent with previous research showing no differences between high-functioning individuals with schizophrenia and healthy controls in task performance (18, 72) and working memory related ERPs (73, 74). Thus, given the preserved working memory performance and lack of significant CDA abnormalities, our findings may be more representative of high-functioning patients. In this context, it is worth noting that, at the time of recruitment and throughout the data gathering phase, our patients were asymptomatic and engaged in psychodynamic group psychotherapy. While this criterion alone need not imply high-functioning status, given the known associations between engagement in psychodynamic psychotherapy and functional outcome (75), it is reasonable to suspect that our patients might potentially be close to high-functioning.

4.2. Schizophrenia patients exhibit decreased suppression of alpha spectral power during visual WM task

Our analysis revealed significantly lower suppression of non-lateralized parietal alpha spectral power during the task preparation, memory encoding, maintenance, and retrieval phases of the visual WM change detection task. Given the recognized role of oscillations in the alpha frequency band in long-range synchronization (38), top-down control (76, 77), attention (78) and cortical inhibition (79, 80), our time-frequency results may reflect a deficit that makes it difficult for patients to inhibit task-irrelevant brain regions and processes and to maintain efficient attention control, regardless of the experimental condition. These results are consistent with existing literature reporting alpha suppression abnormalities in schizophrenia during working memory tasks (24, 38–41). In the presence of these potential inhibitory and attention deficits, patients might have been able to maintain behavioral performance through various compensatory strategies, such as greater attention effort (17) reflected by less alpha suppression.

4.3. Deep attention networks can discriminate high performing individuals with schizophrenia from healthy controls in EEG data after dimensionality reduction

The dense attention network model implemented in this study was able to classify patients and controls with an accuracy significantly above chance, $ACC = 0.69$ outperforming simpler machine learning architectures, while achieving similar performance to more commonly used deep network models. Moreover, our attention model revealed the relative importance of each feature in the input space for the successful classification of patients and controls. This was possible owing to our proposed data aggregation technique (i.e., incremental stepwise averaging), that allowed us to reduce each patient's preprocessed EEG data to a one-dimensional vector, while preserving the temporal characteristics of the signal.

The results show that the time points that were most discriminative for the machine learning algorithm, overlapped with both the preparatory and memory retrieval phases during the task, as well as with ROIs selected from the time-frequency maps. Furthermore, the two highest peaks in The DAN attention

value vector were found to overlap with the significant main effect of *group* found in time-frequency ROIs in the alpha band during task preparation and memory retrieval phases. Based on this congruence, we can conclude with high *confidence* (81) that the DAN model's decision to classify subjects as patients or controls is based on the same aspects of the data that were revealed by the time-frequency analysis. Given that the detected abnormalities are oscillatory in nature and the DAN algorithm partially operates by convolution (82), it might have been specially suited to detect oscillatory signatures in the EEG. Because, similarly, decomposition of the EEG into the time-frequency domain is often accomplished by convolution of the EEG signal with complex Morlet wavelets, which was our method of choice for the time-frequency analysis in this study.

These results add to the rapidly growing body of literature reporting encouraging results in the use of machine learning to classify patients and controls in schizophrenia (46–52), with the ultimate goal of aiding and improving the challenging diagnosis of such heterogeneous disorder (83). Furthermore, the demonstrated interpretability of our model highlights that machine learning can be designed to serve not only as a diagnostic aid in classification, but also to probe the neurophysiological correlates of schizophrenia and, potentially, other psychiatric disorders.

4.4. Limitations and future directions

This study has some limitations. Our sample size was small, which may have affected statistical power. However, this is a consequence of the challenging goal of recruiting a homogeneous group of schizophrenia patients. Furthermore, our sample is constituted exclusively by males, which may limit the translational value of the study. Finally, although the accuracy of our DAN machine learning model is significant and provides additional information about the differences between patients and controls, it is not robust enough to support the direct diagnosis or classification of patients on its own.

Nevertheless, the machine learning and time-frequency results both suggest that in schizophrenia there is a significant impact on working memory processes during the task preparation and maintenance phases. Even in high performing patients that show no significant impact in behavioral performance or ERP correlates, when compared to healthy controls. Furthermore, the features studied could be combined with a broader set of features to support more accurate identification of patients. In that fashion, these techniques could be used as a diagnostic complement to more established clinical assessment methods to help in early detection or differential diagnosis of neuropsychiatric disorders with suspected oscillatory abnormalities. Moreover, the DAN model's accuracy could still be further improved by enriching its input with relevant multimodal data. For instance, as we have argued that the oscillatory abnormalities in the alpha band may indicate an inhibitory and attention deficit, future research could design experiments that would not only include EEG, but also additional techniques such as pupillometry, to measure changes in attention and arousal (84), or non-invasive stimulation, to directly probe the role of inhibitory neural circuits during the task (85). Finally, based on the neurophysiological insight provided by our model, we further encourage the incorporation of interpretable models in schizophrenia research.

Data availability statement

The original contributions presented in the study are publicly available. This data can be found here: https://gitlab.com/MaticKu/shizo.

Ethics statement

The studies involving humans were approved by the Medical Ethics Committee of the Republic of Slovenia. The studies were conducted in accordance with the local legislation and institutional requirements. The participants provided their written informed consent to participate in this study.

Author contributions

JB and GR: study conception and design. JB, RP-A, and IP: data collection. RP-A, MK, BŠkr, and IP: data analysis. RP-A, AO, BŠko, PP, KA-P, GR, and JB: results interpretation. RP-A, AO, and JB: manuscript writing. All authors contributed to the manuscript review and approved the submitted version.

Funding

RP-A was supported by a fellowship from "la Caixa" Foundation (ID 100010434; Fellowship code: LCF/BQ/DI19/11730050). KA-P was financially supported by a Juan de la Cierva-Formacion research grant (FJC2021-047380-I) from the Spanish Ministry of Science and Innovation. IP is supported by a fellowship from "la Caixa" Foundation (ID 100010434; fellowship code LCF/BQ/DI18/11660026). This project has received funding from the European Union's Horizon 2020 Research and Innovation Programme under the Marie Skłodowska-Curie grant agreement No. 713673. This study was supported by Slovenian Research Agency grants P5-0110, P3-0338, J3-1763, and J3-9264.

Acknowledgments

The authors want to thank the participants, without whom this study would not have been possible.

Conflict of interest

GR consults for and holds equity in Neumora Therapeutics and Manifest Technologies.

The remaining authors declare that the research was conducted in the absence of any commercial or financial

relationships that could be construed as a potential conflict of interest.

Publisher's note

All claims expressed in this article are solely those of the authors and do not necessarily represent those of their affiliated organizations, or those of the publisher, the editors and the reviewers. Any product that may be evaluated in this article, or claim that may be made by its manufacturer, is not guaranteed or endorsed by the publisher.

Supplementary material

The Supplementary Material for this article can be found online at: https://www.frontiersin.org/articles/10.3389/fpsyt.2023.1205119/full#supplementary-material

References

1. Charlson FJ, Ferrari AJ, Santomauro DF, Diminic S, Stockings E, Scott JG, et al. Global epidemiology and burden of schizophrenia: Findings from the global burden of disease study 2016. *Schizoph Bull.* (2018) 44:1195–203. doi: 10.1093/schbul/sby058

2. Batinic B. Cognitive models of positive and negative symptoms of schizophrenia and implications for treatment. *Psychiatria Danubina.* (2019) 31:S181–4.

3. Mosolov SN, Yaltonskaya PA. Primary and secondary negative symptoms in schizophrenia. *Front Psychiatry.* (2022) 12:766692. doi: 10.3389/fpsyt.2021.766692

4. Robinson N, Bergen SE. Environmental risk factors for schizophrenia and bipolar disorder and their relationship to genetic risk: current knowledge and future directions. *Front Genet.* (2021) 12:686666. doi: 10.3389/fgene.2021.686666

5. Seidman LJ, Mirsky AF. Evolving notions of schizophrenia as a developmental neurocognitive disorder. *J Int Neuropsychol Soc.* (2017) 23:881–92. doi: 10.1017/S1355617717001114

6. Van Os J, Kenis G, Rutten BPF. The environment and schizophrenia. *Nature.* (2010) 468:203–12. doi: 10.1038/nature09563

7. Howes OD, Shatalina E. Integrating the neurodevelopmental and dopamine hypotheses of schizophrenia and the role of cortical excitation-inhibition balance. *Biol Psychiatry.* (2022) 92:501–13. doi: 10.1016/j.biopsych.2022.06.017

8. Liu Y, Ouyang P, Zheng Y, Mi L, Zhao J, Ning Y, et al. A selective review of the excitatory-inhibitory imbalance in schizophrenia: underlying biology, genetics, microcircuits, and symptoms. *Front Cell Dev Biol.* (2021) 9:664535. doi: 10.3389/fcell.2021.664535

9. Anticevic A, Hu X, Xiao Y, Hu J, Li F, Bi F, et al. Early-course unmedicated schizophrenia patients exhibit elevated prefrontal connectivity associated with longitudinal change. *J Neurosci.* (2015) 35:267–86. doi: 10.1523/JNEUROSCI.2310-14.2015

10. Anticevic A, Murray JD, Barch DM. Bridging levels of understanding in schizophrenia through computational modeling. *Clin Psychol Sci.* (2015) 3:433–59. doi: 10.1177/2167702614562041

11. Hirano Y, Uhlhaas PJ. Current findings and perspectives on aberrant neural oscillations in schizophrenia. *Psychiatry Clin Neurosci.* (2021) 75:358–68. doi: 10.1111/pcn.13300

12. Gold JM, Barch DM, Feuerstahler LM, Carter CS, MacDonald AW, Daniel Ragland J, et al. Working memory impairment across psychotic disorders. *Schizoph Bull.* (2019) 45:804–12. doi: 10.1093/schbul/sby134

13. Tao TJ, Hui CLM, Hui PWM, Ho ECN, Lam BST, Wong AKH, et al. Working memory deterioration as an early warning sign for relapse in remitted psychosis: A one-year naturalistic follow-up study. *Psychiatry Res.* (2023) 319:114976. doi: 10.1016/j.psychres.2022.114976

14. D'Esposito M, Postle BR. The cognitive neuroscience of working memory. *Annu Rev Psychol.* (2015) 66:115–42. doi: 10.1146/annurev-psych-010814-015031

15. Luck SJ, Vogel EK. Visual working memory capacity: From psychophysics and neurobiology to individual differences. *Trends Cogn Sci.* (2013) 17:391–400. doi: 10.1016/j.tics.2013.06.006

16. Barch DM, Ceaser A. Cognition in schizophrenia: Core psychological and neural mechanisms. *Trends Cogn Sci.* (2012) 16:27–34. doi: 10.1016/j.tics.2011.11.015

17. Luck SJ, Hahn B, Leonard CJ, Gold JM. The hyperfocusing hypothesis: a new account of cognitive dysfunction in schizophrenia. *Schizoph Bull.* (2019) 45:991–1000. doi: 10.1093/schbul/sbz063

18. Rentrop M, Rodewald K, Roth A, Simon J, Walther S, Fiedler P, et al. Intra-individual variability in high-functioning patients with schizophrenia. *Psychiatry Res.* (2010) 178:27–32. doi: 10.1016/j.psychres.2010.04.009

19. Johnson MK, McMahon RP, Robinson BM, Harvey AN, Hahn B, Leonard CJ, et al. The relationship between working memory capacity and broad measures of cognitive ability in healthy adults and people with schizophrenia. *Neuropsychology.* (2013) 27:220–9. doi: 10.1037/a0032060

20. Jaeggi SM, Buschkuehl M, Perrig WJ, Meier B. The concurrent validity of the N-back task as a working memory measure. *Memory.* (2010) 18:394–412. doi: 10.1080/09658211003702171

21. Scharinger C, Soutschek A, Schubert T, Gerjets P. Comparison of the working memory load in N-back and working memory span tasks by means of EEG frequency band power and P300 amplitude. *Front Hum Neurosci.* (2017) 11:6. doi: 10.3389/fnhum.2017.00006

22. Luck SJ, Vogel EK. The capacity of visual working memory for features and conjunctions. *Nature.* (1997) 390:279–84. doi: 10.1038/36846

23. Vogel EK, Machizawa MG. Neural activity predicts individual differences in visual working memory capacity. *Nature.* (2004) 428:748–51. doi: 10.1038/nature02447

24. Coffman BA, Haas G, Olson C, Cho R, Ghuman AS, Salisbury DF. Reduced Dorsal Visual Oscillatory Activity During Working Memory Maintenance in the First-Episode Schizophrenia Spectrum. *Front Psychiatry.* (2020) 11:743. doi: 10.3389/fpsyt.2020.00743

25. Driesen NR, Leung HC, Calhoun VD, Constable RT, Gueorguieva R, Hoffman R, et al. Impairment of working memory maintenance and response in schizophrenia: functional magnetic resonance imaging evidence. *Biol Psychiatry.* (2008) 64:1026–34. doi: 10.1016/j.biopsych.2008.07.029

26. Huang AS, Rogers BP, Anticevic A, Blackford JU, Heckers S, Woodward ND. Brain function during stages of working memory in schizophrenia and psychotic bipolar disorder. *Neuropsychopharmacology.* (2019) 44:2136–42. doi: 10.1038/s41386-019-0434-4

27. Wang B, Zartaloudi E, Linden JF, Bramon E. Neurophysiology in psychosis: The quest for disease biomarkers. *Transl Psychiatry.* (2022) 12:1–10. doi: 10.1038/s41398-022-01860-x

28. Luria R, Balaban H, Awh E, Vogel EK. The contralateral delay activity as a neural measure of visual working memory. *Neurosci Biobehav Rev.* (2016) 62:100–8. doi: 10.1016/j.neubiorev.2016.01.003

29. Leonard CJ, Kaiser ST, Robinson BM, Kappenman ES, Hahn B, Gold JM, et al. Toward the neural mechanisms of reduced working memory capacity in schizophrenia. *Cereb Cortex.* (2013) 23:1582–92. doi: 10.1093/cercor/bhs148

30. Wang XJ. Neurophysiological and computational principles of cortical rhythms in cognition. *Physiol Rev.* (2010) 90:1195–268. doi: 10.1152/physrev.00035.2008

31. Lisman JE, Jensen O. The Theta-Gamma Neural Code. *Neuron.* (2013) 77:1002–16. doi: 10.1016/j.neuron.2013.03.007

32. Missonnier P, Prévot A, Herrmann FR, Ventura J, Padée A, Merlo MCG. Disruption of gamma–delta relationship related to working memory deficits in first-episode psychosis. *J Neural Trans.* (2020) 127:103–15. doi: 10.1007/s00702-019-02126-5

33. Sauseng P, Griesmayr B, Freunberger R, Klimesch W. Control mechanisms in working memory: A possible function of EEG theta oscillations. *Neurosci Biobehav Rev.* (2010) 34:1015–22. doi: 10.1016/j.neubiorev.2009.12.006

34. Cao Y, Han C, Peng X, Su Z, Liu G, Xie Y, et al. Correlation between resting theta power and cognitive performance in patients with schizophrenia. *Front Hum Neurosci.* (2022) 16:853994. doi: 10.3389/fnhum.2022.853994

35. Barr MS, Rajji TK, Zomorrodi R, Radhu N, George TP, Blumberger DM, et al. Impaired theta-gamma coupling during working memory performance in schizophrenia. *Schizoph Res.* (2017) 189:104–10. doi: 10.1016/j.schres.2017.01.044

36. Jensen O, Mazaheri A. Shaping functional architecture by oscillatory alpha activity: Gating by inhibition. *Front Hum Neurosci.* (2010) 4:186. doi: 10.3389/fnhum.2010.00186

37. Klimesch W. Alpha-band oscillations, attention, and controlled access to stored information. *Trends Cogn Sci.* (2012) 16:606–17. doi: 10.1016/j.tics.2012.10.007

38. Doesburg SM, Green JJ, McDonald JJ, Ward LM. From local inhibition to long-range integration: A functional dissociation of alpha-band synchronization across cortical scales in visuospatial attention. *Brain Res.* (2009) 1303:97–110. doi: 10.1016/j.brainres.2009.09.069

39. Erickson MA, Albrecht MA, Robinson B, Luck SJ, Gold JM. Impaired Suppression of Delay-Period Alpha and Beta Is Associated With Impaired Working Memory in Schizophrenia. *Biol Psychiatry.* (2017) 2:272–9. doi: 10.1016/j.bpsc.2016.09.003

40. Kustermann T, Rockstroh B, Kienle J, Miller GA, Popov T. Deficient attention modulation of lateralized alpha power in schizophrenia: Deficient lateralized alpha modulation in schizophrenia. *Psychophysiology.* (2016) 53:776–85.

41. Ramyead A, Roach B, Hamilton H, Addington J, Bachman P, Bearden C, et al. O33. EEG Alpha Event-Related Desynchronization Deficits Predict Conversion to Psychosis in Individuals With the Psychosis Risk Syndrome. *Biol Psychiatry.* (2019) 85:S119. doi: 10.1016/j.biopsych.2019.03.298.

42. Scangos KW, State MW, Miller AH, Baker JT, Williams LM. New and emerging approaches to treat psychiatric disorders. *Nat Med.* (2023) 29:317–33. doi: 10.1038/s41591-022-02197-0

43. Williams LM. Precision psychiatry: A neural circuit taxonomy for depression and anxiety. *Lancet Psychiatry.* (2016) 3:472–80. doi: 10.1016/S2215-036600579-9

44. Feczko E, Miranda-Dominguez O, Marr M, Graham AM, Nigg JT, Fair DA. The Heterogeneity Problem: Approaches to Identify Psychiatric Subtypes. *Trends Cogn Sci.* (2019) 23:584–601. doi: 10.1016/j.tics.2019.03.009

45. Martín Noguerol T, Paulano-Godino F, Martín-Valdivia MT, Menias CO, Luna A. Strengths, weaknesses, opportunities, and threats analysis of artificial intelligence and machine learning applications in radiology. *J. Am. Coll. Radiol.* (2019) 16:1239–1247. doi: 10.1016/j.jacr.2019.05.047

46. Johannesen JK, Bi J, Jiang R, Kenney JG, Chen C-MA. Machine learning identification of EEG features predicting working memory performance in schizophrenia and healthy adults. *Neuropsychiatric Electrophysiol.* (2016) 2:1–21. doi: 10.1186/s40810-016-0017-0

47. Kim JW, Lee YS, Han DH, Min KJ, Lee J, Lee K. Diagnostic utility of quantitative EEG in un-medicated schizophrenia. *Neurosci Lett.* (2015) 589:126–31. doi: 10.1016/j.neulet.2014.12.064

48. Phang CR, Noman F, Hussain H, Ting CM, Ombao H. A multi-domain connectome convolutional neural network for identifying schizophrenia from EEG connectivity patterns. *IEEE J Biomed Health Inform.* (2020) 24:1333–43. doi: 10.1109/JBHI.2019.2941222

49. Ruiz de Miras J, Ibáñez-Molina AJ, Soriano MF, Iglesias-Parro S. Schizophrenia classification using machine learning on resting state EEG signal. *Biomed Signal Process Control.* (2023) 79:104233. doi: 10.1016/j.bspc.2022.104233

50. Shim M, Hwang HJ, Kim DW, Lee SH, Im CH. Machine-learning-based diagnosis of schizophrenia using combined sensor-level and source-level EEG features. *Schizoph Res.* (2016) 176:314–9. doi: 10.1016/j.schres.2016.05.007

51. Shoeibi A, Sadeghi D, Moridian P, Ghassemi N, Heras J, Alizadehsani R, et al. Automatic Diagnosis of Schizophrenia in EEG Signals Using CNN-LSTM Models. *Front Neuroinform.* (2021) 15:777977. doi: 10.3389/fninf.2021.777977

52. Sun J, Cao R, Zhou M, Hussain W, Wang B, Xue J, et al. A hybrid deep neural network for classification of schizophrenia using EEG Data. *Sci Rep.* (2021) 11:1–16. doi: 10.1038/s41598-021-83350-6

53. Sheu YH. Illuminating the Black Box: Interpreting Deep Neural Network Models for Psychiatric Research. *Front Psychiatry.* (2020) 11:551299. doi: 10.3389/fpsyt.2020.551299

54. Barros C, Silva CA, Pinheiro AP. Advanced EEG-based learning approaches to predict schizophrenia: Promises and pitfalls. *Artif Intell Med.* (2021) 114:102039.

55. Bahdanau D, Cho KH, Bengio Y. Neural machine translation by jointly learning to align and translate. *Proceedings of the 3rd International Conference on Learning Representations, ICLR 2015 - Conference Track Proceedings*. Vienna (2015).

56. de Santana Correia A, Colombini EL. Attention, please! A survey of neural attention models in deep learning. *Artif Intell Rev.* (2022) 55:6037–124. doi: 10.1007/s10462-022-10148-x

57. Škrlj B, Daeroski S, Lavraè N, Petković M. Feature importance estimation with self-attention networks. *Front Artif Intell Applic.* (2020) 325:1491–8. doi: 10.3233/FAIA200256

58. Kay SR, Fiszbein A, Opler LA. The positive and negative syndrome scale (PANSS) for schizophrenia. *Schizoph Bull.* (1987) 13:261–76. doi: 10.1093/schbul/13.2.261

59. Vogel EK, McCollough AW, Machizawa MG. Neural measures reveal individual differences in controlling access to working memory. *Nature.* (2005) 438:500–3. doi: 10.1038/nature04171

60. Peirce J, Gray JR, Simpson S, MacAskill M, Höchenberger R, Sogo H, et al. PsychoPy2: Experiments in behavior made easy. *Behav Res Methods.* (2019) 51:195–203. doi: 10.3758/s13428-018-01193-y

61. Rouder JN, Morey RD, Morey CC, Cowan N. How to measure working memory capacity in the change detection paradigm. *Psych Bull Rev.* (2011) 18:324–30. doi: 10.3758/s13423-011-0055-3

62. Delorme A, Makeig S. EEGLAB: An open source toolbox for analysis of single-trial EEG dynamics including independent component analysis. *J Neurosci Methods.* (2004) 134:9–21. doi: 10.1016/j.jneumeth.2003.10.009

63. Mullen T. *NITRC: CleanLine: Tool/Resource Info*. New Delhi: NITRC (2012).

64. Hsu SS. *Adaptive Mixture ICA (AMICA): Theory & Practicum*. Lincoln: AMICA (2018).

65. Kingma DP, Ba JL. Adam: A method for stochastic optimization. *Proceedings of the 3rd International Conference on Learning Representations, ICLR 2015 - Conference Track Proceedings*. Vienna (2015).

66. Paszke A, Gross S, Massa F, Lerer A, Bradbury J, Chanan G, et al. PyTorch: An Imperative Style, High-Performance Deep Learning Library. In: Wallach H, Larochelle H, Beygelzimer A, Alché-Buc F, Fox E, Garnett R editors. *Advances in Neural Information Processing Systems*. New York, NY: Curran Associates, Inc (2019).

67. R Core Team. *R: A language and environment for statistical computing*. Vienna: R Foundation for Statistical Computing (2017).

68. Forbes NF, Carrick LA, McIntosh AM, Lawrie SM. Working memory in schizophrenia: A meta-analysis. *Psychol Med.* (2009) 39:889–905. doi: 10.1017/S0033291708004558

69. Gold JM, Luck SJ. Working Memory in People with Schizophrenia. *Curr Topics Behav Neurosci.* (2023) 63:137–52. doi: 10.1007/7854_2022_381

70. Gold JM, Robinson B, Leonard CJ, Hahn B, Chen S, McMahon RP, et al. Selective attention, working memory, and executive function as potential independent sources of cognitive dysfunction in schizophrenia. *Schizoph Bull.* (2018) 44:1227–34. doi: 10.1093/schbul/sbx155

71. Zhao YJ, Ma T, Zhang L, Ran X, Zhang RY, Ku Y. Atypically larger variability of resource allocation accounts for visual working memory deficits in schizophrenia. *PLoS Comput Biol.* (2021) 17:1009544. doi: 10.1371/journal.pcbi.1009544

72. Heinrichs RW, Pinnock F, Muharib E, Hartman L, Goldberg J, McDermid Vaz S. Neurocognitive normality in schizophrenia revisited. *Schizoph Res.* (2015) 2:227–32. doi: 10.1016/j.scog.2015.09.001

73. Light GA, Williams LE, Minow F, Sprock J, Rissling A, Sharp R, et al. Electroencephalography (EEG) and event-related potentials (ERPs) with human participants. *Curr Protoc Neurosci.* (2010) 52:1–24. doi: 10.1002/0471142301.ns0625s52

74. So RP, Kegeles LS, Mao X, Shungu DC, Stanford AD, Chen CMA. Long-range gamma phase synchronization as a compensatory strategy during working memory in high-performing patients with schizophrenia. *J Clin Exp Neuropsychol.* (2018) 40:663–81. doi: 10.1080/13803395.2017.1420142

75. Modesti MN, Arena JF, Palermo N, Del Casale A. A Systematic Review on Add-On Psychotherapy in Schizophrenia Spectrum Disorders. *J Clin Med.* (2023) 12:1021. doi: 10.3390/jcm12031021

76. Von Stein A, Chiang C, König P. Top-down processing mediated by interareal synchronization. *Proc Natl Acad Sci U.S.A.* (2000) 97:14748–53. doi: 10.1073/pnas.97.26.14748

77. Womelsdorf T, Schoffelen JM, Oostenveld R, Singer W, Desimone R, Engel AK, et al. Modulation of neuronal interactions through neuronal synchronization. *Science.* (2007) 316:1609–12. doi: 10.1126/science.1139597

78. Thut G, Nietzel A, Brandt SA, Pascual-Leone A. α-Band electroencephalographic activity over occipital cortex indexes visuospatial attention bias and predicts visual target detection. *J Neurosci.* (2006) 26:9494–502. doi: 10.1523/JNEUROSCI.0875-06.2006

79. Klimesch W, Sauseng P, Hanslmayr S. EEG alpha oscillations: The inhibition-timing hypothesis. *Brain Res Rev.* (2007) 53:63–88. doi: 10.1016/j.brainresrev.2006.06.003

80. Lewis DA, Hashimoto T, Volk DW. Cortical inhibitory neurons and schizophrenia. *Nat Rev Neurosci.* (2005) 6:312–24. doi: 10.1038/nrn1648

81. Avberšek LK, Repovš G. Deep learning in neuroimaging data analysis: Applications, challenges, and solutions. *Front Neuroimag.* (2022) 1:981642. doi: 10.3389/fnimg.2022.981642

82. Cordonnier J-B, Loukas A, Jaggi M. On the relationship between self-attention and convolutional layers. *arXiv [Preprint].* (2019) doi: 10.48550/arXiv.1911.03584

83. Wolfers T, Doan NT, Kaufmann T, Alnæs D, Moberget T, Agartz I, et al. Mapping the heterogeneous phenotype of schizophrenia and bipolar disorder using normative models. *JAMA Psychiatry.* (2018) 75:1146–55. doi: 10.1001/jamapsychiatry.2018.2467

84. Unsworth N, Robison MK. The importance of arousal for variation in working memory capacity and attention control: A latent variable pupillometry study. *J Exp Psychol.* (2017) 43:1962–87. doi: 10.1037/xlm0000421

85. Takahashi S, Ukai S, Kose A, Hashimoto T, Iwatani J, Okumura M, et al. Reduction of cortical GABAergic inhibition correlates with working memory impairment in recent onset schizophrenia. *Schizoph Res.* (2013) 146:238–43. doi: 10.1016/j.schres.2013.02.033

frontiers

Supplementary Material

Dense Attention Network identifies EEG abnormalities during working memory performance of patients with schizophrenia

Ruben Perellón-Alfonso*, Aleš Oblak, Matija Kuclar, Blaž Škrlj, Indre Pileckyte, Borut Škodlar, Peter Pregelj, Kilian Abellaneda-Pérez, David Bartrés-Faz, Grega Repovš, Jurij Bon*

*** Correspondence:** Ruben Perellón-Alfonso: ruben.perellon@ub.edu and Jurij Bon: jurij.bon@mf.uni-lj.si

1 Empirical evaluation of the machine learning models

1.1 Simple feedforward networks

We began our empirical evaluation by implementing a series of simple feedforward neural networks, which took as input the vectors describing individual patients. At this point, we already performed initial experiments with Logistic Regression, where the baseline performance of 65% (F_1 score) was established. Feedforward (or dense) neural networks can be, when properly regularized, suitable for low-data scenarios. These neural networks are composed of layers, comprised of computational units – neurons. The whole neural network is trained via the process of backpropagation, an optimization procedure where errors obtained by comparing the predictions against the target (real) values are propagated and used to update the weights of the neural network.

1.2 The attention mechanism

Recent advancements in natural language processing rely on the notion of neural attention, a simple mechanism which scatters the input signals and highlights only the parts of the feature space which are relevant to the task at hand. This concept is thoroughly explained elsewhere (Škrlj et al., 2020), therefore, we introduce here only the necessary ideas to understand this analysis. Originally, the attention mechanism was used for neural translation purposes, where a mapping between two sequences needed to be learned. Such, attention layer (La) can be formulated as:

$$L_a = softmax(Q^T K) \otimes V$$

where Q, K and V are the query, key and value, respectively. The query and key sequence's indices are thus associated with a given value. Here we explored how a similar idea performs on simple, feedforward neural networks and time-dependent inputs extracted from the reduced EEG data.

1.3 Dense Attention Networks

The attention mechanism is inspired by the recently introduced language models (Devlin et al., 2019), and for our data it can be defined as:

$$L_a = softmax(W^T X + b) \otimes X$$

For the first layer, followed by standard dense layers with additional regularization in form of the dropout. The W thus corresponds to a weight matrix and X to the whole input time series. When used directly as output, such attention layers emit a probability distribution across the input space, offering a window into the inner workings of the neural network and a potential opportunity to identify whether some spurious correlations were learnt.

1.4 Model interpretability

In terms of how models are interpretable, we can distinguish between two main interpretability types. Symbolic models, such as trees or similar, which yield conjuncts of features, are directly interpretable to a human observer. Statistical methods, such as neural networks are commonly interpreted post-hoc – their predictions are approximated one-by-one and aggregated. However, the attention mechanism offers an alternative, as it maintains a bijection with the input space throughout the training (the attention layer corresponds to the input space in a one-to-one manner). The main caveat is that if the network learns correlations which are not causal, the attention will similarly emphasize wrong parts of the input space. We explored qualitatively, whether the attention vectors, once aggregated across all correctly predicted classifications, highlight timepoints that are also relevant with respect to the experimental design. The attention mechanism, thus, offers one approach to understand which segments of the feature space are relevant. However, as the inputs are aggregated prior to being fed to a neural network, this mechanism does not help with explanations related to individual conditions. Here, we developed a different approach which tackles this issue in a different manner altogether. Note that six possible task conditions were measured. As these conditions represent potentially individual parts of the feature space, we can design an evaluation procedure, where the models are trained on subsets of the space of all conditions (results are summarized in supplementary table S3 and figure S1).

2 Time-Frequency statistical analysis results of ROIs in the theta, beta and gamma frequency bands

A mixed design ANOVA with a within-subject factor condition (condition 2, condition 2+2, and condition 4), a within-subject factor task phase (preparation, encoding, maintenance, retrieval), and a between-subject factor group (patient vs. control) on average power in theta range revealed a significant main effect of task phase, $F(3,84) = 50.25$, $p < .001$, $\eta^2 = .067$. A pairwise analysis with Bonferroni correction revealed that theta power was higher during encoding, $M = 0.13$, $SD = 1.88$, than during the maintenance, $M = -1.13$, $SD = 1.81$, $p = .046$. For beta frequency band, we found a significant main effect of task phase, $F(3,84) = 3.53$, $p = .026$, $\eta^2 = .018$, as well as significant interaction between task phase and condition, $F(6, 168) = 5.57$, $p < 001$, $\eta^2 = .009$. A pairwise analysis with Bonferroni correction revealed that beta power was higher during maintenance, $M = -0.50$, $SD = 0.58$, than during the retrieval, $M = -0.69$, $SD = 0.68$, $p = .049$. When task phase was held constant, beta power was different between conditions during the retrieval only, $F(2, 56) = 9.10$, $p = .004$, $\eta^2 = .044$, but not during the other three task phases ($p>0.05$). A pairwise analysis with Bonferroni correction revealed that during the retrieval phase beta power was significantly more negative at condition 2+2, $M = -0.88$, $SD = 0.65$, when compared to condition 2, $M = -0.64$, $SD = 0.66$, $p = .012$, and condition 4, $M = -0.55$, $SD = 0.71$, $p = .004$. Finally, we found a significant main effect of task phase at gamma frequency band, $F(3, 84) = 3.28$, $p = 025$, $\eta^2 = .020$. A pairwise analysis with Bonferroni correction revealed that gamma power was almost significantly different between maintenance and retrieval periods, $p = .053$.

3 Supplementary References

Devlin, J., Chang, M. W., Lee, K., & Toutanova, K. (2019). BERT: Pre-training of deep bidirectional transformers for language understanding. NAACL HLT 2019 - 2019 Conference of the North American Chapter of the Association for Computational Linguistics: Human Language Technologies - Proceedings of the Conference, 1(Mlm), 4171–4186.

Škrlj, B., Džeroski, S., Lavrač, N., & Petković, M. (2020). Feature importance estimation with self-attention networks. ArXiv, 1.

Table S1. Demographics and clinical properties of study participants

Participant property	**Patient group**	**Control group**
Age [mean (SD)]	28.1 (3.87)	26.8 (5.54)
Years of education [mean (SD)]	13.4 (1.12)	14.4 (1.18)
Handedness [N]		
Right	14	13
Left	1	1
Ambidextrous	0	1
Antipsychotic medication [N]		
Aripiprazole	4	0
Olanzapine	3	0
Clozapine	5	0
Quetiapine	2	0
Risperidone	3	0
Paliperidone	1	0

Amisulpride	2	0
ICD-10 F code [N]		
F 20.0	12	0
F 25	3	0
PSP [mean (SD)]	53.73 (8.28)	N/A
EASE [mean (SD)]		
Cognition	35.5 (14.3)	N/A
Presence	42.4 (13.9)	N/A
Body	13.3 (15.3)	N/A
Transitivism	18.7 (22.0)	N/A
Existential	19.1 (14.8)	N/A
Hyperreflexivity	2.1 (0.9)	N/A
PANSS [mean (SD)]	77.07 (15.29)	N/A

Table S2. Working memory task performance. H = hit rate; F = false alarm rate; K = memory capacity index.

WM performance	**Experimental group**	**Control group**
Condition 2		
Errors when different [mean (SD])	7.5 (4.2)	11.4 (8.2)
Errors when same [mean(SD)]	4.2 (4.2)	5.8 (4.3)
All errors [mean(SD)]	11.7 (6.9)	17.2 (10.6)
Accuracy [mean(SD)]	94.5 (3.3)	91.7 (4.9)
H – F [mean(SD)]	0.9 (0.07)	0.84 (0.1)
K	1.79 (0.13)	1.67 (0.21)
Reaction time	840.27 (403.45)	764.10 (372.71)
Condition 4		
Errors when different [mean (SD])	27.8 (15.7)	39.7 (22.3)
Errors when same [mean(SD)]	12.9 (9.2)	8.3 (5.7)
All errors [mean(SD)]	40.7 (20.5)	48.0 (23.2)
Accuracy [mean(SD)]	81.0 (9.5)	77.7 (10.9)
H – F [mean(SD)]	0.64 (0.21)	0.55 (0.22)
K	2.47 (0.77)	2.19 (0.86)
Reaction time	990.21 (497.95)	959.11 (472.68)

Condition 2+2		
Errors when different [mean (SD])	7.7 (7.1)	14.8 (16.7)
Errors when same [mean(SD)]	5.2 (3.7)	7.9 (6.9)
All errors [mean(SD)]	12.9 (9.8)	22.7 (22.1)
Accuracy [mean(SD)]	94.1 (3.6)	89.4 (10.3)
H – F [mean(SD)]	0.89 (0.09)	0.79 (0.21)
K	1.74 (0.19)	1.59 (0.42)
Reaction time	883.18 (435.30)	776.83 (369.26)
Overall reaction time	904.45 (451.60)	833.24 (417.23)

Table S3. Average performance metrics and standard deviation (in parenthesis) for each machine learning model tested in each subset of the feature space (i.e., experimental condition 2, 2+2 and 4 items; for both right and left visual hemifield presentation). CNN, convolutional neural network; DAN, dense attentional network; FFNN, feed forward neural network; KNN, K-nearest neighbour; LR, linear regression; RF, radio frequency machine learning; SVM, support vector machine; rbf, radial basis function.

Model	**Condition**	**Accuracy**	**F1**	**Recall**	**Precision**
CNN	2 left	0.67 ± (0.03)	0.7 ± (0.01)	0.77 ± (0.11)	0.65 ± (0.06)
CNN	2 right	0.71 ± (0.03)	0.73 ± (0.02)	0.77 ± (0.0)	0.69 ± (0.03)
CNN	2+2 left	0.69 ± (0.11)	0.72 ± (0.11)	0.81 ± (0.16)	0.65 ± (0.07)
CNN	2+2 right	0.71 ± (0.03)	0.72 ± (0.03)	0.73 ± (0.05)	0.7 ± (0.02)
CNN	4 left	0.71 ± (0.14)	0.73 ± (0.12)	0.77 ± (0.11)	0.69 ± (0.13)

CNN	4 right	0.71 ± (0.08)	0.73 ± (0.12)	0.81 ± (0.27)	0.68 ± (0.01)
CNN	all	0.69 ± (0.05)	0.72 ± (0.05)	0.81 ± (0.05)	0.66 ± (0.04)
DAN	2 left	0.62 ± (0.05)	0.62 ± (0.09)	0.65 ± (0.16)	0.6 ± (0.03)
DAN	2 right	0.75 ± (0.03)	0.75 ± (0.05)	0.77 ± (0.11)	0.74 ± (0.01)
DAN	2+2 left	0.62 ± (0.05)	0.66 ± (0.05)	0.73 ± (0.05)	0.59 ± (0.04)
DAN	2 right	0.63 ± (0.08)	0.69 ± (0.06)	0.81 ± (0.05)	0.6 ± (0.06)
DAN	4 left	0.56 ± (0.14)	0.65 ± (0.09)	0.81 ± (0.05)	0.54 ± (0.1)
DAN	4 right	0.75 ± (0.03)	0.79 ± (0.02)	0.92 ± (0.0)	0.69 ± (0.03)
DAN	all	0.69 ± (0.05)	0.71 ± (0.07)	0.77 ± (0.11)	0.67 ± (0.03)
FFNN	2 left	0.77 ± (0.0)	0.78 ± (0.01)	0.81 ± (0.05)	0.75 ± (0.03)
FFNN	2 right	0.79 ± (0.03)	0.8 ± (0.02)	0.85 ± (0.0)	0.76 ± (0.04)
FFNN	2+2 left	0.67 ± (0.03)	0.69 ± (0.03)	0.73 ± (0.05)	0.65 ± (0.02)
FFNN	2+2 right	0.67 ± (0.08)	0.72 ± (0.05)	0.85 ± (0.0)	0.63 ± (0.08)
FFNN	4 left	0.67 ± (0.03)	0.7 ± (0.05)	0.77 ± (0.11)	0.64 ± (0.0)
FFNN	4 right	0.67 ± (0.03)	0.71 ± (0.0)	0.81 ± (0.05)	0.64 ± (0.04)
FFNN	all	0.71 ± (0.03)	0.72 ± (0.03)	0.73 ± (0.05)	0.7 ± (0.02)
KNN	2 left	0.62 ± (0.0)	0.55 ± (0.0)	0.46 ± (0.0)	0.67 ± (0.0)
KNN	2 right	0.5 ± (0.0)	0.55 ± (0.0)	0.62 ± (0.0)	0.5 ± (0.0)
KNN	2+2 left	0.54 ± (0.0)	0.6 ± (0.0)	0.69 ± (0.0)	0.53 ± (0.0)
KNN	2+2 right	0.65 ± (0.0)	0.71 ± (0.0)	0.85 ± (0.0)	0.61 ± (0.0)

KNN	4 left	0.54 ± (0.0)	0.57 ± (0.0)	0.62 ± (0.0)	0.53 ± (0.0)
KNN	4 right	0.65 ± (0.0)	0.67 ± (0.0)	0.69 ± (0.0)	0.64 ± (0.0)
KNN	all	0.69 ± (0.0)	0.71 ± (0.0)	0.77 ± (0.0)	0.67 ± (0.0)
LR	2 left	0.73 ± (0.0)	0.72 ± (0.0)	0.69 ± (0.0)	0.75 ± (0.0)
LR	2 right	0.69 ± (0.0)	0.71 ± (0.0)	0.77 ± (0.0)	0.67 ± (0.0)
LR	2+2 left	0.58 ± (0.0)	0.56 ± (0.0)	0.54 ± (0.0)	0.58 ± (0.0)
LR	2+2 right	0.58 ± (0.0)	0.65 ± (0.0)	0.77 ± (0.0)	0.56 ± (0.0)
LR	4 left	0.62 ± (0.0)	0.67 ± (0.0)	0.77 ± (0.0)	0.59 ± (0.0)
LR	4 right	0.62 ± (0.0)	0.64 ± (0.0)	0.69 ± (0.0)	0.6 ± (0.0)
LR	all	0.65 ± (0.0)	0.67 ± (0.0)	0.69 ± (0.0)	0.64 ± (0.0)
RF	2 left	0.6 ± (0.03)	0.55 ± (0.01)	0.5 ± (0.05)	0.62 ± (0.06)
RF	2 right	0.62 ± (0.11)	0.64 ± (0.1)	0.69 ± (0.11)	0.6 ± (0.09)
RF	2+2 left	0.44 ± (0.08)	0.43 ± (0.0)	0.42 ± (0.05)	0.45 ± (0.07)
RF	2+2 right	0.58 ± (0.05)	0.61 ± (0.05)	0.65 ± (0.05)	0.57 ± (0.05)
RF	4 left	0.38 ± (0.11)	0.36 ± (0.15)	0.35 ± (0.16)	0.37 ± (0.13)
RF	4 right	0.58 ± (0.05)	0.57 ± (0.1)	0.58 ± (0.16)	0.57 ± (0.04)
RF	all	0.56 ± (0.08)	0.58 ± (0.09)	0.62 ± (0.11)	0.55 ± (0.07)
SVM linear	2 left	0.73 ± (0.0)	0.72 ± (0.0)	0.69 ± (0.0)	0.75 ± (0.0)
SVM linear	2 right	0.58 ± (0.0)	0.59 ± (0.0)	0.62 ± (0.0)	0.57 ± (0.0)
SVM linear	2+2 left	0.54 ± (0.0)	0.5 ± (0.0)	0.46 ± (0.0)	0.55 ± (0.0)

SVM linear	2+2 right	0.65 ± (0.0)	0.67 ± (0.0)	0.69 ± (0.0)	0.64 ± (0.0)
SVM linear	4 left	0.62 ± (0.0)	0.64 ± (0.0)	0.69 ± (0.0)	0.6 ± (0.0)
SVM linear	4 right	0.58 ± (0.0)	0.56 ± (0.0)	0.54 ± (0.0)	0.58 ± (0.0)
SVM linear	all	0.62 ± (0.0)	0.62 ± (0.0)	0.62 ± (0.0)	0.62 ± (0.0)
SVM poly	2 left	0.54 ± (0.0)	0.4 ± (0.0)	0.31 ± (0.0)	0.57 ± (0.0)
SVM poly	2 right	0.73 ± (0.0)	0.72 ± (0.0)	0.69 ± (0.0)	0.75 ± (0.0)
SVM poly	2+2 left	0.62 ± (0.0)	0.55 ± (0.0)	0.46 ± (0.0)	0.67 ± (0.0)
SVM poly	2+2 right	0.5 ± (0.0)	0.48 ± (0.0)	0.46 ± (0.0)	0.5 ± (0.0)
SVM poly	4 left	0.5 ± (0.0)	0.38 ± (0.0)	0.31 ± (0.0)	0.5 ± (0.0)
SVM poly	4 right	0.62 ± (0.0)	0.62 ± (0.0)	0.62 ± (0.0)	0.62 ± (0.0)
SVM poly	all	0.62 ± (0.0)	0.58 ± (0.0)	0.54 ± (0.0)	0.64 ± (0.0)
SVM rbf	2 left	0.42 ± (0.0)	0.44 ± (0.0)	0.46 ± (0.0)	0.43 ± (0.0)
SVM rbf	2 right	0.5 ± (0.0)	0.48 ± (0.0)	0.46 ± (0.0)	0.5 ± (0.0)
SVM rbf	2+2 left	0.42 ± (0.0)	0.4 ± (0.0)	0.38 ± (0.0)	0.42 ± (0.0)
SVM rbf	2+2 right	0.38 ± (0.0)	0.38 ± (0.0)	0.38 ± (0.0)	0.38 ± (0.0)
SVM rbf	4 left	0.27 ± (0.0)	0.24 ± (0.0)	0.23 ± (0.0)	0.25 ± (0.0)
SVM rbf	4 right	0.42 ± (0.0)	0.44 ± (0.0)	0.46 ± (0.0)	0.43 ± (0.0)
SVM rbf	all	0.58 ± (0.0)	0.62 ± (0.0)	0.69 ± (0.0)	0.56 ± (0.0)

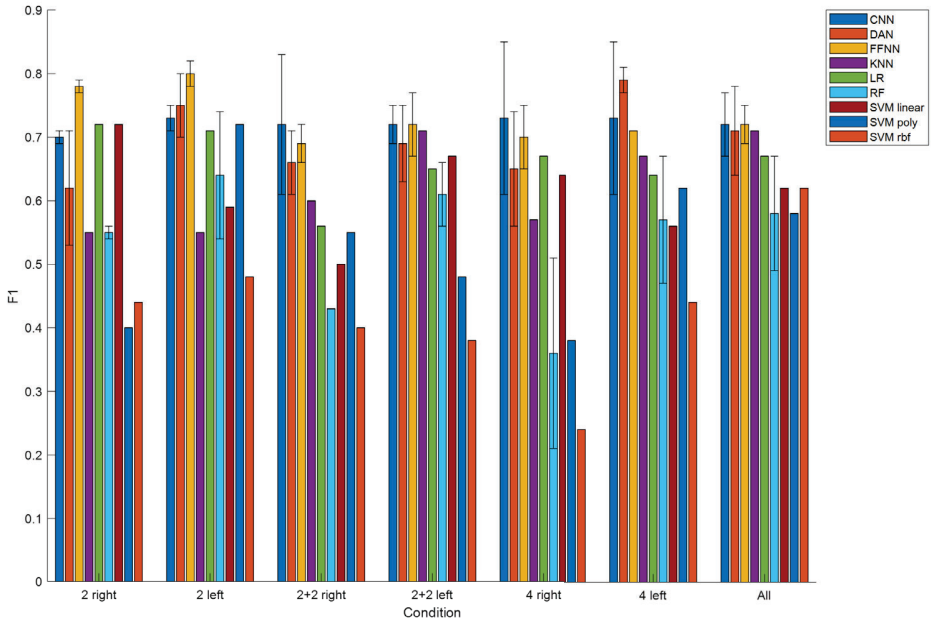

Figure S1. Bar graph ilustrating average performance metrics (black bars show standard deviations) for each machine learning model tested in each subset of the feature space (i.e., experimental condition 2, 2+2 and 4 items; for both right and left visual hemifield presentation). CNN, convolutional neural network; DAN, dense attentional network; FFNN, feed forward neural network; KNN, K-nearest neighbour; LR, linear regression; RF, radio frequency machine learning; SVM, support vector machine; rbf, radial basis function.

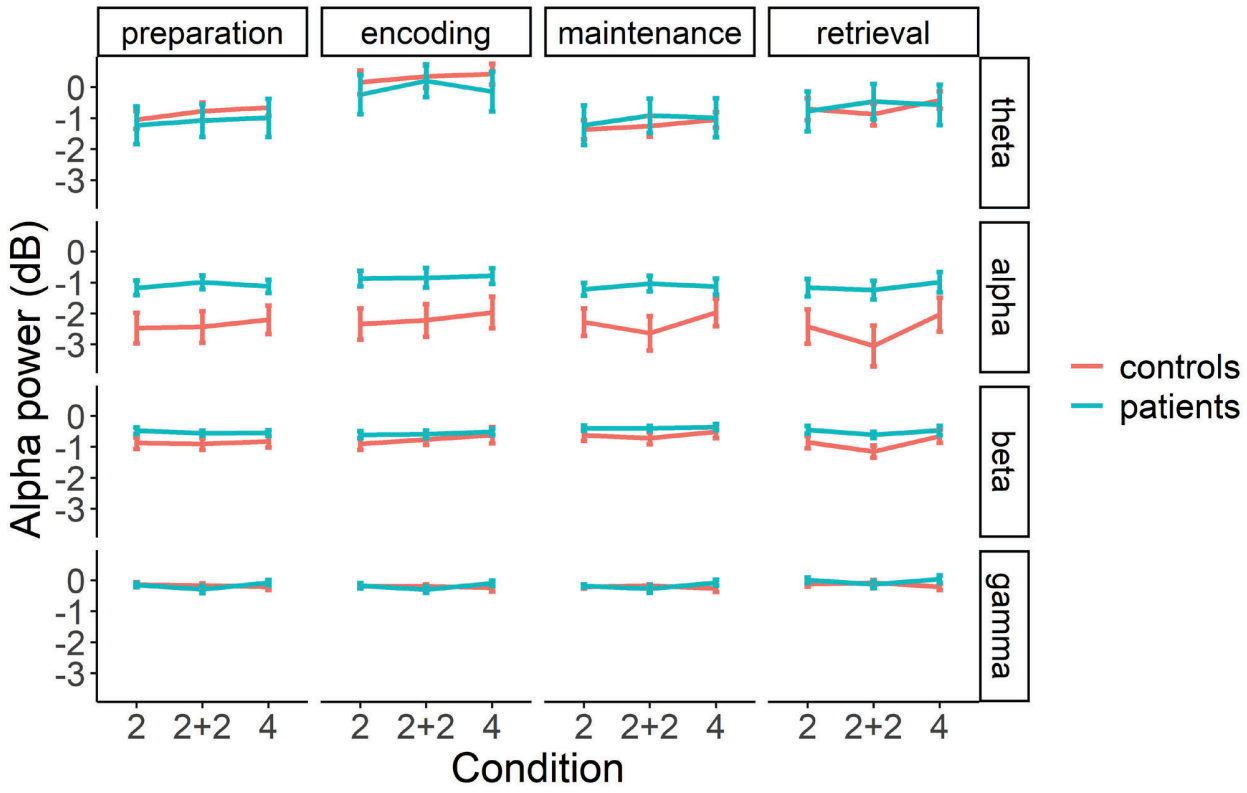

Figure S2. Average power values for patients (blue line) and controls (red line) in four WM task phases (preparation, encoding, maintenance, and retrieval) and four frequency bands (theta, alpha, beta, and gamma). The error bars represent standard error of mean.

3.3. STUDY 3

Perellón-Alfonso, R., Abellaneda-Pérez, K., Pileckyte, I., Cabello-Toscano, M., Mulet-Pons, L., Vaqué-Alcázar, L., Cattaneo G., Redondo-Camós, M., España-Irla, G., Delgado-Gallen, S., Sánchez, JS., Zetterberg, H., Tormos JM., Franzmeier N., Pascual-Leone A., Bartrés-Faz D. Spontaneous and perturbation-based EEG markers of cortical excitability are associated with blood p-tau181 concentration in healthy middle aged adults. Under Review.

Spontaneous and perturbation-based EEG cortical excitability markers are associated with plasma p-tau181 concentration in healthy middle-aged adults

Ruben Perellón-Alfonso[1,2,3,*], Kilian Abellaneda-Pérez[3,4,5], Indre Pileckyte[6], María Cabello-Toscano[1,2], Lídia Mulet-Pons[1,2], Lídia Vaqué-Alcázar[1,2,7], Gabriele Cattaneo[3,4,5], María Redondo-Camós[3,4,5], Goretti España-Irla[8,9,10], Selma Delgado-Gallen[3,4,5], Javier Solana Sánchez[3,4,5], Henrik Zetterberg[11,12,13,14,15,16] Jose M. Tormos[17], Nicolai Franzmeier[18,19,20], Alvaro Pascual-Leone[21,22,23,+], David Bartrés-Faz[1,2,3,+,*]

[1]Department of Medicine, Faculty of Medicine and Health Sciences, and Institute of Neurosciences, University of Barcelona, Barcelona, Spain.
[2]Institut d'Investigacions Biomèdiques August Pi i Sunyer (IDIBAPS), Barcelona, Spain.
[3]Institut Guttmann, Institut Universitari de Neurorehabilitació adscrit a la Universitat Autònoma de Barcelona, Barcelona, Spain.
[4]Universitat Autònoma de Barcelona, Bellaterra (Cerdanyola del Vallès), Spain
[5]Fundació Institut d'Investigació en Ciències de la Salut Germans Trias i Pujol, Badalona, Spain.
[6]Center for Brain and Cognition, Pompeu Fabra University, Barcelona, Spain.
[7]Sant Pau Memory Unit, Department of Neurology, Institut d'Investigacions Biomèdiques Sant Pau-Hospital de Sant Pau, Universitat Autònoma de Barcelona, Barcelona, Spain.
[8]Department of Psychology, Northeastern University, Boston, MA, USA
[9]Center for Cognitive & Brain Health, Northeastern University, Boston, MA, USA
[10]Department of Physical Therapy, Movement, & Rehabilitation Sciences, Northeastern University, Boston, MA, USA
[11]Department of Psychiatry and Neurochemistry, Institute of Neuroscience and Physiology, the Sahlgrenska Academy at the University of Gothenburg, Mölndal, Sweden
[12]Clinical Neurochemistry Laboratory, Sahlgrenska University Hospital, Mölndal, Sweden
[13]Department of Neurodegenerative Disease, UCL Institute of Neurology, Queen Square, London, UK
[14]UK Dementia Research Institute at UCL, London, UK
[15]Hong Kong Center for Neurodegenerative Diseases, Clear Water Bay, Hong Kong, China
[16]Wisconsin Alzheimer's Disease Research Center, University of Wisconsin School of Medicine and Public Health, University of Wisconsin-Madison, Madison, WI, USA
[17]Centro de Investigación Translacional San Alberto Magno - Facultad Ciencias de la Salud - Universidad Católica de Valencia
[18]Institute for Stroke and Dementia Research (ISD), University Hospital, LMU Munich, Germany
[19]Munich Cluster for Systems Neurology (SyNergy), Munich, Germany
[20]University of Gothenburg, The Sahlgrenska Academy, Institute of Neuroscience and Physiology, Department of Psychiatry and Neurochemistry
[21]Hinda and Arthur Marcus Institute for Aging Research and Deanna and Sidney Wolk Center for Memory Health, Hebrew SeniorLife, Boston, MA, USA
[22]Department of Neurology, Harvard Medical School, Boston, MA, USA
[23]Linus Health, Inc., Boston, MA, USA
[*]Corresponding authors
[+]Joint senior authors

Abstract:
In early-stage Alzheimer's disease (AD) amyloid-β (Aβ) deposition can induce neuronal hyperactivity, thereby potentially triggering activity-dependent neuronal secretion of phosphorylated tau (p-tau), ensuing tau aggregation and spread. Therefore, cortical excitability is a candidate biomarker for early AD detection. Moreover, lowering neuronal excitability could potentially complement strategies to reduce Aβ and tau buildup. There is, however, a lack of understanding of the relationship between cortical excitability and p-tau increase *in vivo*. Therefore, in a sample of 658 healthy middle-aged (between 40-65 years of age) participants of the Barcelona Brain Health Initiative cohort study, we examined the relation of blood-based tau, phosphorylated at amino acid 181 (p-tau181), reflecting neuronal p-tau secretion; neurofilament light chain (NfL), as a passively released control for p-tau181; and electroencephalography (EEG) markers of cortical excitability. A subsample of 47 participants also completed a controlled brain perturbation approach via transcranial magnetic stimulation (TMS) with concurrent EEG. Results show that both spontaneous (i.e., resting-state) and perturbation-based TMS-EEG markers, are associated with blood p-tau181, particularly in older individuals. The perturbation-based marker was found to be a significantly more sensitive predictor of p-tau181 concentration than the spontaneous EEG-based marker. The relationships observed are not present for the NfL control. These results show that relationships between p-tau181 and cortical excitability are present in healthy middle-aged subjects and that p-tau181 increases may reflect activity-dependent secretion.

Keywords: Alzheimer's Disease; Tau; EEG; Transcranial Magnetic Stimulation;

INTRODUCTION

In early-stage Alzheimer's disease (AD), the buildup of amyloid-β (Aβ) plaques triggers increased levels of soluble phosphorylated tau protein (p-tau), which can be detected using cerebrospinal fluid (CSF) and blood-based biomarkers.[1] Recent research shows that this rise is strongly predictive of the accumulation and spread of insoluble tau aggregates and subsequent cognitive decline.[2]

Hyperexcitability is a hallmark of early AD and research in human patients and mouse models consistently show hyperexcitability at the single neuron level, as well as in neural networks or entire brain systems.[3,4] Further evidence from research in mice shows that extracellular soluble Aβ induces neuronal hyperexcitability.[5] Subsequently, this hyperexcitability contributes to trigger the secretion of tau, which propagates through trans-synaptic transmission to affect distal brain regions.[6] Functional magnetic resonance imaging (fMRI) research in humans has further shown that the spread of tau pathology occurs preferentially through functionally connected brain regions,[7] leading to neuronal degeneration. Therefore, changes in neuronal excitability potentially constitute a pathophysiologically relevant biomarker for early detection of AD.

Emerging interventions for AD focus on clearing Aβ to reduce tau pathology and spread,[8] however, given that Aβ may trigger the release of phosphorylated tau by stimulating neuronal excitability, reducing it could further complement these treatments.[9] Readily available antiepileptic medications, for instance, can effectively reduce overall cortical excitability,[10] but they often produce unwanted side-effects and affect whole brain neurotransmitter systems. Conversely, non-invasive brain stimulation techniques can reduce cortical excitability in specific brain regions, without comparable side-effects, via long term depression-like mechanisms,[11–14] and could be applied on specific functional connectivity nodes,[15,16] to target specific pathways of preferential tau spread.

Therefore, cortical excitability is a modifiable factor that could provide a new avenue of potentially disease-modifying interventions targeting the Aβ-tau axis in AD. While the link between hyperexcitability and tau pathology is better established in the early stages of AD,[3] and there is a relation between cortical hyperexcitability and cognitive dysfunction,[4] we still lack understanding of how cortical excitability might be related to Aβ and tau in cognitively-unimpaired populations.

The relationships between Aβ, tau, and excitability have been mainly investigated in animal models of AD. However, we now have available tools to study these relationships *in vivo* in humans. Blood-based biomarkers have been recently developed,[17] paving the way for research at any clinical stage, as well as in preclinical healthy populations.[18] Moreover, recent developments in electroencephalography (EEG), make it possible to study cortical excitability non-invasively, either based on spontaneous activity during resting-state, or elicited by controlled brain perturbations using transcranial magnetic stimulation (TMS). Specifically, recent studies have shown that the EEG power spectrum's 1/*f*-like activity partially reflects the overall cortical balance of excitation and inhibition,[19,20] and its abnormality in AD has been established[21] and shown to relate to cognitive function.[22] Whereas single-pulse TMS produces a repeatable evoked EEG response, its later components (160 to 240ms after the pulse) directly relating to voltage-gated sodium channel (VGSC)-mediated excitability, as the response can be directly inhibited by VGSC blockers such as carbamazepine.[23,24]

In this study, we aim at establishing the relationships between cortical excitability and p-tau detectable in blood plasma in a healthy middle-aged population. To achieve this objective, we first tested the relationship between cortical excitability, measured as the EEG brain reactivity to a controlled TMS perturbation, and blood phosphorylated tau at amino acid 181 (p-tau181) concentration, and compared it to neurofilament light chain (NfL) concentration in blood, which is thought to be passively released into the blood stream as a result of axonal damage and cell death, irrespective of the underlying cause.[25] Second, we tested the relationship between cortical excitation/inhibition balance, measured from spontaneous resting state EEG activity, and plasma p-tau181 concentration, comparing it to NfL. Finally, we compared the value of the spontaneous and perturbation-based measures of cortical excitability in explaining p-tau181 concentration. Given the evidence that excitability might stimulate the secretion and propagation of tau,[5,6] we hypothesized that higher excitability would correlate with higher concentration of p-tau181, but not with NfL. We also hypothesized that perturbation-based measures would be a more sensitive predictor of p-tau181 concentration, because spontaneous-based excitation/inhibition balance represents a more heterogeneous measure of complex excitatory and inhibitory interactions,[26] which precludes a direct estimation of net excitability.

MATERIAL AND METHODS

Study Participants

Participants were recruited from the Barcelona Brain Health Initiative project (BBHI)[27] an ongoing longitudinal study that investigates brain health determinants in middle-aged adults. A main inclusion criterion for the project is absence of any neurological or psychiatric condition. For the present study we selected all participants who completed both blood extraction and resting-state EEG, and whose data survived preprocessing. The final sample included consists of 648 subjects aged 40-65 years, *M*=52.3 *SD*=7.2, 307 female. A subsample of 47 participants (aged 40-64 years, *M*=54.8 *SD*=7.1, 16 female) additionally completed TMS with concurrent EEG (from now on TMS-EEG). The study protocols were approved by the Comitè Ètic d'Investigació (CEIm) de la Fundació Unió Catalana d'Hospitals (ref. CEIC 17/06) and all participants gave their informed consent to participate in accordance to the declaration of Helsinki.

Blood-based biomarkers

Ethylenediaminetetraacetic acid plasma samples were collected through venipuncture. Plasma concentrations of phosphorylated p-tau181 and NfL were measured using Single molecule array (Simoa) methods on an HD-X instrument (Quanterix, Billerica, MA, USA), as previously described.[28,29]

TMS-EEG recording and preprocessing

TMS was applied over the left dorsolateral prefrontal cortex (L-PFC) and the left inferior parietal lobule (L-IPL). Stimulation was guided by a BrainSight neuronavigation system (RogueResearch, Inc., Canada). The targets were determined based on either anatomy – for subjects recorded before 2019 (*n*=27)– or the functional cortical parcellation by Yeo and colleagues[30] –for subjects studied after 2019 (*n*=20). See supplementary materials for MRI acquisition parameters and detailed target determination procedures. Stimulation was set to 120% of resting motor threshold, determined as the lowest intensity needed to produce motor evoked potentials of no less than 50μV peak-to-peak in the first dorsal interosseous muscle on the relaxed right hand, achieving this in a minimum of 3 out of 6

attempts.[31] For each designated target, a series of 120 single biphasic pulses were administered using an MCF-B65 butterfly coil attached to a MagPro X100 stimulator (Magventure, Inc., Denmark). Pulses were spaced randomly, ranging between four to six seconds apart. The sequence in which targets were stimulated was shuffled for every participant. To diminish the auditory responses triggered by the click from the TMS coil, participants were equipped with earplug-earbuds emitting white noise at their maximum tolerated volume. EEG was recorded concurrently using a TMS-compatible ActiChamp 64-channel amplifier system, paired with an ActiCap Slim featuring active electrodes (from BrainProducts, GmbH., Germany). Electrode impedance was consistently monitored and maintained below 5kΩ throughout the recording. EEG data was captured from DC to 500Hz and converted into a digital format at a rate of 1KHz. The preprocessed TMS-evoked potential data was then used for source localization (see supplementary materials for source localization procedures).

Resting-state EEG recording and preprocessing

EEG was recorded for 10 minutes at rest (i.e., 5 minutes eyes closed, 5 minutes eyes open) using an Enobio 32 channel system (Neuroelectrics, Spain) at a sampling rate of 512 Hz with a 50Hz notch filter of order 1. Electrode impedance for all channels was kept below 25 kΩ. We included only eyes closed data in the analysis, as it contains less eye and muscle related artifacts, and hence guarantees a higher survival rate and quality during automatic data preprocessing.

Data was preprocessed using a fully automated pipeline developed in house (see supplementary materials for pipeline script and details) and consisting of EEGLAB[32] and custom-made MATLAB functions (The MathWorks INC. USA). The pipeline ran through all the 748 EEG resting-state datasets and logged the number of bad channels and epochs. For the current analysis we kept only those datasets that retained at least 22 out of 32 channels and 100 artifact free epochs, resulting in 648 individual clean recordings for subsequent statistical analysis.

TMS-EEG perturbation based cortical excitability

To quantify VGSC mediated excitability at each stimulation target location we first defined a region of interest (ROI) of 100 vertices around each subject's stimulation target coordinate, which corresponds to a cortex surface area of approximately 10 cm^2. To allow group level statistics, the TMS-evoked potential (TEP) time-series in source space of each vertex within the target ROI were rectified, averaged together, and then normalized via z-score transformation:

$$z=(TEP-\mu)/\sigma$$

Where μ is the average of the pre-stimulus baseline (from -500 ms to -3 ms relative to the TMS pulse) and σ is the standard deviation of the baseline. Finally, we computed the trapezoidal integration (i.e., area under the curve) of the normalized TEP between 160 and 240ms after the TMS pulse (Figure 1, B).

Spontaneous resting state EEG cortical excitation/inhibition balance

To estimate excitation/inhibition balance, first the EEG power spectrum was computed via the Welch's method, whereby the fast Fourier transform of each 2 second epoch is computed and then all epochs' spectra are averaged together. The aperiodic component of the EEG spectrum (i.e., $1/f$-like activity) was estimated using the *fooof* toolbox,[20] and then the exponent (i.e., slope) of the aperiodic fit line was taken as the estimate of $1/f$-

like activity and, hence, as a proxy of cortical inhibition/excitation balance,[19] with stepper slopes (i.e., higher values) indicating a shift in the balance towards inhibition and vice-versa (Figure 1, D).

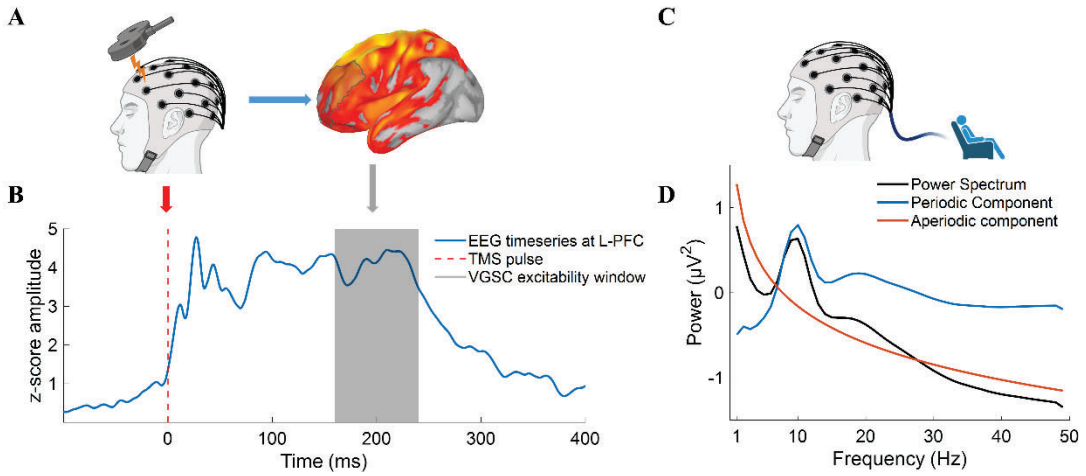

Figure 1. Illustration of EEG cortical excitability markers. A) illustrates the TMS-evoked perturbation of the EEG and the spatial region of interest in source space (grey transparent patch over L-PFC) and, B) the time-window taken from the TMS-evoked EEG timeseries to compute the perturbation-based marker of VGSC excitability (grey transparency spanning from 160 to 240ms after TMS pulse). C) illustrates the recording of resting state EEG and, D) the decomposition of the power spectrum at rest to isolate the aperiodic component, the slope of which we take here as the spontaneous marker for excitation/inhibition balance. In both B and D panels, grand average waveforms for all participants included in the study are shown. EEG, electroencephalography; L-PFC, left prefrontal cortex; VGSC, voltage-gated sodium channel.

Statistical analysis

All statistical analyses were performed in R version 4.2.3 (R Foundation for Statistical Computing, Vienna, Austria).

To determine the relation of perturbation-based VGSC mediated excitability and p-tau181 in the TMS-EEG subsample (n=47), we used stepwise general linear modeling to determine the best fitting model and discard irrelevant predictors. The criterion for removing predictors was the models' chi-squared test of the change in the deviance that results from removing the term. The starting model included all main effects and interactions of perturbation-based excitability (at both L-IPL and L-PFC targets), age, biological sex and TMS targeting method (i.e., functional or anatomical). The final model reported in the results section included the main effects of age and VGSC excitability at the L-PFC target as well as their interaction.

To determine the relation of spontaneous excitation/inhibition balance, during resting-state EEG, with p-tau181 concentration, in the full sample (n=648), we analogously used stepwise general linear modeling. The starting model included all possible main effects and interactions of spontaneous excitability, age, and biological sex. The final model reported in the results section included the main effects of age and spontaneous excitability, as well as their interaction. Due to the gamma-like distribution of p-tau181 values in this sample, models were fitted with a gamma distribution and a "log" link function.

To compare the predictive value of the spontaneous excitation/inhibition balance and perturbation-based excitability, we used an additional model including the predictors from both models.

Finally, to show that cortical excitability markers are more likely related to secreted proteins that pass into the blood stream, rather than passively released proteins, we contrasted these models with NfL, by running the final models with NfL instead of p-tau181 as the response variable.

RESULTS

Perturbation-based cortical excitability is positively correlated with secreted p-tau181 after 61 years of age

To investigate the relationship between perturbation-based cortical excitability and p-tau181 concentration, we fitted a linear regression model with a response variable *p-tau181*, and the predictors *age, perturbation-based-excitability*, and their interaction, $F(43, 4)=5.86$, $p=.002$, $\eta^2=.29$, revealing a trend level main effect of *perturbation-based-excitability*, $\beta=-.019$, $p=.061$, and a significant interaction between *perturbation-based-excitability* and *age*, $\beta=3.6e\text{-}4$, $p=.036$. A Johnson-Neyman interaction analysis was used to further study the interaction between *age* and *perturbation-based-excitability*, revealing that *perturbation-based-excitability* significantly predicts p-tau181 concentration starting at age 61 (Figure 2).

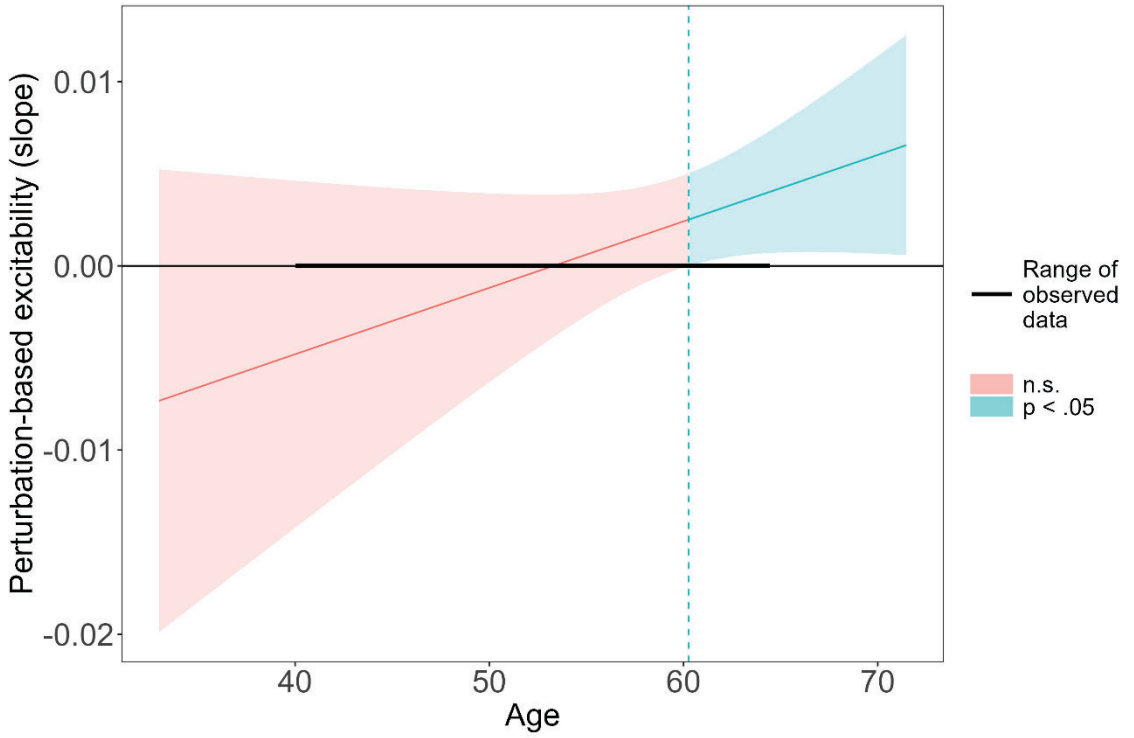

Figure 2. Johnson-Neyman interval plot illustrating the age interval at which the relationship between perturbation-based excitability and p-tau181 is significant (i.e., 61 to 65 years of age). n.s.= non-significant.

To show that the relationship is specific to potentially secreted p-tau protein, rather than passively released proteins, we fitted a linear regression model replacing the response variable *p-tau181* with *NfL*, $F(43, 4)=6.32$ -value, $p=.001$, $\eta^2=.31$, revealing no significant main effect of *age*, $p=.109$, *perturbation-based excitability*, $p=.649$, or interaction between them, $p=.556$.

Spontaneous cortical excitation/inhibition balance is positively correlated with secreted p-tau181 after 54 years of age

To investigate the relationship between spontaneous cortical excitation/inhibition balance and p-tau181 concentration, we fitted a general linear model with a response variable *p-tau181*, and the predictors *age, spontaneous-excitability*, and their interactions, $F(644, 4)=5.07$, $p=.002$, $\eta^2=.03$, revealing a trend level main effect of *spontaneous-excitability*, $\beta=-.45$, $p=.060$, and a significant interaction between *spontaneous-excitability* and *age*, $\beta=.009$, $p=.029$. A Johnson-Neyman interval analysis was used to probe the interaction between *age* and *spontaneous-excitability*, revealing that *spontaneous-excitability* significantly predicts p-tau181 concentration starting at age 54 (Figure 3).

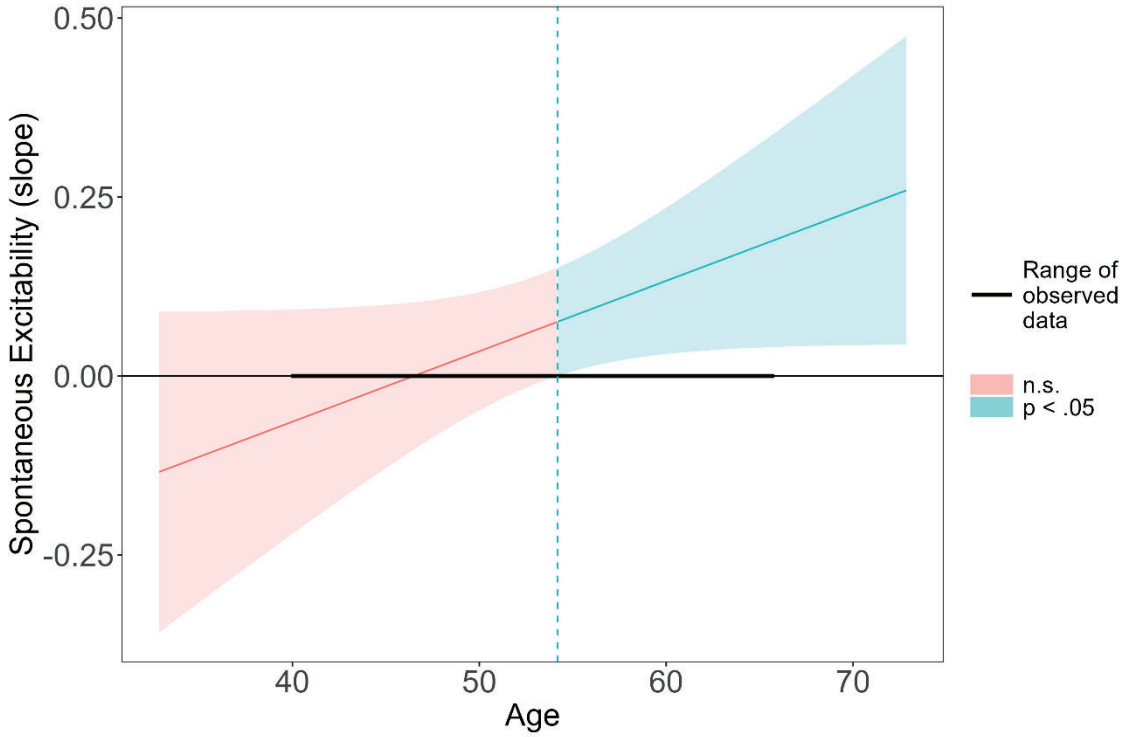

Figure 3. Johnson-Neyman interval plot illustrating the age interval at which the relationship between spontaneous excitability and p-tau181 is significant (i.e., 54-65 years of age). n.s.= non-significant.

To show that the relationship is specific to potentially secreted p-tau protein, rather than passively released proteins, we fitted a linear regression model replacing the response variable *p-tau181* with *NfL*, $F(644, 4)=62.9$ -value, $p<.001$, $\eta^2=.22$, revealing a significant main effect of *age*, $\beta=-.021$ $p<.001$, but no significant main effect of *spontaneous-excitability*, $p=.339$, or interaction between *age* and *spontaneous-excitability*, $p=.311$.

Perturbation based excitability is a better predictor of p-tau181 concentration than spontaneous excitation/inhibition balance

To compare the predictive value of perturbation based excitability against spontaneous excitation/inhibition balance, we fitted a full linear regression model with a response variable *p-tau181*, and the predictors *age, perturbation-based-excitability*, their interaction, and *spontaneous-excitability*, and its interaction with age $F(41, 6)=3.627$, $p=.008$, $\eta^2=.31$, revealing a trend level main effect of *perturbation-based excitability*, $\beta=-.021$, $p=.051$, and a significant interaction between *perturbation-based excitability* and *age*, $\beta=3.8e-04$ $p=.031$. However, there was no significant main effect of *spontaneous-excitability*, $p=.834$, or an interaction with *age*, $p=.926$.

Model comparisons between this full model and the reduced one (i.e., with only perturbation-based excitability, age, and their interaction as predictors), revealed that the reduced model is a better fit to the response variable *p-tau181,* because the full model is not significantly better than the reduced one, p=.616. Moreover, smaller Akaike Information Criterion (AIC) and Bayesian Information Criterion (BIC) values, as well as the larger Bayes factor, further support the reduced model as the better fitting of the two (Table 1).

Table 1. Model comparisons results of the full (spontaneous+perturbation) Vs reduced (perturbation only) model.

Regression Model	***AIC***	***BIC***	***Bayes Factor***	***p***	***η²***
Spontaneous + Perturbation	181.8	194.7	.03	.616	.31
Perturbation only	178.9	188.1	26.9		.29

DISCUSSION

We established the relationship between cortical excitability and secreted p-tau in a healthy middle-aged population and did so by leveraging non-invasive and potentially scalable methods.

As hypothesized, the more sensitive and direct marker of cortical excitability, induced by TMS perturbation, shows that the higher the cortical excitability, the higher the p-tau181 concentration is. This result is consistent with the recently shown synergic relationship between Aβ and tau,[33] where in the presence of Aβ, the inhibitory effect of tau on neuronal activity becomes ineffective.[34] Nonetheless, the lack of a selective Aβ biomarker in this study precludes us from directly testing this hypothesis. Moreover, our sample consists of healthy middle-aged adults, and it is currently unknown what is the nature of the interplay between Aβ and p-tau and its compounded impact on neuronal excitability in the healthy adult brain.

Conversely, the results also show that cortical excitation/inhibition balance is positively correlated with p-tau181 concentration. Computational modeling, as well as evidence from research in mice and macaques,[19] suggest that flatter slopes in the aperiodic component of the power spectrum might indicate an inhibitory deficit, thus stepper slopes might indicate that the balance is shifter towards inhibition. In this context, our results would indicate that the more the excitation/inhibition balance is shifted towards inhibition (i.e., steeper slopes) the higher the p-tau181 concentrations are. While this may appear in opposition with the finding obtained in the perturbation-based model, it is important to note that the perturbation-based marker is location specific, and more importantly, it is specific to VGSC excitability. Thus, it more directly reflects the excitability of pyramidal neurons at the stimulation site.[23,24] In contrast, the spontaneous marker is an heterogeneous measure likely reflecting the global complex interplay of multiple excitatory and inhibitory neurotransmission pathways throughout the cortex.[26,35] Thus, it lacks the spatial and neurophysiological specificity of the perturbation-based metric. Therefore, the relationship we observed is not directly comparable or analogous between spontaneous and perturbation-based metrics, and the former might not be sensitive enough to detect the subtle and localized excitability increases that the later revealed to be associated with higher ptau181 concentration.

Interestingly, our results show that relationships between excitability and p-tau are dependent on age, becoming significant after the ages of 54 and 61 for spontaneous and perturbation-based excitability, respectively. There is ample evidence that in normal

aging there is measurable structural and functional brain deterioration of the brain,[36,37] encompassing biochemical, metabolic, cellular, and molecular changes.[38] Therefore, a possible explanation for the non-linear associations we report here, might be that at late middle age, normal aging-related brain deterioration may reach a critical threshold from which aberrant interactions between Aβ and p-tau might start to manifest, at least in part, in the form of changes in cortical excitability. Similarly, recent research on the same BBHI cohort also shows that even in the absence of pathology, subtle decreases in dual-task gait performance become noticeable only after 54 years of age.[39]

We have also shown that the relationships observed between cortical excitability markers and p-tau do not hold for NfL. This highlights that the presented markers of cortical excitability are probably related to secreted protein passing to the blood stream when dissolved, rather than being passively released as a byproduct of axonal damage and cell death. Although both NfL and tau can be either passively released or secreted into the extracellular space, tau secretion has been observed in a regulated manner in healthy and pathological conditions,[40] while passive release of tau has been mostly observed as a byproduct of cell death or injury after an acute stroke.[41] Conversely, NfL concentration have been shown to increase in CSF and blood proportionally to the degree of axonal damage, both in normal aging and in neurodegenerative diseases,[25] suggesting that NfL is mostly passively released as a byproduct of cell injury.

This study is limited as it lacks a selective Aβ biomarker to better interpret the results, and our sample only includes middle aged subjects. This precludes us from exploring how the relationships described progress into older ages and pathology. Nevertheless, we have shown, for the first time, that cortical excitability changes are related to p-tau concentration starting at late middle age, even in the absence of obvious amyloid and tau pathology or cognitive decline. Research in preclinical healthy populations is crucial if we are to detect individuals at risk of developing disease and be able to delay or prevent it via modifiable lifestyle factors or specific therapies aiming at reducing Aβ and p-tau buildup early on. In this regard, we have shown that readily available blood-based biomarkers and non-invasive electrophysiology can be used to study the associations between cortical excitability and proteins implicated in the pathophysiology of neurodegenerative disorders. This is important from an early disease detection standpoint, but also provides neurophysiological insights about the relationships between p-tau and cortical excitability, which represents a potentially modifiable and complementary target to combat disease early on, as cortical excitability can be effectively reduced using pharmacological and non-invasive brain stimulation interventions.

Acknowledgements
Authors thank the Barcelona Brain Health Initiative project participants, whose invaluable contribution made this research possible.

Data availability
The script used to preprocess the resting state EEG data is available as a supplementary material. The data that support the findings of this study are available from the corresponding author, upon reasonable request.

Funding
R.P-A. was supported by a fellowship from “la Caixa” Foundation (ID 100010434; Fellowship code: LCF/BQ/DI19/11730050).

K.A.-P. was financially supported by a Juan de la Cierva research grant (FJC2021-047380-I) of the Spanish Ministry of Science and Innovation.

I.P. was supported by a fellowship from “la Caixa” Foundation (ID 100010434; fellowship code LCF/BQ/DI18/11660026).

L.V.-A. was supported by a Margarita Salas junior postdoctoral fellowship from NextGenerationUE.

A.P-L. was partly supported by the Barcelona Brain Health Initiative, National Institutes of Health (R01AG076708, R01AG059089, R03AG072233), and the Bright Focus Foundation.

H.Z. is a Wallenberg Scholar supported by grants from the Swedish Research Council (#2023-00356; #2022-01018 and #2019-02397), the European Union’s Horizon Europe research and innovation programme under grant agreement No 101053962, Swedish State Support for Clinical Research (#ALFGBG-71320), the Alzheimer Drug Discovery Foundation (ADDF), USA (#201809-2016862), the AD Strategic Fund and the Alzheimer's Association (#ADSF-21-831376-C, #ADSF-21-831381-C, #ADSF-21-831377-C, and #ADSF-24-1284328-C), the Bluefield Project, Cure Alzheimer’s Fund, the Olav Thon Foundation, the Erling-Persson Family Foundation, Stiftelsen för Gamla Tjänarinnor, Hjärnfonden, Sweden (#FO2022-0270), the European Union’s Horizon 2020 research and innovation programme under the Marie Skłodowska-Curie grant agreement No 860197 (MIRIADE), the European Union Joint Programme – Neurodegenerative Disease Research (JPND2021-00694), the National Institute for Health and Care Research University College London Hospitals Biomedical Research Centre, and the UK Dementia Research Institute at UCL (UKDRI-1003).

This project has received funding from the European Union’s Horizon 2020 Research and Innovation Programme under the Marie Skłodowska-Curie grant agreement No. 713673

Conflicts of interest

A.P-L. serves as a paid member of the scientific advisory boards for Neuroelectrics, Magstim Inc., TetraNeuron, Skin2Neuron, MedRhythms, and Hearts Radiant. He is co-founder of TI solutions and co-founder and chief medical officer of Linus Health where he has shares and share-options. A.P-L is listed as an inventor on several issued and pending patents on the real-time integration of transcranial magnetic stimulation with electroencephalography and magnetic resonance imaging, and applications of noninvasive brain stimulation in various neurological disorders; as well as digital biomarkers of cognition and digital assessments for early diagnosis of dementia.

H.Z. has served at scientific advisory boards and/or as a consultant for Abbvie, Acumen, Alector, Alzinova, ALZPath, Annexon, Apellis, Artery Therapeutics, AZTherapies, Cognito Therapeutics, CogRx, Denali, Eisai, Merry Life, Nervgen, Novo Nordisk, Optoceutics, Passage Bio, Pinteon Therapeutics, Prothena, Red Abbey Labs, reMYND, Roche, Samumed, Siemens Healthineers, Triplet Therapeutics, and Wave, has given lectures in symposia sponsored by Alzecure, Biogen, Cellectricon, Fujirebio, Lilly, and Roche, and is a co-founder of Brain Biomarker Solutions in Gothenburg AB (BBS),

which is a part of the GU Ventures Incubator Program (outside submitted work). D.B-F. serves as a paid member of the scientific advisory board for Linus Health.

The remaining authors declare that the research was conducted in the absence of any commercial or financial relationships that could be construed as a potential conflict of interest.

References:

1. Hansson O. Biomarkers for neurodegenerative diseases. *Nat Med*. 2021;27(6):954-963. doi:10.1038/s41591-021-01382-x
2. Pichet Binette A, Franzmeier N, Spotorno N, et al. Amyloid-associated increases in soluble tau relate to tau aggregation rates and cognitive decline in early Alzheimer's disease. *Nat Commun*. 2022;13(1):6635. doi:10.1038/s41467-022-34129-4
3. Targa Dias Anastacio H, Matosin N, Ooi L. Neuronal hyperexcitability in Alzheimer's disease: what are the drivers behind this aberrant phenotype? *Transl Psychiatry*. 2022;12(1). doi:10.1038/s41398-022-02024-7
4. Zadey S, Buss SS, McDonald K, Press DZ, Pascual-Leone A, Fried PJ. Higher motor cortical excitability linked to greater cognitive dysfunction in Alzheimer's disease: results from two independent cohorts. *Neurobiol Aging*. 2021;108:24-33. doi:10.1016/j.neurobiolaging.2021.06.007
5. Busche MA, Chen X, Henning HA, et al. Critical role of soluble amyloid-β for early hippocampal hyperactivity in a mouse model of Alzheimer's disease. *Proc Natl Acad Sci U S A*. 2012;109(22):8740-8745. doi:10.1073/pnas.1206171109
6. Schultz MK, Gentzel R, Usenovic M, et al. Pharmacogenetic neuronal stimulation increases human tau pathology and trans-synaptic spread of tau to distal brain regions in mice. *Neurobiol Dis*. 2018;118(July):161-176. doi:10.1016/j.nbd.2018.07.003
7. Franzmeier N, Neitzel J, Rubinski A, et al. Functional brain architecture is associated with the rate of tau accumulation in Alzheimer's disease. *Nat Commun*. 2020;11(1):1-17. doi:10.1038/s41467-019-14159-1
8. Zhang Y, Chen H, Li R, Sterling K, Song W. Amyloid β-based therapy for Alzheimer's disease: challenges, successes and future. *Signal Transduct Target Ther*. 2023;8(1):1-26. doi:10.1038/s41392-023-01484-7
9. Kondo A, Shahpasand K, Mannix R, et al. Antibody against early driver of neurodegeneration cis P-tau blocks brain injury and tauopathy. *Nature*. 2015;523(7561):431-436. doi:10.1038/nature14658
10. Meisel C, Schulze-Bonhage A, Freestone D, Cook MJ, Achermann P, Plenz D. Intrinsic excitability measures track antiepileptic drug action and uncover increasing/decreasing excitability over the wake/sleep cycle. *Proc Natl Acad Sci U S A*. 2015;112(47):14694-14699. doi:10.1073/pnas.1513716112
11. Huang YZ, Edwards MJ, Rounis E, Bhatia KP, Rothwell JC. Theta burst stimulation of the human motor cortex. *Neuron*. 2005;45(2):201-206. doi:10.1016/j.neuron.2004.12.033
12. Houdayer E, Degardin A, Cassim F, Bocquillon P, Derambure P, Devanne H. The effects of low- and high-frequency repetitive TMS on the input/output properties of the human corticospinal pathway. *Exp Brain Res*. 2008;187(2):207-217. doi:10.1007/s00221-008-1294-z
13. Valero-Cabré A, Payne BR, Pascual-Leone A. Opposite impact on 14C-2-deoxyglucose brain metabolism following patterns of high and low frequency

repetitive transcranial magnetic stimulation in the posterior parietal cortex. *Exp Brain Res*. 2007;176(4):603-615. doi:10.1007/s00221-006-0639-8
14. Pascual-Leone A, Valls-Solé J, Wassermann EM, Hallett M. Responses to rapid-rate transcranial magnetic stimulation of the human motor cortex. *Brain*. 1994;117(4):847-858. doi:10.1093/brain/117.4.847
15. Lynch CJ, Elbau IG, Ng TH, et al. Automated optimization of TMS coil placement for personalized functional network engagement. *Neuron*. 2022;110(20):3263-3277.e4. doi:10.1016/j.neuron.2022.08.012
16. Momi D, Ozdemir RA, Tadayon E, et al. Network-level macroscale structural connectivity predicts propagation of transcranial magnetic stimulation. *Neuroimage*. 2021;229(July 2020):117698. doi:10.1016/j.neuroimage.2020.117698
17. Teunissen CE, Verberk IMW, Thijssen EH, et al. Blood-based biomarkers for Alzheimer's disease: towards clinical implementation. *Lancet Neurol*. 2022;21(1):66-77.
18. Mattsson-Carlgren N, Salvadó G, Ashton NJ, et al. Prediction of Longitudinal Cognitive Decline in Preclinical Alzheimer Disease Using Plasma Biomarkers. *JAMA Neurol*. 2023;80(4):360-369. doi:10.1001/jamaneurol.2022.5272
19. Gao R, Peterson EJ, Voytek B. Inferring synaptic excitation/inhibition balance from field potentials. *Neuroimage*. 2017;158(March):70-78. doi:10.1016/j.neuroimage.2017.06.078
20. Donoghue T, Haller M, Peterson EJ, et al. Parameterizing neural power spectra into periodic and aperiodic components. *Nat Neurosci*. 2020;23(12):1655-1665. doi:10.1038/s41593-020-00744-x
21. Kopčanová M, Tait L, Donoghue T, et al. Resting-state EEG signatures of Alzheimer's disease are driven by periodic but not aperiodic changes. *bioRxiv Prepr Serv Biol*. 2023;190(July 2023). doi:10.1101/2023.06.11.544491
22. Benwell CSY, Davila-Pérez P, Fried PJ, et al. EEG spectral power abnormalities and their relationship with cognitive dysfunction in patients with Alzheimer's disease and type 2 diabetes. *Neurobiol Aging*. 2020;85:83-95. doi:10.1016/j.neurobiolaging.2019.10.004
23. Darmani G, Bergmann TO, Zipser C, Baur D, Müller-Dahlhaus F, Ziemann U. Effects of antiepileptic drugs on cortical excitability in humans: A TMS-EMG and TMS-EEG study. *Hum Brain Mapp*. 2019;40(4):1276-1289. doi:10.1002/hbm.24448
24. Premoli I, Biondi A, Carlesso S, Rivolta D, Richardson MP. Lamotrigine and levetiracetam exert a similar modulation of TMS-evoked EEG potentials. *Epilepsia*. 2017;58(1):42-50. doi:10.1111/epi.13599
25. Gaetani L, Blennow K, Calabresi P, Di Filippo M, Parnetti L, Zetterberg H. Neurofilament light chain as a biomarker in neurological disorders. *J Neurol Neurosurg Psychiatry*. Published online 2019:870-881. doi:10.1136/jnnp-2018-320106
26. Ahmad J, Ellis C, Leech R, et al. From mechanisms to markers: novel noninvasive EEG proxy markers of the neural excitation and inhibition system in humans. *Transl Psychiatry*. 2022;12(1). doi:10.1038/s41398-022-02218-z
27. Cattaneo G, Bartrés-Faz D, Morris TP, et al. The Barcelona brain health initiative: A cohort study to define and promote determinants of brain health. *Front Aging Neurosci*. 2018;10(OCT). doi:10.3389/fnagi.2018.00321
28. Karikari TK, Pascoal TA, Ashton NJ, et al. Blood phosphorylated tau 181 as a biomarker for Alzheimer's disease: a diagnostic performance and prediction

modelling study using data from four prospective cohorts. *Lancet Neurol*. 2020;19(5):422-433. doi:10.1016/S1474-4422(20)30071-5
29. Gisslén M, Price RW, Andreasson U, et al. Plasma Concentration of the Neurofilament Light Protein (NFL) is a Biomarker of CNS Injury in HIV Infection: A Cross-Sectional Study. *EBioMedicine*. 2016;3:135-140. doi:10.1016/j.ebiom.2015.11.036
30. Thomas Yeo BT, Krienen FM, Sepulcre J, et al. The organization of the human cerebral cortex estimated by intrinsic functional connectivity. *J Neurophysiol*. 2011;106(3):1125-1165. doi:10.1152/jn.00338.2011
31. Rossini PM, Burke D, Chen R, et al. Clinical Neurophysiology Non-invasive electrical and magnetic stimulation of the brain , spinal cord , roots and peripheral nerves : Basic principles and procedures for routine clinical and research application . An updated report from an. *Clin Neurophysiol*. 2015;126(6):1071-1107. doi:10.1016/j.clinph.2015.02.001
32. Delorme A, Makeig S. EEGLAB: An open source toolbox for analysis of single-trial EEG dynamics including independent component analysis. *J Neurosci Methods*. 2004;134(1):9-21. doi:10.1016/j.jneumeth.2003.10.009
33. Busche MA, Hyman BT. Synergy between amyloid-β and tau in Alzheimer's disease. *Nat Neurosci*. 2020;23(10):1183-1193. doi:10.1038/s41593-020-0687-6
34. DeVos SL, Corjuc BT, Commins C, et al. Tau reduction in the presence of amyloid-β prevents tau pathology and neuronal death in vivo. *Brain*. 2018;141(7):2194-2212. doi:10.1093/brain/awy117
35. Voytek B, Knight RT. Dynamic network communication as a unifying neural basis for cognition, development, aging, and disease. *Biol Psychiatry*. 2015;77(12):1089-1097. doi:10.1016/j.biopsych.2015.04.016
36. Fjell AM, Walhovd KB. Structural brain changes in aging: Courses, causes and cognitive consequences. *Rev Neurosci*. 2010;21(3):187-221. doi:10.1515/REVNEURO.2010.21.3.187
37. Tomasi D, Volkow ND. Aging and functional brain networks. *Mol Psychiatry*. 2012;17(5):549-558. doi:10.1038/mp.2011.81
38. Lee J, Kim HJ. Normal Aging Induces Changes in the Brain and Neurodegeneration Progress: Review of the Structural, Biochemical, Metabolic, Cellular, and Molecular Changes. *Front Aging Neurosci*. 2022;14(June):1-15. doi:10.3389/fnagi.2022.931536
39. Zhou J, Cattaneo G, Yu W, et al. The age-related contribution of cognitive function to dual-task gait in middle-aged adults in Spain: observations from a population-based study. *Lancet Heal Longev*. 2023;4(3):e98-e106. doi:10.1016/S2666-7568(23)00009-0
40. Merezhko M, Uronen R, Huttunen HJ. The Cell Biology of Tau Secretion. 2020;13(September):1-20. doi:10.3389/fnmol.2020.569818
41. Hampel H, Blennow K, Shaw LM, Hoessler YC, Zetterberg H, Trojanowski JQ. Total and phosphorylated tau protein as biological markers of Alzheimer ' s disease. *Exp Gerontol*. 2010;45(1):30-40. doi:10.1016/j.exger.2009.10.010

Supplementary Materials for

Spontaneous and perturbation-based EEG cortical excitability markers are associated with plasma pTau181 concentration in healthy middle-aged adults

Included here:

Automated preprocessing pipeline for resting EEG

Structural MRI acquisition parameters

TMS target determination procedures

Source localization of TMS evoked potentials

Supplementary References

Automated preprocessing pipeline for resting EEG

First, data is down-sampled to 250Hz and high pass filtered at 1Hz. Then line noise at 50Hz and harmonic frequencies is further attenuated using the *Cleanline* algorithm (Mullen, 2012). Excessively noisy or disconnected electrode channels are detected using the *clean_artifacts* function (Kothe & Makeig, 2013) and spherically interpolated from neighboring channels. Data is then re-referenced to the average of all channels. Next, the continuous electroencephalogram (EEG) is segmented into non-overlapping two-second-long epochs. Finally, a custom-made function detects and removes noisy epochs based on Kurtosis, joint probability, and amplitude thresholding (±100 μV).

Structural MRI acquisition parameters

All participants received T1- and T2-weighted anatomical MRI scans, which served as a basis for neuronavigation and EEG source reconstruction. These high-resolution (0.8x0.8x0.8mm3) scans included a 3D MP-RAGE T1-weighted structural MRI from a 3T Siemens Magnetom Prisma at the Unitat d'Imatge per Ressonància Magnètica IDIBAPS (Institut d'Investigacions Biomèdiques August Pi i Sunyer) at Hospital Clínic de Barcelona. The T1 scan comprised 208 axial slices captured sequentially with specific parameters (TR = 2400ms, TE = 2.22ms, TI = 1000ms, flip angle = 8º, slice thickness = 0.8 mm, and FOV = 256mm). Similarly, a 3D SPC T2-weighted MRI was acquired using the same equipment, with its own set of parameters (rTR = 3200ms, TE = 563ms, flip angle = 120º, slice thickness = 0.8 mm, and FOV = 256mm). María Cabello-Toscano and Lídia Mulet-Pons meticulously checked the images for quality, ensuring no MRI artifacts or excessive motion were present. The T1 images

facilitated neuronavigation, while both T1 and T2 images contributed to producing detailed segmentations and meshes vital for EEG source reconstruction.

TMS target determination procedures

For the 27 subjects recorded during 2018, personalized targets subjects were identified anatomically. The superior portion of the middle frontal gyrus, about 3 cm ahead of the precentral sulcus, was the focus for Left Prefrontal Cortex (L-PFC) stimulation. Similarly, the Left Inferior Parietal lobule (L-IPL) aimed at the top edge of the angular gyrus, nearly 1 cm below the intraparietal sulcus. For the subsequent 20 participants recorded from 2019 to 2020, target identification relied on the group-level analysis of the seven functional networks parcellation by Yeo et al. (2011), employing a technique initially proposed by Ozdemir et al. (2020). This method utilized confidence maps from a 1000-healthy subject dataset, where each vertex was assigned a confidence score between -1 and 1, indicating its association with a specific network. The most stable and reliable areas within the angular gyrus and middle frontal gyrus were chosen at the group level. Each subject's T1 image was linearly transformed into MNI space and then inversely transformed back to individual native space using the FSL's FNIRT tool (Woolrich et al., 2009). These coordinates where used to guide precise stimulation using a BrainSight neuronavigation system (RogueResearch, Inc., Canada).

Anatomically targeted mean MNI coordinates were x=-44, y=-67, z=44 for IPL and x=-33, y=37, z=48 for L-PFC. Functionally targeted coordinates were x=-53, y=-51, z=18 for IPL and x=-43, y=34, z=42 for L-PFC, as depicted in Figure S1 on the MNI template. To explore the impact of the targeting method on relevant predictors, an interaction term for each perturbation-based marker (i.e., at each target) was integrated into the main statistical analysis.

Source localization of TMS evoked potentials

Brainstorm software (Tadel et al., 2019) was employed for source reconstruction. A forward model was created for each participant using the openMEEG algorithm (Kybic et al., 2005). The process adhered to standard settings, including three layers with 1922 vertices each, skull and scalp conductivities set at 1, and a brain conductivity of 0.0125, along with adaptive integration. This model was formulated based on each individual's T1 and T2 weighted MRI scans and the positions of electrodes as recorded. The minimum norm imaging method (Salmelin & Baillet, 2009) was then used to estimate the inverse solution. Subsequently, sources were derived as current density maps, with a focus on constrained orientations, specifically normal to the cortex).

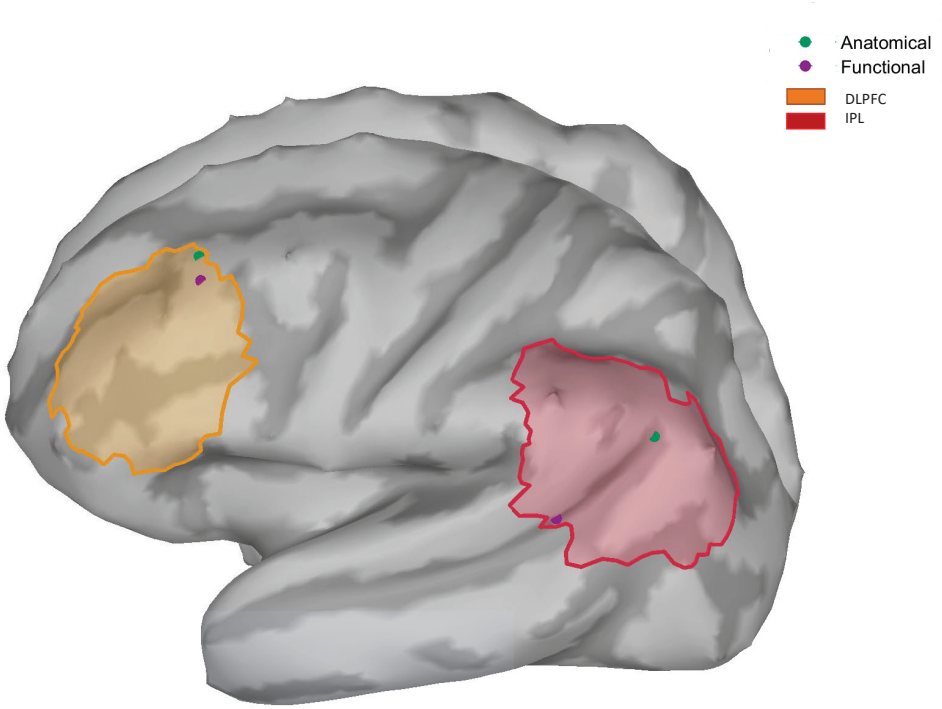

Fig. S1. The average coordinates for L-IPL and L-DLPFC from each targeting technique were superimposed on the MNI template. The regions of interest (ROIs) were highlighted

in yellow and red, representing the projected areas of the PFC and IPL, respectively. These projections were derived from the 17-network Schaefer partition of the Yeo atlas (Schaefer et al., 2018). Figure extracted from supplementary materials of Perellón-Alfonso et. al. (Perellón-Alfonso et al., 2022).

Supplementary References

Kothe, C. A., & Makeig, S. (2013). BCILAB: A platform for brain-computer interface development. *Journal of Neural Engineering*, *10*(5). https://doi.org/10.1088/1741-2560/10/5/056014

Kybic, J., Clerc, M., Abboud, T., Faugeras, O., Keriven, R., & Papadopoulo, T. (2005). A common formalism for the integral formulations of the forward EEG problem. *IEEE Transactions on Medical Imaging*, *24*(1), 12–28. https://doi.org/10.1109/TMI.2004.837363

Mullen, T. (2012, February 9). *NITRC: CleanLine: Tool/Resource Info*. https://www.nitrc.org/projects/cleanline

Ozdemir, R. A., Tadayon, E., Boucher, P., Momi, D., Karakhanyan, K. A., Fox, M. D., Halko, M. A., Pascual-Leone, A., Shafi, M. M., & Santarnecchi, E. (2020). Individualized perturbation of the human connectome reveals reproducible biomarkers of network dynamics relevant to cognition. *Proceedings of the National Academy of Sciences of the United States of America*, *117*(14), 8115–8125. https://doi.org/10.1073/pnas.1911240117

Perellón-Alfonso, R., Redondo-Camós, M., Abellaneda-Pérez, K., Cattaneo, G., Delgado-Gallén, S., España-Irla, G., Solana Sánchez, J., Tormos, J. M., Pascual-Leone, A., & Bartrés-Faz, D. (2022). Prefrontal reactivity to TMS perturbation as a toy model of mental health outcomes during the COVID-19 pandemic. *Heliyon*, *8*(8), 10208. https://doi.org/10.1016/j.heliyon.2022.e10208

Salmelin, R., & Baillet, S. (2009). Electromagnetic brain imaging. *Human Brain Mapping*, *30*(6), 1753–1757. https://doi.org/10.1002/hbm.20795

Schaefer, A., Kong, R., Gordon, E. M., Laumann, T. O., Zuo, X.-N., Holmes, A. J., Eickhoff, S. B., & Yeo, B. T. T. (2018). Local-Global Parcellation of the Human Cerebral Cortex from Intrinsic Functional Connectivity MRI. *Cerebral Cortex*, *28*(9), 3095–3114. https://doi.org/10.1093/cercor/bhx179

Tadel, F., Bock, E., Niso, G., Mosher, J. C., Cousineau, M., Pantazis, D., Leahy, R. M., & Baillet, S. (2019). MEG/EEG group analysis with brainstorm. *Frontiers in Neuroscience*, *13*(FEB), 1–21. https://doi.org/10.3389/fnins.2019.00076

Thomas Yeo, B. T., Krienen, F. M., Sepulcre, J., Sabuncu, M. R., Lashkari, D., Hollinshead, M., Roffman, J. L., Smoller, J. W., Zöllei, L., Polimeni, J. R., Fisch, B., Liu, H., & Buckner, R. L. (2011). The organization of the human cerebral cortex estimated by intrinsic functional connectivity. *Journal of Neurophysiology*, *106*(3), 1125–1165. https://doi.org/10.1152/jn.00338.2011

Woolrich, M. W., Jbabdi, S., Patenaude, B., Chappell, M., Makni, S., Behrens, T., Beckmann, C., Jenkinson, M., & Smith, S. M. (2009). Bayesian analysis of neuroimaging data in FSL. *NeuroImage*, *45*(1 Suppl), S173–S186.

https://doi.org/10.1016/j.neuroimage.2008.10.055

CHAPTER 4. General Discussion

In this thesis, comprised of three studies, we have unveiled novel candidate biomarkers of brain health in the context of mental health resilience, schizophrenia, and early Alzheimer's disease. Importantly, this has been accomplished using non-invasive and scalable methods, consisting of resting state and task-based EEG, concurrent TMS-EEG, and blood-based p-tau and NfL concentration measurements. Thus, we have shown that EEG —by itself or in combination with transcranial magnetic stimulation— can be effectively used to reveal potential biomarkers for a variety of brain health challenges. Indeed, the conditions that are the object of this thesis, are, at the fundamental level, intrinsically related; they involve risk factors or disfunctions which are grounded in inhibitory and excitatory neuronal processes that are essentially electrophysiological in nature and, hence, can be potentially captured and interfered with EEG and TMS, respectively. Moreover, the findings reported here advance our understanding of the neurophysiological mechanisms underlying the resilience or vulnerability to psychosocial stressors, here associated with the COVID-19 pandemic; the subtle oscillatory abnormalities in working memory subprocesses in cognitively preserved schizophrenia patients; and the associations between cortical excitability and proteins implicated in AD pathology. It is also worth noting that the populations sampled in these three studies are healthy, or asymptomatic, which showcases the sensitivity of the proposed biomarkers to detect subtle potential abnormalities, even in the absence of obvious pathology. This underscores the potential of these candidate biomarkers to capture warning signs of intrinsic vulnerability, subtle disfunction or impending pathology. This predictive capability is of crucial importance for early detection and, hence, to provide a preclinical window of opportunity to implement timely interventions to prevent the occurrence of pathology, ameliorate symptoms, or even delay their onset and, hence, promote the best possible functional outcome, that is, optimal brain health. In this context, the choice of electrophysiological correlates in this thesis, has the intended benefit of informing potential interventions that could effectively modify them, with the specific corollary objectives of promoting mental health resilience, ameliorating the cognitive impact of oscillatory abnormalities in schizophrenia, and reducing the spread of protein pathology in preclinical AD. As

described in greater detail in the introduction chapter, we can modulate brain activity by tapping into the excitatory and inhibitory processes of the brain using either pharmacological interventions or electric and magnetic brain stimulation techniques.

In the first study, we presented a toy-model concept to investigate candidate biomarkers of resilience and vulnerability to the deleterious mental health impacts of the psychosocial stressors of the COVID-19 pandemic and associated lockdowns. We used a controlled TMS brain perturbation to model the stressor, and the EEG reactivity to it to model the organism response. The idea that single pulse TMS can be understood as a "perturbation" or temporary insult might be considered controversial, as typically the term has been tied to lesional rTMS protocols that effectively inhibit a particular brain function, such as in speech arrest paradigms, whereby a short (i.e., few seconds) train of TMS pulses is delivered at 2Hz over the inferior frontal gyrus while the subject counts backwards (Borowczyk et al., 2022). However, there is evidence that a single TMS pulse interferes with brain activity by injecting a current that effectively disrupts endogenous electrical brain activity. In support of this point of view, concurrent TMS-EEG studies have shown that the pulse induces phase resetting — an external event related change in brain oscillatory activity— (Rocchi et al., 2018), and possibly reflects deterministic properties of the stimulated neuronal circuits that propagate through anatomically and functionally connected brain regions (Casarotto et al., 2010; Momi et al., 2021). Moreover, evidence from research in epilepsy shows that single pulse TMS stimulation can trigger a cascade of synchronous neuronal excitability resulting in epileptiform discharges (Kimiskidis, 2019; Kimiskidis et al., 2017), which is suggestive of the perturbational nature of the stimulus. Further supporting this notion, it has been shown that the fMRI and EEG response profile to single pulse TMS in patients with epilepsy was consistent with hyperexcitability. If we are therefore defining single pulse TMS as a brain perturbation, we can also consider it a stressor or transitory insult to the brain.

This non-invasive perturbation modeling approach, combining EEG and TMS to predict the mental health outcome of psychosocial stressors associated with the COVID-19 pandemic, revealed that subjects who experienced a measurable negative

impact in mental health, also had an exaggerated EEG evoked response to the controlled and targeted TMS perturbation —months before the pandemic— when compared to those who had no negative impact. The revealed signature was localized to the left prefrontal cortex (L-PFC), as there were no group differences after stimulation of the left inferior parietal lobule (L-IPL), which served as control, nor when comparing the global whole-brain response to stimulation. The groups significantly separated in the TMS evoked EEG response of the L-PFC between 202 and 262ms after the pulse. This time-window overlaps with the 160-240ms time-window when the P180 component typically occurs, which possibly reflects VGSC-mediated excitability. Pharmacological studies have shown that VGSC blockers can effectively inhibit this TMS evoked EEG component (G Darmani et al., 2019; I Premoli et al., 2017). Moreover, the evoked responses 180ms after the pulse have also been shown to be modulated by GABA-B inhibitory interneurons, as the evoked response is effectively reduced after application of long-interval intracortical inhibition, using paired-pulse TMS paradigms (de Goede et al., 2020). Therefore, we can interpret this resilience signature as reflecting the brain's capacity to withstand or successfully inhibit a stressor, transient insult, or disturbance of a critical node or anchor within the networks and brain regions underlying psychological resilience. Importantly, the discovery that vulnerability might be linked to the disruption of parvalbumin-positive cells (i.e., the largest group of GABAergic interneurons) and, consequently, of perineuronal nets, which encase these cells and play a pivotal role in neurodevelopmental and post-injury plasticity (Fawcett et al., 2019), underscores the potential translatability of this candidate biomarker to pathologies involving disruption of these neuronal populations. Such pathologies include traumatic brain injury, schizophrenia, or Alzheimer's disease (AD), where we can thus conceivable predict that these conditions would be associated with a loss of resilience and increased susceptibility to stressors, as suggested by epidemiological findings on the presence of psychiatric comorbidities in these disorders (Buckley et al., 2009; Ehrenberg et al., 2018; Hammond et al., 2019). Finally, the revealed resilience signature could serve explain the considerable variability observed in mental health trajectories during the pandemic and associated lockdowns observed in a recent two-year post-COVID 19 outbreak follow-up (Bayes-Marin et al., 2023).

In the second study we investigated subtle oscillatory abnormalities in schizophrenia patients, using EEG during a visual WM task. Contrary to our initial hypothesis, we show that our sample of patients do not exhibit lesser working memory performance nor higher reaction time variability than healthy matched controls. We also did not see any significant differences in the EEG event related response —contralateral delay activity (CDA)— that indexes neural memory capacity during the task. This supports that our sample of patients had preserved working memory performance and could be considered high-functioning individuals, which typically perform comparably to healthy controls in cognitive tasks (Heinrichs et al., 2015; Rentrop et al., 2010b), and do not exhibit WM related differences in CDA amplitude or latency (Light et al., 2010; So et al., 2018). This is further supported by the fact that our patients were asymptomatic at the time of recruitment and were engaged in psychodynamic psychotherapy, which has been shown to positively correlate with overall functional outcome (Modesti et al., 2023). However, even in high-functioning patients, it is thought that working memory related subprocesses are still fundamentally affected. However, due to either above average cognitive performance or successful compensatory mechanisms —such as attentional hyperfocus— these abnormalities are masked, effectively yielding normal working memory performance (Luck et al., 2019). However, a data driven approach on the oscillatory components of the EEG evoked response, revealed that patients had significantly lower alpha suppression in all phases of the working memory task (i.e., task preparation, memory encoding, maintenance, and retrieval), when compared to controls. There is ample evidence of abnormalities in the alpha band, which plays a crucial role in basic processes subtending cognitive functioning, such as long-range brain synchrony and top-down control (Doesburg et al., 2009; Scheeringa et al., 2012; Von Stein et al., 2000) —fundamental drivers of functional connectivity— and, importantly, attentional and cortical inhibitory processes (Jensen and Mazaheri, 2010; Klimesch, 2012; Klimesch et al., 2007; Thut et al., 2006), which have been found to be consistently affected in schizophrenia (Lewis et al., 2005; Radhu et al., 2015; Trajkovic et al., 2021). Our results coincide with previous findings reporting decreased alpha suppression in schizophrenia spectrum during working memory, suggestive of inhibitory deficits (Doesburg et al., 2009; Erickson et al., 2017; Kustermann et al., 2016; Ramyead et al., 2019), likely

related to known disfunctions in parvalbumin-positive cells in schizophrenia (Kaar et al., 2019). We then implemented a custom machine learning architecture, incorporating the attention mechanism, which was used to differentiate patients from controls based on standardly preprocessed EEG data alone. This interpretable model revealed that the temporal windows throughout the WM task time-course that were most discriminative between patients and controls, overlapped with the task phases which were also found to be significantly different between groups in the exploratory oscillatory analysis. This indicates that the machine learning model was able to detect the same oscillatory abnormalities, indicative of inhibitory deficits in schizophrenia. This shows that interpretable machine learning models can be used to distinguish patients from controls, even when cognitive performance is preserved, and at the same time, provide mechanistic insights on the neurophysiological underpinnings of the disease. Therefore, we have shown that decreased event related desynchronization of alpha oscillations during working memory is a sensitive candidate biomarker for schizophrenia detection and differentiation —linked to inhibitory deficits— that can be revealed by either time-frequency decomposition of the EEG or interpretable machine learning models, which showcases the potential for individual diagnostic applications in a precision psychiatry framework.

In the third study we established, for the first time, the relationship between cortical excitability and p-tau in a healthy middle-aged population, by leveraging non-invasive methods. We have shown that p-tau concentration in plasma is partially explainable by spontaneous and perturbation-based excitability metrics. Specifically, higher perturbation-based excitability, as indexed by the late components (i.e., 160-240ms) of the TMS evoked EEG response, is correlated with higher concentrations of p-tau. It has been shown that tau and Aβ have an antagonistic effect on cortical excitability (Busche et al., 2019), when considered independently; the former would promote excitability (Palop and Mucke, 2016) and the latter inhibition (Marinković et al., 2019). Recent findings however, show that Aβ and tau interact in a synergic manner, whereby higher levels of Aβ render the inhibitory effects of tau ineffective (Busche and Hyman, 2020; DeVos et al., 2018). Moreover, it has also been shown that soluble Aβ actively promotes the secretion of p-tau, possibly through the promotion of

neuronal excitability (Pichet Binette et al., 2022). Therefore, our results might reflect this synergic relationship, which would predict both higher levels of p-tau as well as higher excitability. Conversely, and contrary to our initial hypothesis, the spontaneous EEG metric of inhibition/excitation balance, showed that the stepper the slope of the aperiodic component of the EEG spectra —meaning the balance is shifted towards inhibition—, the higher the p-tau concentration. However, it must be noted that this metric is an heterogeneous measure possibly reflecting the complex interaction of excitatory and inhibitory intraneuronal populations (Ahmad et al., 2022), which precludes direct quantification of net excitation and inhibition. In contrast, the perturbation marker reflects VGSC mediated excitability, which more directly quantifies net cortical pyramidal neuron excitability, regardless of interneuron interactions. Moreover, the results further show that the perturbation marker is more sensitive than the spontaneous one, as it better predicts p-tau concentrations in a subsample an order of magnitude smaller. Importantly, we also found that the correlation between excitability and p-tau concentration becomes significant only at late middle age. These non-linear relationships with age could indicate early potentially pathological processes in Aβ and tau, related to changes associated with the aging brain. It is well known that, even in non-pathological aging, there is widespread brain deterioration, with changes spanning from the molecular and cell level up to and including whole brain systems (Fjell and Walhovd, 2010; Lee and Kim, 2022; Tomasi and Volkow, 2012). Finally, we have shown that cortical excitability is related to secreted p-tau, rather than passively released proteins, such as NfL. This is significant, as it shows that cortical excitability is likely associated with p-tau secretion, which stands as a fundamental driver in AD pathology in its early stages. This underscores the potential relevance of the proposed candidate biomarkers for early detection of protein pathology implicated in AD.

In this thesis we have discovered three candidate biomarkers of brain health that are relevant to fundamental pathological threats, based on non-invasive, readily available methods, and thus potentially scalable and translatable to a clinical preventive and diagnostic screening scenario. Studies 1 and 3 leveraged the same sample of participants, belonging to the Barcelona Brain Health Initiative project (Cattaneo et al., 2018), to show that using TMS to transitorily perturb ongoing brain

activity can reveal preclinical EEG signatures of inhibitory and excitatory processes with high spatial and neurophysiological specificity, that are predictive of an individual's brain health status and potential resilience. Specifically, in study 1 we have shown that we can model the future mental health impact —months later— of psychosocial stressors, by encouraging a brain reaction in a controlled experimental framework by using TMS perturbations. Similarly, in study 3 we have shown that the same methodology can be used to tap into the role of cortical excitability in protein secretion mechanisms implicated in the early stages of AD. In study 2, we selected a sample of asymptomatic and likely high-functioning schizophrenia patients to investigate subtle oscillatory abnormalities associated with inhibitory deficits in working memory, showcasing the potential of interpretable machine learning algorithms to detect these EEG signatures and use them to differentiate patients form controls, even when conventional neuropsychological and psychophysics methods could not distinguish them. All three of the identified correlates of brain health are grounded on and reflect the excitatory and inhibitory processes that constitute causative neurophysiological disfunctions in synaptic transmission of highly prevalent neuropsychiatric and neurodegenerative disorders.

These studies were intrinsically limited by the characteristics of the samples and other methodological constraints. In study 1 and the subsample receiving TMS-EEG in study 3, some of the subjects received stimulation based on anatomical targeting while others based on functionally determined targeting, while the topographic distances between targets where relatively small, this introduced an additional variable that needed to be accounted for, however this was controlled directly in statistical analysis in each study by adding a targeting method interaction term to the predictors of interest. Moreover, in this sample not all participants completed stimulation at both L-PFC and L-IPL stimulation targets; for study 1 this required running regression analysis for each target separately, potentially hindering statistical power. Moreover, in study 1, the mental health changes during the pandemic timepoints sampled, when compared to pre-pandemic measurements, were relatively small, in most cases not reaching clinical thresholds for anxiety and depression. Therefore, the predictive clinical value of the revealed resilience and vulnerability signatures would have benefited from a

sample incorporating a sufficient sample of clinically affected individuals. In study 3 participants were healthy middle-aged individuals, therefore, while the revealed relationships of cortical excitability and p-tau might be relevant to AD pathology, further validation on early-stage AD patients or older individuals would be needed to corroborate the relationships observed and determine how they might change with aging and the onset of protein pathology. Moreover, in study 3 our interpretation of results partially relies on Aβ, for which we did not have a selective biomarker in this sample. Nevertheless, given the known high correlation between PET-Aβ and p-tau181 concentration in plasma (Mielke et al., 2018), it is reasonable to assume that higher concentration of p-tau implies higher concentration of Aβ. In study 2, to properly validate the differential diagnostic value of the detected oscillatory signature and evaluate its potential in tackling the heterogeneity problem in psychiatry, it would be necessary to include different subtypes of schizophrenia with varying degrees of working memory impairment, as well as other disorders presenting similar impairments and dysfunctions in working memory subprocesses, such as bipolar disorder (Saldarini et al., 2022).

Despite these limitations, the proposed candidate biomarkers reflect excitatory and inhibitory processes that are known to play a fundamental role in the neruophysiopathology of mental health and neurodegenerative disorders. This is important, because as described in greater detail in the introduction chapter, synaptic transmission can be effectively modified via non-invasive brain stimulation protocols. In study 1, we showed that hyperactivity in response to a TMS perturbation of the L-PFC was predictive of higher mental health vulnerability to psychosocial stressors, we argued this excitability could be caused by deficient GABAergic inhibition. Moreover, while the resilience 'toy model' we proposed was applied to the psychosocial stressors associated with the COVID-19 pandemic and lockdowns, this model is meant to be translatable to resilience when facing other potentially stressful scenarios, such as hip replacement surgery (Zhang et al., 2022) or exposure to potential trauma (e.g., disaster relief or warzone workers), as well as . Therefore, a plausible intervention would consist in promoting inhibition at the L-PFC via low frequency rTMS, cTBS or cathodal tDCS, thus potentially increasing resilience by targeting the hypothesized inhibitory

disfunction at the critical L-PFC target. Similarly, in study 2 we have shown that high-performing schizophrenia patients exhibit alpha suppression abnormalities in bilateral parietal-occipital cortex, which is likely related to deficient inhibition in critical subprocesses of working memory (i.e., task preparation, encoding, maintenance and retrieval). Therefore, a plausible intervention would consist in promoting inhibition of the parietal-occipital cortex using low-frequency rTMS, cTBS, or cathodal tDCS. Finally, in study 3 we have shown that higher cortical excitability is correlated with higher p-tau concentrations, which likely promotes the spread of tau pathology throughout the cortex. Current interventions targeting the removal of Aβ and tau could be complemented by targeting the hypothesized mediating mechanism —cortical excitability. Thus, a plausible intervention would consist in promoting inhibition as an addon treatment to protein removal therapies, whereby low-frequency rTMS, cTBS or cathodal tDCS would be delivered over a tau epicenter, such as the temporal cortex (Figure 8).

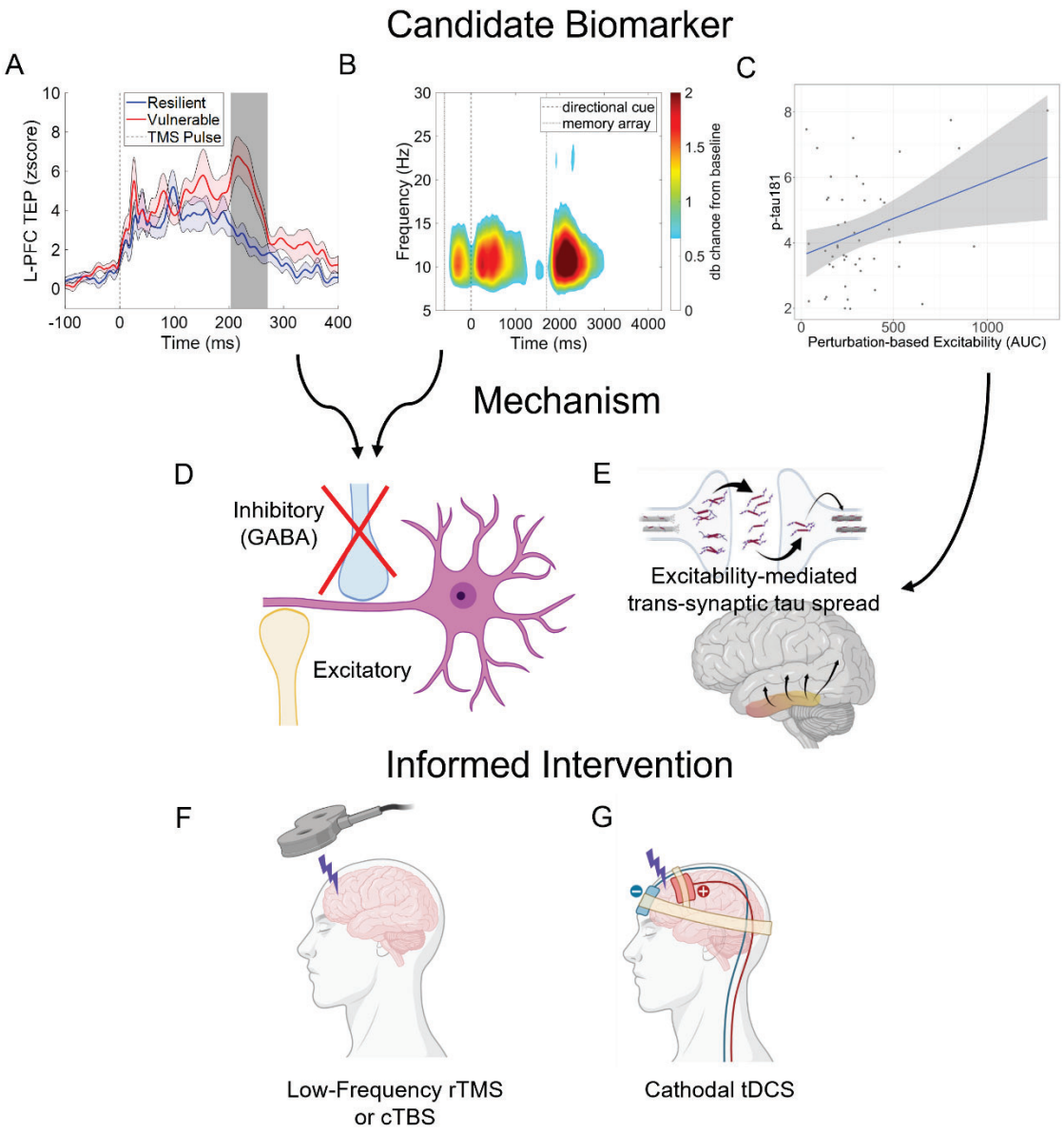

Figure 8. Proposed workflow from candidate biomarkers, through dysfunctional mechanisms, to biomarker-informed NIBS intervention. A) illustrates the perturbation-based EEG signature of resilience. Extracted from Perellón-Alfonso et al., (2022). B) Illustrates the oscillatory EEG signature of WM disfunction in schizophrenia. Modified from Perellón-Alfonso et al., (2023). C) Illustrates the perturbation-based EEG cortical excitability marker of p-tau concentration. Original made with R version 4.2.3 (R Foundation for Statistical Computing, Vienna, Austria). D) Schematic of synaptic transmission dysfunction rooted in GABAergic inhibitory deficits. Original made with BioRender.com. E) Schematic illustration of excitability mediated transsynaptic spread

of tau pathology in AD. Adapted from Binette et. al., (2022). F) and G) illustrate the proposed inhibitory TES and TMS interventions. Original made with BioRender.com.

Remarkably these interventions are inexpensive, readily available and produce minimal or no side effects. TMS is delivered through expensive equipment that requires trained and experienced technicians to operate it, therefore treatments must be administered at a clinic and typically require multiple daily sessions to produce long-lasting plastic changes. In contrast, transcranial electric current stimulation is relatively inexpensive and can be delivered at home with minimal remote guidance (Paneva et al., 2022), which offers a solution potentially scalable to mass population usage. This is supported by a growing number of successful home TES clinical trials targeting mental health disorders, such as depression and anxiety, or neurologic disorders affecting cognition, such as dementia or multiple sclerosis (Antonenko et al., 2022; Charvet et al., 2023b, 2023a; Pilloni, 2023; Pilloni et al., 2022; Silva-Filho et al., 2022). These studies have shown that home-based neuromodulation using TES is feasible and safe in a variety of conditions. For instance, in a recent pilot study not included in this thesis, we stablished the feasibility and safety of a home-based TES intervention targeting the left angular gyrus, which produced memory performance improvements in all participants (Cappon et al., 2023).

CONCLUSIONS

1. Mental health resilience can be modeled as the brain's response to a controlled perturbation that predicts future vulnerability to psychosocial stressors associated with the COVID-19 pandemic and indicates potentially decreased inhibitory capacity.

2. Interpretable machine learning algorithms can detect inhibitory deficits in schizophrenia based on electroencephalographic data alone, even when cognitive performance is preserved.

3. Electroencephalography markers of cortical excitability are associated with plasma p-tau concentration in healthy middle-aged subjects, aligning with the putative role of neuronal excitability in the Aβ-promotion of p-tau secretion in early Alzheimer's disease.

4. Spontaneous and perturbation-based electroencephalography revealed non-invasive candidate biomarkers of brain health that are rooted in inhibitory and excitatory synaptic transmission.

BIBLIOGRAPHY

1. Abi-Dargham A, Moeller SJ, Ali F, DeLorenzo C, Domschke K, Horga G, et al. Candidate biomarkers in psychiatric disorders: state of the field. World Psychiatry 2023;22:236–62. https://doi.org/10.1002/wps.21078.
2. Ahmad J, Ellis C, Leech R, Voytek B, Garces P, Jones E, et al. From mechanisms to markers: novel noninvasive EEG proxy markers of the neural excitation and inhibition system in humans. Transl Psychiatry 2022;12. https://doi.org/10.1038/s41398-022-02218-z.
3. Alnæs D, Kaufmann T, Van Der Meer D, Córdova-Palomera A, Rokicki J, Moberget T, et al. Brain Heterogeneity in Schizophrenia and Its Association with Polygenic Risk. JAMA Psychiatry 2019;76:739–48. https://doi.org/10.1001/jamapsychiatry.2019.0257.
4. Anticevic A, Hu X, Xiao Y, Hu J, Li F, Bi F, et al. Early-course unmedicated schizophrenia patients exhibit elevated prefrontal connectivity associated with longitudinal change. J Neurosci 2015a;35:267–86. https://doi.org/10.1523/JNEUROSCI.2310-14.2015.
5. Anticevic A, Murray JD, Barch DM. Bridging Levels of Understanding in Schizophrenia Through Computational Modeling. Clin Psychol Sci 2015b;3:433–59. https://doi.org/10.1177/2167702614562041.
6. Antonenko D, Rocke M, Thams F, Hummel FC, Maceira-Elvira P, Meinzer M, et al. Complementary practical considerations to home-based, remotely-controlled and independently self-applied tES combined with cognitive training. Brain Stimul 2022;15:1351–3. https://doi.org/10.1016/j.brs.2022.09.010.
7. Arias C, Arrieta I, Tapia R. Beta-Amyloid peptide fragment 25--35 potentiates the calcium-dependent release of excitatory amino acids from depolarized hippocampal slices. J Neurosci Res 1995;41:561–6.
8. Arispe N, Pollard HB, Rojas E. Giant multilevel cation channels formed by Alzheimer disease amyloid beta-protein [A beta P-(1-40)] in bilayer membranes. Proc Natl Acad Sci 1993;90:10573–7.
9. Atagun MI, Drukker M, Hall MH, Altun IK, Tatli SZ, Guloksuz S, et al. Meta-analysis of auditory P50 sensory gating in schizophrenia and bipolar disorder. Psychiatry Res Neuroimaging 2020;300:111078.
10. Baddeley A. Working memory. Curr Biol 2010;20:136–40. https://doi.org/10.1016/j.cub.2009.12.014.
11. Bahdanau D, Cho KH, Bengio Y. Neural machine translation by jointly learning to align and translate. 3rd Int Conf Learn Represent ICLR 2015 - Conf Track Proc 2015:1–15.
12. Barch DM, Ceaser A. Cognition in schizophrenia: Core psychological and neural mechanisms. Trends Cogn Sci 2012;16:27–34. https://doi.org/10.1016/j.tics.2011.11.015.
13. Barros C, Silva CA, Pinheiro AP. Advanced EEG-based learning approaches to

predict schizophrenia: Promises and pitfalls. Artif Intell Med 2021;114:102039.

14. Bartos M, Vida I, Jonas P. Synaptic mechanisms of synchronized gamma oscillations in inhibitory interneuron networks. Nat Rev Neurosci 2007;8:45–56.

15. Batinic B. Cognitive models of positive and negative symptoms of schizophrenia and implications for treatment. Psychiatr Danub 2019;31:S181–4.

16. Bayes-Marin I, Cabello-Toscano M, Cattaneo G, Solana-Sánchez J, Fernández D, Portellano-Ortiz C, et al. COVID-19 after two years: trajectories of different components of mental health in the Spanish population. Epidemiol Psychiatr Sci 2023;32:e19.

17. Bear M, Connors B, Paradiso MA. Neuroscience: exploring the brain, enhanced edition: exploring the brain. Jones & Bartlett Learning; 2020.

18. Begré S, Federspiel A, Kiefer C, Schroth G, Dierks T, Strik WK. Reduced hippocampal anisotropy related to anteriorization of alpha EEG in schizophrenia. Neuroreport 2003;14:739–42.

19. Belardinelli P, König F, Liang C, Premoli I, Desideri D, Müller-Dahlhaus F, et al. TMS-EEG signatures of glutamatergic neurotransmission in human cortex. Sci Rep 2021;11:1–14. https://doi.org/10.1038/s41598-021-87533-z.

20. Bhattacharya A, Mrudula K, Sreepada SS, Sathyaprabha TN, Pal PK, Chen R, et al. An Overview of Noninvasive Brain Stimulation: Basic Principles and Clinical Applications. Can J Neurol Sci 2022;49:479–92. https://doi.org/10.1017/cjn.2021.158.

21. Bialer M, White HS. Key factors in the discovery and development of new antiepileptic drugs. Nat Rev Drug Discov 2010;9:68–82.

22. Biswal B, Zerrin Yetkin F, Haughton VM, Hyde JS. Functional connectivity in the motor cortex of resting human brain using echo-planar MRI. Magn Reson Med 1995;34:537–41.

23. Blennow K, Hampel H, Weiner M, Zetterberg H. Cerebrospinal fluid and plasma biomarkers in Alzheimer disease. Nat Rev Neurol 2010;6:131–44.

24. Bolsinger J, Seifritz E, Kleim B, Manoliu A. Neuroimaging Correlates of Resilience to Traumatic Events—A Comprehensive Review. Front Psychiatry 2018;9. https://doi.org/10.3389/fpsyt.2018.00693.

25. Borowczyk M, Wojtysiak M, Chmielarz-Czarnocińska A, Braszka M, Danielewski P, Bryndal A, et al. Speech arrest by repetitive Transcranial Magnetic Stimulation - does it still work? Old experiences with new improvements. Restor Neurol Neurosci 2022;40:125–35. https://doi.org/10.3233/RNN-211237.

26. Bosia M, Bechi M, Bosinelli F, Politi E, Buonocore M, Spangaro M, et al. From cognitive and clinical substrates to functional profiles: Disentangling heterogeneity in schizophrenia. Psychiatry Res 2019;271:446–53. https://doi.org/10.1016/j.psychres.2018.12.026.

27. Boudewyn MA, Carter CS. Electrophysiological correlates of adaptive control and attentional engagement in patients with first episode schizophrenia and healthy young adults. Psychophysiology 2018;55:e12820.

28. Breijyeh Z, Karaman R. Comprehensive Review on Alzheimer ' s Disease Causes and treatment. Molecules. 2020;25(24):5789. https://doi.org/10.3390/molecules25245789

29. Brodmann K. Vergleichende Lokalisationslehre der Grosshirnrinde in ihren Prinzipien dargestellt auf Grund des Zellenbaues. Barth; 1909.

30. Brunoni AR, Nitsche MA, Bolognini N, Bikson M, Wagner T, Merabet L, et al. Clinical research with transcranial direct current stimulation (tDCS): Challenges and future directions. Brain Stimul 2012;5:175–95. https://doi.org/10.1016/j.brs.2011.03.002.

31. Buckley PF, Miller BJ, Lehrer DS, Castle DJ. Psychiatric comorbidities and schizophrenia. Schizophr Bull 2009;35:383–402. https://doi.org/10.1093/schbul/sbn135.

32. Bueno-Notivol J, Gracia-García P, Olaya B, Lasheras I, López-Antón R, Santabárbara J. Prevalence of depression during the COVID-19 outbreak: A meta-analysis of community-based studies. Int J Clin Heal Psychol 2021;21. https://doi.org/10.1016/j.ijchp.2020.07.007.

33. Busche MA, Chen X, Henning HA, Reichwald J, Staufenbiel M, Sakmann B, et al. Critical role of soluble amyloid-β for early hippocampal hyperactivity in a mouse model of Alzheimer's disease. Proc Natl Acad Sci U S A 2012;109:8740–5. https://doi.org/10.1073/pnas.1206171109.

34. Busche MA, Eichhoff G, Adelsberger H, Abramowski D, Wiederhold K-H, Haass C, et al. Clusters of hyperactive neurons near amyloid plaques in a mouse model of Alzheimer's disease. Science (80-) 2008;321:1686–9.

35. Busche MA, Hyman BT. Synergy between amyloid-β and tau in Alzheimer's disease. Nat Neurosci 2020;23:1183–93. https://doi.org/10.1038/s41593-020-0687-6.

36. Busche MA, Wegmann S, Dujardin S, Commins C, Schiantarelli J, Klickstein N, et al. Tau impairs neural circuits, dominating amyloid-β effects, in Alzheimer models in vivo. Nat Neurosci 2019;22:57–64. https://doi.org/10.1038/s41593-018-0289-8.

37. Buzsáki G, Anastassiou CA, Koch C. The origin of extracellular fields and currents-EEG, ECoG, LFP and spikes. Nat Rev Neurosci 2012;13:407–20. https://doi.org/10.1038/nrn3241.

38. Campbell-Sills L, Forde DR, Stein MB. Demographic and childhood environmental predictors of resilience in a community sample. J Psychiatr Res 2009;43:1007–12. https://doi.org/10.1016/j.jpsychires.2009.01.013.

39. Capocchi G, Zampolini M, Larson J. Theta burst stimulation is optimal for induction of LTP at both apical and basal dendritic synapses on hippocampal CA1 neurons. Brain Res 1992;591:332–6.

https://doi.org/10.1016/0006-8993(92)91715-Q.

40. Cappon D, Fox R, den Boer T, Yu W, LaGanke N, Cattaneo G, et al. Tele-supervised home-based transcranial alternating current stimulation (tACS) for Alzheimer's

disease: a pilot study. Front Hum Neurosci 2023;17. https://doi.org/10.3389/fnhum.2023.1168673.

41. Carson RE, Naganawa M, Toyonaga T, Koohsari S, Yang Y, Chen M-K, et al. Imaging of synaptic density in neurodegenerative disorders. J Nucl Med 2022;63:60S--67S.

42. Casarotto S, Lauro LJR, Bellina V, Casali AG, Rosanova M, Pigorini A, et al. EEG responses to TMS are sensitive to changes in the perturbation parameters and repeatable over time. PLoS One 2010;5. https://doi.org/10.1371/journal.pone.0010281.

43. Cash RFH, Ziemann U. Paired-pulse interactions. Oxford Handb. Transcranial Stimul., Oxford University Press; 2021. https://doi.org/10.1093/oxfordhb/9780198832256.013.13.

44. Cathomas F, Murrough JW, Nestler EJ, Han MH, Russo SJ. Neurobiology of Resilience: Interface Between Mind and Body. Biol Psychiatry 2019;86:410–20. https://doi.org/10.1016/j.biopsych.2019.04.011.

45. Cattaneo G, Bartrés-Faz D, Morris TP, Sánchez JS, Macià D, Tarrero C, et al. The Barcelona brain health initiative: A cohort study to define and promote determinants of brain health. Front Aging Neurosci 2018;10. https://doi.org/10.3389/fnagi.2018.00321.

46. Chan AS, Kwok IC, Chiu H, Lam L, Pang A, Chow L. Memory and organizational strategies in chronic and acute schizophrenic patients. Schizophr Res 2000;41:431–45.

47. Charlson FJ, Ferrari AJ, Santomauro DF, Diminic S, Stockings E, Scott JG, et al. Global epidemiology and burden of schizophrenia: Findings from the global burden of disease study 2016. Schizophr Bull 2018;44:1195–203. https://doi.org/10.1093/schbul/sby058.

48. Charvet L, George A, Charlson E, Lustberg M, Vogel-Eyny A, Eilam-Stock T, et al. Home-administered transcranial direct current stimulation is a feasible intervention for depression: an observational cohort study. Front Psychiatry 2023a;14. https://doi.org/10.3389/fpsyt.2023.1199773.

49. Charvet L, Pilloni G, Lustberg M, Malik M, Feinberg C, Gutman J, et al. Hand Dexterity Improves in Patients with Progressive Multiple Sclerosis (MS) with Telerehabilitation Using Transcranial Direct Current Stimulation (tDCS). Brain Stimul 2023b;16:280. https://doi.org/10.1016/j.brs.2023.01.483.

50. Chen M-H, Chang W-C, Bai Y-M, Huang K-L, Tu P-C, Su T-P, et al. Cortico-thalamic dysconnection in early-stage schizophrenia: a functional connectivity magnetic resonance imaging study. Eur Arch Psychiatry Clin Neurosci 2020;270:351–8.

51. Chételat G, Arbizu J, Barthel H, Garibotto V, Law I, Morbelli S, et al. Amyloid-PET and 18F-FDG-PET in the diagnostic investigation of Alzheimer's disease and other dementias. Lancet Neurol 2020;19:951–62.

52. Chimthanawala NM, Haria A, Sathaye S. Non-invasive biomarkers for early detection of Alzheimer's disease: a new-age perspective. Mol Neurobiol

2023;19:1-2.

53. Clements GM, Bowie DC, Gyurkovics M, Low KA, Fabiani M, Gratton G. Spontaneous alpha and theta oscillations are related to complementary aspects of cognitive control in younger and older adults. Front Hum Neurosci 2021;15:621620.

54. Cohen MX. Where Does EEG Come From and What Does It Mean? Trends Neurosci 2017;40:208–18. https://doi.org/10.1016/j.tins.2017.02.004.

55. Cortes-Briones JA, Tapia-Rivas NI, D'Souza DC, Estevez PA. Going deep into schizophrenia with artificial intelligence. Schizophr Res 2022;245:122–40. https://doi.org/10.1016/j.schres.2021.05.018.

56. Cortes C, Vapnik V. Support-vector networks. Mach Learn 1995;20:273–97.

57. Craig-Schapiro R, Perrin RJ, Roe CM, Xiong C, Carter D, Cairns NJ, et al. YKL-40: a novel prognostic fluid biomarker for preclinical Alzheimer's disease. Biol Psychiatry 2010;68:903–12.

58. D'Esposito M, Postle BR. The cognitive neuroscience of working memory. Annu Rev Psychol 2015;66:115–42. https://doi.org/10.1146/annurev-psych-010814-015031.

59. Dabiri M, Dehghani Firouzabadi F, Yang K, Barker PB, Lee RR, Yousem DM. Neuroimaging in schizophrenia: A review article. Front Neurosci 2022;16:1042814.

60. Darmani Ghazaleh, Bergmann TO, Zipser C, Baur D, Müller-Dahlhaus F, Ziemann U. Effects of antiepileptic drugs on cortical excitability in humans: A TMS-EMG and TMS-EEG study. Hum Brain Mapp 2019;40:1276–89. https://doi.org/10.1002/hbm.24448.

61. Darmani G, Bergmann TO, Zipser C, Baur D, Müller-Dahlhaus F, Ziemann U. Effects of antiepileptic drugs on cortical excitability in humans: a TMS-EMG and TMS-EEG study. Hum Brain Mapp 2019;40:1276–89.

62. Darmani G, Ziemann U. Pharmacophysiology of TMS-evoked EEG potentials: A mini-review. Brain Stimul 2019;12:829–31. https://doi.org/10.1016/j.brs.2019.02.021.

63. Darmani G, Zipser CM, Böhmer GM, others. Effects of the selective alpha5-GABAAR antagonist S44819 on excitability in the human brain: a TMS-EMG and TMS-EEG phase I study. J Neurosci 2016;36:12312–20.

64. DeVos SL, Corjuc BT, Commins C, Dujardin S, Bannon RN, Corjuc D, et al. Tau reduction in the presence of amyloid-β prevents tau pathology and neuronal death in vivo. Brain 2018;141:2194–212. https://doi.org/10.1093/brain/awy117.

65. Dienel SJ, Schoonover KE, Lewis DA. Cognitive Dysfunction and Prefrontal Cortical Circuit Alterations in Schizophrenia: Developmental Trajectories. Biol Psychiatry 2022;92:450–9. https://doi.org/10.1016/j.biopsych.2022.03.002.

66. Doesburg SM, Green JJ, McDonald JJ, Ward LM. From local inhibition to long-range integration: A functional dissociation of alpha-band synchronization across cortical scales in visuospatial attention. Brain Res 2009;1303:97–110.

https://doi.org/10.1016/j.brainres.2009.09.069.

67. Dollfus S, Brazo P. Clinical heterogeneity of schizophrenia. Psychopathology 1997;30:275–81. https://doi.org/10.1159/000285059.

68. Donoghue T, Haller M, Peterson EJ, Varma P, Sebastian P, Gao R, et al. Parameterizing neural power spectra into periodic and aperiodic components. Nat Neurosci 2020;23:1655–65. https://doi.org/10.1038/s41593-020-00744-x.

69. Du X, Rowland LM, Summerfelt A, Choa F-S, Wittenberg GF, Wisner K, et al. Cerebellar-stimulation evoked prefrontal electrical synchrony is modulated by GABA. The Cerebellum 2018;17:550–63. https://doi.org/10.1007/s12311-018-0945-2.

70. Duman RS, Aghajanian GK. Synaptic dysfunction in depression: Potential therapeutic targets. Science 2012;338:68–72. https://doi.org/10.1126/science.1222939.

71. Ehrenberg AJ, Suemoto CK, França Resende E de P, Petersen C, Leite REP, Rodriguez RD, et al. Neuropathologic Correlates of Psychiatric Symptoms in Alzheimer's Disease. J Alzheimers Dis 2018;66:115–26. https://doi.org/10.3233/JAD-180688.

72. Erickson MA, Albrecht MA, Robinson B, Luck SJ, Gold JM. Impaired Suppression of Delay-Period Alpha and Beta Is Associated With Impaired Working Memory in Schizophrenia. Biol Psychiatry Cogn Neurosci Neuroimaging 2017;2:272–9. https://doi.org/10.1016/j.bpsc.2016.09.003.

73. Erickson MA, Ruffle A, Gold JM. A meta-analysis of mismatch negativity in schizophrenia: from clinical risk to disease specificity and progression. Biol Psychiatry 2016;79:980–7.

74. European Commission. An EU Comprehensive Approach That Prioritises Sound Mental Health for All 2023:1–30.

75. Ewers M, Luan Y, Frontzkowski L, Neitzel J, Rubinski A, Dichgans M, et al. Segregation of functional networks is associated with cognitive resilience in Alzheimer's disease. Brain 2021;144:2176–85. https://doi.org/10.1093/brain/awab112.

76. Fawcett JW, Oohashi T, Pizzorusso T. The roles of perineuronal nets and the perinodal extracellular matrix in neuronal function. Nat Rev Neurosci 2019;20:451–65. https://doi.org/10.1038/s41583-019-0196-3.

77. Feczko E, Miranda-Dominguez O, Marr M, Graham AM, Nigg JT, Fair DA. The Heterogeneity Problem: Approaches to Identify Psychiatric Subtypes. Trends Cogn Sci 2019;23:584–601. https://doi.org/10.1016/j.tics.2019.03.009.

78. Ferrarelli F, Massimini M, Sarasso S, others. Breakdown in cortical effective connectivity during midazolam-induced loss of consciousness. Proc Natl Acad Sci U S A 2010;107:2681–6.

79. Fjell AM, Walhovd KB. Structural brain changes in aging: Courses, causes and cognitive consequences. Rev Neurosci 2010;21:187–221. https://doi.org/10.1515/REVNEURO.2010.21.3.187.

80. Fodor JA. The modularity of mind. MIT press; 1983.

81. Frankish H, Horton R. Prevention and management of dementia: a priority for public health. Lancet 2017;390:2614–5. https://doi.org/10.1016/S0140-6736(17)31756-7.

82. Franzmeier N, Hartmann J, Taylor ANW, Araque-Caballero M, Simon-Vermot L, Kambeitz-Ilankovic L, et al. The left frontal cortex supports reserve in aging by enhancing functional network efficiency Rik Ossenkoppele. Alzheimer's Res Ther 2018;10:1–12. https://doi.org/10.1186/s13195-018-0358-y.

83. Franzmeier N, Hartmann JC, Taylor ANW, Caballero MÁA, Simon-Vermot L, Buerger K, et al. Left frontal hub connectivity during memory performance supports reserve in aging and mild cognitive impairment. J Alzheimer's Dis 2017;59:1381–92. https://doi.org/10.3233/JAD-170360.

84. Fries P. Neuronal gamma-band synchronization as a fundamental process in cortical computation. Annu Rev Neurosci 2009;32:209–24.

85. Fries P, Nikolić D, Singer W. The gamma cycle. Trends Neurosci 2007;30:309–16.

86. Frisoni GB, Fox NC, Jack Jr CR, Scheltens P, Thompson PM. The clinical use of structural MRI in Alzheimer disease. Nat Rev Neurol 2010;6:67–77.

87. Fu S, Czajkowski N, Rund BR, Torgalsbøen A-K. The relationship between level of cognitive impairments and functional outcome trajectories in first-episode schizophrenia. Schizophr Res 2017;190:144–9.

88. Gaetani L, Blennow K, Calabresi P, Di Filippo M, Parnetti L, Zetterberg H. Neurofilament light chain as a biomarker in neurological disorders. J Neurol Neurosurg Psychiatry 2019:870–81. https://doi.org/10.1136/jnnp-2018-320106.

89. Galton F. Regression towards mediocrity in hereditary stature. J Anthropol Inst Gt Britain Irel 1886;15:246–63.

90. Gao R, Peterson EJ, Voytek B. Inferring synaptic excitation/inhibition balance from field potentials. Neuroimage 2017;158:70–8. https://doi.org/10.1016/j.neuroimage.2017.06.078.

91. Gelfo F, Mandolesi L, Serra L, Sorrentino G, Caltagirone C. The Neuroprotective Effects of Experience on Cognitive Functions: Evidence from Animal Studies on the Neurobiological Bases of Brain Reserve. Neuroscience 2018;370:218–35. https://doi.org/10.1016/j.neuroscience.2017.07.065.

92. Georgescu I. Toy model. Nat Phys 2012;8:444. https://doi.org/10.1038/nphys2340.

93. Ghatak S, Dolatabadi N, Trudler D, Zhang X, Wu Y, Mohata M, et al. Mechanisms of hyperexcitability in Alzheimer's disease hiPSC-derived neurons and cerebral organoids vs isogenic controls. Elife 2019;8:e50333.

94. Glickfeld LL, Roberts JD, Somogyi P, Scanziani M. Interneurons hyperpolarize pyramidal cells along their entire somatodendritic axis. Nat Neurosci 2009;12:21–3. https://doi.org/10.1038/nn.2230.

95. de Goede AA, Cumplido-Mayoral I, van Putten MJAM. Spatiotemporal Dynamics

of Single and Paired Pulse TMS-EEG Responses. Brain Topogr 2020;33:425–37. https://doi.org/10.1007/s10548-020-00773-6.

96. Gold JM, Barch DM, Feuerstahler LM, Carter CS, MacDonald AW, Daniel Ragland J, et al. Working Memory Impairment across Psychotic disorders. Schizophr Bull 2019;45:804–12. https://doi.org/10.1093/schbul/sby134.

97. Gustavsson A, Norton N, Fast T, Frölich L, Georges J, Holzapfel D, et al. Global estimates on the number of persons across the Alzheimer's disease continuum. Alzheimer's Dement 2023;19:658–70. https://doi.org/10.1002/alz.12694.

98. Gyurkovics M, Clements GM, Low KA, Fabiani M, Gratton G. The impact of 1/f activity and baseline correction on the results and interpretation of time-frequency analyses of EEG/MEG data: A cautionary tale. Neuroimage 2021;237:118192.

99. Hachinski V. Integral brain health: Cerebral/mental/social provisional definitions. Alzheimer's Dement 2023;19:3226–30. https://doi.org/10.1002/alz.13010.

100. Hachinski V, Avan A, Gilliland J, Oveisgharan S. A new definition of brain health. Lancet Neurol 2021;20:335–6. https://doi.org/10.1016/S1474-4422(21)00102-2.

101. Hallett M. Transcranial magnetic stimulation and the human brain. Nature 2000;406:147–50. https://doi.org/10.1038/35018000.

102. Hammond FM, Corrigan JD, Ketchum JM, Malec JF, Dams-O'Connor K, Hart T, et al. Prevalence of Medical and Psychiatric Comorbidities Following Traumatic Brain Injury. J Head Trauma Rehabil 2019;34:E1–10. https://doi.org/10.1097/HTR.0000000000000465.

103. Hansen ECA, Battaglia D, Spiegler A, Deco G, Jirsa VK. Functional connectivity dynamics: modeling the switching behavior of the resting state. Neuroimage 2015;105:525–35. https://doi.org/10.1016/j.neuroimage.2014.11.001

104. Hansson O. Biomarkers for neurodegenerative diseases. Nat Med 2021;27:954–63. https://doi.org/10.1038/s41591-021-01382-x.

105. Hare BD, Duman RS. Prefrontal cortex circuits in depression and anxiety: contribution of discrete neuronal populations and target regions. Mol Psychiatry 2020;25:2742–58. https://doi.org/10.1038/s41380-020-0685-9.

106. Heinrichs RW, Pinnock F, Muharib E, Hartman L, Goldberg J, McDermid Vaz S. Neurocognitive normality in schizophrenia revisited. Schizophr Res Cogn 2015;2:227–32. https://doi.org/10.1016/j.scog.2015.09.001.

107. Hirano Y, Uhlhaas PJ. Current findings and perspectives on aberrant neural oscillations in schizophrenia. Psychiatry Clin Neurosci 2021;75:358–68. https://doi.org/10.1111/pcn.13300.

108. Ho R, Ortiz D, Shea TB. Amyloid-β promotes calcium influx and neurodegeneration via stimulation of L voltage-sensitive calcium channels rather than NMDA channels in cultured neurons. J Alzheimer's Dis 2001;3:479–83.

109. Houdayer E, Degardin A, Cassim F, Bocquillon P, Derambure P, Devanne H. The effects of low- and high-frequency repetitive TMS on the input/output properties of the human corticospinal pathway. Exp Brain Res 2008;187:207–17.

https://doi.org/10.1007/s00221-008-1294-z.

110. Howes OD, Cummings C, Chapman GE, Shatalina E. Neuroimaging in schizophrenia: an overview of findings and their implications for synaptic changes. Neuropsychopharmacology 2023;48:151–67. https://doi.org/10.1038/s41386-022-01426-x.

111. Howes OD, Shatalina E. Integrating the Neurodevelopmental and Dopamine Hypotheses of Schizophrenia and the Role of Cortical Excitation-Inhibition Balance. Biol Psychiatry 2022;92:501–13. https://doi.org/10.1016/j.biopsych.2022.06.017.

112. Hu M-L, Zong X-F, Mann JJ, Zheng J-J, Liao Y-H, Li Z-C, et al. A review of the functional and anatomical default mode network in schizophrenia. Neurosci Bull 2017;33:73–84.

113. Huang YZ, Edwards MJ, Rounis E, Bhatia KP, Rothwell JC. Theta burst stimulation of the human motor cortex. Neuron 2005a;45:201–6. https://doi.org/10.1016/j.neuron.2004.12.033.

114. Huang YZ, Edwards MJ, Rounis E, Bhatia KP, Rothwell JC. Theta burst stimulation of the human motor cortex. Neuron 2005b;45:201–6. https://doi.org/10.1016/j.neuron.2004.12.033.

115. Jablensky A. The diagnostic concept of schizophrenia: its history, evolution, and future prospects. Dialogues Clin Neurosci 2010;12:271–87. https://doi.org/10.31887/dcns.2010.12.3/ajablensky.

116. Jack CR, Holtzman DM. Biomarker modeling of Alzheimer's disease. Neuron 2013;80:1347–58. https://doi.org/10.1016/j.neuron.2013.12.003.

117. Jack CRJ, Bennett DA, Blennow K, Carrillo MC, Dunn B, Haeberlein SB, et al. NIA-AA Research Framework: Toward a biological definition of Alzheimer's disease. Alzheimers Dement 2018;14:535–62. https://doi.org/10.1016/j.jalz.2018.02.018.

118. Jamil A, Batsikadze G, Kuo HI, Labruna L, Hasan A, Paulus W, et al. Systematic evaluation of the impact of stimulation intensity on neuroplastic after-effects induced by transcranial direct current stimulation. J Physiol 2017;595:1273–88. https://doi.org/10.1113/JP272738.

119. Jenkins LM, Bodapati AS, Sharma RP, Rosen C. Working memory predicts presence of auditory verbal hallucinations in schizophrenia and bipolar disorder with psychosis. J Clin Exp Neuropsychol 2018;40:84–94. https://doi.org/10.1080/13803395.2017.1321106.

120. Jensen O, Mazaheri A. Shaping functional architecture by oscillatory alpha activity: Gating by inhibition. Front Hum Neurosci 2010;4:1–8. https://doi.org/10.3389/fnhum.2010.00186.

121. Jog MA, Anderson C, Kubicki A, Boucher M, Leaver A, Hellemann G, et al. Transcranial direct current stimulation (tDCS) in depression induces structural plasticity. Sci Rep 2023;13:2841.

122. Johannesen JK, Bi J, Jiang R, Kenney JG, Chen C-MA. Machine learning identification of EEG features predicting working memory performance in

schizophrenia and healthy adults. Neuropsychiatr Electrophysiol 2016;2:1–21. https://doi.org/10.1186/s40810-016-0017-0.

123. Kaar SJ, Angelescu I, Marques TR, Howes OD. Pre-frontal parvalbumin interneurons in schizophrenia: a meta-analysis of post-mortem studies. J Neural Transm 2019;126:1637–51. https://doi.org/10.1007/s00702-019-02080-2.

124. Kabakov AY, Muller PA, Pascual-Leone A, Jensen FE, Rotenberg A. Contribution of axonal orientation to pathway-dependent modulation of excitatory transmission by direct current stimulation in isolated rat hippocampus. J Neurophysiol 2012;107:1881–9. https://doi.org/10.1152/jn.00715.2011.

125. Kaplan EL, Meier P. Nonparametric estimation from incomplete observations. Break. Stat. Methodol. Distrib., Springer; 1958, p. 319–37.

126. Kayser J, Tenke CE, Kroppmann CJ, Alschuler DM, Fekri S, Ben-David S, et al. Auditory event-related potentials and alpha oscillations in the psychosis prodrome: neuronal generator patterns during a novelty oddball task. Int J Psychophysiol 2014;91:104–20. https://doi.org/10.1016/j.ijpsycho.2013.12.003.

127. Kearney-Ramos TE, Lench DH, Hoffman M, Correia B, Dowdle LT, Hanlon CA. Gray and white matter integrity influence TMS signal propagation: A multimodal evaluation in cocaine-dependent individuals. Sci Rep 2018;8:1–11. https://doi.org/10.1038/s41598-018-21634-0.

128. Kimiskidis V. The dynamics of TMS-induced seizures and epileptiform discharges. Brain Stimul 2019;12:484. https://doi.org/10.1016/j.brs.2018.12.582.

129. Kimiskidis VK, Tsimpiris A, Ryvlin P, Kalviainen R, Koutroumanidis M, Valentin A, et al. TMS combined with EEG in genetic generalized epilepsy: A phase II diagnostic accuracy study. Clin Neurophysiol 2017;128:367–81. https://doi.org/10.1016/j.clinph.2016.11.013.

130. Klimesch W. Alpha-band oscillations, attention, and controlled access to stored information. Trends Cogn Sci 2012;16:606–17. https://doi.org/10.1016/j.tics.2012.10.007.

131. Klimesch W, Sauseng P, Hanslmayr S. EEG alpha oscillations: The inhibition-timing hypothesis. Brain Res Rev 2007;53:63–88. https://doi.org/10.1016/j.brainresrev.2006.06.003.

132. Kong F, Wang X, Hu S, Liu J. Neural correlates of psychological resilience and their relation to life satisfaction in a sample of healthy young adults. Neuroimage 2015;123:165–72. https://doi.org/10.1016/j.neuroimage.2015.08.020.

133. Kraguljac NV, Guerreri M, Strickland MJ, Zhang H. Neurite orientation dispersion and density imaging in psychiatric disorders: a systematic literature review and a technical note. Biol Psychiatry Glob Open Sci 2023;3:10–21. https://doi.org/10.1016/j.bpsgos.2021.12.012.

134. Krizhevsky A, Sutskever I, Hinton GE. Imagenet classification with deep convolutional neural networks. Adv Neural Inf Process Syst 2012;25.

135. Kronberg G, Bridi M, Abel T, Bikson M, Parra LC. Direct current stimulation modulates LTP and LTD: activity dependence and dendritic effects. Brain Stimul

2017;10:51–8. https://doi.org/10.1016/j.brs.2016.10.001.

136. Kunze T, Hunold A, Haueisen J, Jirsa V, Spiegler A. Transcranial direct current stimulation changes resting state functional connectivity: A large-scale brain network modeling study. Neuroimage 2016;140:174–87. https://doi.org/10.1016/j.neuroimage.2016.02.015.

137. Kuo SS, Pogue-Geile MF. Variation in fourteen brain structure volumes in schizophrenia: A comprehensive meta-analysis of 246 studies. Neurosci & Biobehav Rev 2019;98:85–94. https://doi.org/10.1016/j.neubiorev.2018.12.030.

138. Kural MA, Duez L, Sejer Hansen V, Larsson PG, Rampp S, Schulz R, et al. Criteria for defining interictal epileptiform discharges in EEG: A clinical validation study. Neurology 2020;94:e2139-e2147. https://doi.org/10.1212/WNL.0000000000009439

139. Kustermann T, Rockstroh B, Kienle J, Miller GA, Popov T. Deficient attention modulation of lateralized alpha power in schizophrenia: Deficient lateralized alpha modulation in schizophrenia. Psychophysiology 2016;53:776–85. https://doi.org/10.1111/psyp.12626.

140. Landgraf D, Long J, Der-Avakian A, Streets M, Welsh DK. Dissociation of learned helplessness and fear conditioning in mice: A mouse model of depression. PLoS One 2015;10:1–17. https://doi.org/10.1371/journal.pone.0125892.

141. Larson J, Munkácsy E. Theta-burst LTP. Brain Res 2015;1621:38–50. https://doi.org/10.1016/j.brainres.2014.10.034.

142. Lee J, Kim HJ. Normal Aging Induces Changes in the Brain and Neurodegeneration Progress: Review of the Structural, Biochemical, Metabolic, Cellular, and Molecular Changes. Front Aging Neurosci 2022;14:1–15. https://doi.org/10.3389/fnagi.2022.931536.

143. Lefaucheur JP, André-Obadia N, Antal A, Ayache SS, Baeken C, Benninger DH, et al. Evidence-based guidelines on the therapeutic use of repetitive transcranial magnetic stimulation (rTMS). Clin Neurophysiol 2014;125:2150–206. https://doi.org/10.1016/j.clinph.2014.05.021.

144. Lefaucheur JP, Wendling F. Mechanisms of action of tDCS: A brief and practical overview. Neurophysiol Clin 2019;49:269–75. https://doi.org/10.1016/j.neucli.2019.07.013.

145. Lewis DA, Hashimoto T, Volk DW. Cortical inhibitory neurons and schizophrenia. Nat Rev Neurosci 2005;6:312–24. https://doi.org/10.1038/nrn1648.

146. Li S, Hong S, Shepardson NE, Walsh DM, Shankar GM, Selkoe D. Soluble oligomers of amyloid Beta protein facilitate hippocampal long-term depression by disrupting neuronal glutamate uptake. Neuron 2009;62:788–801. https://doi.org/10.1016/j.neuron.2009.05.012.

147. Light GA, Williams LE, Minow F, Sprock J, Rissling A, Sharp R, et al. Electroencephalography (EEG) and event-related potentials (ERPs) with human participants. Curr Protoc Neurosci 2010:1–24. https://doi.org/10.1002/0471142301.ns0625s52.

148. Liu Y, Ouyang P, Zheng Y, Mi L, Zhao J, Ning Y, et al. A Selective Review of the Excitatory-Inhibitory Imbalance in Schizophrenia: Underlying Biology, Genetics, Microcircuits, and Symptoms. Front Cell Dev Biol 2021;9:1–15. https://doi.org/10.3389/fcell.2021.664535.

149. Livingston G, Sommerlad A, Orgeta V, Costafreda SG, Huntley J, Ames D, et al. The Lancet International Commission on Dementia Prevention and Care. Lancet 2017;390:2673–2734.

150. Long S, Benoist C, Weidner W. World Alzheimer Report 2023: reducing dementia risk: never too early, never too late. London, Engl Alzheimer's Dis Int 2023.

151. Luck SJ, Hahn B, Leonard CJ, Gold JM. The Hyperfocusing Hypothesis: A New Account of Cognitive Dysfunction in Schizophrenia. Schizophr Bull 2019;45:991–1000. https://doi.org/10.1093/schbul/sbz063.

152. Luck SJ, Vogel EK. Visual working memory capacity: From psychophysics and neurobiology to individual differences. Trends Cogn Sci 2013;17:391–400. https://doi.org/10.1016/j.tics.2013.06.006.

153. Lynch CJ, Elbau IG, Ng TH, Wolk D, Zhu S, Ayaz A, et al. Automated optimization of TMS coil placement for personalized functional network engagement. Neuron 2022;110:3263-3277.e4. https://doi.org/10.1016/j.neuron.2022.08.012.

154. Maier SF, Watkins LR. Role of the medial prefrontal cortex in coping and resilience. Brain Res 2010;1355:52–60. https://doi.org/10.1016/j.brainres.2010.08.039.

155. Di Marco LY, Marzo A, Muñoz-Ruiz M, Ikram MA, Kivipelto M, Ruefenacht D, et al. Modifiable Lifestyle Factors in Dementia: A Systematic Review of Longitudinal Observational Cohort Studies. J Alzheimer's Dis 2014;42:119–35. https://doi.org/10.3233/JAD-132225.

156. Marinković P, Blumenstock S, Goltstein PM, Korzhova V, Peters F, Knebl A, et al. In vivo imaging reveals reduced activity of neuronal circuits in a mouse tauopathy model. Brain 2019;142:1051–62. https://doi.org/10.1093/brain/awz035.

157. Marzuoli A. Toy models in physics and the reasonable effectiveness of mathematics. Deduction, Comput. Exp., Springer; 2008, p. 49–64.

158. Mattsson-Carlgren N, Salvadó G, Ashton NJ, Tideman P, Stomrud E, Zetterberg H, et al. Prediction of Longitudinal Cognitive Decline in Preclinical Alzheimer Disease Using Plasma Biomarkers. JAMA Neurol 2023;80:360–9. https://doi.org/10.1001/jamaneurol.2022.5272.

159. McIntyre RS, Alsuwaidan M, Baune BT, Berk M, Demyttenaere K, Goldberg JF, et al. Treatment-resistant depression: definition, prevalence, detection, management, and investigational interventions. World Psychiatry 2023;22:394–412. https://doi.org/10.1002/wps.21120.

160. Meisel C, Schulze-Bonhage A, Freestone D, Cook MJ, Achermann P, Plenz D. Intrinsic excitability measures track antiepileptic drug action and uncover increasing/decreasing excitability over the wake/sleep cycle. Proc Natl Acad Sci U S A 2015;112:14694–9. https://doi.org/10.1073/pnas.1513716112.

161. Menon V, Uddin LQ. Saliency, switching, attention and control: a network model of insula function. Brain Struct Funct 2010;214:655–67. https://doi.org/10.1007/s00429-010-0262-0.

162. Mielke MM, Hagen CE, Xu J, Chai X, Vemuri P, Lowe VJ, et al. Plasma phospho-tau181 increases with Alzheimer ' s disease clinical severity and is associated with tau- and amyloid-positron emission tomography 2018;14:989–97. https://doi.org/10.1016/j.jalz.2018.02.013.

163. Modesti MN, Arena JF, Palermo N, Del Casale A. A Systematic Review on Add-On Psychotherapy in Schizophrenia Spectrum Disorders. J Clin Med 2023;12. https://doi.org/10.3390/jcm12031021.

164. Momi D, Ozdemir RA, Tadayon E, Boucher P, Shafi MM, Pascual-Leone A, et al. Network-level macroscale structural connectivity predicts propagation of transcranial magnetic stimulation. Neuroimage 2021;229:117698. https://doi.org/10.1016/j.neuroimage.2020.117698.

165. Monte-Silva K, Kuo MF, Hessenthaler S, Fresnoza S, Liebetanz D, Paulus W, et al. Induction of late LTP-like plasticity in the human motor cortex by repeated non-invasive brain stimulation. Brain Stimul 2013;6:424–32. https://doi.org/10.1016/j.brs.2012.04.011.

166. Monte-Silva K, Kuo MF, Liebetanz D, Paulus W, Nitsche MA. Shaping the optimal repetition interval for cathodal transcranial direct current stimulation (tDCS). J Neurophysiol 2010;103:1735–40. https://doi.org/10.1152/jn.00924.2009.

167. Montine TJ, Phelps CH, Beach TG, Bigio EH, Cairns NJ, Dickson DW, et al. National Institute on Aging--Alzheimer's Association guidelines for the neuropathologic assessment of Alzheimer's disease: a practical approach. Acta Neuropathol 2012;123:1–11.

168. Moore TM, White LK, Barzilay R, Calkins ME, Jones JD, Young JF, et al. Development of a scale battery for rapid assessment of risk and resilience. Psychiatry Res 2020;288:112996. https://doi.org/10.1016/j.psychres.2020.112996.

169. Mørup MF, Kymes SM, Åström DO. A modelling approach to estimate the prevalence of treatment-resistant schizophrenia in the United States. PLoS One 2020;15:1–10. https://doi.org/10.1371/journal.pone.0234121.

170. Mosolov SN, Yaltonskaya PA. Primary and Secondary Negative Symptoms in Schizophrenia. Front Psychiatry 2022;12:1–12. https://doi.org/10.3389/fpsyt.2021.766692.

171. Murphy M, Öngür D. Decreased peak alpha frequency and impaired visual evoked potentials in first episode psychosis. NeuroImage Clin 2019;22:101693. https://doi.org/10.1016/j.nicl.2019.101693.

172. Nazeri A, Mulsant BH, Rajji TK, Levesque ML, Pipitone J, Stefanik L, et al. Gray matter neuritic microstructure deficits in schizophrenia and bipolar disorder. Biol Psychiatry 2017;82:726–36. https://doi.org/10.1016/j.biopsych.2016.12.005.

173. Neitzel J, Franzmeier N, Rubinski A, Ewers M. Left frontal connectivity attenuates

the adverse effect of entorhinal tau pathology on memory. Neurology 2019;93:E347–57. https://doi.org/10.1212/WNL.0000000000007822.

174. Nichols E, Steinmetz JD, Vollset SE, Fukutaki K, Chalek J, Abd-Allah F, et al. Estimation of the global prevalence of dementia in 2019 and forecasted prevalence in 2050: an analysis for the Global Burden of Disease Study 2019. Lancet Public Heal 2022;7:e105–25. https://doi.org/10.1016/S2468-2667(21)00249-8.

175. Onwordi EC, Halff EF, Whitehurst T, Mansur A, Cotel M-C, Wells L, et al. Synaptic density marker SV2A is reduced in schizophrenia patients and unaffected by antipsychotics in rats. Nat Commun 2020;11:246. https://doi.org/10.1038/s41467-019-14122-0.

176. van Oort J, Tendolkar I, Hermans EJ, Mulders PC, Beckmann CF, Schene AH, et al. How the brain connects in response to acute stress: A review at the human brain systems level. Neurosci Biobehav Rev 2017;83:281–97. https://doi.org/10.1016/j.neubiorev.2017.10.015.

177. Van Os J, Kenis G, Rutten BPF. The environment and schizophrenia. Nature 2010;468:203–12. https://doi.org/10.1038/nature09563.

178. Ossenkoppele R, Schonhaut DR, Schöll M, Lockhart SN, Ayakta N, Baker SL, et al. Tau PET patterns mirror clinical and neuroanatomical variability in Alzheimer's disease. Brain 2016;139:1551–67. https://doi.org/10.1093/brain/aww027.

179. Ozdemir RA, Boucher P, Fried PJ, Momi D, Jannati A, Pascual-Leone A, et al. Reproducibility of cortical response modulation induced by intermittent and continuous theta-burst stimulation of the human motor cortex. Brain Stimul 2021a;14:949–64. https://doi.org/10.1016/j.brs.2021.05.013.

180. Ozdemir RA, Tadayon E, Boucher P, Momi D, Karakhanyan KA, Fox MD, et al. Individualized perturbation of the human connectome reveals reproducible biomarkers of network dynamics relevant to cognition. Proc Natl Acad Sci U S A 2020;117:8115–25. https://doi.org/10.1073/pnas.1911240117.

181. Ozdemir RA, Tadayon E, Boucher P, Sun H, Momi D, Ganglberger W, et al. Cortical Responses to Noninvasive Perturbations Enable Individual Brain Fingerprinting. Brain Stimul 2021b;14. https://doi.org/10.1016/j.brs.2021.02.005.

182. Palaniyappan L, Liddle PF. Does the salience network play a cardinal role in psychosis? An emerging hypothesis of insular dysfunction. J Psychiatry Neurosci 2012;37:17–27. https://doi.org/10.1503/jpn.100176.

183. Palop JJ, Mucke L. Network abnormalities and interneuron dysfunction in Alzheimer disease. Nat Rev Neurosci 2016;17:777–92. https://doi.org/10.1038/nrn.2016.141.

184. Pandis D, Scarmeas N. Seizures in alzheimer disease: clinical and epidemiological data. Epilepsy Curr 2012;12:184–7. https://doi.org/10.5698/1535-7511-12.5.184.

185. Paneva J, Leunissen I, Schuhmann T, de Graaf TA, Jønsson MG, Onarheim B, et al. Using Remotely Supervised At-Home TES for Enhancing Mental Resilience. Front Hum Neurosci 2022;16:1–7. https://doi.org/10.3389/fnhum.2022.838187.

186. Parpura-Gill A, Beitz D, Uemura E. The inhibitory effects of Beta-amyloid on glutamate and glucose uptakes by cultured astrocytes. Brain Res 1997;754:65–71. https://doi.org/10.1016/s0006-8993(97)00043-7.

187. Pascual-Leone A, Bartres-Faz D. Human Brain Resilience: A Call to Action. Ann Neurol 2021;90:336–49. https://doi.org/10.1002/ana.26157.

188. Pascual-Leone A, Valls-Solé J, Wassermann EM, Hallett M. Responses to rapid-rate transcranial magnetic stimulation of the human motor cortex. Brain 1994;117:847–58. https://doi.org/10.1093/brain/117.4.847.

189. Pascual-Marqui RD, Lehmann D, Koenig T, Kochi K, Merlo MCG, Hell D, et al. Low resolution brain electromagnetic tomography (LORETA) functional imaging in acute, neuroleptic-naive, first-episode, productive schizophrenia. Psychiatry Res Neuroimaging 1999;90:169–79. https://doi.org/10.1016/s0925-4927(99)00013-x.

190. Perellón-Alfonso R, Oblak A, Kuclar M, Škrlj B, Pileckyte I, Škodlar B, et al. Dense attention network identifies EEG abnormalities during working memory performance of patients with schizophrenia. Front Psychiatry 2023;14. https://doi.org/10.3389/fpsyt.2023.1205119.

191. Perellón-Alfonso R, Redondo-Camós M, Abellaneda-Pérez K, Cattaneo G, Delgado-Gallén S, España-Irla G, et al. Prefrontal reactivity to TMS perturbation as a toy model of mental health outcomes during the COVID-19 pandemic. Heliyon 2022;8:10208. https://doi.org/10.1016/j.heliyon.2022.e10208.

192. Perucca P, Gilliam FG. Adverse effects of antiepileptic drugs. Lancet Neurol 2012;11:792–802. https://doi.org/10.1016/S1474-4422(12)70153-9.

193. Phang CR, Noman F, Hussain H, Ting CM, Ombao H. A Multi-Domain Connectome Convolutional Neural Network for Identifying Schizophrenia from EEG Connectivity Patterns. IEEE J Biomed Heal Informatics 2020;24:1333–43. https://doi.org/10.1109/JBHI.2019.2941222.

194. Pichet Binette A, Franzmeier N, Spotorno N, Ewers M, Brendel M, Biel D, et al. Amyloid-associated increases in soluble tau relate to tau aggregation rates and cognitive decline in early Alzheimer's disease. Nat Commun 2022;13:6635. https://doi.org/10.1038/s41467-022-34129-4.

195. Picó-Pérez M, Vieira R, Fernández-Rodriguez M, De Barros MAP, Radua J, Morgado P. Multimodal meta-analysis of structural gray matter, neurocognitive and social cognitive fMRI findings in schizophrenia patients. Psychol Med 2022;52:614–24. https://doi.org/10.1017/s0033291721005523.

196. Pilloni G. Home-based transcranial electrical stimulation to scale clinical trials: methodology, safety, and beyond. Brain Stimul 2023;16:114. https://doi.org/10.1016/j.brs.2023.01.1665.

197. Pilloni G, Vogel-Eyny A, Lustberg M, Best P, Malik M, Walton-Masters L, et al. Tolerability and feasibility of at-home remotely supervised transcranial direct current stimulation (RS-tDCS): Single-center evidence from 6,779 sessions. Brain Stimul 2022;15:707–16. https://doi.org/10.1016/j.brs.2022.04.014.

198. Pizzagalli DA, Roberts AC. Prefrontal cortex and depression.

Neuropsychopharmacology 2022;47:225–46. https://doi.org/10.1038/s41386-021-01101-7.

199. Pooler AM, Phillips EC, Lau DHW, Noble W, Hanger DP. Physiological release of endogenous tau is stimulated by neuronal activity. EMBO Rep 2013;14:389–94.

200. Portelius E, Zetterberg H, Skillbäck T, Törnqvist U, Andreasson U, Trojanowski JQ, et al. Cerebrospinal fluid neurogranin: relation to cognition and neurodegeneration in Alzheimer's disease. Brain 2015;138:3373–85. https://doi.org/10.1038/embor.2013.15.

201. Premoli Isabella, Biondi A, Carlesso S, Rivolta D, Richardson MP. Lamotrigine and levetiracetam exert a similar modulation of TMS-evoked EEG potentials. Epilepsia 2017;58:42–50. https://doi.org/10.1111/epi.13599.

202. Premoli I, Biondi A, Carlesso S, Rivolta D, Richardson MP. Lamotrigine and levetiracetam exert a similar modulation of TMS-evoked EEG potentials. Epilepsia 2017;58:42–50. https://doi.org/10.1111/epi.13599.

203. Premoli Isabella, Castellanos N, Rivolta D, Belardinelli P, Bajo R, Zipser C, et al. TMS-EEG signatures of GABAergic neurotransmission in the human cortex. J Neurosci 2014;34:5603–12. https://doi.org/10.1523/jneurosci.5089-13.2014.

204. Premoli I, Rivolta D, Espenhahn S, others. Characterization of GABAB-receptor mediated neurotransmission in the human cortex by paired-pulse TMS-EEG. Neuroimage 2014;103C:152–62. https://doi.org/10.1016/j.neuroimage.2014.09.028.

205. Pujol J, Pujol N, Mané A, Martínez-Vilavella G, Deus J, Pérez-Sola V, et al. Mapping alterations in the local synchrony of the cerebral cortex in schizophrenia. Eur Psychiatry 2023;66. https://doi.org/10.1192/j.eurpsy.2023.2463.

206. Qiu Y, Tang Y, Chan RCK, Sun X, He J. P300 aberration in first-episode schizophrenia patients: a meta-analysis. PLoS One 2014;9:e97794. https://doi.org/10.1371/journal.pone.0097794.

207. Quinlan JR. Induction of decision trees. Mach Learn 1986;1:81–106. https://doi.org/10.1007/BF00116251.

208. Radhakrishnan R, Skosnik PD, Ranganathan M, Naganawa M, Toyonaga T, Finnema S, et al. In vivo evidence of lower synaptic vesicle density in schizophrenia. Mol Psychiatry 2021;26:7690–8. https://doi.org/10.1038/s41380-021-01184-0.

209. Radhu N, Dominguez LG, Farzan F, Richter MA, Semeralul MO, Chen R, et al. Evidence for inhibitory deficits in the prefrontal cortex in schizophrenia. Brain 2015;138:483–97. https://doi.org/10.1093/brain/awu360.

210. Raichle ME, MacLeod AM, Snyder AZ, Powers WJ, Gusnard DA, Shulman GL. A default mode of brain function. Proc Natl Acad Sci 2001;98:676–82. https://doi.org/10.1073/pnas.98.2.676.

211. Rajan KB, Weuve J, Barnes LL, McAninch EA, Wilson RS, Evans DA. Population estimate of people with clinical Alzheimer's disease and mild cognitive

impairment in the United States (2020--2060). Alzheimer's & Dement 2021;17:1966–75. https://doi.org/10.1002/alz.12362.

212. Ramsay IS, Mueller B, Ma Y, Shen C, Sponheim SR. Thalamocortical connectivity and its relationship with symptoms and cognition across the psychosis continuum. Psychol Med 2023;53:5582–91. https://doi.org/10.1017/s0033291722002793.

213. Ramyead A, Kometer M, Studerus E, Koranyi S, Ittig S, Gschwandtner U, et al. Aberrant current source-density and lagged phase synchronization of neural oscillations as markers for emerging psychosis. Schizophr Bull 2015;41:919–29. https://doi.org/10.1093/schbul/sbu134.

214. Ramyead A, Roach B, Hamilton H, Addington J, Bachman P, Bearden C, et al. O33. EEG Alpha Event-Related Desynchronization Deficits Predict Conversion to Psychosis in Individuals With the Psychosis Risk Syndrome. Biol Psychiatry 2019;85:S119. https://doi.org/10.1016/j.biopsych.2019.03.298.

215. Ramyead A, Studerus E, Kometer M, Heitz U, Gschwandtner U, Fuhr P, et al. Neural oscillations in antipsychotic-naive patients with a first psychotic episode. World J Biol Psychiatry 2016;17:296–307. https://doi.org/10.3109/15622975.2016.1156742.

216. Reilly TJ, Nottage JF, Studerus E, Rutigliano G, De Micheli AI, Fusar-Poli P, et al. Gamma band oscillations in the early phase of psychosis: A systematic review. Neurosci & Biobehav Rev 2018;90:381–99. https://doi.org/10.1016/j.neubiorev.2018.04.006.

217. Rentrop M, Rodewald K, Roth A, Simon J, Walther S, Fiedler P, et al. Intra-individual variability in high-functioning patients with schizophrenia. Psychiatry Res 2010a;178:27–32. https://doi.org/10.1016/j.psychres.2010.04.009.

218. Rentrop M, Rodewald K, Roth A, Simon J, Walther S, Fiedler P, et al. Intra-individual variability in high-functioning patients with schizophrenia. Psychiatry Res 2010b;178:27–32. https://doi.org/10.1016/j.psychres.2010.04.009.

219. Robinson N, Bergen SE. Environmental Risk Factors for Schizophrenia and Bipolar Disorder and Their Relationship to Genetic Risk: Current Knowledge and Future Directions. Front Genet 2021;12. https://doi.org/10.3389/fgene.2021.686666.

220. Rocchi L, Ibáñez J, Benussi A, Hannah R, Rawji V, Casula E, et al. Variability and predictors of response to continuous theta burst stimulation: A TMS-EEG study. Front Neurosci 2018;12:1–11. https://doi.org/10.3389/fnins.2018.00400.

221. Rodman AM, Jenness JL, Weissman DG, Pine DS, McLaughlin KA. Neurobiological Markers of Resilience to Depression Following Childhood Maltreatment: The Role of Neural Circuits Supporting the Cognitive Control of Emotion. Biol Psychiatry 2019;86:464–73. https://doi.org/10.1016/j.biopsych.2019.04.033.

222. Rosburg T. Auditory N100 gating in patients with schizophrenia: a systematic meta-analysis. Clin Neurophysiol 2018;129:2099–111. https://doi.org/10.1016/j.clinph.2018.07.012.

223. Rossini PM, Burke D, Chen R, Cohen LG, Daskalakis Z, Di Iorio R, et al. Clinical

Neurophysiology Non-invasive electrical and magnetic stimulation of the brain , spinal cord , roots and peripheral nerves : Basic principles and procedures for routine clinical and research application . An updated report from an. Clin Neurophysiol 2015;126:1071–107. https://doi.org/10.1016/j.clinph.2015.02.001.

224. Roux F, Wibral M, Mohr HM, Singer W, Uhlhaas PJ. Gamma-band activity in human prefrontal cortex codes for the number of relevant items maintained in working memory. J Neurosci 2012;32:12411–20. https://doi.org/10.1523/jneurosci.0421-12.2012.

225. Rubinov M, Sporns O. Complex network measures of brain connectivity: uses and interpretations. Neuroimage 2010;52:1059–69. https://doi.org/10.1016/j.neuroimage.2009.10.003.

226. Ruiz De Miras J, Ibáñez-Molina AJ, Soriano MF, Iglesias-Parro S. Schizophrenia classification using machine learning on resting state EEG signal. Biomed Signal Process Control 2023;79:104233. https://doi.org/10.1016/j.bspc.2022.104233.

227. Rumelhart DE, Hinton GE, Williams RJ. Learning representations by back-propagating errors. Nature 1986;323:533–6. https://doi.org/10.1038/323533a0

228. Russo SJ, Murrough JW, Han MH, Charney DS, Nestler EJ. Neurobiology of resilience. Nat Neurosci 2012;15:1475–84. https://doi.org/10.1038/nn.3234.

229. Rutter M. Resilience as a dynamic concept. Dev Psychopathol 2012;24:335–44. https://doi.org/10.1017/S0954579412000028.

230. Salavati B, Rajji TK, Zomorrodi R, others. Pharmacological manipulation of cortical inhibition in the dorsolateral prefrontal cortex. Neuropsychopharmacology 2018;43:354–61. https://doi.org/10.1038/npp.2017.104.

231. Saldarini F, Gottlieb N, Stokes PRA. Neural correlates of working memory function in euthymic people with bipolar disorder compared to healthy controls : A systematic review and. J Affect Disord 2022;297:610–22. https://doi.org/10.1016/j.jad.2021.10.084.

232. Samudra N, Ranasinghe K, Kirsch H, Rankin K, Miller B. Etiology and Clinical Significance of Network Hyperexcitability in Alzheimer's Disease: Unanswered Questions and Next Steps. J Alzheimer's Dis 2023;92:13–27. https://doi.org/10.3233/JAD-220983.

233. de Santana Correia A, Colombini EL. Attention, please! A survey of neural attention models in deep learning. vol. 55. Springer Netherlands; 2022. https://doi.org/10.1007/s10462-022-10148-x.

234. Santomauro DF, Mantilla Herrera AM, Shadid J, Zheng P, Ashbaugh C, Pigott DM, et al. Global prevalence and burden of depressive and anxiety disorders in 204 countries and territories in 2020 due to the COVID-19 pandemic. Lancet 2021;398:1700–12. https://doi.org/10.1016/S0140-6736(21)02143-7.

235. Sarasso S, Boly M, Napolitani M, others. Consciousness and complexity during unresponsiveness induced by propofol, xenon, and ketamine. Curr Biol 2015;25:3099–105. https://doi.org/10.1016/j.cub.2015.10.014.

236. Sasabayashi D, Takahashi T, Takayanagi Y, Suzuki M. Anomalous brain gyrification

patterns in major psychiatric disorders: a systematic review and transdiagnostic integration. Transl Psychiatry 2021;11. https://doi.org/10.1038/s41398-021-01297-8.

237. Scangos KW, State MW, Miller AH, Baker JT, Williams LM. New and emerging approaches to treat psychiatric disorders. Nat Med 2023;29:317–33. https://doi.org/10.1038/s41591-022-02197-0.

238. Scheeringa R, Petersson KM, Kleinschmidt A, Jensen O, Bastiaansen MCM. EEG alpha power modulation of fMRI resting-state connectivity. Brain Connect 2012;2:254–64. https://doi.org/10.1089/brain.2012.0088.

239. Schmidt SH, Brandt SA. Motor threshold, motor evoked potential, central motor conduction time. Oxford Handb. Transcranial Stimul., Oxford University Press; 2021. https://doi.org/10.1093/oxfordhb/9780198832256.013.11.

240. Schultz MK, Gentzel R, Usenovic M, Gretzula C, Ware C, Parmentier-Batteur S, et al. Pharmacogenetic neuronal stimulation increases human tau pathology and trans-synaptic spread of tau to distal brain regions in mice. Neurobiol Dis 2018;118:161–76. https://doi.org/10.1016/j.nbd.2018.07.003.

241. Seidman LJ, Mirsky AF. Evolving notions of schizophrenia as a developmental neurocognitive disorder. J Int Neuropsychol Soc 2017;23:881–92. https://doi.org/10.1017/S1355617717001114.

242. Seligman ME, Rosellini RA, Kozak MJ. Learned helplessness in the rat: time course, immunization, and reversibility. J Comp Physiol Psychol 1975;88:542–7. https://doi.org/10.1037/h0076431.

243. Sheu YH. Illuminating the Black Box: Interpreting Deep Neural Network Models for Psychiatric Research. Front Psychiatry 2020;11:1–14. https://doi.org/10.3389/fpsyt.2020.551299.

244. Shim M, Hwang HJ, Kim DW, Lee SH, Im CH. Machine-learning-based diagnosis of schizophrenia using combined sensor-level and source-level EEG features. Schizophr Res 2016;176:314–9. https://doi.org/10.1016/j.schres.2016.05.007.

245. Shoeibi A, Sadeghi D, Moridian P, Ghassemi N, Heras J, Alizadehsani R, et al. Automatic Diagnosis of Schizophrenia in EEG Signals Using CNN-LSTM Models. Front Neuroinform 2021;15:1–16. https://doi.org/10.3389/fninf.2021.777977.

246. Silva-Filho E, Pilloni G, Charvet LE, Fregni F, Brunoni AR, Bikson M. Factors supporting availability of home-based Neuromodulation using remote supervision in middle-income countries; Brazil experience. Brain Stimul 2022;15:385–7. https://doi.org/10.1016/j.brs.2022.02.005.

247. Simrén J, Leuzy A, Karikari TK, Hye A, Benedet AL, Lantero-Rodriguez J, et al. The diagnostic and prognostic capabilities of plasma biomarkers in Alzheimer's disease. Alzheimer's & Dement 2021;17:1145–56. https://doi.org/10.1002/alz.12283.

248. Škrlj B, Džeroski S, Lavrač N, Petkovič M. Feature Importance Estimation with Self-Attention Networks. arXiv preprint 2020;2002.04464. https://doi.org/10.48550/arXiv.2002.04464.

249. Smucny J, Dienel SJ, Lewis DA, Carter CS. Mechanisms underlying dorsolateral prefrontal cortex contributions to cognitive dysfunction in schizophrenia. Neuropsychopharmacology 2022;47:292–308. https://doi.org/10.1038/s41386-021-01089-0.

250. So RP, Kegeles LS, Mao X, Shungu DC, Stanford AD, Chen CMA. Long-range gamma phase synchronization as a compensatory strategy during working memory in high-performing patients with schizophrenia. J Clin Exp Neuropsychol 2018;40:663–81. https://doi.org/10.1080/13803395.2017.1420142.

251. Von Stein A, Chiang C, König P. Top-down processing mediated by interareal synchronization. Proc Natl Acad Sci U S A 2000;97:14748–53. https://doi.org/10.1073/pnas.97.26.14748.

252. Steward A, Biel D, Brendel M, Dewenter A, Roemer S, Rubinski A, et al. Functional network segregation is associated with attenuated tau spreading in Alzheimer's disease. Alzheimer's Dement 2023;19:2034–46. https://doi.org/10.1002/alz.12867.

253. Sun J, Cao R, Zhou M, Hussain W, Wang B, Xue J, et al. A hybrid deep neural network for classification of schizophrenia using EEG Data. Sci Rep 2021;11:1–16. https://doi.org/10.1038/s41598-021-83350-6.

254. Tao TJ, Hui CLM, Hui PWM, Ho ECN, Lam BST, Wong AKH, et al. Working memory deterioration as an early warning sign for relapse in remitted psychosis: A one-year naturalistic follow-up study. Psychiatry Res 2023;319:114976. https://doi.org/10.1016/j.psychres.2022.114976.

255. Targa Dias Anastacio H, Matosin N, Ooi L. Neuronal hyperexcitability in Alzheimer's disease: what are the drivers behind this aberrant phenotype? Transl Psychiatry 2022;12. https://doi.org/10.1038/s41398-022-02024-7.

256. Teunissen CE, Verberk IMW, Thijssen EH, Vermunt L, Hansson O, Zetterberg H, et al. Blood-based biomarkers for Alzheimer's disease: towards clinical implementation. Lancet Neurol 2022;21:66–77. https://doi.org/10.1016/s1474-4422(21)00361-6.

257. Thomas Yeo BT, Krienen FM, Sepulcre J, Sabuncu MR, Lashkari D, Hollinshead M, et al. The organization of the human cerebral cortex estimated by intrinsic functional connectivity. J Neurophysiol 2011;106:1125–65. https://doi.org/10.1152/jn.00338.2011.

258. Thut G, Nietzel A, Brandt SA, Pascual-Leone A. α-Band electroencephalographic activity over occipital cortex indexes visuospatial attention bias and predicts visual target detection. J Neurosci 2006;26:9494–502. https://doi.org/10.1523/JNEUROSCI.0875-06.2006.

259. Tikka SK, Yadav S, Nizamie SH, Das B, Tikka DL, Goyal N. Schneiderian first rank symptoms and gamma oscillatory activity in neuroleptic naive first episode schizophrenia: a 192 channel EEG study. Psychiatry Investig 2014;11:467. https://doi.org/10.4306%2Fpi.2014.11.4.467.

260. Tomasi D, Volkow ND. Aging and functional brain networks. Mol Psychiatry 2012;17:549–58. https://doi.org/10.1038/mp.2011.81.

261. Tost H, Champagne FA, Meyer-Lindenberg A. Environmental influence in the brain, human welfare and mental health. Nat Neurosci 2015;18:4121–31. https://doi.org/10.1038/nn.4108.

262. Townsend L, Pillinger T, Selvaggi P, Veronese M, Turkheimer F, Howes O. Brain glucose metabolism in schizophrenia: a systematic review and meta-analysis of 18FDG-PET studies in schizophrenia. Psychol Med 2023;53:4880–97. https://doi.org/10.1017/s003329172200174x.

263. Trajkovic J, Di Gregorio F, Ferri F, Marzi C, Diciotti S, Romei V. Resting state alpha oscillatory activity is a valid and reliable marker of schizotypy. Sci Rep 2021;11:1–13. https://doi.org/10.1038/s41598-021-89690-7.

264. Valenza M, Scuderi C. How useful are biomarkers for the diagnosis of Alzheimer's disease and especially for its therapy? Neural Regen Res 2022;17:2205–7. https://doi.org/10.4103/1673-5374.335791.

265. Valero-Cabré A, Payne BR, Pascual-Leone A. Opposite impact on 14C-2-deoxyglucose brain metabolism following patterns of high and low frequency repetitive transcranial magnetic stimulation in the posterior parietal cortex. Exp Brain Res 2007;176:603–15. https://doi.org/10.1007/s00221-006-0639-8.

266. Varela JA, Wang J, Christianson JP, Maier SF, Cooper DC. Control over stress, but not stress per Se increases prefrontal cortical pyramidal neuron excitability. J Neurosci 2012;32:12848–53. https://doi.org/10.1523/JNEUROSCI.2669-12.2012.

267. Vink JJT, Mandija S, Petrov PI, van den Berg CAT, Sommer IEC, Neggers SFW. A novel concurrent TMS-fMRI method to reveal propagation patterns of prefrontal magnetic brain stimulation. Hum Brain Mapp 2018;39:4580–92. https://doi.org/10.1002/hbm.24307.

268. Voineskos AN, Farzan F, Barr MS, Lobaugh NJ, Mulsant BH, Chen R, et al. The Role of the Corpus Callosum in Transcranial Propagation. BPS 2010;68:825–31. https://doi.org/10.1016/j.biopsych.2010.06.021.

269. Wagner T, Valero-Cabre A, Pascual-Leone A. Noninvasive human brain stimulation. Annu Rev Biomed Eng 2007;9:527–65. https://doi.org/10.1146/annurev.bioeng.9.061206.133100.

270. Watanabe N, Takeda M. Neurophysiological dynamics for psychological resilience: A view from the temporal axis. Neurosci Res 2022;175:53–61. https://doi.org/10.1016/j.neures.2021.11.004.

271. Waugh CE, Wager TD, Fredrickson BL, Noll DC, Taylor SF. The neural correlates of trait resilience when anticipating and recovering from threat. Soc Cogn Affect Neurosci 2008;3:322–32.

272. Wei Y, Xue K, Yang M, Wang H, Chen J, Han S, et al. Aberrant cerebello-thalamo-cortical functional and effective connectivity in first-episode schizophrenia with auditory verbal hallucinations. Schizophr Bull 2022;48:1336–43.

273. Wolfers T, Doan NT, Kaufmann T, Alnæs D, Moberget T, Agartz I, et al. Mapping the Heterogeneous Phenotype of Schizophrenia and Bipolar Disorder Using Normative Models. JAMA Psychiatry 2018;75:1146–55.

https://doi.org/10.1001/jamapsychiatry.2018.2467.

274. Womelsdorf T, Schoffelen JM, Oostenveld R, Singer W, Desimone R, Engel AK, et al. Modulation of neuronal interactions through neuronal synchronization. Science (80-) 2007;316:1609–12. https://doi.org/10.1126/science.1139597.

275. Word Health Organization. Optimizing brain health across the life course: WHO position paper. 2022.

276. Wright MO, Masten AS, Narayan AJ. Resilience Processes in Development: Four Waves of Research on Positive Adaptation in the Context of Adversity. In: Goldstein S, Brooks RB, editors. Handb. Resil. Child., Boston, MA: Springer US; 2013, p. 15–37. https://doi.org/10.1007/978-1-4614-3661-4_2.

277. Wu JW, Hussaini SA, Bastille IM, Rodriguez GA, Mrejeru A, Rilett K, et al. Neuronal activity enhances tau propagation and tau pathology in vivo. Nat Neurosci 2016;19:1085–92. https://doi.org/10.1038/nn.4328.

278. Wu S-Z, Bodles AM, Porter MM, Griffin WST, Basile AS, Barger SW. Induction of serine racemase expression and D-serine release from microglia by amyloid Beta-peptide. J Neuroinflammation 2004;1:1–11. https://doi.org/10.1186/1742-2094-1-2.

279. Yamada K, Holth JK, Liao F, Stewart FR, Mahan TE, Jiang H, et al. Neuronal activity regulates extracellular tau in vivo. J Exp Med 2014;211:387–93. https://doi.org/10.1084/jem.20131685.

280. Yamada Y, Sumiyoshi T. Neurobiological Mechanisms of Transcranial Direct Current Stimulation for Psychiatric Disorders; Neurophysiological, Chemical, and Anatomical Considerations. Front Hum Neurosci 2021;15:1–10. https://doi.org/10.3389/fnhum.2021.631838.

281. Zhang Z, Xing Q, Zhong D, Pan Y, He T, Hu Y. The Impact of Psychological Health on Patient Recovery After Arthroplasty 2022;13:1–9. https://doi.org/10.3389/fpsyt.2022.817716.

282. Ziemann U, Reis J, Schwenkreis P, others. TMS and drugs revisited 2014. Clin Neurophysiol 2015;126:1847–68. https://doi.org/10.1016/j.clinph.2014.08.028.

283. Zilles K, Armstrong E, Schleicher A, Kretschmann H-J. The human pattern of gyrification in the cerebral cortex. Anat Embryol (Berl) 1988;179:173–9. https://doi.org/10.1007/bf00304699.

284. Zott B, Simon MM, Hong W, Unger F, Chen-Engerer H-J, Frosch MP, et al. A vicious cycle of Beta amyloid-dependent neuronal hyperactivation. Science 2019;365:559–65. https://doi.org/10.1126/science.aay0198.